5-2024

# Inhibition of pro-inflammatory lipid mediators by Yersinia pestis.

Amanda Brady
*University of Louisville*

# INHIBITION OF PRO-INFLAMMATORY LIPID MEDIATORS BY *YERSINIA PESTIS*

By

Amanda Brady
B.S., University of Northern Colorado, 2017
M.S., University of Louisville, 2020

A Dissertation
Submitted to the Faculty of the
School of Medicine of the University of Louisville
In Partial Fulfillment of the Requirements
for the Degree of

Doctor of Philosophy
In Microbiology and Immunology

Department of Microbiology and Immunology
University of Louisville
Louisville, Kentucky

May 2024

INHIBITION OF PRO-INFLAMMATORY LIPID MEDIATORS BY *YERSINIA PESTIS*

By

Amanda Brady

A Dissertation Approved on

March 25, 2024

By the following Dissertation Committee

Dissertation Chair: Dr. Matthew B. Lawrenz

Dissertation Co-Chair: Dr. Silvia M. Uriarte

Committee member: Dr. Juhi Bagaitkar

Committee member: Dr. Hari Bodduluri

Committee member: Dr. Yousef Abu-Kwaik

DEDICATION

Gage, this is as much yours as it is mine.

&

Mami, you said I could, so I did.

ACKNOWLEDGEMENTS

I would like to thank those who have contributed to my world of science in one way or another:

My PI, Dr. Matthew Lawrenz, thank you for guiding me through the dark times when I thought none of my science was working, for helping me grow as a scientist and pushing me to find solutions from different angles.

My co-mentor, Dr. Silvia Uriarte, thank you for being my role model as a Latina woman in science, for providing your expertise as an immunologist, and being a major supporter throughout these years.

My fellow plague doctors, i.e. lab mates, thank you for being team players and optimistic.

My dissertation committee, thank you for providing valuable feedback that helped my presentation and critical thinking skills.

Thank you to my collaborators for not only providing me with material and expertise, but also giving me opportunities to perform experiments outside of my dissertation project.

Thank you to my friends, who have become my family:

My Kentucky peeps, thank you for being with me through the ups and downs of a PhD, the journey has been better with your companionship.

My Colorado peeps, thank you for not seeing distance as an obstacle, and always finding ways to help me push through.

Thank you to my family (both by marriage and by blood), for being understanding throughout these years of me/us being consumed by this PhD.

10 billion thank yous to my husband, Gage. You have given me love, support, and encouragement throughout this wild ride. I couldn’t have done it without you.

ABSTRACT

INHIBITION OF PRO-INFLAMMATORY LIPID MEDIATORS BY *YERSINIA PESTIS*

Amanda Brady

March 25, 2024

*Yersinia pestis* causes the human disease known as plague. A key manifestation of plague is a delayed inflammatory response. Because this delay in inflammation is required for virulence, I was interested in defining the molecular mechanisms used by *Y. pestis* to evade immune recognition. Eicosanoids are produced early during infection and necessary to initiate a rapid inflammatory response. Despite the importance of these lipids in mediating inflammation, the role of eicosanoids during plague has not been previously investigated. Using an intranasal mouse model infection, I determined the kinetics of eicosanoid synthesis during pneumonic plague. I further demonstrated that $LTB_4$ synthesis by neutrophils, macrophages, and mast cells is actively inhibited by a set of *Y. pestis* proteins that are directly injected into host leukocytes via a type 3 secretion system (T3SS). I also showed that the T3SS is a conserved PAMP recognized by leukocytes. While phagocytosis is not required for $LTB_4$ synthesis by neutrophils, inhibition of phagocytosis in macrophages significantly decreases $LTB_4$ production. Furthermore, I showed that activation of the CASP1/11 inflammasome is required for an enhanced $LTB_4$ response in macrophages, but CASP1/11 is not required for synthesis by neutrophils. Instead, the SKAP2 signaling pathway is required for T3SS-mediated $LTB_4$ production by neutrophils. Together, these data represent the first characterization of the eicosanoid response during pneumonic plague and suggest that *Y. pestis* inhibition of $LTB_4$ synthesis is important for the delayed inflammatory

response associated with plague. These data also highlight significant differences in the signaling pathways induced by the T3SS between macrophages and neutrophils. Importantly, despite multiple mechanisms to recognize the *Y. pestis* T3SS, *Y. pestis* has evolved virulence mechanisms to counteract these signaling pathways to inhibit $LTB_4$ synthesis.

TABLE OF CONTENTS

LIST OF FIGURES

LIST OF TABLES

# CHAPTER 1:

# INTRODUCTION

## 1-1. *Yersinia pestis*: A select agent

Within the genus *Yersinia,* three species are pathogenic to humans: *Y. enterocolitica, Y. pseudotuberculosis*, and *Y. pestis*. *Y. enterocolitica* and *Y. pseudotuberculosis* are enteric gastrointestinal pathogens that cause diarrhea and septicemia.[1, 2] *Y. pestis*, which emerged from *Y. pseudotuberculosis*, causes a more acute disease known as the plague. Plague can manifest in three forms: bubonic, septicemic, and pneumonic. Transmitted by the flea, bubonic plague is the result of *Y. pestis* colonizing the lymphatic system and subsequently spreading to other organs. If left untreated, bubonic plague has a fatality rate of 30-60% within six days as a result of the bacteria entering the blood stream, i.e., septicemic plague.[3-5] Transmitted via aerosols, or secondary to bubonic plague, pneumonic plague has a 100% fatality rate within three days of exposure if treatment is not provided within 36 hours of the bacteria colonizing the lungs.[5-8] Additionally, *Y. pestis* has a history of misuse as a biological weapon.[9, 10] Thus, *Y. pestis* has been categorized as a Tier 1 select agent.

## 1-2. Biphasic inflammatory response during plague

The reservoir hosts of *Y. pestis* are rodents and it exists in an enzootic cycle between these rodents and the flea vector that transmits it.[11] Within the flea, *Y. pestis* is exposed to a temperature of ~26°C and expresses transmission factors required for flea colonization.[12, 13] Spillover into humans occurs when humans come into contact with these *Y. pestis*-infested fleas. As the fleas attempt to feed, the fleas can regurgitate the bacteria into the open bite site.[12-16] At the site of infection, which has a temperature closer to the fleas, *Y. pestis* expresses TLR4 activating LPS and is not synthesizing the type 3 secretion system (T3SS). This allows neutrophils and macrophages, the first responders to *Y. pestis*, to phagocytose the bacteria.[17-19] If engulfed by neutrophils, the bacteria are typically degraded. However, a small percentage of infected neutrophils are efferocytosed by macrophages (the process generally involved in the removal of apoptotic cells[20]).[21, 22] Bacteria taken up by efferocytosis, or directly by macrophages, can inhibit phagosome maturation, and survive within these phagocytes.[22, 23] A subset of extracellular *Y. pestis* also appear to directly enter the lymphatics to evade dermal leukocytes and establish infection in the draining lymph nodes.[24] Eventually, as *Y. pestis* acclimates to the temperature of the mammalian host (~37°C), it will change its lipid A structure from hexa-acylated to tetra-acylated, which is a TLR4-antagonist. It also induces synthesis of the T3SS.[25, 26] These changes allow *Y. pestis* to continue to evade and inhibit the host innate immune response and replicate to high numbers, eventually resulting in the hallmark swollen lymph nodes referred to as buboes.[27]

This initial stage of colonization is accompanied by the absence of robust inflammation, typically referred to in the field as the pre-inflammatory phase of plague.[8, 27-29] Reaching exponential growth within the lymph node, the host transitions to an inflammatory phase;[6] however, *Y. pestis* is still able to re-enter the lymphatics or disseminate into the blood, resulting in septicemic plague. It also spreads and colonizes other organs, such as the spleen, liver, or lungs. Dissemination to the lungs results in the development of secondary pneumonic plague. As the bacteria replicate in the lungs, *Y. pestis* can then be transmitted through aerosolized droplets, allowing for person-to-person transmission, in which primary pneumonic plague manifests, and the process of evading the host innate immune response is repeated.[7, 25]

A similar biphasic inflammatory response is well documented to occur during pneumonic plague.[6, 8, 19, 28, 30-32] In addition to changes in LPS, the secretion of effector proteins through the T3SS allows *Y. pestis* to target neutrophils to both prevent phagocytosis and inflammation, while simultaneously prolonging neutrophil survival.[8, 33 19, 34] Goldman's group showed that YopM, an effector protein secreted by the T3SS, promotes neutrophil survival within the lung lesions during pneumonic plague, potentially by inhibiting NET formation or degranulation.[35] They also showed that YopH and YopE can inhibit primary granule release of neutrophils via inhibiting $Ca^{2+}$ flux and

Rac2 activation, respectively, during pneumonic plague.[36] The T3SS has also been shown to delay cytokine and chemokine release within the lungs and lymph nodes.[6, 8] Importantly, it has been shown that this delay in inflammation is crucial for the progression of disease.[31] Mamroud's group has shown that inducing the inflammatory phase earlier in pneumonic plague, via proxy of inducing neutrophil influx into the lungs, results in an increase in mouse survival and a decrease in bacterial replication.[31] These data suggest that it is therefore critical to fully define all of the bacterial factors contributing to a non-inflammatory environment beneficial to *Y. pestis* colonization to understand the virulence of this organism.

<u>1-2a. The inflammatory cascade</u>

Inflammation can occur in response to pathogen associated molecular patterns (PAMPs) or damage associated molecular patterns (DAMPs). These signals activate pattern recognition receptors (PRRs) triggering the release of lipid mediators by sentinel leukocytes. These lipid mediators are recognized by resident cells, inducing the release of more lipid mediators and of cytokines and chemokines. Together these inflammatory mediators trigger chemotaxis and migration of circulating immune cells to the site of infection.[37] These cells are further activated by the surrounding lipid mediators and cytokines, thus amplifying the inflammatory response until the pathogen has been cleared.[38-40] This process, the inflammatory cascade, is a domino and amplifying effect triggered by the initial release of lipid mediators. Despite lipid mediators playing a critical role in initiating the inflammatory cascade, there is little known about the lipid mediator response during plague.

## 1-3. The *Y. pestis* Ysc Type 3 Secretion System

The *Y. pestis* T3SS, encoded on the pCD1 plasmid, is a molecular syringe that spans the bacterial inner and outer membranes and allows *Y. pestis* to inject *Yersinia* outer proteins (Yops) directly into host cells. These Yop effectors play a major role in altering a plethora of host responses by neutrophils and macrophages on a molecular, cellular, and host level.[26, 41-45] Transcription of the T3SS is controlled by the master regulator LcrF.[4, 46] LcrF is activated by an increase in temperature and a decrease in iron availability. [46-48] Additionally, when $Ca^{2+}$ levels drop, it triggers maximum induction of the transcription of the T3SS components, including the Yops. The release of the Yop effectors occurs when the needle makes contact with the host cell.[4, 49-52]

With transcription initiated, the injectosome begins assembling into a basal body, needle, and pore complex. The basal body, which spans the bacterial inner and outer membrane, is oligomerized into an OM ring and an MS ring, respectively.[26, 53] This occurs via the activation of the scaffolding proteins YscC, YscD and YscJ, the integral membrane proteins YscR, YscS, YscT, YscU, and YscV, and the ATPase complex YscN, YscK, and YscL. Once completed, the basal body secretes the proteins necessary for assembling the needle. YscI forms a rod that spans the inner membrane, allowing YscF to be secreted and polymerize into the needle, with the help of YopR. YscP then regulates the length of the needle. Once the appropriate length of the needle has been reached, YscP interacts with YscU to trigger the secretion of the translocator proteins LcrV, YopB, and YopD. LcrV polymerizes with YscF forming a needle tip complex. The tip complex acts as a platform, tightly binding to the host cell, allowing for YopB and YopD, which contain transmembrane domains, to insert into the host cell membrane forming a translocase pore.[54] Contact with the host membrane initiates the translocation and secretion of the seven effector proteins YpkA, YopE, YopH, YopJ, YopK, YopM, and YopT into the host cell.[26, 55-58]

1-3a. YopB and YopD are required to translocate other Yop effectors

The YopB/D translocase functions to generate a pore needed for Yop secretion, translocation, and regulation.[59, 60] In order for the translocase to be fully functional, YopB and YopD are both needed to form a complex within the membrane.[61, 62] YopB appears to be the major component responsible for inducing pore formation,[4, 63] while YopD has chaperone-like activity and is primarily responsible for the translocation of the effectors[64-66] However, the translocation of YopB and YopD, and insertion into the plasma membrane, is tightly controlled, and hyper-translocation of these proteins can trigger NLRP3 activation and inflammasome-mediated pyroptosis. Hyper-translocation appears to be prevented by YopK.[67, 68]

<u>1-3b. The Yop effectors and their host targets</u>

Upon translocation into the cell, each of the Yop effector proteins have different enzymatic activities and target different components of the cell (Table 1-1).[41, 42, 45, 69, 70] *Yersinia* protein kinase A, or YpkA, is a serine/threonine protein kinase. Having a Rho-GTPase binding domain, YpkA binds to RhoA and Rac1, preventing actin cytoskeleton rearrangement and phagocytosis.[71, 72] Phagocytosis is also inhibited by YpkA directly binding and phosphorylating actin and G protein subunit G$\alpha$q. Phosphorylating G$\alpha$q can also inhibit $Ca^{2+}$ signaling.[26, 73-76] Additionally, RhoA, Rac1, and G$\alpha$q have also been linked to MAPK signaling, therefore YpkA can also contribute to MAPK signaling inhibition.[44, 75, 77-81] Finally, YpkA has also been shown to induce apoptosis.[82]

YopE is a GTPase activating protein (GAP) that binds RhoA, Rac1, and Cdc42 inhibiting downstream signaling. The RhoA, Rac1, and Cdc42 proteins regulate actin cytoskeleton rearrangement, and can trigger MAPK and NF$\kappa$B signaling pathways.[83-85] Thus, YopE has been shown to directly inhibit phagocytosis, MAPK phosphorylation, and cytokine release.[42, 86, 87] YopE GAP activity also triggers pyrin, which leads to inflammasome activation and pyroptosis.[88] However, YopM disrupts the pyrin activation of the inflammasome via binding protein kinase C-related kinases (PRK) and ribosomal S6 kinases (RPK), thereby preventing pyrin phosphorylation.[89, 90] Additionally, excessive YopE activity can induce macrophage cell death, but YopT competes with YopE in interacting with Rho GTPases, minimizing host recognition of YopE.[44, 91, 92] Finally, YopE can also inhibit degranulation by neutrophils[36, 93, 94] and limit the translocation of other effectors.[56]

YopH is a tyrosine phosphatase, and thus removes phosphates from tyrosine residues on proteins. This enzymatic activity has been shown to target focal adhesion complexes such as SLP-76, SKAP2, PRAM, Vav, LCK, Fak, SKAP-HOM, and Fyb. [42, 95-99] Targeting these complexes results in inhibiting $Ca^{2+}$ signaling,[97, 98, 100] phagocytosis,[99] cytokine release,[101, 102] and ROS production.[98] Studies have also shown that YopH can inhibit ERK phosphorylation in neutrophils.[97, 98, 100, 103] Additionally, YopH has been shown to be critical for virulence, as an infection with a YopH mutant is attenuated in the mouse model.[104]

YopJ is a serine/threonine acetyltransferase that plays a major role in inhibiting inflammation during plague. YopJ uses acetyl-coenzyme A (CoA) to modify the serine and threonine sites of proteins, such as TAK1, in the mitogen-activated protein (MAP), and IκB pathways, blocking their activation.[41, 42, 55, 105, 106] It has also been shown to deubiquitinate TRAF6 and TRAF2 in the NF-κB pathway as well.[107] As such, YopJ inhibits pro-inflammatory cytokine release,[108-110] contributes to inhibiting degranulation by neutrophils,[36, 93, 111] and induces apoptosis.[112, 113] This apoptosis has been seen coupled with caspase-1 activation, but inflammasome assembly is prevented by YopM binding to IQGAP1 (IQ motif- containing GTPase-activating protein 1)[114] and to caspase-1 preventing full activation in *Y. pseudotuberculosis*.[115-117] Even further, with *Y. pestis* expressing a TLR4-antagonist LPS, cells do not receive the primary signal required, therefore complete inflammasome activation is not fulfilled.[118, 119]

While termed an outer protein, YopK is typically not considered an effector, as it had not been shown to target host components and mostly functions to regulate the T3SS translocase pore size, and thus the translocation rate of the effector proteins.[28, 57] This regulation contributes to YopJ induced apoptosis, which in turn promotes spread of *Y. pestis* and disease progression.[28] YopK also inhibits host recognition of YopB from activating the NLRP3 and NLRC4 inflammasomes.[67, 68] Furthermore, studies have found YopK targets the host receptor for activated C kinase (RACK1) preventing phagocytosis[120] and binds directly to matrix adaptor protein matrilin-2 (MATN2) promoting the bacteria binding to cells.[121] YopK has also been shown to be critical for *Y. pseudotuberculosis* colonizing the gut.[122]

YopM, which lacks catalytic activity, has leucine rich repeats which allow it to bind to host proteins.[42, 44] It has been shown to be an adaptor protein binding to RSK and PRK inhibiting their activity.[123] RSKs are downstream of MAPK signaling and are involved in cell proliferation, survival, growth, and motility.[124, 125] PRKs regulate the phosphorylation of serine and threonine residues.[126] Importantly, binding to these proteins inhibits pyrin phosphorylation, and thereby prevents pyrin inflammasome activation.[89, 90, 114, 115] YopM has also been shown to inhibit cytokine release,[110] and induce caspase-3 activation, to promote bacterial survival.[127]

YopT is a cysteine protease and the third Yop effector that targets RhoA, Rac1, and Cdc42. However, YopT renders their inhibition irreversible by cleaving the proteins from the plasma membrane.[42, 87, 128] This results in YopT inhibiting phagocytosis and MAPK signaling.[26, 41, 129]

While each Yop effector targets different components in the cell, as summarized in Table 1-1, it is clear that there is functional redundancy in the effectors. Importantly, the overarching outcome of targeting these different components results in inhibiting inflammation to establish a non-inflammatory environment and slow the host innate immune responses required for the clearance of *Y. pestis*.

| Yop | Biochemical function | Cell targets | Cellular effects |
|---|---|---|---|
| **YpkA** | Serine/threonine kinase | Gαq, RhoA, Rac1, actin | Disruption of actin cytoskeleton<br>Inhibits phagocytosis<br>Inhibits Gαq signaling<br>Inhibits $Ca^{2+}$ signaling<br>Induces apoptosis<br>Inhibits MAPK signaling |
| **YopE** | GTPase activating protein | RhoA, Rac1, Cdc42 | Disruption of actin cytoskeleton<br>Inhibits phagocytosis<br>Inhibit degranulation<br>Regulates Yop translocation<br>Inhibits MAPK signaling |
| **YopH** | Protein tyrosine phosphatase | Focal adhesion complexes | Inhibits ROS production<br>Inhibits phagocytosis<br>Inhibits $Ca^{2+}$ signaling<br>Inhibits cytokine release<br>Inhibits MAPK signaling |
| **YopJ** | Acetyl-transferase, deubiquitinase | MAPKK, IKK, and NF-κB family proteins | Induces apoptosis<br>Inhibits MAPK signaling |
| **YopK** | Yop regulator | Yersinia translocation machinery | Regulates Yop translocation<br>Inhibits phagocytosis<br>Inhibits inflammasome activation<br>Promotes colonization |
| **YopM** | Leucine-rich repeat containing protein | Pyrin activation | Inhibits pyrin activation<br>Inhibits cytokine release |
| **YopT** | Cysteine protease | RhoA, Rac1, Cdc42 | Inhibits phagocytosis<br>Inhibits MAPK signaling |

Table 1-1. Summary of Yop cellular targets and effects

## 1-4. *Y. pestis* inhibits leukocyte responses

While *Y. pestis* and *Y. pseudotuberculosis* are closely related, studies have found distinct immunomodulatory differences between them.[130-133] Additionally, a recent review goes into detail of the role of neutrophils in the *Yersinia* infectious model, with a strong focus on *Y. pseudotuberculosis.*[134] Therefore, here I will focus on *Y. pestis* specific studies .

### 1-4a. *Y. pestis* and neutrophils

In 1969, Janssen and Surgalla[135] using an *ex vivo* approach, were the first to show *Y. pestis* survived within neutrophils and macrophages. Since then, there have been several studies to explore the implications of the host being unable to clear the bacteria. By 12 h post infection, neutrophils have been shown to be the primary targets for Yop translocation during plague.[19, 34] The Yop effectors have been shown to promote neutrophil survival,[8, 33] inhibiting $Ca^{2+}$ flux, and Rac2 activation.[36] Additionally, using human neutrophils, Hinnebusch's group has shown that *Y. pestis* inhibits phagocytosis[136] and YopJ inhibits IL-8 secretion.[109] Towards this, Kobayashi's group has also shown the T3SS inhibits phagocytosis, ROS production,[103, 137] and apoptosis.[137] They also showed *Y. pestis* resists neutrophil antimicrobial responses via the two-component regulator, PhoP.[138] Finally, studies have shown a redundant, cooperative role by the Yop effectors to inhibit neutrophil degranulation.[93, 111]

### 1-4b. *Y. pestis* and macrophages

The immunomodulatory effects of *Y. pestis* on macrophages have been extensively studied. It has been shown that *Y. pestis* prevents phagolysosome fusion to prevent phagocytic killing by the macrophages if the bacteria become phagocytosed.[17, 139, 140] However, the bacteria can evade uptake entirely, by inhibiting macrophage recognition.[69, 133, 141-143] *Y. pestis* can also induces macrophage non-inflammatory apoptosis, thereby promoting spread and the progression of disease.[28, 112, 133, 144] Moreover, the bacterium prevents pro-inflammatory cytokine release,[133, 145] nitric oxide synthesis,[133] and proinflammatory M1 polarization,[133] and changes the antigen presentation profile of macrophages.[133, 146]

1-4c. *Y. pestis* and mast cells

Exploring the host-pathogen interaction between *Y. pestis* and mast cells is severely lacking. To my knowledge, there has been a singular study to date in which mast cells isolated from the peritoneum were infected with *Y. pestis* and measured for degranulation.[147] Even after treatment with a powerful degranulation inducer, ionophore A23187, the level of mast cell degranulation was dramatically decreased in the *Y. pestis* infected group. They further showed this inhibition was attributed to the tyrosine phosphatase activity of YopH.[147]

**1-5. $LTB_4$: A powerful inflammatory modulator**

Lipid mediators are omega-6 polyunsaturated fatty acids (PUFA) that play a critical role in enhancing innate and adaptive immune inflammatory responses.[148] Derived from linoleic, arachidonic, eicosapentaenoic, and docosahexaenoic acid, the host can produce both pro-resolving lipid mediators (lipoxin, resolvins, and protectins) and pro-inflammatory lipid mediators (thromboxane, prostaglandins, and leukotrienes) (Fig 5-1).[149] Of the proinflammatory mediators, leukotriene B4 ($LTB_4$) is recognized as a potent chemoattractant and activator of cells.[150, 151]

1-5a. $LTB_4$ synthesis

$LTB_4$ is synthesized by leukocytes, primarily mast cells, neutrophils, and macrophages.[150, 152, 153] A PAMP binding to a PRR initiates MAPK and $Ca^{2+}$ signaling. The combination of these signaling pathways leads to complete activation of the enzymes cytosolic phospholipase A2 ($cPLA_2$) and 5-Lipoxygenase (5-LOX). These fully activated enzymes congregate at the nuclear membrane or lipidisome to form a complex with 5-LOX activating protein (FLAP) in which FLAP presents the free arachidonic acid (AA) to 5-LOX. 5-LOX oxidizes AA to H-pETE, and then rapidly converts it to leukotriene A4 ($LTA_4$). $LTA_4$ leaves the nuclear membrane and is hydrolyzed to $LTB_4$ by $LTA_4$

hydrolase ($LTA_4H$). $LTB_4$ is then released from the cell (Fig 1-1). Because $LTB_4$ has a significant effect on inflammation, its synthesis must be highly regulated, otherwise chronic detrimental inflammation can occur.

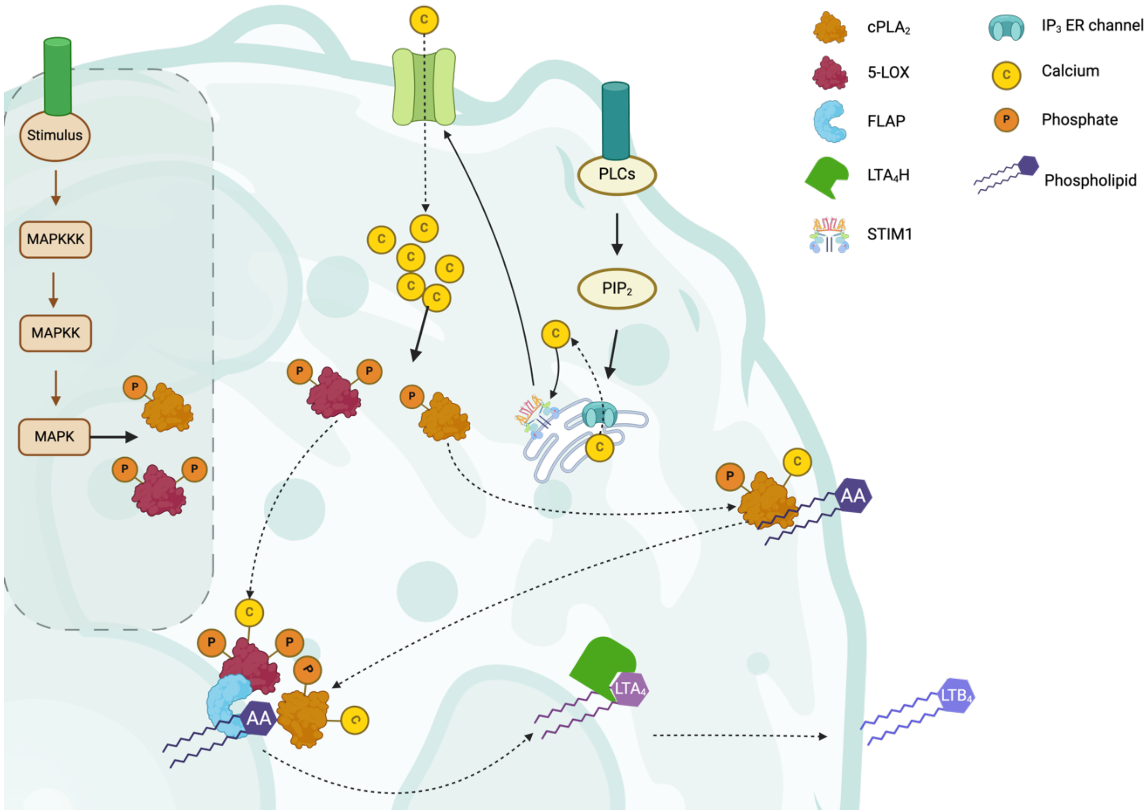


Figure 1-1. Leukotriene $B_4$ synthesis pathway

LTB$_4$ is synthesized when the enzymes cPLA$_2$ and 5-LOX/FLAP convert arachidonic acid (AA) into LTA$_4$. LTA$_4$H then rapidly converts LTA$_4$ to LTB$_4$, which then gets released from the cell. The enzymes become fully activated via phosphorylation and $Ca^{2+}$ binding. Dashed arrows denote movement of molecule. Solid arrows denote signaling pathways.

1-5b. $cPLA_2$ regulation

Through MAPK signaling, $cPLA_2$ is phosphorylated at Ser505, triggering the enzyme to translocate to the plasma membrane. Then, through $Ca^{2+}$ signaling, the influx of $Ca^{2+}$ leads to binding to $cPLA_2$ to fully activate the enzymes.[152, 154] Importantly, $Ca^{2+}$ concentrations need to reach a threshold for an extended period before returning to resting level to activate $cPLA_2$ to discriminate against false activation.[155, 156] $Ca^{2+}$ binding also induces conformational changes that promote translocation of these proteins to the nuclear membrane or lipidisome.[157] Prior to translocation, $cPLA_2$ cleaves AA from the plasma membrane and carries it towards 5-LOX.[157] AA release from the plasma membrane has been linked to epidermal growth factor (EGF) signaling.[158, 159] If this signaling continues longer than 24 hours, P11, a unique s100 calcium binding enzyme that binds to proteins instead of $Ca^{2+}$, becomes transcriptionally activated and turns off $cPLA_2$ activity by binding directly to the enzymes catalytic region.[160, 161] Another mechanism to inactivate $cPLA_2$ is thiol modification of Cys331 which alters the activity of the enzyme.[162]

1-5c. Arachidonic acid

Rapid synthesis of $LTB_4$ is possible due to the quick sequential release of AA from the plasma membrane, and not requiring de novo synthesis. With PLC activation, $PIP_2$ is cleaved to produce inositol 1,4,5-triphosphate ($IP_3$) and diacylglycerol (DAG). DAG then becomes cleaved into AA.[163, 164] $cPLA_2$ is then able to cleave AA free from the plasma membrane.[165, 166]

1-5d. 5-LOX regulation

5-LOX becomes partially activated upon phosphorylation at Ser-271 by p38[167] or at Ser-663 by ERK signaling.[168] Unlike $cPLA_2$, 5-LOX does not require a high concentration of $Ca^{2+}$, nor does that threshold need to be maintained.[152, 169] Once $Ca^{2+}$ binds, supported by the chaperone coactosin-like protein (CLP), it stimulates 5-LOX enzymatic activity and induces nuclear membrane association.[152, 169, 170] As a form of regulation, glutathione peroxidase-1 (GPx-1) inhibits 5-LOX from binding to lipid hydroperoxide (LOOH). LOOH converts the ferrous iron ($Fe^{2+}$), located on the C-terminus of 5-LOX, to ferric iron ($Fe^{3+}$), which activates the catalytic activity and stabilizes 5-LOX.[169, 171] In addition to GPx-1, 5-LOX is also inhibited by cAMP signaling activating the protein kinase A (PKA) pathway, which in turn phosphorylates the 5-LOX at Ser523, inactivating the enzyme.[169, 172]

1-5e. 5-lipoxygenase activating protein (FLAP) is required for cPLA2-5-LOX complex formation

Transcription of FLAP has been shown to be triggered by cytokines IL-3 and IL-5, granulocyte-monocyte colony stimulating factor (GM-CSF), LPS, and TNF-$\alpha$ depending on cell type.[173-177] FLAP was also identified as a critical component for 5-LOX to associate with the membrane and form the complex with $cPLA_2$.[178]

1-5f. $LTA_4$ hydrolase regulation

$LTA_4$ hydrolase ($LTA_4H$) is a soluble, monomeric zinc-metalloenzyme that has two catalytic activities: it is a protease and epoxide hydrolase. The N-terminus β-sheet functions to recognize peptide substrates, and the C-terminus has an α-helical domain that faces the catalytic domain and together house a zinc molecule.[179, 180] The zinc is ligated to the enzyme at His-295, His-299, and Glu-318. Without the presence of zinc, at a 1:1 ratio, the enzyme is completely inactive for both catalytic activities. In addition to zinc, a water molecule is required to fully activate $LTA_4H$. Once $LTA_4$ binds to Tyr-378 of $LTA_4H$, and $LTA_4$ is hydrolyzed to $LTB_4$, $LTA_4H$ undergoes suicide inactivation as a form of regulation.[179, 181]

1-5g. $LTB_4$ receptors

As an autocrine and paracrine signal, $LTB_4$ binds to G-protein coupled receptors (GPCR) BLT1 and BLT2 with a high and low affinity, respectively. BLT1 is expressed primarily by leukocytes and BLT2 is primarily expressed by epithelial and endothelial cells.[182-185] Additionally, $LTB_4$ can bind to peroxisome proliferator-activated receptor-α (PPAR-α) as a form of regulation. Binding to PPAR-α leads to the catabolism of the lipid, and thus a form of resolving the inflammatory response.[186, 187]

## **1-6. BLT1-LTB$_4$ axis in disease**

1-6a. Sterile inflammation

A recent detailed review summarizes numerous studies that have investigated the significance of LTB$_4$ and inflammatory diseases.[185] In brief, it has been established that the LTB$_4$-BLT1 axis contributes to diseases such as rheumatoid arthritis, obesity, diabetes, tumor development, lung fibrosis, and asthma.[186-191] Recently, a study also showed that there is an elevated level of LTB$_4$ in macrophages collected from patients with systemic lupus erythematosus, which was increased through NF-κB signaling, and thus the increase of pro-inflammatory cytokine production.[192] In the gout model, LTB$_4$ induces macrophage ROS production, which leads to caspase-1 cleavage and NLRP3 inflammasome activation, compared to vehicle controls.[193] Even further, LTB$_4$ has also been linked to increasing inflammatory conditions following cardiac infarction. BLT1$^{-/-}$ mice showed increased survival due to decreased leukocyte infiltration, decreased cell death, and decreased pro-inflammatory cytokine production.[194]

1-6b. Infection-mediated inflammation

While LTB$_4$ can be detrimental during sterile inflammation, it is critical in inducing antimicrobial activity in defense of viral, fungal, parasitic, and bacterial infections.[195-197] While there are reviews that have addressed the relationship between LTB$_4$ and pathological infections, these reviews are primarily focused on viral studies.[185, 196]

LTB$_4$ has been linked to inducing activation of leukocytes in response to pathogens. Peters-Golden's group has shown that not only does opsonized *K. pneumoniae* induce LTB$_4$ synthesis by alveolar macrophages (AM), but when BLT1-LTB$_4$ signaling is blocked, phagocytosis of *K. pneumoniae* is significantly reduced. Using alveolar macrophages isolated from 5-LOX$^{-/-}$ mice, they were able to rescue phagocytosis by exogenous treatment of LTB$_4$.[198] They then went on to show human neutrophils and mouse peritoneal neutrophils treated with LTB$_4$ successfully phagocytosed

*K. pneumoniae*.[199] Furthermore, they were able to show that AM bactericidal activity is enhanced by $LTB_4$ activating NADPH oxidase.[200] While these experiments were performed *in vitro*, they had previously determined the result of removing $LTB_4$ synthesis *in vivo*. They found that 5-LOX$^{-/-}$ mice infected with *K. pneumoniae* had a decrease in mouse survival, when compared to wildtype mice. This phenotype was attributed to the decrease in neutrophil infiltration into the lungs, phagocytosis, and intracellular killing, and an increase in bacterial survival.[201]

In another study, wildtype and 5-LOX$^{-/-}$ mice were intranasally infected with *Streptococcus pneumoniae* and then treated with aerosolized $LTB_4$ 24 h post infection. Not only did they find that treatment dramatically improved macrophage and neutrophil infiltration and decreased bacterial load, compared to mice treated with the vehicle, but they also found that the mode of administration of $LTB_4$ treatment dramatically changes the outcome, with aerosolized administration being the most effective.[202]

When $LTB_4$ synthesis is inhibited in zebrafish, there is a reduction of macrophage aggregation in response to *Streptococcus iniae*. However, this phenotype was reversed when neutrophil derived $LTB_4$ producing zebrafish were crossed with $LTA_4H$ deficient zebrafish.[203] Also in zebrafish, a study showed that a balanced production of $LTB_4$ is critical for controlling a *Mycobacterium* infection and preventing severe disease. More importantly, while they experimented with zebrafish, they were able to correlate these results with human susceptibility to tuberculosis and leprosy.[204] This balance was also observed in a 5-LOX$^{-/-}$ mouse model. Compared to wildtype mice, 5-LOX$^{-/-}$ mice had a better survival rate when infected with *Mycobacterium tuberculosis*, which the authors attribute to the decrease in inflammatory response.[205]

An *ex* vivo approach showed $LTB_4$ treatment not only increased human neutrophil secretion of antimicrobial proteins, but also decreased overall survival of *Staphylococcus aureus* and *Escherichia coli*.[197] Additionally, $LTB_4$ produced by macrophages induces neutrophil migration, the formation of abscesses, and the clearance of MRSA from mouse skin infections.[206] It has also been shown that *E. coli* induces the synthesis of $LTB_4$ by mouse bone marrow derived mast cells, which then improves neutrophil recruitment.[207] Another study showed mouse peritoneal macrophages improved phagocytosis of *Salmonella enterica* Typhimurium and *Pseudomonas aeruginosa* when treated with $LTB_4$.[208] More recently, it has been shown that the treatment of $LTB_4$ to macrophages isolated from $BLT1^{-/-}$ mice restored phagocytosis of *Borrelia burgdorferi*.[209] The same group also showed the augmenting effect $LTB_4$ has on the human neutrophil killing of *Mycobacterium bovis*.[210] Another study showed *Streptococcus pyogenes* induces $LTB_4$ synthesis *in vivo*, and when human and mouse macrophages are treated with $LTB_4$, phagocytosis is improved.[211] Lastly, a study in 1992 identified the ability of intracellular bacteria, *Y. enterocolitica* and *Listeria monocytogenes*, to reduce the production of $LTB_4$ by human neutrophils when compared to extracellular bacteria, *E. coli*.[155] In conclusion, these studies have shown the importance of $LTB_4$ in controlling infection models, by using exogenous $LTB_4$ treatment. Nonetheless, these studies lack information regarding the direct host $LTB_4$ response to these pathogens.

1-6c. $LTB_4$ and the inflammasome

$LTB_4$ binding to BLT1 plays a critical role in the migration, activation, and proliferation of both innate and adaptive immune cells[196, 212-214] and in the activation and differentiation of non-immune cells.[215, 216] The role of $LTB_4$ in inflammasome activity has been shown to be beneficial and detrimental depending on the infectious model. In a parasitic model, $LTB_4$ is critical for clearance of *Leishmania amazonensis*. Activation of the P2X7 receptor by ATP, activates $LTB_4$ synthesis, initiating a cascade leading to NLRP3 inflammasome activation.[217] Finally, a group studying methicillin-resistant *Staphylococcus aureus* (MRSA) skin infection found $LTB_4$ to be critical in activating NLRP3, improving clearance of the infection.[218] On the contrary, a study found an opposite effect of $LTB_4$ on inflammasome activation. Wild type mice inoculated with *Tityus* *serrulatus* scorpion venom had increased survival, compared to Alox5$^{-/-}$ (5-LOX deficient) mice, which was attributed to a decrease in inflammasome activation. The authors propose that in this context, $PGE_2$ (an alternative AA product) is responsible for the inflammasome activation.[219]

Regarding $LTB_4$ synthesis specifically, Hedge et al.[153] found no connection to the inflammasome during a crystalline silica sterile inflammation model in both macrophages and neutrophils. On the contrary, von Moltke et al.[220] showed $LTB_4$ synthesis in macrophages depended on MyD88/Trif in response to the artificially delivered *Legionella pneumophila* flagellin (FlaA) fused to *Bacillus anthracis* lethal factor (LFn) mediated by the anthrax protective antigen (PA) channel. Zoccal et al.[219] identified NLRP3 as an essential component for $LTB_4$ synthesis in response to scorpion venom. These studies highlight the importance of $LTB_4$ in activating the inflammasome, but also allude to a potential requirement of inflammasome activity for $LTB_4$ synthesis in a bacterial infection model.

### 1-6d. $LTB_4$ and neutrophil swarming

$LTB_4$ has been shown to be absolutely required for the phenomenon known as neutrophil swarming.[221-223] Once triggered, neutrophils release $LTB_4$ in a feedforward amplification gradient, which results in an exponential accumulation of neutrophils at the site of infection or damage.[224-226] *In vivo* studies have shown without $LTB_4$, there is an absence of an effective neutrophil response to sterile injury to the dermis of mice[227] and damaged tissue in zebra fish.[228, 229] Interestingly, an ex vivo microscale "arena" model using human neutrophils showed the importance of $LTB_4$ in swarming.[230]

## 1-7. This dissertation: A rationale for the madness

*Y. pestis* has been shown to alter the host inflammatory response resulting in immune evasion and the generation of a non-inflammatory environment beneficial for its colonization. However, despite the critical role lipid mediators play in producing a robust immune response that is essential for the clearance of pathogens, the impact of lipid mediator synthesis on *Y. pestis* infection has not previously been explored. However, our lab has shown that *Y. pestis* can inhibit $LTB_4$ synthesis by infected human neutrophils,[93] leading to my central hypothesis that *Y. pestis* inhibits $LTB_4$ synthesis during infection to generate a non-inflammatory environment beneficial for the progression of disease. In my dissertation I set out to specifically test this hypothesis and explored the following questions:

1. What is the inflammatory lipid mediator response during plague?
2. Does *Y. pestis* manipulate this response?
3. Does *Y. pestis* target $LTB_4$ synthesis by other leukocytes?
4. How are the Yop effectors inhibiting $LTB_4$ synthesis in the neutrophils?
5. How are the neutrophils recognizing *Y. pestis* and triggering this $LTB_4$ response?
6. Finally, what are the consequences of altering the host lipid mediator responses?

CHAPTER 2:

TYPE 3 SECRETION SYSTEM INDUCED LEUKOTRIENE $B_4$ SYNTHESIS BY LEUKOCYTES IS ACTIVELY INHIBITED BY *YERSINIA PESTIS* TO EVADE EARLY IMMUNE RECOGNITION[1]

[1]Brady A, Sheneman KR, Pulsifer AR, Price SL, Garrison TM, Maddipati KR, Bodduluri SR, Pan J, Boyd NL, Zheng JJ, Rai SN, Hellmann J, Haribabu B, Uriarte SM, Lawrenz MB. Type 3 secretion system induced leukotriene B4 synthesis by leukocytes is actively inhibited by *Yersinia pestis* to evade early immune recognition. PLoS Pathog. 2024; 20(1): e1011280. PMID: 38271464

## 2-1. Introduction

*Yersinia pestis* causes the human disease known as the plague. Although typically characterized as a disease of our past, in the aftermath of the 3rd plague pandemic, *Y. pestis* became endemic in rodent populations in several countries, increasing the potential for spillover into human populations through contact with infected animals and fleas.[3, 231, 232] Human plague manifests in three forms: bubonic, septicemic, or pneumonic plague. Bubonic plague resulting from flea transmission arises when bacteria colonize and replicate within lymph nodes. Septicemic plague results when *Y. pestis* gains access to the bloodstream, either directly from a flea bite or via dissemination from an infected lymph node, and results in uncontrolled bacterial replication and sepsis. Finally, secondary pneumonic plague, wherein *Y. pestis* disseminates to the lungs via the blood, results in a pneumonia that can promote direct person-to-person transmission via aerosols. While treatable with antibiotics, if left untreated, all forms of plague are associated with high mortality rates, and the probability of successful treatment decreases the longer initiation of treatment is delayed post-exposure.[3-5, 233] Regardless of the route of infection, one of the key virulence determinants for *Y. pestis* to colonize the host is the Ysc type 3 secretion system (T3SS) encoded on the pCD1 plasmid.[4, 234] This secretion system allows direct translocation of bacterial effector proteins, called Yops, into host cells.[4, 56, 235] The Yop effectors target specific host factors to disrupt normal host cell signaling pathways and functions.[6, 8, 28, 102, 236, 237] Because the T3SS and Yops are required for mammalian but not flea infection, the expression of the genes encoding these virulence factors are differentially expressed within these two hosts.[4, 26, 56, 238] The primary signal leading to T3SS and Yop expression is a shift in temperature from that of the flea vector (<28°C) to that of the mammalian host (>30°C). During mammalian infection, *Y. pestis* primarily targets neutrophils and macrophages for T3SS-mediated injection of the Yop effectors.[19, 98, 239] The outcomes of Yop injection into these cells include inhibition of phagocytosis, reactive oxygen species (ROS) synthesis, degranulation by neutrophils, and inflammatory cytokine and chemokine release required to recruit circulating neutrophils to infection sites.[36, 93, 103, 109, 136, 137] Importantly, previous work suggests that inhibition of neutrophil influx and establishing a non-inflammatory environment is crucial for *Y. pestis* virulence.[31, 240] Therefore, defining the molecular mechanisms used by *Y. pestis* to subvert the host immune response is fundamental to understanding the pathogenesis of this organism. Moreover, defining the host mechanisms targeted by *Y. pestis* to inhibit inflammation can also provide novel insights into how the host responds to bacterial pathogens to control infection.

A cascade of events tightly regulates inflammation to ensure rapid responses to control infection and effective immune resolution after clearance of pathogens to limit tissue damage.[38, 148] This inflammatory cascade is initiated by synthesizing potent lipid mediators and is sustained and amplified by the subsequent production of protein mediators.[37, 241] Polyunsaturated fatty acid (PUFA)-derived lipid mediators are potent modulators of the innate and adaptive immune responses.[148, 242] Of these, the eicosanoids, including the leukotrienes and the prostaglandins, are key regulators of the inflammatory cascade during infection.[37, 241] Leukotriene B4 ($LTB_4$) is rapidly synthesized from arachidonic acid upon activation of 5-lipoxygenase (5-LOX), cytosolic phospholipase $A_2$ ($cPLA_2$), 5-LOX activating protein (FLAP), and $LTA_4$ hydrolase (Fig 2-1A).[152] Upon synthesis and release, $LTB_4$ is recognized by the high affinity BLT1 receptor on immune cells to promote chemotaxis and initiate the inflammatory cascade leading to production of pro-inflammatory cytokines and chemokines.[37, 150, 151, 183, 185, 241, 243] Together these inflammatory mediators promote the recruitment of circulating leukocytes to infected tissue.[37] Importantly, because of its critical role in initiating the inflammatory cascade, disruption in the timely production of $LTB_4$ can slow the subsequent downstream release of cytokines and chemokines and the ability of the host to mount a rapid inflammatory response required to control infection.

Despite active proliferation of *Y. pestis* within the lungs in the mouse model*,* there appears to be an absence of pro-inflammatory cytokines, chemokines, and neutrophil influx for the first 36 hours of primary pneumonic plague.[6, 8, 28, 102, 237] This phenotype dramatically differs from pulmonary infection with attenuated mutants of *Y. pestis* lacking the T3SS or Yop effectors or by other pulmonary pathogens, such as *Klebsiella pneumoniae*, which induce significant inflammation within 24 hours of bacterial exposure.[6, 8, 28, 102, 237] Surprisingly, despite the importance of lipid mediators in initiating the inflammatory cascade, the role of inflammatory lipids during plague has not been previously investigated. However, using human peripheral blood neutrophils, Pulsifer et al.[93] previously demonstrated that *Y. pestis* can actively inhibit the synthesis of $LTB_4$ *in vitro* in a T3SS/Yop-dependent manner, suggesting that $LTB_4$ synthesis may be inhibited during plague. In this chapter, I expand on these observations by investigating $LTB_4$ synthesis by the mammalian host in response to *Y. pestis*. Using the murine model of plague, I demonstrate dysregulation in the production of $LTB_4$ by *Y. pestis* and provide the lipidomic profile of other host inflammatory lipids during the initial 48 h of pneumonic plague. I further show that exogenous treatment with $LTB_4$ inhibits bacterial proliferation in the murine model. Using *Y. pestis* mutants, I also discovered that leukocyte interactions with the *Y. pestis* T3SS triggers $LTB_4$ synthesis, but synthesis is inhibited by multiple Yop effectors secreted via the same T3SS. Together, these data suggest that modulation in the production of host inflammatory lipids is an additional virulence mechanism used by *Y. pestis* to inhibit the rapid recruitment of immune cells needed to control infection.

## 2-2. Results

### 2-2a. $LTB_4$ synthesis is delayed during pneumonic plague

Based on my lab's previous observations that *Y. pestis* inhibits $LTB_4$ synthesis by human neutrophils,[93] I sought to determine if $LTB_4$ was synthesized during infection using the murine model of pneumonic plague. C57BL/6J mice were intranasally infected with *Y. pestis* KIM5+ and $LTB_4$ was measured in the lungs during the non-inflammatory stage of disease (6, 12, and 24 h post-infection). I did not observe a statistically significant increase in $LTB_4$ synthesis at any time point, with only 3 of the 15 samples having elevated $LTB_4$ concentrations over the entire 24 h period (Fig 2-1B). Moreover, I did not observe a significant increase in 20-hydroxy $LTB_4$ (Fig 2-1C), which is the direct degradation product of $LTB_4$ (Fig 2-1A). To confirm these results, $LTB_4$ was measured in the lungs from a second independent group of C57BL/6J mice, this time expanding the analysis to include the pro-inflammatory stage of disease (36 and 48 h post-infection). Again, I did not observe statistically significant increases in $LTB_4$ or 20-hydroxy $LTB_4$ during the first 24 h of infection (Fig 2-1D and 2-1E). However, by 36 h post-infection, both lipids were statistically elevated compared to uninfected samples ($p \leq 0.05$). Moreover, I observed a significant increase in 5-HETE as early as 6 h post-infection (Fig 2-1F; $p \leq 0.01$), which can result if 5-LOX does not complete the synthesis of $LTA_4$ from arachidonic acid.[244, 245] While the synthesis of $LTB_4$ appears absent during the first 24 h of infection, the synthesis of other inflammatory lipids increased during the same period, including the prostaglandins, which are another group of eicosanoids whose synthesis is regulated via the cyclooxygenase pathway (Fig 2-1G-I). Globally, I observed significant changes in the synthesis of 63 lipids during pneumonic plague, including lipids generally considered to be pro-inflammatory (18 lipids), anti-inflammatory (41 lipids), or pro-resolving (4 lipids) (Table 2-1 & Fig 5-1).[246, 247] Together these data indicate $LTB_4$ synthesis is delayed during pneumonic plague.

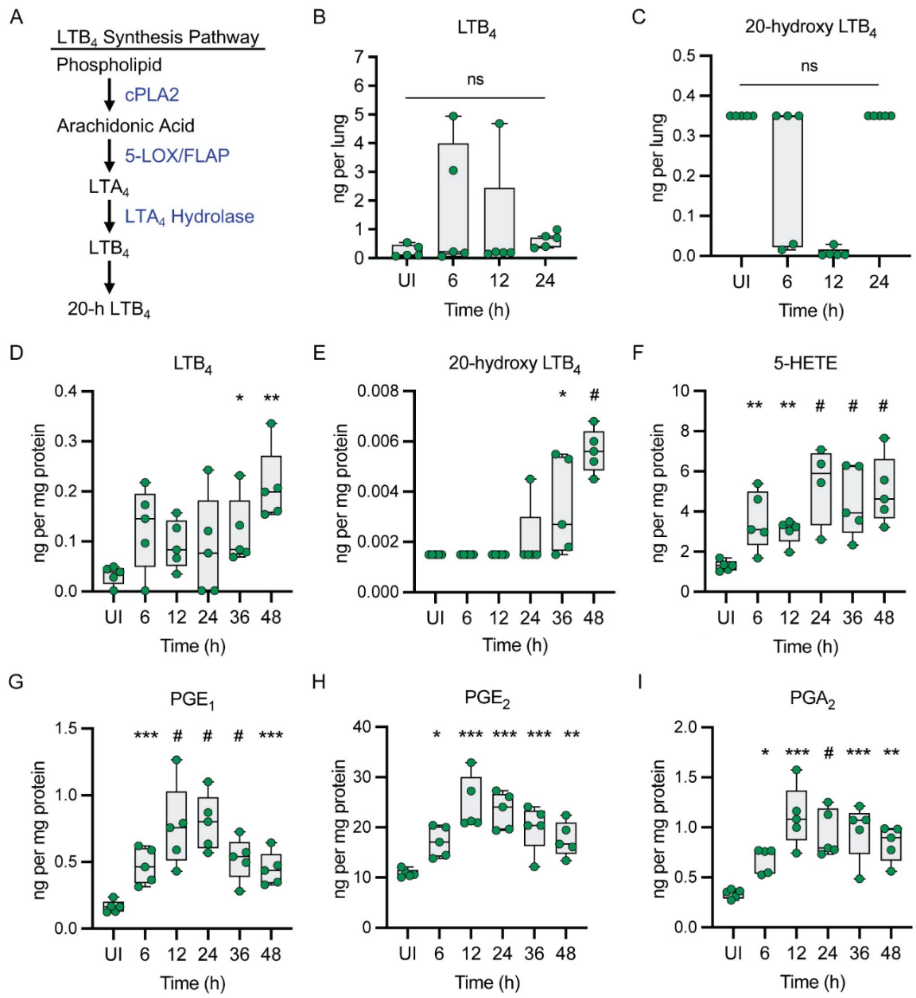


<u>Figure 2-1. $LTB_4$ synthesis is blunted during pneumonic plague</u>

(A) The $LTB_4$ synthesis pathway. (B-I) C56BL/6J mice were infected with 10 x the $LD_{50}$ *Y. pestis* KIM5+ and lungs were harvested at the indicated times (n=5) to measure host lipids by LC-MS. UI= samples from uninfected animals. (B) $LTB_4$ concentrations. (C) 20-hydroxy $LTB_4$ concentrations. (D) $LTB_4$ concentrations. (E) 20-hydroxy $LTB_4$ concentrations. (F) 5-HETE Concentrations. (G) $PGE_1$ concentrations. (H) $PGE_2$ concentrations. (I) $PGA_2$ concentrations. Each symbol represents an individual mouse and the box plot represents the median of the group ± the range. Changes in lipid concentrations were compared to the UI sample using (B-C) One-way ANOVA with Dunnett's *post hoc* test or (D-I) the LIMMA - Moderated t-test. ns = not significant, *=p≤0.05, **=p≤0.01, ***=p≤0.001, #=p≤0.0001.

| | | | | | | *Y. pestis* infection | | | | | | |
|---|---|---|---|---|---|---|---|---|---|---|---|---|
| | Uninfected (UI) | | | | | 6 hr | | | | | | |
| **Lipid** | **1** | **2** | **3** | **4** | **5** | **1** | **2** | **3** | **4** | **5** | **LogFC** | **p-value** |
| 10-HDoHE | 0.1791 | 0.0015 | 0.2581 | 0.2886 | 0.3397 | 0.3781 | 0.4022 | 0.6471 | 0.3494 | 0.5986 | 2.2669 | **0.0149** |
| 10(11)-EpDPE | 0.0326 | 0.0156 | 0.0317 | 0.0196 | 0.0443 | 0.0295 | 0.0357 | 0.0272 | 0.0286 | 0.0493 | 0.2269 | 0.8208 |
| 10S,17S-DiHDoHE | 0.0015 | 0.0015 | 0.0015 | 0.0015 | 0.0015 | 0.0015 | 0.0015 | 0.0015 | 0.0015 | 0.0015 | 0.0000 | 1.0000 |
| 11-HDoHE | 0.0015 | 0.0015 | 0.4672 | 0.0015 | 0.0015 | 0.0015 | 0.0015 | 0.0015 | 0.0015 | 0.0015 | -1.6280 | 0.6540 |
| 11-HEPE | 0.3896 | 0.2435 | 0.3743 | 0.3234 | 0.3701 | 0.7055 | 0.3681 | 0.7554 | 0.3916 | 0.7163 | 0.6029 | 0.6540 |
| 11-HETE | 79.7221 | 93.6908 | 66.3016 | 71.2922 | 70.8498 | 84.3431 | 53.6769 | 64.9328 | 50.3294 | 94.3760 | -0.0490 | 0.8445 |
| 11,12-DiHETrE | 0.3019 | 0.3424 | 0.2642 | 0.3698 | 0.1507 | 0.1170 | 0.0993 | 0.1533 | 0.1452 | 0.2108 | -0.8986 | **0.0245** |
| 11(12)-EpETrE | 0.0782 | 0.0015 | 0.1706 | 0.1312 | 0.1970 | 0.1217 | 0.1277 | 0.0870 | 0.0824 | 0.2782 | 1.1942 | 0.6240 |
| 11(R)-HEDE | 1.7474 | 1.6548 | 1.4651 | 1.4726 | 1.8574 | 3.1981 | 1.9851 | 3.2213 | 1.8652 | 2.9416 | 0.5844 | 0.2634 |
| 11dh-2,3-dinor TXB2 | 0.0108 | 0.0148 | 0.0071 | 0.0200 | 0.0080 | 0.0098 | 0.0119 | 0.0108 | 0.0182 | 0.0147 | 0.3595 | 0.8208 |
| 11dh-TXB2 | 0.0015 | 0.0015 | 0.0015 | 0.0015 | 0.0015 | 0.0015 | 0.0015 | 0.0015 | 0.0015 | 0.0015 | 0.0000 | 1.0000 |
| 12-HEPE | 2.9162 | 2.2473 | 2.4298 | 3.0685 | 6.7805 | 6.0638 | 10.3187 | 19.6205 | 7.3016 | 18.4246 | 1.7220 | **0.0006** |
| 12-HETE | 72.5816 | 78.9431 | 61.3581 | 78.7440 | 122.5452 | 97.6870 | 148.7784 | 289.9760 | 111.3355 | 203.9594 | 0.9200 | **0.0000** |
| 12,13-DiHOME | 2.1580 | 1.7970 | 1.4632 | 1.5488 | 0.6811 | 0.4536 | 0.3306 | 0.7981 | 0.9416 | 0.6386 | -1.2427 | **0.0038** |
| 12(13)-EpOME | 0.6150 | 0.4682 | 0.4531 | 0.4299 | 0.5792 | 0.4128 | 0.5144 | 1.1274 | 0.4831 | 0.7461 | 0.2904 | 0.5411 |
| 12(S)-HHTrE | 25.4892 | 26.8030 | 23.4114 | 17.5795 | 20.8156 | 10.0625 | 8.0426 | 12.3596 | 4.6230 | 11.3536 | -1.3695 | **0.0000** |
| 13-HDoHE | 1.1767 | 1.5264 | 1.2935 | 1.5491 | 1.4563 | 3.1412 | 1.8155 | 2.3320 | 2.1895 | 3.3984 | 0.8381 | **0.0192** |
| 13-HODE | 102.5982 | 95.7632 | 76.3926 | 74.8717 | 73.3199 | 136.1293 | 52.4990 | 138.3853 | 100.5133 | 106.7603 | 0.1975 | 0.4609 |
| 13-OxoODE | 4.1100 | 3.5354 | 3.4325 | 2.6608 | 4.4553 | 4.7412 | 2.3906 | 5.1264 | 2.7443 | 3.7786 | 0.0503 | 0.9291 |
| 13,14dh-15k-PGD2 | 1.6960 | 1.5422 | 1.2874 | 1.2029 | 1.1678 | 1.9161 | 1.1229 | 1.8841 | 1.5599 | 2.4745 | 0.3980 | 0.4488 |
| 13,14dh-15k-PGE1 | 0.0182 | 0.0099 | 0.0176 | 0.0015 | 0.0170 | 0.0192 | 0.0113 | 0.0154 | 0.0098 | 0.0107 | 0.6536 | 0.6540 |
| 13,14dh-15k-PGE2 | 0.4777 | 0.5916 | 0.5485 | 0.5033 | 0.4110 | 0.8218 | 0.6211 | 0.5531 | 0.6693 | 0.8952 | 0.4919 | 0.2828 |
| 13,14dh-15k-PGF2a | 0.0547 | 0.0785 | 0.0912 | 0.0525 | 0.0810 | 0.0516 | 0.0241 | 0.0456 | 0.0400 | 0.0495 | -0.7833 | 0.5124 |
| 13(14)-EpDPE | 0.0112 | 0.0098 | 0.0015 | 0.0096 | 0.0132 | 0.0015 | 0.0122 | 0.0015 | 0.0015 | 0.0288 | -0.8127 | 0.6540 |
| 13(S)-HOTrE | 1.8809 | 1.0374 | 1.2444 | 1.3337 | 1.1165 | 1.7870 | 0.4103 | 2.0556 | 2.0710 | 0.8830 | 0.0398 | 0.9799 |
| 14-HDoHE | 4.0850 | 3.8589 | 4.0309 | 5.0897 | 5.2854 | 6.9826 | 5.7477 | 7.3503 | 6.9959 | 10.1087 | 0.7709 | **0.0178** |
| 14,15-DiHETrE | 0.4157 | 0.5778 | 0.5527 | 0.4511 | 0.2352 | 0.4122 | 0.2830 | 0.3453 | 0.3440 | 0.5106 | -0.2018 | 0.6987 |
| 14(15)-EpETrE | 0.0015 | 0.0015 | 0.0015 | 0.0015 | 0.0015 | 0.0015 | 0.1958 | 0.0015 | 0.1029 | 0.0015 | 2.7111 | 0.2634 |
| 15-epi LXA4 | 0.0015 | 0.0050 | 0.0015 | 0.0015 | 0.0025 | 0.0015 | 0.0015 | 0.0015 | 0.0015 | 0.0015 | -0.4976 | 0.3642 |
| 15-HETE | 20.1300 | 23.4669 | 18.4581 | 17.9891 | 21.4737 | 20.5317 | 12.9361 | 14.0834 | 14.2272 | 19.3192 | -0.4318 | **0.0223** |
| 15-keto PGE1 | 0.0015 | 0.0015 | 0.0015 | 0.0015 | 0.0015 | 0.0015 | 0.0074 | 0.0015 | 0.0015 | 0.0015 | 0.1272 | 0.9291 |
| 15-keto PGE2 | 0.2065 | 0.4942 | 0.4060 | 0.4265 | 0.3602 | 0.2522 | 0.3139 | 0.1834 | 0.2245 | 0.5252 | -0.3032 | 0.6724 |
| 15-keto PGF2a | 0.5871 | 0.6055 | 0.5364 | 0.5491 | 0.4648 | 0.9721 | 0.7192 | 0.6634 | 0.8164 | 1.0654 | 0.5406 | 0.1885 |
| 15-OxoETE | 0.0015 | 0.4128 | 0.5018 | 0.0015 | 0.4084 | 0.0015 | 0.0015 | 0.0015 | 0.0015 | 0.0015 | -4.9123 | 0.1648 |
| 15(R)-PGE1 | 0.0959 | 0.1149 | 0.0778 | 0.0793 | 0.0015 | 0.0015 | 0.0015 | 0.0015 | 0.0015 | 0.1627 | -3.5400 | 0.0788 |
| 15(S)-HEDE | 0.1069 | 0.0890 | 0.1130 | 0.1090 | 0.1254 | 0.1961 | 0.0854 | 0.1880 | 0.1402 | 0.1549 | 0.4878 | 0.7354 |
| 15(S)-HEPE | 0.4564 | 0.0015 | 0.2618 | 0.2662 | 0.2317 | 0.3695 | 0.1150 | 0.4643 | 0.2896 | 0.2812 | 1.4949 | 0.4488 |
| 15d-D12,14-PGJ2 | 0.0519 | 0.0727 | 0.0757 | 0.0773 | 0.0691 | 0.0774 | 0.0437 | 0.0464 | 0.0537 | 0.0797 | -0.2129 | 0.7009 |
| 16-HDoHE | 0.4735 | 0.3834 | 0.4376 | 0.4385 | 0.5883 | 0.7286 | 0.5709 | 0.8418 | 0.5093 | 1.1021 | 0.6522 | **0.0192** |
| 16(17)-EpDPE | 0.0097 | 0.0126 | 0.0015 | 0.0080 | 0.0183 | 0.0125 | 0.0125 | 0.0015 | 0.0015 | 0.0015 | -1.0189 | 0.5124 |
| 17-HDoHE | 0.3356 | 0.1855 | 0.1926 | 0.2292 | 0.2906 | 0.5825 | 0.1667 | 0.3805 | 0.4905 | 0.3732 | 0.6164 | 0.6724 |
| 17(18)-EpETE | 0.0015 | 0.0015 | 0.0015 | 0.0052 | 0.0015 | 0.0015 | 0.0099 | 0.0015 | 0.0029 | 0.0015 | 0.2706 | 0.8208 |
| 18-carboxy dinor LTB4 | 0.0015 | 0.0015 | 0.0015 | 0.0015 | 0.0015 | 0.0015 | 0.0015 | 0.0015 | 0.0015 | 0.0015 | 0.0000 | 1.0000 |
| 18-HEPE | 0.0015 | 0.0015 | 0.0485 | 0.0015 | 0.0444 | 0.0015 | 0.0015 | 0.0856 | 0.0357 | 0.0404 | 1.0775 | 0.6540 |
| 19,20-DiHDoPE | 0.1499 | 0.2146 | 0.1943 | 0.2219 | 0.0830 | 0.1550 | 0.0646 | 0.1272 | 0.1855 | 0.1684 | -0.3157 | 0.7699 |
| 19(20)-EpDPE | 0.0298 | 0.0203 | 0.0284 | 0.0189 | 0.0378 | 0.0252 | 0.0321 | 0.0270 | 0.0273 | 0.0491 | 0.3531 | 0.6788 |
| 19(R)-OH PGF2a & 20-OH PGF2a | 0.0015 | 0.0015 | 0.0015 | 0.0015 | 0.0015 | 0.0079 | 0.0015 | 0.0015 | 0.0015 | 0.0015 | 0.5715 | 0.5516 |
| 20-HDoHE | 0.4596 | 0.5278 | 0.4812 | 0.5438 | 0.5025 | 0.5971 | 0.4777 | 0.7571 | 0.4932 | 0.8761 | 0.3685 | 0.7864 |
| 20-HETE | 0.0015 | 0.7678 | 0.8797 | 0.7748 | 1.0269 | 0.0015 | 0.4052 | 0.0015 | 0.0015 | 0.0015 | -5.5373 | 0.1627 |
| 20-hydroxy LTB4 | 0.0015 | 0.0015 | 0.0015 | 0.0015 | 0.0015 | 0.0015 | 0.0015 | 0.0015 | 0.0015 | 0.0015 | 0.0000 | 1.0000 |
| 4-HDoHE | 0.1009 | 0.1166 | 0.1178 | 0.1438 | 0.2012 | 0.1979 | 0.1387 | 0.2104 | 0.1521 | 0.2442 | 0.5018 | 0.6724 |
| 5-HEPE | 0.0015 | 0.0015 | 0.0015 | 0.0754 | 0.0854 | 0.0015 | 0.1485 | 0.3060 | 0.1379 | 0.2492 | 3.3159 | 0.0721 |
| 5-HETE | 1.1215 | 1.3183 | 1.0202 | 1.3526 | 1.6977 | 1.6854 | 3.1099 | 4.6121 | 2.9764 | 5.3962 | 1.3995 | **0.0013** |
| 5-oxoETE | 0.0881 | 0.0988 | 0.1752 | 0.1365 | 0.2091 | 0.1563 | 0.0796 | 0.1144 | 0.1006 | 0.1455 | -0.2301 | 0.8830 |
| 5,6-DiHETE(EPA) | 0.0015 | 0.0015 | 0.0015 | 0.0151 | 0.0015 | 0.0015 | 0.0015 | 0.0015 | 0.0015 | 0.0015 | -0.7101 | 0.3150 |
| 5,6-DiHETrE | 0.0116 | 0.0015 | 0.0015 | 0.0144 | 0.0052 | 0.0036 | 0.0015 | 0.0015 | 0.0015 | 0.0068 | -0.7368 | 0.5195 |
| 5(6)-EpETrE | 0.1433 | 0.1314 | 0.1363 | 0.1291 | 0.1562 | 0.0468 | 0.0760 | 0.0421 | 0.0564 | 0.0730 | -1.2186 | 0.0721 |
| 5(S)-HETrE | 0.0015 | 0.0089 | 0.0072 | 0.0015 | 0.0178 | 0.0160 | 0.0245 | 0.0343 | 0.0232 | 0.0423 | 2.7882 | **0.0001** |
| 5(S),12(S)-DiHETE | 0.1200 | 0.2146 | 0.1380 | 0.1362 | 0.1033 | 0.0265 | 0.0646 | 0.0934 | 0.0233 | 0.0701 | -1.4612 | 0.1256 |
| 5(S),15(S)-DiHEPE | 0.0015 | 0.0954 | 0.0015 | 0.0015 | 0.0350 | 0.0015 | 0.0015 | 0.0263 | 0.0015 | 0.0015 | -1.1976 | 0.5584 |
| 5(S),15(S)-DiHETE | 0.0015 | 0.0015 | 0.0015 | 0.0015 | 0.0015 | 0.0015 | 0.0013 | 0.0044 | 0.0015 | 0.0015 | 0.2890 | 0.7699 |
| 6-keto PGE1 | 0.0015 | 0.0172 | 0.0149 | 0.0154 | 0.0136 | 0.0145 | 0.0054 | 0.0015 | 0.0015 | 0.0143 | -0.7677 | 0.6540 |
| 6kPGF1a | 3.6156 | 6.1570 | 5.2604 | 5.9817 | 6.4715 | 0.0015 | 0.0015 | 0.0015 | 0.0015 | 0.0015 | -11.7313 | **0.0019** |
| 7-HDoHE | 0.0884 | 0.0780 | 0.0788 | 0.1264 | 0.1118 | 0.1175 | 0.2103 | 0.2701 | 0.1761 | 0.3609 | 1.1041 | **0.0024** |
| 7(8)-EpDPE | 0.0033 | 0.0054 | 0.0054 | 0.0074 | 0.0108 | 0.0035 | 0.0078 | 0.0015 | 0.0035 | 0.0083 | -0.3674 | 0.7485 |
| 8-HDoHE | 0.0938 | 0.1141 | 0.1405 | 0.0758 | 0.1676 | 0.1518 | 0.0866 | 0.1038 | 0.0832 | 0.2353 | 0.0976 | 0.9618 |
| 8-HEPE | 0.0015 | 0.0015 | 0.0015 | 0.0015 | 0.0498 | 0.0398 | 0.0432 | 0.1254 | 0.0333 | 0.0926 | 4.3256 | **0.0024** |
| 8-HETE | 1.0683 | 0.7753 | 0.9253 | 1.0993 | 0.9928 | 1.3829 | 0.7802 | 1.2278 | 0.8928 | 1.3179 | 0.3404 | 0.2634 |
| 8-isoPGF2a & 11bPGF2a | 0.0015 | 0.1033 | 0.0638 | 0.0015 | 0.0970 | 0.0803 | 0.0576 | 0.0511 | 0.0425 | 0.0608 | 1.7774 | 0.5411 |
| 8,9-DiHETrE | 0.0321 | 0.0314 | 0.0422 | 0.0336 | 0.0253 | 0.0227 | 0.0172 | 0.0177 | 0.0202 | 0.0353 | -0.4730 | 0.4488 |
| 8(9)-EpETrE | 0.0015 | 0.0015 | 0.0395 | 0.0015 | 0.0015 | 0.0157 | 0.0015 | 0.0015 | 0.0015 | 0.0015 | -0.0196 | 1.0000 |
| 8(S)-HETrE | 0.1078 | 0.1475 | 0.1140 | 0.1546 | 0.1888 | 0.1290 | 0.2890 | 0.3881 | 0.2082 | 0.4278 | 1.0208 | 0.3150 |
| 9-HEPE | 0.1265 | 0.0015 | 0.1298 | 0.1464 | 0.2553 | 0.1856 | 0.3996 | 1.0143 | 0.3042 | 0.7883 | 2.9059 | 0.1475 |
| 9-HETE | 0.0015 | 0.0015 | 0.0015 | 0.0015 | 0.0015 | 0.0015 | 0.0015 | 0.0015 | 0.0015 | 0.0015 | 0.0000 | 1.0000 |
| 9-HODE | 13.1826 | 17.9999 | 14.7776 | 15.0953 | 0.0015 | 0.0015 | 0.0015 | 0.0015 | 12.2472 | 0.0015 | -7.9394 | **0.0432** |
| 9-OxoODE | 4.1273 | 3.4742 | 3.2389 | 2.9265 | 3.3894 | 3.2473 | 1.7810 | 3.7651 | 2.0240 | 2.9063 | -0.4286 | 0.1881 |
| 9-OxoOTrE | 0.0664 | 0.0015 | 0.0438 | 0.0509 | 0.0824 | 0.0721 | 0.0321 | 0.1032 | 0.0556 | 0.0369 | 0.9673 | 0.6540 |
| 9,10-DiHOME | 2.3010 | 1.1255 | 1.1798 | 1.2964 | 0.5984 | 0.3202 | 0.2295 | 0.5036 | 0.5791 | 0.5728 | -1.5768 | **0.0003** |
| 9(10)-EpOME | 1.2526 | 0.9361 | 1.0894 | 0.7780 | 1.2517 | 1.0080 | 1.2110 | 1.7993 | 1.3750 | 1.8010 | 0.4448 | 0.7699 |
| 9(S)-HOTrE | 0.3026 | 0.1751 | 0.2697 | 0.2057 | 0.4403 | 0.3576 | 0.2475 | 0.9490 | 0.4147 | 0.4311 | 0.6652 | 0.6789 |
| Bicyclo PGE1 | 3.2853 | 5.6863 | 4.1312 | 3.1560 | 4.1412 | 2.7398 | 2.9279 | 4.4070 | 1.3258 | 4.2940 | -0.5821 | 0.4609 |
| Bicyclo PGE2 | 0.0401 | 0.0476 | 0.0262 | 0.0309 | 0.0386 | 0.0758 | 0.0555 | 0.0569 | 0.0739 | 0.0841 | 1.0858 | 0.2931 |
| LTB4 | 0.0283 | 0.0446 | 0.0495 | 0.0015 | 0.0388 | 0.0015 | 0.1456 | 0.1731 | 0.0965 | 0.2176 | 1.7016 | 0.2480 |
| LXA5 | 0.0015 | 0.0047 | 0.0015 | 0.0015 | 0.0013 | 0.0015 | 0.0015 | 0.0015 | 0.0015 | 0.0022 | -0.3054 | 0.7864 |
| PD1(n-3, DPA) | 3.8907 | 11.0489 | 4.1335 | 6.3073 | 1.6294 | 1.2818 | 0.7911 | 0.3559 | 0.8236 | 0.7211 | -2.5707 | **0.0149** |
| PGA2 | 0.3540 | 0.3827 | 0.3073 | 0.2715 | 0.3636 | 0.7593 | 0.5253 | 0.5468 | 0.7660 | 0.7691 | 0.9961 | **0.0209** |
| PGD2 | 0.0015 | 0.0015 | 0.0015 | 0.0015 | 0.0015 | 0.7737 | 0.0015 | 0.6089 | 0.7119 | 0.0015 | 5.2632 | 0.0788 |
| PGD3 | 0.0258 | 0.0956 | 0.1062 | 0.0015 | 0.0820 | 0.0015 | 0.0015 | 0.0015 | 0.0015 | 0.0015 | -4.2958 | **0.0245** |
| PGE1 | 0.1287 | 0.2363 | 0.1247 | 0.1645 | 0.1673 | 0.6203 | 0.3147 | 0.3661 | 0.4621 | 0.5886 | 1.4997 | **0.0003** |
| PGE2 | 10.9409 | 12.1142 | 10.5898 | 10.3617 | 10.0851 | 20.0090 | 13.8080 | 14.4604 | 17.0902 | 20.4174 | 0.6890 | **0.0432** |
| PGE3 | 0.0314 | 0.0405 | 0.0273 | 0.0380 | 0.0373 | 0.0893 | 0.0716 | 0.0709 | 0.0872 | 0.1159 | 1.6078 | 0.1093 |
| PGF1a | 0.0360 | 0.0483 | 0.0286 | 0.0170 | 0.0389 | 0.0670 | 0.0575 | 0.0609 | 0.0266 | 0.0797 | 0.7022 | 0.5551 |
| PGF2a | 1.3802 | 1.3584 | 1.2208 | 0.6895 | 1.2415 | 1.1884 | 0.8811 | 1.0897 | 0.8387 | 1.1770 | -0.1534 | 0.8091 |
| PGJ2 | 0.1498 | 0.1779 | 0.1303 | 0.1310 | 0.1644 | 0.3818 | 0.2650 | 0.2719 | 0.3872 | 0.4006 | 1.1964 | **0.0245** |
| RvD1 & AT-RvD1 | 0.1682 | 0.0015 | 0.0015 | 0.0015 | 0.1145 | 0.0015 | 0.0015 | 0.0379 | 0.0015 | 0.0015 | -1.8212 | 0.6375 |
| RvD5(n-3DPA) (7,17-DiHDoPE) | 0.0356 | 0.0633 | 0.0591 | 0.0926 | 0.0284 | 0.0230 | 0.0254 | 0.0446 | 0.0272 | 0.0271 | -0.7297 | 0.6540 |
| RvD6 (4,17-DiHDoHE) | 0.0015 | 0.0015 | 0.0015 | 0.0015 | 0.0015 | 0.0015 | 0.0056 | 0.0061 | 0.0065 | 0.0076 | 1.3271 | 0.0875 |
| RvE3 | 0.6231 | 1.9823 | 1.2107 | 1.5691 | 0.3361 | 0.1809 | 0.2053 | 0.1072 | 0.2183 | 0.3128 | -2.3389 | **0.0088** |
| tetranor 12-HETE | 0.0550 | 0.0659 | 0.0563 | 0.0908 | 0.0015 | 0.0458 | 0.0642 | 0.0977 | 0.0794 | 0.1194 | 1.2683 | 0.4752 |
| tetranor PGEM | 0.0022 | 0.0015 | 0.0018 | 0.0015 | 0.0011 | 0.0020 | 0.0015 | 0.0016 | 0.0015 | 0.0026 | -0.0164 | 1.0000 |
| TXB2 | 0.0015 | 3.6118 | 2.9670 | 2.9934 | 2.9566 | 2.1481 | 1.7680 | 2.7872 | 0.0015 | 2.3648 | -0.4723 | 0.9096 |
| TXB3 | 0.0015 | 0.0015 | 0.0015 | 0.0015 | 0.0015 | 0.0162 | 0.0121 | 0.0249 | 0.0134 | 0.0015 | 2.7660 | **0.0100** |

| | Uninfected (UI) | | | | | *Y. pestis* infection 12 hr | | | | | | |
|---|---|---|---|---|---|---|---|---|---|---|---|---|
| **Lipid** | **1** | **2** | **3** | **4** | **5** | **1** | **2** | **3** | **4** | **5** | **LogFC** | **p-value** |
| 10-HDoHE | 0.1791 | 0.0015 | 0.2581 | 0.2886 | 0.3397 | 0.2856 | 0.2420 | 0.3386 | 0.4070 | 0.3723 | 1.8241 | **0.0407** |
| 10(11)-EpDPE | 0.0326 | 0.0156 | 0.0317 | 0.0196 | 0.0443 | 0.0174 | 0.0296 | 0.0269 | 0.0299 | 0.0114 | -0.5657 | 0.5281 |
| 10S,17S-DiHDoHE | 0.0015 | 0.0015 | 0.0015 | 0.0015 | 0.0015 | 0.0015 | 0.0015 | 0.0015 | 0.0015 | 0.0015 | 0.0000 | 1.0000 |
| 11-HDoHE | 0.0015 | 0.0015 | 0.4672 | 0.0015 | 0.0015 | 0.8195 | 0.5656 | 0.0015 | 0.0015 | 0.0015 | 1.8574 | 0.5281 |
| 11-HEPE | 0.3896 | 0.2435 | 0.3743 | 0.3234 | 0.3701 | 0.8876 | 0.6439 | 0.5296 | 0.6317 | 0.4455 | 0.9404 | 0.3914 |
| 11-HETE | 79.7221 | 93.6908 | 66.3016 | 71.2922 | 70.8498 | 100.2319 | 70.9247 | 74.4882 | 89.9584 | 76.8310 | 0.1349 | 0.5281 |
| 11,12-DiHETrE | 0.3019 | 0.3424 | 0.2642 | 0.3698 | 0.1507 | 0.1296 | 0.1171 | 0.1131 | 0.1169 | 0.0955 | -1.1543 | **0.0037** |
| 11(12)-EpETrE | 0.0782 | 0.0015 | 0.1706 | 0.1312 | 0.1970 | 0.1199 | 0.1003 | 0.1303 | 0.0956 | 0.0015 | -0.1816 | 0.9282 |
| 11(R)-HEDE | 1.7474 | 1.6548 | 1.4651 | 1.4726 | 1.8574 | 3.5258 | 3.0259 | 2.6492 | 2.6707 | 2.1981 | 0.6896 | 0.1359 |
| 11dh-2,3-dinor TXB2 | 0.0108 | 0.0148 | 0.0071 | 0.0200 | 0.0080 | 0.0382 | 0.0243 | 0.0183 | 0.0280 | 0.0320 | 1.4767 | 0.2235 |
| 11dh-TXB2 | 0.0015 | 0.0015 | 0.0015 | 0.0015 | 0.0015 | 0.0015 | 0.0015 | 0.0052 | 0.0015 | 0.0015 | 0.6379 | 0.4961 |
| 12-HEPE | 2.9162 | 2.2473 | 2.4298 | 3.0685 | 6.7805 | 6.8698 | 6.2748 | 6.8620 | 8.6344 | 8.9916 | 1.1190 | **0.0205** |
| 12-HETE | 72.5816 | 78.9431 | 61.3581 | 78.7440 | 122.5452 | 123.8943 | 107.1726 | 123.5936 | 134.6523 | 165.9993 | 0.6833 | **0.0003** |
| 12,13-DiHOME | 2.1580 | 1.7970 | 1.4632 | 1.5488 | 0.6811 | 0.7688 | 0.7557 | 0.5810 | 0.6019 | 0.3301 | -1.3223 | **0.0018** |
| 12(13)-EpOME | 0.6150 | 0.4682 | 0.4531 | 0.4299 | 0.5792 | 0.5479 | 0.5876 | 0.4792 | 0.6298 | 0.3370 | -0.0654 | 0.8837 |
| 12(S)-HHTrE | 25.4892 | 26.8030 | 23.4114 | 17.5795 | 20.8156 | 14.5344 | 11.2410 | 8.9680 | 14.1555 | 12.0447 | -0.8494 | **0.0013** |
| 13-HDoHE | 1.1767 | 1.5264 | 1.2935 | 1.5491 | 1.4563 | 3.1923 | 2.4876 | 2.5095 | 2.5712 | 2.4144 | 0.8224 | **0.0189** |
| 13-HODE | 102.5982 | 95.7632 | 76.3926 | 74.8717 | 73.3199 | 137.8055 | 103.3344 | 103.9469 | 104.8757 | 105.4479 | 0.3765 | 0.0759 |
| 13-OxoODE | 4.1100 | 3.5354 | 3.4325 | 2.6608 | 4.4553 | 4.5176 | 3.1514 | 2.9965 | 3.6716 | 3.6021 | -0.0071 | 1.0000 |
| 13,14dh-15k-PGD2 | 1.6960 | 1.5422 | 1.2874 | 1.2029 | 1.1678 | 2.7122 | 2.3656 | 1.6323 | 2.7718 | 1.5151 | 0.6330 | 0.1333 |
| 13,14dh-15k-PGE1 | 0.0182 | 0.0099 | 0.0176 | 0.0015 | 0.0170 | 0.0282 | 0.0158 | 0.0162 | 0.0303 | 0.0246 | 1.4931 | 0.1922 |
| 13,14dh-15k-PGE2 | 0.4777 | 0.5916 | 0.5485 | 0.5033 | 0.4110 | 1.3257 | 0.9952 | 0.7998 | 1.0487 | 0.9497 | 0.9684 | **0.0151** |
| 13,14dh-15k-PGF2a | 0.0547 | 0.0785 | 0.0912 | 0.0525 | 0.0810 | 0.0409 | 0.0316 | 0.0287 | 0.0397 | 0.0833 | -0.5633 | 0.5889 |
| 13(14)-EpDPE | 0.0112 | 0.0098 | 0.0015 | 0.0096 | 0.0132 | 0.0015 | 0.0015 | 0.0015 | 0.0015 | 0.0015 | -2.2654 | 0.0922 |
| 13(S)-HOTrE | 1.8809 | 1.0374 | 1.2444 | 1.3337 | 1.1165 | 1.3194 | 0.9578 | 0.9853 | 1.2299 | 2.0578 | -0.1133 | 0.8656 |
| 14-HDoHE | 4.0850 | 3.8589 | 4.0309 | 5.0897 | 5.2854 | 6.2344 | 4.6459 | 6.2348 | 5.6768 | 8.0515 | 0.3836 | 0.2380 |
| 14,15-DiHETrE | 0.4157 | 0.5778 | 0.5527 | 0.4511 | 0.2352 | 0.3574 | 0.3035 | 0.3245 | 0.2927 | 0.2939 | -0.4197 | 0.3255 |
| 14(15)-EpETrE | 0.0015 | 0.0015 | 0.0015 | 0.0015 | 0.0015 | 0.1006 | 0.0015 | 0.2017 | 0.0015 | 0.3637 | 4.3093 | **0.0407** |
| 15-epi LXA4 | 0.0015 | 0.0050 | 0.0015 | 0.0015 | 0.0025 | 0.0015 | 0.0015 | 0.0015 | 0.0009 | 0.0015 | -0.5359 | 0.2548 |
| 15-HETE | 20.1300 | 23.4669 | 18.4581 | 17.9891 | 21.4737 | 25.7467 | 21.0120 | 19.1299 | 22.7413 | 18.3913 | 0.0485 | 0.8541 |
| 15-keto PGE1 | 0.0015 | 0.0015 | 0.0015 | 0.0015 | 0.0015 | 0.0015 | 0.0015 | 0.0051 | 0.0042 | 0.0117 | 1.2276 | 0.1559 |
| 15-keto PGE2 | 0.2065 | 0.4942 | 0.4060 | 0.4265 | 0.3602 | 0.5676 | 0.4101 | 0.2832 | 0.3449 | 0.5794 | 0.2159 | 0.7467 |
| 15-keto PGF2a | 0.5871 | 0.6055 | 0.5364 | 0.5491 | 0.4648 | 1.6871 | 1.1605 | 1.0210 | 1.2873 | 1.0324 | 1.1666 | **0.0019** |
| 15-OxoETE | 0.0015 | 0.4128 | 0.5018 | 0.0015 | 0.4084 | 0.9815 | 0.7231 | 0.0015 | 1.3662 | 1.2545 | 2.5963 | 0.4952 |
| 15(R)-PGE1 | 0.0959 | 0.1149 | 0.0778 | 0.0793 | 0.0015 | 0.0015 | 0.0015 | 0.0015 | 0.0015 | 0.0015 | -4.7888 | **0.0138** |
| 15(S)-HEDE | 0.1069 | 0.0890 | 0.1130 | 0.1090 | 0.1254 | 0.2312 | 0.1716 | 0.1667 | 0.1729 | 0.1915 | 0.8480 | 0.4961 |
| 15(S)-HEPE | 0.4564 | 0.0015 | 0.2618 | 0.2662 | 0.2317 | 1.2100 | 1.2070 | 0.7624 | 0.9064 | 0.9455 | 3.3547 | **0.0267** |
| 15d-D12,14-PGJ2 | 0.0519 | 0.0727 | 0.0757 | 0.0773 | 0.0691 | 0.0754 | 0.0532 | 0.0764 | 0.0592 | 0.0888 | 0.1451 | 0.8010 |
| 16-HDoHE | 0.4735 | 0.3834 | 0.4376 | 0.4385 | 0.5883 | 0.6831 | 0.5858 | 0.5186 | 0.5993 | 0.4788 | 0.2790 | 0.3300 |
| 16(17)-EpDPE | 0.0097 | 0.0126 | 0.0015 | 0.0080 | 0.0183 | 0.0015 | 0.0090 | 0.0015 | 0.0097 | 0.0015 | -1.5632 | 0.1996 |
| 17-HDoHE | 0.3356 | 0.1855 | 0.1926 | 0.2292 | 0.2906 | 0.4501 | 0.2949 | 0.4180 | 0.5868 | 0.7996 | 0.9816 | 0.4264 |
| 17(18)-EpETE | 0.0015 | 0.0015 | 0.0015 | 0.0052 | 0.0015 | 0.0015 | 0.0015 | 0.0015 | 0.0015 | 0.0015 | -0.4099 | 0.7251 |
| 18-carboxy dinor LTB4 | 0.0015 | 0.0015 | 0.0015 | 0.0015 | 0.0015 | 0.0015 | 0.0061 | 0.0015 | 0.0015 | 0.0015 | 0.5093 | 0.7645 |
| 18-HEPE | 0.0015 | 0.0015 | 0.0485 | 0.0015 | 0.0444 | 0.0542 | 0.0015 | 0.0015 | 0.0327 | 0.0327 | 0.8860 | 0.6750 |
| 19,20-DiHDoPE | 0.1499 | 0.2146 | 0.1943 | 0.2219 | 0.0830 | 0.1209 | 0.0904 | 0.0953 | 0.0891 | 0.0695 | -0.8855 | 0.2857 |
| 19(20)-EpDPE | 0.0298 | 0.0203 | 0.0284 | 0.0189 | 0.0378 | 0.0190 | 0.0240 | 0.0285 | 0.0265 | 0.0183 | -0.2908 | 0.7287 |
| 19(R)-OH PGF2a & 20-OH PGF2a | 0.0015 | 0.0015 | 0.0015 | 0.0015 | 0.0015 | 0.0015 | 0.0015 | 0.0015 | 0.0074 | 0.0015 | 0.0920 | 0.9182 |
| 20-HDoHE | 0.4596 | 0.5278 | 0.4812 | 0.5438 | 0.5025 | 0.7287 | 0.5038 | 0.5274 | 0.5402 | 0.4561 | 0.1285 | 0.9182 |
| 20-HETE | 0.0015 | 0.7678 | 0.8797 | 0.7748 | 1.0269 | 0.0015 | 0.5258 | 0.0015 | 0.0015 | 0.0015 | -5.5844 | 0.1333 |
| 20-hydroxy LTB4 | 0.0015 | 0.0015 | 0.0015 | 0.0015 | 0.0015 | 0.0015 | 0.0015 | 0.0015 | 0.0015 | 0.0015 | 0.0000 | 1.0000 |
| 4-HDoHE | 0.1009 | 0.1166 | 0.1178 | 0.1438 | 0.2012 | 0.1114 | 0.1772 | 0.1450 | 0.1879 | 0.1310 | 0.1953 | 0.8664 |
| 5-HEPE | 0.0015 | 0.0015 | 0.0015 | 0.0754 | 0.0854 | 0.0824 | 0.1383 | 0.1142 | 0.1530 | 0.1150 | 4.0315 | **0.0206** |
| 5-HETE | 1.1215 | 1.3183 | 1.0202 | 1.3526 | 1.6977 | 3.0408 | 3.3308 | 3.4971 | 3.2391 | 1.9678 | 1.1997 | **0.0040** |
| 5-oxoETE | 0.0881 | 0.0988 | 0.1752 | 0.1365 | 0.2091 | 0.0015 | 0.1193 | 0.0989 | 0.0959 | 0.0644 | -1.8077 | 0.0922 |
| 5,6-DiHETE(EPA) | 0.0015 | 0.0015 | 0.0015 | 0.0151 | 0.0015 | 0.0015 | 0.0015 | 0.0015 | 0.0015 | 0.0015 | -0.7101 | 0.2567 |
| 5,6-DiHETrE | 0.0116 | 0.0015 | 0.0015 | 0.0144 | 0.0052 | 0.0015 | 0.0036 | 0.0015 | 0.0042 | 0.0015 | -1.2069 | 0.1862 |
| 5(6)-EpETrE | 0.1433 | 0.1314 | 0.1363 | 0.1291 | 0.1562 | 0.0366 | 0.0586 | 0.0458 | 0.0350 | 0.0202 | -1.9054 | **0.0035** |
| 5(S)-HETrE | 0.0015 | 0.0089 | 0.0072 | 0.0015 | 0.0178 | 0.0290 | 0.0198 | 0.0239 | 0.0215 | 0.0155 | 2.3073 | **0.0007** |
| 5(S),12(S)-DiHETE | 0.1200 | 0.2146 | 0.1380 | 0.1362 | 0.1033 | 0.0254 | 0.0216 | 0.0463 | 0.0755 | 0.1015 | -1.6142 | 0.0730 |
| 5(S),15(S)-DiHEPE | 0.0015 | 0.0954 | 0.0015 | 0.0015 | 0.0350 | 0.0710 | 0.0015 | 0.0623 | 0.1426 | 0.0719 | 2.6192 | 0.0981 |
| 5(S),15(S)-DiHETE | 0.0015 | 0.0015 | 0.0015 | 0.0015 | 0.0015 | 0.0015 | 0.0016 | 0.0015 | 0.0015 | 0.0015 | 0.1024 | 0.9182 |
| 6-keto PGE1 | 0.0015 | 0.0172 | 0.0149 | 0.0154 | 0.0136 | 0.0015 | 0.0066 | 0.0077 | 0.0055 | 0.0015 | -0.8276 | 0.5791 |
| 6kPGF1a | 3.6156 | 6.1570 | 5.2604 | 5.9817 | 6.4715 | 0.0015 | 0.0015 | 0.0015 | 6.2952 | 2.9810 | -7.1122 | **0.0482** |
| 7-HDoHE | 0.0884 | 0.0780 | 0.0788 | 0.1264 | 0.1118 | 0.1120 | 0.1598 | 0.1467 | 0.1412 | 0.0787 | 0.4265 | 0.2456 |
| 7(8)-EpDPE | 0.0033 | 0.0054 | 0.0054 | 0.0074 | 0.0108 | 0.0055 | 0.0040 | 0.0051 | 0.0084 | 0.0015 | -0.5705 | 0.5618 |
| 8-HDoHE | 0.0938 | 0.1141 | 0.1405 | 0.0758 | 0.1676 | 0.0799 | 0.1173 | 0.1312 | 0.0938 | 0.0904 | -0.1885 | 0.8664 |
| 8-HEPE | 0.0015 | 0.0015 | 0.0015 | 0.0015 | 0.0498 | 0.0454 | 0.0507 | 0.0558 | 0.0241 | 0.0015 | 2.7469 | **0.0470** |
| 8-HETE | 1.0683 | 0.7753 | 0.9253 | 1.0993 | 0.9928 | 0.9516 | 0.8276 | 1.1066 | 1.0895 | 0.9997 | 0.1623 | 0.5916 |
| 8-isoPGF2a & 11bPGF2a | 0.0015 | 0.1033 | 0.0638 | 0.0015 | 0.0970 | 0.0840 | 0.0015 | 0.0723 | 0.1330 | 0.0757 | 1.1879 | 0.6565 |
| 8,9-DiHETrE | 0.0321 | 0.0314 | 0.0422 | 0.0336 | 0.0253 | 0.0240 | 0.0150 | 0.0161 | 0.0182 | 0.0161 | -1.0437 | **0.0278** |
| 8(9)-EpETrE | 0.0015 | 0.0015 | 0.0395 | 0.0015 | 0.0015 | 0.0015 | 0.0015 | 0.0015 | 0.0015 | 0.0015 | -0.7912 | 0.5674 |
| 8(S)-HETrE | 0.1078 | 0.1475 | 0.1140 | 0.1546 | 0.1888 | 0.1797 | 0.2216 | 0.2415 | 0.2014 | 0.2341 | 0.6470 | 0.5281 |
| 9-HEPE | 0.1265 | 0.0015 | 0.1298 | 0.1464 | 0.2553 | 0.3526 | 0.2611 | 0.2400 | 0.4024 | 0.3551 | 2.3238 | 0.2235 |
| 9-HETE | 0.0015 | 0.0015 | 0.0015 | 0.0015 | 0.0015 | 0.0015 | 0.0015 | 0.0015 | 0.0015 | 0.0015 | 0.0000 | 1.0000 |
| 9-HODE | 13.1826 | 17.9999 | 14.7776 | 15.0953 | 0.0015 | 0.0015 | 0.0015 | 0.0015 | 0.0015 | 0.0015 | -10.5488 | **0.0055** |
| 9-OxoODE | 4.1273 | 3.4742 | 3.2389 | 2.9265 | 3.3894 | 2.7368 | 2.5733 | 2.2684 | 2.9556 | 2.6956 | -0.3984 | 0.1922 |
| 9-OxoOTrE | 0.0664 | 0.0015 | 0.0438 | 0.0509 | 0.0824 | 0.0388 | 0.0508 | 0.0015 | 0.0500 | 0.0414 | -0.3315 | 0.8664 |
| 9,10-DiHOME | 2.3010 | 1.1255 | 1.1798 | 1.2964 | 0.5984 | 0.4318 | 0.4297 | 0.2748 | 0.3642 | 0.2312 | -1.9341 | **0.0000** |
| 9(10)-EpOME | 1.2526 | 0.9361 | 1.0894 | 0.7780 | 1.2517 | 1.2015 | 1.3144 | 0.0015 | 1.5504 | 0.9977 | -1.7309 | 0.1359 |
| 9(S)-HOTrE | 0.3026 | 0.1751 | 0.2697 | 0.2057 | 0.4403 | 0.4785 | 0.3317 | 0.3268 | 0.3257 | 0.4042 | 0.5122 | 0.7467 |
| Bicyclo PGE1 | 3.2853 | 5.6863 | 4.1312 | 3.1560 | 4.1412 | 0.5813 | 0.7103 | 0.4652 | 1.6072 | 2.8614 | -2.0080 | **0.0013** |
| Bicyclo PGE2 | 0.0401 | 0.0476 | 0.0262 | 0.0309 | 0.0386 | 0.1845 | 0.1155 | 0.0830 | 0.1484 | 0.1089 | 1.9427 | **0.0278** |
| LTB4 | 0.0283 | 0.0446 | 0.0495 | 0.0015 | 0.0388 | 0.0663 | 0.0831 | 0.1263 | 0.1568 | 0.0345 | 2.1338 | 0.0981 |
| LXA5 | 0.0015 | 0.0047 | 0.0015 | 0.0015 | 0.0013 | 0.0015 | 0.0015 | 0.0013 | 0.0015 | 0.0015 | -0.4411 | 0.6669 |
| PD1(n-3, DPA) | 3.8907 | 11.0489 | 4.1335 | 6.3073 | 1.6294 | 0.7133 | 0.6374 | 0.6761 | 0.9065 | 1.6687 | -2.3651 | **0.0205** |
| PGA2 | 0.3540 | 0.3827 | 0.3073 | 0.2715 | 0.3636 | 1.5743 | 1.0815 | 0.7436 | 1.1636 | 0.9987 | 1.6749 | **0.0002** |
| PGD2 | 0.0015 | 0.0015 | 0.0015 | 0.0015 | 0.0015 | 1.8134 | 0.0015 | 1.1918 | 1.2492 | 0.7350 | 7.6612 | **0.0071** |
| PGD3 | 0.0258 | 0.0956 | 0.1062 | 0.0015 | 0.0820 | 0.1143 | 0.0015 | 0.0015 | 0.1152 | 0.1346 | -0.5081 | 0.8541 |
| PGE1 | 0.1287 | 0.2363 | 0.1247 | 0.1645 | 0.1673 | 0.7915 | 0.7583 | 0.5901 | 1.2659 | 0.4300 | 2.2740 | **0.0000** |
| PGE2 | 10.9409 | 12.1142 | 10.5898 | 10.3617 | 10.0851 | 32.9111 | 20.8675 | 20.9553 | 27.2644 | 21.2875 | 1.1467 | **0.0008** |
| PGE3 | 0.0314 | 0.0405 | 0.0273 | 0.0380 | 0.0373 | 0.1716 | 0.1432 | 0.0862 | 0.1221 | 0.1177 | 2.0864 | **0.0267** |
| PGF1a | 0.0360 | 0.0483 | 0.0286 | 0.0170 | 0.0389 | 0.0928 | 0.0754 | 0.0867 | 0.0992 | 0.0560 | 1.2195 | 0.1922 |
| PGF2a | 1.3802 | 1.3584 | 1.2208 | 0.6895 | 1.2415 | 1.9375 | 1.4436 | 1.2307 | 1.7319 | 1.3715 | 0.4720 | 0.3397 |
| PGJ2 | 0.1498 | 0.1779 | 0.1303 | 0.1310 | 0.1644 | 0.8339 | 0.5541 | 0.4143 | 0.5457 | 0.5029 | 1.9667 | **0.0003** |
| RvD1 & AT-RvD1 | 0.1682 | 0.0015 | 0.0015 | 0.0015 | 0.1145 | 0.0015 | 0.0015 | 0.0650 | 0.0591 | 0.0793 | 0.5989 | 0.8664 |
| RvD5(n-3DPA) (7,17-DiHDoPE) | 0.0356 | 0.0633 | 0.0591 | 0.0926 | 0.0284 | 0.0976 | 0.0292 | 0.0919 | 0.0586 | 0.0695 | 0.3838 | 0.8118 |
| RvD6 (4,17-DiHDoHE) | 0.0015 | 0.0015 | 0.0015 | 0.0015 | 0.0015 | 0.0107 | 0.0065 | 0.0038 | 0.0083 | 0.0081 | 2.1056 | **0.0044** |
| RvE3 | 0.6231 | 1.9823 | 1.2107 | 1.5691 | 0.3361 | 0.0916 | 0.0862 | 0.0892 | 0.0845 | 0.0999 | -3.4687 | **0.0002** |
| tetranor 12-HETE | 0.0550 | 0.0659 | 0.0563 | 0.0908 | 0.0015 | 0.1193 | 0.0997 | 0.0975 | 0.1058 | 0.1285 | 1.8201 | 0.2001 |
| tetranor PGEM | 0.0022 | 0.0015 | 0.0018 | 0.0015 | 0.0011 | 0.0063 | 0.0017 | 0.0035 | 0.0020 | 0.0015 | 0.3921 | 0.7467 |
| TXB2 | 0.0015 | 3.6118 | 2.9670 | 2.9934 | 2.9566 | 3.2110 | 2.5067 | 1.9897 | 2.4730 | 2.1603 | 1.7995 | 0.5332 |
| TXB3 | 0.0015 | 0.0015 | 0.0015 | 0.0015 | 0.0015 | 0.0015 | 0.0165 | 0.0015 | 0.0143 | 0.0015 | 1.1963 | 0.2597 |

| | | | | | | *Y. pestis* infection | | | | | | |
|---|---|---|---|---|---|---|---|---|---|---|---|---|
| | Uninfected (UI) | | | | | 24 hr | | | | | | |
| **Lipid** | **1** | **2** | **3** | **4** | **5** | **1** | **2** | **3** | **4** | **5** | **LogFC** | **p-value** |
| 10-HDoHE | 0.1791 | 0.0015 | 0.2581 | 0.2886 | 0.3397 | 3.2512 | 7.7324 | 0.9583 | 0.8571 | 0.4860 | 3.8839 | **0.0000** |
| 10(11)-EpDPE | 0.0326 | 0.0156 | 0.0317 | 0.0196 | 0.0443 | 0.2262 | 1.1098 | 0.0459 | 0.0710 | 0.0317 | 0.7733 | 0.3504 |
| 10S,17S-DiHDoHE | 0.0015 | 0.0015 | 0.0015 | 0.0015 | 0.0015 | 0.0015 | 0.0015 | 0.1971 | 0.2193 | 0.0015 | 3.1431 | 0.1290 |
| 11-HDoHE | 0.0015 | 0.0015 | 0.4672 | 0.0015 | 0.0015 | 0.0015 | 4.3588 | 0.0015 | 0.0015 | 0.0015 | 0.5752 | 0.9054 |
| 11-HEPE | 0.3896 | 0.2435 | 0.3743 | 0.3234 | 0.3701 | 0.0015 | 1.5071 | 1.3559 | 0.9009 | 0.5520 | 0.0370 | 0.9827 |
| 11-HETE | 79.7221 | 93.6908 | 66.3016 | 71.2922 | 70.8498 | 89.1092 | 139.9957 | 94.0023 | 88.0173 | 46.4367 | 0.0110 | 0.9827 |
| 11,12-DiHETrE | 0.3019 | 0.3424 | 0.2642 | 0.3698 | 0.1507 | 0.2062 | 0.4379 | 0.1425 | 0.2196 | 0.1135 | -0.6263 | 0.1048 |
| 11(12)-EpETrE | 0.0782 | 0.0015 | 0.1706 | 0.1312 | 0.1970 | 0.0015 | 2.2658 | 0.1410 | 0.2209 | 0.0821 | 1.0254 | 0.5731 |
| 11(R)-HEDE | 1.7474 | 1.6548 | 1.4651 | 1.4726 | 1.8574 | 1.3956 | 3.6186 | 4.6287 | 3.8461 | 2.7729 | 0.9715 | **0.0250** |
| 11dh-2,3-dinor TXB2 | 0.0108 | 0.0148 | 0.0071 | 0.0200 | 0.0080 | 0.3671 | 0.1702 | 0.0382 | 0.0250 | 0.0384 | 1.6924 | 0.1366 |
| 11dh-TXB2 | 0.0015 | 0.0015 | 0.0015 | 0.0015 | 0.0015 | 0.0015 | 0.0015 | 0.0078 | 0.0084 | 0.0015 | 0.6364 | 0.4500 |
| 12-HEPE | 2.9162 | 2.2473 | 2.4298 | 3.0685 | 6.7805 | 16.0197 | 22.4273 | 22.9464 | 25.4610 | 11.0931 | 2.2301 | **0.0000** |
| 12-HETE | 72.5816 | 78.9431 | 61.3581 | 78.7440 | 122.5452 | 228.1547 | 324.5402 | 186.9982 | 211.6215 | 95.5733 | 1.2980 | **0.0000** |
| 12,13-DiHOME | 2.1580 | 1.7970 | 1.4632 | 1.5488 | 0.6811 | 1.2079 | 1.4150 | 0.6761 | 0.6441 | 0.4181 | -0.8852 | **0.0263** |
| 12(13)-EpOME | 0.6150 | 0.4682 | 0.4531 | 0.4299 | 0.5792 | 5.3778 | 7.7017 | 0.6275 | 0.8881 | 0.5060 | 1.5057 | **0.0000** |
| 12(S)-HHTrE | 25.4892 | 26.8030 | 23.4114 | 17.5795 | 20.8156 | 17.8385 | 19.0009 | 13.4913 | 10.7791 | 4.9176 | -1.0695 | **0.0000** |
| 13-HDoHE | 1.1767 | 1.5264 | 1.2935 | 1.5491 | 1.4563 | 2.3465 | 8.4028 | 5.9416 | 4.8808 | 2.5390 | 1.5909 | **0.0000** |
| 13-HODE | 102.5982 | 95.7632 | 76.3926 | 74.8717 | 73.3199 | 197.9743 | 292.1332 | 141.5172 | 110.3109 | 56.7586 | 0.6777 | **0.0006** |
| 13-OxoODE | 4.1100 | 3.5354 | 3.4325 | 2.6608 | 4.4553 | 24.4580 | 27.1372 | 4.3849 | 4.1791 | 2.3991 | 1.4481 | **0.0000** |
| 13,14dh-15k-PGD2 | 1.6960 | 1.5422 | 1.2874 | 1.2029 | 1.1678 | 1.6514 | 1.2689 | 2.3567 | 2.0853 | 1.4668 | 0.6172 | 0.1232 |
| 13,14dh-15k-PGE1 | 0.0182 | 0.0099 | 0.0176 | 0.0015 | 0.0170 | 0.0015 | 0.0015 | 0.0168 | 0.0201 | 0.0109 | -0.9885 | 0.3955 |
| 13,14dh-15k-PGE2 | 0.4777 | 0.5916 | 0.5485 | 0.5033 | 0.4110 | 1.0631 | 0.8052 | 1.1100 | 1.0109 | 0.7818 | 0.9214 | **0.0148** |
| 13,14dh-15k-PGF2a | 0.0547 | 0.0785 | 0.0912 | 0.0525 | 0.0810 | 0.0015 | 0.0015 | 0.0223 | 0.0349 | 0.0317 | -3.5261 | **0.0001** |
| 13(14)-EpDPE | 0.0112 | 0.0098 | 0.0015 | 0.0096 | 0.0132 | 0.1921 | 0.6005 | 0.0181 | 0.0285 | 0.0104 | 1.8389 | 0.1509 |
| 13(S)-HOTrE | 1.8809 | 1.0374 | 1.2444 | 1.3337 | 1.1165 | 5.2469 | 5.3282 | 2.8776 | 1.4350 | 0.8051 | 0.9322 | **0.0338** |
| 14-HDoHE | 4.0850 | 3.8589 | 4.0309 | 5.0897 | 5.2854 | 11.2845 | 18.3026 | 18.3964 | 15.4581 | 7.5814 | 1.3183 | **0.0000** |
| 14,15-DiHETrE | 0.4157 | 0.5778 | 0.5527 | 0.4511 | 0.2352 | 0.4876 | 0.6636 | 0.4098 | 0.7071 | 0.3929 | 0.3192 | 0.4500 |
| 14(15)-EpETrE | 0.0015 | 0.0015 | 0.0015 | 0.0015 | 0.0015 | 9.0856 | 3.6965 | 0.2020 | 0.2734 | 0.1252 | 8.8263 | **0.0000** |
| 15-epi LXA4 | 0.0015 | 0.0050 | 0.0015 | 0.0015 | 0.0025 | 0.0015 | 0.0015 | 0.0026 | 0.0015 | 0.0015 | -0.1754 | 0.7716 |
| 15-HETE | 20.1300 | 23.4669 | 18.4581 | 17.9891 | 21.4737 | 23.2851 | 30.5492 | 26.6282 | 20.2262 | 11.8165 | -0.0311 | 0.9397 |
| 15-keto PGE1 | 0.0015 | 0.0015 | 0.0015 | 0.0015 | 0.0015 | 0.0015 | 0.0015 | 0.0015 | 0.0015 | 0.0015 | 0.2433 | 0.8619 |
| 15-keto PGE2 | 0.2065 | 0.4942 | 0.4060 | 0.4265 | 0.3602 | 0.5806 | 0.4222 | 0.4235 | 0.4352 | 0.3148 | -0.0527 | 0.9771 |
| 15-keto PGF2a | 0.5871 | 0.6055 | 0.5364 | 0.5491 | 0.4648 | 1.3174 | 0.9377 | 1.3197 | 1.1315 | 0.9993 | 1.2566 | **0.0004** |
| 15-OxoETE | 0.0015 | 0.4128 | 0.5018 | 0.0015 | 0.4084 | 34.8442 | 0.0015 | 0.0015 | 0.0015 | 0.0015 | -2.1184 | 0.5401 |
| 15(R)-PGE1 | 0.0959 | 0.1149 | 0.0778 | 0.0793 | 0.0015 | 0.0015 | 0.0015 | 0.1624 | 0.1510 | 0.1455 | -0.5157 | 0.8678 |
| 15(S)-HEDE | 0.1069 | 0.0890 | 0.1130 | 0.1090 | 0.1254 | 0.0015 | 0.0015 | 0.3384 | 0.2900 | 0.1732 | -1.0416 | 0.3667 |
| 15(S)-HEPE | 0.4564 | 0.0015 | 0.2618 | 0.2662 | 0.2317 | 0.0015 | 0.0015 | 1.0893 | 0.5652 | 0.4616 | -0.1674 | 0.9771 |
| 15d-D12,14-PGJ2 | 0.0519 | 0.0727 | 0.0757 | 0.0773 | 0.0691 | 0.0015 | 0.0559 | 0.0724 | 0.0754 | 0.0367 | -1.8185 | **0.0000** |
| 16-HDoHE | 0.4735 | 0.3834 | 0.4376 | 0.4385 | 0.5883 | 2.2619 | 8.5047 | 1.3574 | 1.3014 | 0.7345 | 2.0841 | **0.0000** |
| 16(17)-EpDPE | 0.0097 | 0.0126 | 0.0015 | 0.0080 | 0.0183 | 0.0015 | 0.2300 | 0.0134 | 0.0213 | 0.0114 | -0.0595 | 0.9827 |
| 17-HDoHE | 0.3356 | 0.1855 | 0.1926 | 0.2292 | 0.2906 | 1.2449 | 1.7813 | 1.7938 | 1.1023 | 0.5808 | 2.4713 | **0.0199** |
| 17(18)-EpETE | 0.0015 | 0.0015 | 0.0015 | 0.0052 | 0.0015 | 0.0015 | 0.0015 | 0.0015 | 0.0015 | 0.0015 | -0.1666 | 0.9320 |
| 18-carboxy dinor LTB4 | 0.0015 | 0.0015 | 0.0015 | 0.0015 | 0.0015 | 1.5605 | 1.2422 | 0.0070 | 0.0015 | 0.0015 | 3.8272 | **0.0028** |
| 18-HEPE | 0.0015 | 0.0015 | 0.0485 | 0.0015 | 0.0444 | 0.0015 | 0.0015 | 0.0950 | 0.1067 | 0.0554 | 1.4142 | 0.4500 |
| 19,20-DiHDoPE | 0.1499 | 0.2146 | 0.1943 | 0.2219 | 0.0830 | 0.0015 | 0.2099 | 0.1977 | 0.2314 | 0.1289 | -1.1265 | 0.1457 |
| 19(20)-EpDPE | 0.0298 | 0.0203 | 0.0284 | 0.0189 | 0.0378 | 0.0015 | 0.6529 | 0.0556 | 0.0745 | 0.0380 | 0.1249 | 0.9320 |
| 19(R)-OH PGF2a & 20-OH PGF2a | 0.0015 | 0.0015 | 0.0015 | 0.0015 | 0.0015 | 0.0015 | 0.0015 | 0.0015 | 0.0015 | 0.0015 | 0.2433 | 0.8189 |
| 20-HDoHE | 0.4596 | 0.5278 | 0.4812 | 0.5438 | 0.5025 | 0.0015 | 6.7935 | 1.2099 | 1.1683 | 0.6170 | 0.0272 | 0.9827 |
| 20-HETE | 0.0015 | 0.7678 | 0.8797 | 0.7748 | 1.0269 | 0.0015 | 14.2400 | 0.0015 | 0.0015 | 0.0015 | -4.7077 | 0.1848 |
| 20-hydroxy LTB4 | 0.0015 | 0.0015 | 0.0015 | 0.0015 | 0.0015 | 0.0015 | 0.0015 | 0.0015 | 0.0045 | 0.0015 | 0.3397 | 0.3934 |
| 4-HDoHE | 0.1009 | 0.1166 | 0.1178 | 0.1438 | 0.2012 | 0.0015 | 4.7001 | 0.3990 | 0.4508 | 0.2286 | 0.8067 | 0.3955 |
| 5-HEPE | 0.0015 | 0.0015 | 0.0015 | 0.0754 | 0.0854 | 0.0015 | 0.0015 | 0.3224 | 0.4866 | 0.2177 | 3.0218 | 0.0740 |
| 5-HETE | 1.1215 | 1.3183 | 1.0202 | 1.3526 | 1.6977 | 5.4351 | 17.8135 | 6.3763 | 7.0810 | 2.6094 | 2.3034 | **0.0000** |
| 5-oxoETE | 0.0881 | 0.0988 | 0.1752 | 0.1365 | 0.2091 | 0.0015 | 0.0015 | 0.1364 | 0.1956 | 0.0690 | -2.7423 | **0.0058** |
| 5,6-DiHETE(EPA) | 0.0015 | 0.0015 | 0.0015 | 0.0151 | 0.0015 | 0.0015 | 0.0015 | 0.0015 | 0.0015 | 0.0015 | -0.4668 | 0.4561 |
| 5,6-DiHETrE | 0.0116 | 0.0015 | 0.0015 | 0.0144 | 0.0052 | 0.0015 | 0.0015 | 0.0036 | 0.0116 | 0.0066 | -0.5491 | 0.5556 |
| 5(6)-EpETrE | 0.1433 | 0.1314 | 0.1363 | 0.1291 | 0.1562 | 0.1901 | 0.4521 | 0.0331 | 0.0256 | 0.0142 | -2.5679 | **0.0000** |
| 5(S)-HETrE | 0.0015 | 0.0089 | 0.0072 | 0.0015 | 0.0178 | 0.0015 | 0.0015 | 0.0507 | 0.0346 | 0.0238 | 0.5160 | 0.4500 |
| 5(S),12(S)-DiHETE | 0.1200 | 0.2146 | 0.1380 | 0.1362 | 0.1033 | 0.4280 | 0.8904 | 0.0843 | 0.1166 | 0.0416 | -0.5427 | 0.5676 |
| 5(S),15(S)-DiHEPE | 0.0015 | 0.0954 | 0.0015 | 0.0015 | 0.0350 | 11.6452 | 2.6190 | 0.1678 | 0.1194 | 0.1695 | 6.3311 | **0.0000** |
| 5(S),15(S)-DiHETE | 0.0015 | 0.0015 | 0.0015 | 0.0015 | 0.0015 | 0.0015 | 0.0597 | 0.0015 | 0.0015 | 0.0022 | 1.3264 | 0.0644 |
| 6-keto PGE1 | 0.0015 | 0.0172 | 0.0149 | 0.0154 | 0.0136 | 0.0015 | 0.0015 | 0.0092 | 0.0015 | 0.0015 | -1.6396 | 0.2004 |
| 6kPGF1a | 3.6156 | 6.1570 | 5.2604 | 5.9817 | 6.4715 | 6.8445 | 3.0809 | 0.0015 | 0.0015 | 0.0015 | -7.6132 | **0.0274** |
| 7-HDoHE | 0.0884 | 0.0780 | 0.0788 | 0.1264 | 0.1118 | 0.6605 | 3.6455 | 0.3446 | 0.4728 | 0.2030 | 2.6791 | **0.0000** |
| 7(8)-EpDPE | 0.0033 | 0.0054 | 0.0054 | 0.0074 | 0.0108 | 0.0015 | 0.3253 | 0.0015 | 0.0122 | 0.0048 | -0.0827 | 0.9771 |
| 8-HDoHE | 0.0938 | 0.1141 | 0.1405 | 0.0758 | 0.1676 | 0.7868 | 4.9039 | 0.2620 | 0.2968 | 0.1774 | 2.3022 | **0.0056** |
| 8-HEPE | 0.0015 | 0.0015 | 0.0015 | 0.0015 | 0.0498 | 0.0015 | 0.0015 | 0.0830 | 0.1302 | 0.0381 | 2.1106 | 0.1219 |
| 8-HETE | 1.0683 | 0.7753 | 0.9253 | 1.0993 | 0.9928 | 3.4333 | 12.6075 | 1.4048 | 1.5584 | 0.8277 | 1.4778 | **0.0000** |
| 8-isoPGF2a & 11bPGF2a | 0.0015 | 0.1033 | 0.0638 | 0.0015 | 0.0970 | 0.0015 | 0.0015 | 0.0015 | 0.0015 | 0.0768 | -1.9497 | 0.3955 |
| 8,9-DiHETrE | 0.0321 | 0.0314 | 0.0422 | 0.0336 | 0.0253 | 0.0015 | 0.1078 | 0.0246 | 0.0359 | 0.0220 | -1.6585 | **0.0003** |
| 8(9)-EpETrE | 0.0015 | 0.0015 | 0.0395 | 0.0015 | 0.0015 | 0.0015 | 0.0015 | 0.0015 | 0.0015 | 0.0015 | -0.5479 | 0.7046 |
| 8(S)-HETrE | 0.1078 | 0.1475 | 0.1140 | 0.1546 | 0.1888 | 0.0015 | 2.0481 | 0.3936 | 0.4372 | 0.1668 | 0.4228 | 0.6828 |
| 9-HEPE | 0.1265 | 0.0015 | 0.1298 | 0.1464 | 0.2553 | 0.0015 | 0.0015 | 0.8685 | 1.0544 | 0.0015 | -1.2658 | 0.5159 |
| 9-HETE | 0.0015 | 0.0015 | 0.0015 | 0.0015 | 0.0015 | 0.0015 | 5.8028 | 0.0015 | 0.0015 | 0.0015 | 2.2875 | **0.0336** |
| 9-HODE | 13.1826 | 17.9999 | 14.7776 | 15.0953 | 0.0015 | 0.0015 | 22.9802 | 0.0015 | 0.0015 | 0.0015 | -7.6210 | **0.0338** |
| 9-OxoODE | 4.1273 | 3.4742 | 3.2389 | 2.9265 | 3.3894 | 18.3710 | 22.7061 | 3.3894 | 3.0926 | 1.6322 | 0.9578 | **0.0006** |
| 9-OxoOTrE | 0.0664 | 0.0015 | 0.0438 | 0.0509 | 0.0824 | 0.6946 | 0.0015 | 0.0854 | 0.0783 | 0.0135 | -0.1406 | 0.9771 |
| 9,10-DiHOME | 2.3010 | 1.1255 | 1.1798 | 1.2964 | 0.5984 | 1.0611 | 1.2534 | 0.5860 | 0.7122 | 0.4740 | -0.6747 | 0.0942 |
| 9(10)-EpOME | 1.2526 | 0.9361 | 1.0894 | 0.7780 | 1.2517 | 8.6811 | 16.4249 | 1.7242 | 1.8294 | 0.9156 | 1.6924 | 0.1248 |
| 9(S)-HOTrE | 0.3026 | 0.1751 | 0.2697 | 0.2057 | 0.4403 | 1.4363 | 2.0747 | 0.5217 | 0.3651 | 0.2883 | 1.4349 | 0.2576 |
| Bicyclo PGE1 | 3.2853 | 5.6863 | 4.1312 | 3.1560 | 4.1412 | 3.8898 | 9.4218 | 0.4020 | 3.8820 | 1.3192 | -0.7688 | 0.2014 |
| Bicyclo PGE2 | 0.0401 | 0.0476 | 0.0262 | 0.0309 | 0.0386 | 0.0015 | 0.0015 | 0.1148 | 0.1336 | 0.0852 | -0.6157 | 0.5159 |
| LTB4 | 0.0283 | 0.0446 | 0.0495 | 0.0015 | 0.0388 | 0.0015 | 0.0015 | 0.1212 | 0.2428 | 0.0766 | 0.3410 | 0.8678 |
| LXA5 | 0.0015 | 0.0047 | 0.0015 | 0.0015 | 0.0013 | 0.1295 | 0.0015 | 0.0015 | 0.0015 | 0.0015 | 0.9751 | 0.2518 |
| PD1(n-3, DPA) | 3.8907 | 11.0489 | 4.1335 | 6.3073 | 1.6294 | 75.6719 | 140.5792 | 0.4055 | 0.7046 | 0.5481 | 0.1353 | 0.9687 |
| PGA2 | 0.3540 | 0.3827 | 0.3073 | 0.2715 | 0.3636 | 0.7950 | 0.7331 | 1.2517 | 1.1268 | 0.7774 | 1.5747 | **0.0001** |
| PGD2 | 0.0015 | 0.0015 | 0.0015 | 0.0015 | 0.0015 | 0.7727 | 0.0015 | 1.0803 | 1.1180 | 0.6297 | 7.6643 | **0.0047** |
| PGD3 | 0.0258 | 0.0956 | 0.1062 | 0.0015 | 0.0820 | 0.0015 | 0.5087 | 0.0015 | 0.0015 | 0.0015 | -2.7827 | 0.1290 |
| PGE1 | 0.1287 | 0.2363 | 0.1247 | 0.1645 | 0.1673 | 0.6357 | 0.8712 | 1.1004 | 0.8020 | 0.5697 | 2.2293 | **0.0000** |
| PGE2 | 10.9409 | 12.1142 | 10.5898 | 10.3617 | 10.0851 | 26.1303 | 19.6568 | 27.2916 | 24.0679 | 19.3973 | 1.1293 | **0.0004** |
| PGE3 | 0.0314 | 0.0405 | 0.0273 | 0.0380 | 0.0373 | 0.2521 | 0.0015 | 0.2282 | 0.2264 | 0.1730 | 1.9004 | **0.0336** |
| PGF1a | 0.0360 | 0.0483 | 0.0286 | 0.0170 | 0.0389 | 0.0015 | 0.0015 | 0.0848 | 0.0748 | 0.0490 | -1.4297 | 0.1048 |
| PGF2a | 1.3802 | 1.3584 | 1.2208 | 0.6895 | 1.2415 | 0.9931 | 0.8823 | 1.3823 | 1.2271 | 0.8801 | 0.0280 | 0.9827 |
| PGJ2 | 0.1498 | 0.1779 | 0.1303 | 0.1310 | 0.1644 | 0.4517 | 0.3046 | 0.6195 | 0.5601 | 0.3520 | 1.3191 | **0.0083** |
| RvD1 & AT-RvD1 | 0.1682 | 0.0015 | 0.0015 | 0.0015 | 0.1145 | 4.6956 | 6.8695 | 0.0015 | 0.0963 | 0.0015 | 2.4345 | 0.3955 |
| RvD5(n-3DPA) (7,17-DiHDoPE) | 0.0356 | 0.0633 | 0.0591 | 0.0926 | 0.0284 | 1.1148 | 1.4635 | 0.0272 | 0.0221 | 0.0241 | 0.0053 | 0.9956 |
| RvD6 (4,17-DiHDoHE) | 0.0015 | 0.0015 | 0.0015 | 0.0015 | 0.0015 | 0.0015 | 0.0015 | 0.0056 | 0.0123 | 0.0015 | 0.6801 | 0.3934 |
| RvE3 | 0.6231 | 1.9823 | 1.2107 | 1.5691 | 0.3361 | 0.0015 | 0.0015 | 0.0864 | 0.1485 | 0.0662 | -5.9992 | **0.0000** |
| tetranor 12-HETE | 0.0550 | 0.0659 | 0.0563 | 0.0908 | 0.0015 | 0.0015 | 0.0015 | 0.1710 | 0.1610 | 0.1136 | 0.0403 | 0.9827 |
| tetranor PGEM | 0.0022 | 0.0015 | 0.0018 | 0.0015 | 0.0011 | 0.0308 | 0.0397 | 0.0026 | 0.0034 | 0.0024 | 1.9274 | **0.0336** |
| TXB2 | 0.0015 | 3.6118 | 2.9670 | 2.9934 | 2.9566 | 3.0566 | 1.9095 | 3.3498 | 3.0330 | 2.0149 | 1.9911 | 0.4500 |
| TXB3 | 0.0015 | 0.0015 | 0.0015 | 0.0015 | 0.0015 | 0.0015 | 0.0015 | 0.0781 | 0.0472 | 0.0302 | 2.2502 | **0.0232** |

| | Uninfected (UI) | | | | | *Y. pestis* infection 36 hr | | | | | | |
|---|---|---|---|---|---|---|---|---|---|---|---|---|
| Lipid | 1 | 2 | 3 | 4 | 5 | 1 | 2 | 3 | 4 | 5 | LogFC | p-value |
| 10-HDoHE | 0.1791 | 0.0015 | 0.2581 | 0.2886 | 0.3397 | 0.5089 | 0.4986 | 0.3696 | 0.8152 | 0.5768 | 2.4809 | **0.0043** |
| 10(11)-EpDPE | 0.0326 | 0.0156 | 0.0317 | 0.0196 | 0.0443 | 0.0430 | 0.0483 | 0.0394 | 0.0505 | 0.0559 | 0.6517 | 0.4279 |
| 10S,17S-DiHDoHE | 0.0015 | 0.0015 | 0.0015 | 0.0015 | 0.0015 | 0.1208 | 0.0965 | 0.0015 | 0.0015 | 0.0992 | 3.6972 | 0.0788 |
| 11-HDoHE | 0.0015 | 0.0015 | 0.4672 | 0.0015 | 0.0015 | 0.0015 | 0.0015 | 0.0015 | 0.0015 | 0.0015 | -1.6280 | 0.5562 |
| 11-HEPE | 0.3896 | 0.2435 | 0.3743 | 0.3234 | 0.3701 | 0.7092 | 0.8029 | 0.3768 | 1.1592 | 0.8385 | 1.0488 | 0.3259 |
| 11-HETE | 79.7221 | 93.6908 | 66.3016 | 71.2922 | 70.8498 | 69.8169 | 54.1486 | 27.0377 | 68.0528 | 76.5154 | -0.4214 | **0.0192** |
| 11,12-DiHETrE | 0.3019 | 0.3424 | 0.2642 | 0.3698 | 0.1507 | 0.1126 | 0.1233 | 0.1094 | 0.3318 | 0.2228 | -0.6210 | 0.1084 |
| 11(12)-EpETrE | 0.0782 | 0.0015 | 0.1706 | 0.1312 | 0.1970 | 0.1830 | 0.1480 | 0.1037 | 0.1935 | 0.1765 | 1.5143 | 0.4082 |
| 11(R)-HEDE | 1.7474 | 1.6548 | 1.4651 | 1.4726 | 1.8574 | 2.9524 | 2.6171 | 1.3507 | 3.0300 | 3.5297 | 0.6189 | 0.1652 |
| 11dh-2,3-dinor TXB2 | 0.0108 | 0.0148 | 0.0071 | 0.0200 | 0.0080 | 0.0163 | 0.0569 | 0.0015 | 0.0157 | 0.0155 | 0.1124 | 0.9672 |
| 11dh-TXB2 | 0.0015 | 0.0015 | 0.0015 | 0.0015 | 0.0015 | 0.0034 | 0.0015 | 0.0015 | 0.0015 | 0.0015 | 0.3185 | 0.6992 |
| 12-HEPE | 2.9162 | 2.2473 | 2.4298 | 3.0685 | 6.7805 | 14.6863 | 14.3977 | 6.0943 | 22.9909 | 12.8370 | 1.9441 | **0.0001** |
| 12-HETE | 72.5816 | 78.9431 | 61.3581 | 78.7440 | 122.5452 | 144.9652 | 108.9554 | 50.3418 | 138.2811 | 111.1358 | 0.3943 | **0.0234** |
| 12,13-DiHOME | 2.1580 | 1.7970 | 1.4632 | 1.5488 | 0.6811 | 0.4126 | 0.5116 | 0.5573 | 0.8174 | 0.5393 | -1.3652 | **0.0010** |
| 12(13)-EpOME | 0.6150 | 0.4682 | 0.4531 | 0.4299 | 0.5792 | 0.7155 | 0.6881 | 0.5514 | 1.2455 | 0.8306 | 0.5976 | 0.0901 |
| 12(S)-HHTrE | 25.4892 | 26.8030 | 23.4114 | 17.5795 | 20.8156 | 7.0319 | 8.3530 | 3.6835 | 14.7995 | 9.8756 | -1.4458 | **0.0000** |
| 13-HDoHE | 1.1767 | 1.5264 | 1.2935 | 1.5491 | 1.4563 | 3.3772 | 2.7826 | 1.9205 | 4.3176 | 4.1561 | 1.1339 | **0.0010** |
| 13-HODE | 102.5982 | 95.7632 | 76.3926 | 74.8717 | 73.3199 | 82.7508 | 86.4948 | 47.1794 | 136.1056 | 76.9026 | -0.0939 | 0.6871 |
| 13-OxoODE | 4.1100 | 3.5354 | 3.4325 | 2.6608 | 4.4553 | 2.9277 | 3.2403 | 2.2792 | 5.3606 | 3.4583 | -0.1325 | 0.6992 |
| 13,14dh-15k-PGD2 | 1.6960 | 1.5422 | 1.2874 | 1.2029 | 1.1678 | 1.6612 | 1.7216 | 1.1426 | 2.2383 | 2.0350 | 0.3775 | 0.3881 |
| 13,14dh-15k-PGE1 | 0.0182 | 0.0099 | 0.0176 | 0.0015 | 0.0170 | 0.0015 | 0.0164 | 0.0015 | 0.0015 | 0.0109 | -1.1999 | 0.2997 |
| 13,14dh-15k-PGE2 | 0.4777 | 0.5916 | 0.5485 | 0.5033 | 0.4110 | 0.9973 | 0.8484 | 0.5458 | 1.0380 | 1.0440 | 0.7566 | **0.0493** |
| 13,14dh-15k-PGF2a | 0.0547 | 0.0785 | 0.0912 | 0.0525 | 0.0810 | 0.0285 | 0.0015 | 0.0315 | 0.0467 | 0.0424 | -1.9093 | **0.0276** |
| 13(14)-EpDPE | 0.0112 | 0.0098 | 0.0015 | 0.0096 | 0.0132 | 0.0259 | 0.0254 | 0.0134 | 0.0278 | 0.0167 | 1.5194 | 0.2699 |
| 13(S)-HOTrE | 1.8809 | 1.0374 | 1.2444 | 1.3337 | 1.1165 | 1.2377 | 1.4079 | 0.7988 | 2.6679 | 0.9292 | 0.0117 | 0.9937 |
| 14-HDoHE | 4.0850 | 3.8589 | 4.0309 | 5.0897 | 5.2854 | 9.0899 | 8.8225 | 5.2917 | 14.8542 | 11.9397 | 1.1151 | **0.0004** |
| 14,15-DiHETrE | 0.4157 | 0.5778 | 0.5527 | 0.4511 | 0.2352 | 0.3284 | 0.3352 | 0.3741 | 0.7898 | 0.6628 | 0.1722 | 0.6992 |
| 14(15)-EpETrE | 0.0015 | 0.0015 | 0.0015 | 0.0015 | 0.0015 | 0.1509 | 0.0752 | 0.2334 | 0.1759 | 0.2091 | 6.7303 | **0.0013** |
| 15-epi LXA4 | 0.0015 | 0.0050 | 0.0015 | 0.0015 | 0.0025 | 0.0015 | 0.0015 | 0.0015 | 0.0020 | 0.0019 | -0.3970 | 0.4097 |
| 15-HETE | 20.1300 | 23.4669 | 18.4581 | 17.9891 | 21.4737 | 16.9082 | 16.5269 | 7.0203 | 20.2204 | 18.3023 | -0.5185 | **0.0041** |
| 15-keto PGE1 | 0.0015 | 0.0015 | 0.0015 | 0.0015 | 0.0015 | 0.0094 | 0.0015 | 0.0035 | 0.0015 | 0.0015 | 0.8185 | 0.3691 |
| 15-keto PGE2 | 0.2065 | 0.4942 | 0.4060 | 0.4265 | 0.3602 | 0.5127 | 0.4680 | 0.2028 | 0.3670 | 0.3366 | -0.0324 | 0.9822 |
| 15-keto PGF2a | 0.5871 | 0.6055 | 0.5364 | 0.5491 | 0.4648 | 1.0635 | 1.0508 | 0.6271 | 1.1559 | 1.1819 | 0.8438 | **0.0191** |
| 15-OxoETE | 0.0015 | 0.4128 | 0.5018 | 0.0015 | 0.4084 | 1.0888 | 0.6292 | 1.0468 | 1.0035 | 1.3011 | 4.4355 | 0.1652 |
| 15(R)-PGE1 | 0.0959 | 0.1149 | 0.0778 | 0.0793 | 0.0015 | 0.0015 | 0.1206 | 0.0853 | 0.1643 | 0.1844 | 0.3577 | 0.9099 |
| 15(S)-HEDE | 0.1069 | 0.0890 | 0.1130 | 0.1090 | 0.1254 | 0.2016 | 0.2063 | 0.0843 | 0.2579 | 0.2180 | 0.7420 | 0.5301 |
| 15(S)-HEPE | 0.4564 | 0.0015 | 0.2618 | 0.2662 | 0.2317 | 2.1295 | 1.5306 | 1.1329 | 1.7074 | 1.5532 | 4.0247 | **0.0059** |
| 15d-D12,14-PGJ2 | 0.0519 | 0.0727 | 0.0757 | 0.0773 | 0.0691 | 0.0471 | 0.0502 | 0.0486 | 0.0787 | 0.0644 | -0.2177 | 0.6629 |
| 16-HDoHE | 0.4735 | 0.3834 | 0.4376 | 0.4385 | 0.5883 | 0.7942 | 0.7079 | 0.4913 | 1.0657 | 1.0658 | 0.7605 | **0.0041** |
| 16(17)-EpDPE | 0.0097 | 0.0126 | 0.0015 | 0.0080 | 0.0183 | 0.0015 | 0.0132 | 0.0072 | 0.0211 | 0.0177 | 0.1033 | 0.9672 |
| 17-HDoHE | 0.3356 | 0.1855 | 0.1926 | 0.2292 | 0.2906 | 1.0108 | 0.0015 | 0.4717 | 1.5572 | 0.8907 | 0.0392 | 0.9930 |
| 17(18)-EpETE | 0.0015 | 0.0015 | 0.0015 | 0.0052 | 0.0015 | 0.0119 | 0.0015 | 0.0120 | 0.0124 | 0.0015 | 1.2799 | 0.1557 |
| 18-carboxy dinor LTB4 | 0.0015 | 0.0015 | 0.0015 | 0.0015 | 0.0015 | 0.0015 | 0.0015 | 0.0053 | 0.0045 | 0.0051 | 0.7182 | 0.6417 |
| 18-HEPE | 0.0015 | 0.0015 | 0.0485 | 0.0015 | 0.0444 | 0.0507 | 0.0506 | 0.0495 | 0.1169 | 0.0836 | 3.6671 | **0.0276** |
| 19,20-DiHDoPE | 0.1499 | 0.2146 | 0.1943 | 0.2219 | 0.0830 | 0.1336 | 0.1259 | 0.1267 | 0.2348 | 0.3020 | 0.0761 | 0.9672 |
| 19(20)-EpDPE | 0.0298 | 0.0203 | 0.0284 | 0.0189 | 0.0378 | 0.0496 | 0.0506 | 0.0470 | 0.0750 | 0.0676 | 1.2133 | 0.0585 |
| 19(R)-OH PGF2a & 20-OH PGF2a | 0.0015 | 0.0015 | 0.0015 | 0.0015 | 0.0015 | 0.0015 | 0.0015 | 0.0085 | 0.0132 | 0.0015 | 1.1483 | 0.1060 |
| 20-HDoHE | 0.4596 | 0.5278 | 0.4812 | 0.5438 | 0.5025 | 0.7121 | 0.7012 | 0.4048 | 1.1183 | 0.9594 | 0.6139 | 0.5927 |
| 20-HETE | 0.0015 | 0.7678 | 0.8797 | 0.7748 | 1.0269 | 0.8282 | 0.0015 | 0.3907 | 0.9544 | 0.8414 | -0.1986 | 0.9822 |
| 20-hydroxy LTB4 | 0.0015 | 0.0015 | 0.0015 | 0.0015 | 0.0015 | 0.0015 | 0.0018 | 0.0027 | 0.0053 | 0.0055 | 0.8751 | **0.0144** |
| 4-HDoHE | 0.1009 | 0.1166 | 0.1178 | 0.1438 | 0.2012 | 0.2473 | 0.2707 | 0.1809 | 0.2977 | 0.3699 | 1.0203 | 0.2840 |
| 5-HEPE | 0.0015 | 0.0015 | 0.0015 | 0.0754 | 0.0854 | 0.2351 | 0.2547 | 0.2121 | 0.5822 | 0.4417 | 5.4547 | **0.0015** |
| 5-HETE | 1.1215 | 1.3183 | 1.0202 | 1.3526 | 1.6977 | 3.5606 | 3.9356 | 2.3316 | 6.2934 | 6.2652 | 1.6832 | **0.0001** |
| 5-oxoETE | 0.0881 | 0.0988 | 0.1752 | 0.1365 | 0.2091 | 0.0925 | 0.1029 | 0.0772 | 0.1834 | 0.2328 | -0.0955 | 0.9672 |
| 5,6-DiHETE(EPA) | 0.0015 | 0.0015 | 0.0015 | 0.0151 | 0.0015 | 0.0015 | 0.0015 | 0.0015 | 0.0080 | 0.0061 | -0.2395 | 0.6992 |
| 5,6-DiHETrE | 0.0116 | 0.0015 | 0.0015 | 0.0144 | 0.0052 | 0.0043 | 0.0052 | 0.0064 | 0.0102 | 0.0108 | 0.6503 | 0.4950 |
| 5(6)-EpETrE | 0.1433 | 0.1314 | 0.1363 | 0.1291 | 0.1562 | 0.0239 | 0.0187 | 0.0173 | 0.0235 | 0.0305 | -2.6607 | **0.0001** |
| 5(S)-HETrE | 0.0015 | 0.0089 | 0.0072 | 0.0015 | 0.0178 | 0.0229 | 0.0323 | 0.0159 | 0.0399 | 0.0371 | 2.8384 | **0.0000** |
| 5(S),12(S)-DiHETE | 0.1200 | 0.2146 | 0.1380 | 0.1362 | 0.1033 | 0.0436 | 0.0015 | 0.0169 | 0.1120 | 0.0704 | -2.4885 | **0.0041** |
| 5(S),15(S)-DiHEPE | 0.0015 | 0.0954 | 0.0015 | 0.0015 | 0.0350 | 0.0811 | 0.0015 | 0.0341 | 0.0969 | 0.0412 | 2.1614 | 0.1652 |
| 5(S),15(S)-DiHETE | 0.0015 | 0.0015 | 0.0015 | 0.0015 | 0.0015 | 0.0013 | 0.0044 | 0.0015 | 0.0015 | 0.0015 | 0.6247 | 0.4279 |
| 6-keto PGE1 | 0.0015 | 0.0172 | 0.0149 | 0.0154 | 0.0136 | 0.0062 | 0.0082 | 0.0047 | 0.0015 | 0.0079 | -0.5880 | 0.6871 |
| 6kPGF1a | 3.6156 | 6.1570 | 5.2604 | 5.9817 | 6.4715 | 0.0015 | 4.0415 | 0.0015 | 3.5370 | 2.9582 | -5.1335 | 0.1557 |
| 7-HDoHE | 0.0884 | 0.0780 | 0.0788 | 0.1264 | 0.1118 | 0.2469 | 0.2387 | 0.2858 | 0.5036 | 0.4877 | 1.8674 | **0.0000** |
| 7(8)-EpDPE | 0.0033 | 0.0054 | 0.0054 | 0.0074 | 0.0108 | 0.0080 | 0.0074 | 0.0041 | 0.0085 | 0.0107 | 0.1499 | 0.9103 |
| 8-HDoHE | 0.0938 | 0.1141 | 0.1405 | 0.0758 | 0.1676 | 0.2031 | 0.2553 | 0.1695 | 0.3131 | 0.2656 | 1.0567 | 0.2396 |
| 8-HEPE | 0.0015 | 0.0015 | 0.0015 | 0.0015 | 0.0498 | 0.0418 | 0.0731 | 0.0503 | 0.0876 | 0.0464 | 4.3409 | **0.0015** |
| 8-HETE | 1.0683 | 0.7753 | 0.9253 | 1.0993 | 0.9928 | 1.0628 | 1.0770 | 0.4855 | 1.2524 | 1.6767 | 0.2492 | 0.3833 |
| 8-isoPGF2a & 11bPGF2a | 0.0015 | 0.1033 | 0.0638 | 0.0015 | 0.0970 | 0.0487 | 0.0723 | 0.0447 | 0.0987 | 0.0796 | 1.9712 | 0.4039 |
| 8,9-DiHETrE | 0.0321 | 0.0314 | 0.0422 | 0.0336 | 0.0253 | 0.0198 | 0.0207 | 0.0158 | 0.0455 | 0.0328 | -0.3355 | 0.5278 |
| 8(9)-EpETrE | 0.0015 | 0.0015 | 0.0395 | 0.0015 | 0.0015 | 0.0015 | 0.0015 | 0.0015 | 0.0015 | 0.0015 | -0.7912 | 0.5447 |
| 8(S)-HETrE | 0.1078 | 0.1475 | 0.1140 | 0.1546 | 0.1888 | 0.2664 | 0.2464 | 0.1211 | 0.3412 | 0.3163 | 0.8415 | 0.3691 |
| 9-HEPE | 0.1265 | 0.0015 | 0.1298 | 0.1464 | 0.2553 | 0.5175 | 0.5709 | 0.2659 | 0.9727 | 0.4871 | 3.0149 | 0.0956 |
| 9-HETE | 0.0015 | 0.0015 | 0.0015 | 0.0015 | 0.0015 | 0.0015 | 0.0015 | 0.0015 | 0.0015 | 0.0015 | 0.0000 | 1.0000 |
| 9-HODE | 13.1826 | 17.9999 | 14.7776 | 15.0953 | 0.0015 | 0.0015 | 0.0015 | 0.0015 | 0.0015 | 0.0015 | -10.5488 | **0.0043** |
| 9-OxoODE | 4.1273 | 3.4742 | 3.2389 | 2.9265 | 3.3894 | 2.1003 | 2.4979 | 2.0297 | 4.3854 | 3.3262 | -0.3999 | 0.1652 |
| 9-OxoOTrE | 0.0664 | 0.0015 | 0.0438 | 0.0509 | 0.0824 | 0.0320 | 0.0566 | 0.0424 | 0.0600 | 0.0449 | 0.7618 | 0.6732 |
| 9,10-DiHOME | 2.3010 | 1.1255 | 1.1798 | 1.2964 | 0.5984 | 0.4241 | 0.4844 | 0.7475 | 1.0082 | 0.6042 | -0.9744 | **0.0144** |
| 9(10)-EpOME | 1.2526 | 0.9361 | 1.0894 | 0.7780 | 1.2517 | 1.7908 | 1.5952 | 1.4686 | 2.2481 | 1.8809 | 0.8199 | 0.5089 |
| 9(S)-HOTrE | 0.3026 | 0.1751 | 0.2697 | 0.2057 | 0.4403 | 0.4832 | 0.3245 | 0.2997 | 0.4368 | 0.3320 | 0.4918 | 0.6992 |
| Bicyclo PGE1 | 3.2853 | 5.6863 | 4.1312 | 3.1560 | 4.1412 | 2.9925 | 0.8480 | 2.4907 | 1.7216 | 1.7194 | -1.0214 | 0.0901 |
| Bicyclo PGE2 | 0.0401 | 0.0476 | 0.0262 | 0.0309 | 0.0386 | 0.1073 | 0.1122 | 0.0487 | 0.1302 | 0.1275 | 1.6390 | 0.0585 |
| LTB4 | 0.0283 | 0.0446 | 0.0495 | 0.0015 | 0.0388 | 0.0687 | 0.0785 | 0.0838 | 0.1324 | 0.2318 | 2.6820 | **0.0276** |
| LXA5 | 0.0015 | 0.0047 | 0.0015 | 0.0015 | 0.0013 | 0.0015 | 0.0015 | 0.0015 | 0.0015 | 0.0015 | -0.4028 | 0.6732 |
| PD1(n-3, DPA) | 3.8907 | 11.0489 | 4.1335 | 6.3073 | 1.6294 | 0.6113 | 0.4724 | 0.7548 | 0.8736 | 0.7266 | -2.6846 | **0.0059** |
| PGA2 | 0.3540 | 0.3827 | 0.3073 | 0.2715 | 0.3636 | 0.9773 | 1.0729 | 0.4864 | 1.2130 | 1.0754 | 1.4802 | **0.0004** |
| PGD2 | 0.0015 | 0.0015 | 0.0015 | 0.0015 | 0.0015 | 0.0015 | 0.0015 | 0.0015 | 0.0015 | 0.0015 | 0.0000 | 1.0000 |
| PGD3 | 0.0258 | 0.0956 | 0.1062 | 0.0015 | 0.0820 | 0.0015 | 0.0015 | 0.0015 | 0.0015 | 0.0015 | -4.2958 | **0.0186** |
| PGE1 | 0.1287 | 0.2363 | 0.1247 | 0.1645 | 0.1673 | 0.5719 | 0.4959 | 0.2805 | 0.5410 | 0.7261 | 1.6277 | **0.0001** |
| PGE2 | 10.9409 | 12.1142 | 10.5898 | 10.3617 | 10.0851 | 20.3727 | 20.3837 | 12.1757 | 24.1056 | 22.5965 | 0.8633 | **0.0067** |
| PGE3 | 0.0314 | 0.0405 | 0.0273 | 0.0380 | 0.0373 | 0.1737 | 0.1777 | 0.1153 | 0.2542 | 0.2096 | 2.5898 | **0.0043** |
| PGF1a | 0.0360 | 0.0483 | 0.0286 | 0.0170 | 0.0389 | 0.0514 | 0.0530 | 0.0015 | 0.0302 | 0.0559 | -0.5059 | 0.6191 |
| PGF2a | 1.3802 | 1.3584 | 1.2208 | 0.6895 | 1.2415 | 0.9068 | 0.8342 | 0.3463 | 0.8367 | 0.9504 | -0.7163 | 0.1187 |
| PGJ2 | 0.1498 | 0.1779 | 0.1303 | 0.1310 | 0.1644 | 0.4775 | 0.4831 | 0.2263 | 0.6094 | 0.5008 | 1.5504 | **0.0029** |
| RvD1 & AT-RvD1 | 0.1682 | 0.0015 | 0.0015 | 0.0015 | 0.1145 | 0.0600 | 0.0015 | 0.0581 | 0.1301 | 0.0574 | 1.8047 | 0.5400 |
| RvD5(n-3DPA) (7,17-DiHDoPE) | 0.0356 | 0.0633 | 0.0591 | 0.0926 | 0.0284 | 0.0182 | 0.0227 | 0.0283 | 0.0236 | 0.0244 | -1.1659 | 0.3691 |
| RvD6 (4,17-DiHDoHE) | 0.0015 | 0.0015 | 0.0015 | 0.0015 | 0.0015 | 0.0015 | 0.0088 | 0.0047 | 0.0056 | 0.0100 | 1.5831 | **0.0265** |
| RvE3 | 0.6231 | 1.9823 | 1.2107 | 1.5691 | 0.3361 | 0.1330 | 0.0652 | 0.0778 | 0.1018 | 0.1052 | -3.4463 | **0.0001** |
| tetranor 12-HETE | 0.0550 | 0.0659 | 0.0563 | 0.0908 | 0.0015 | 0.1468 | 0.0947 | 0.1418 | 0.1752 | 0.1938 | 2.2302 | 0.1000 |
| tetranor PGEM | 0.0022 | 0.0015 | 0.0018 | 0.0015 | 0.0011 | 0.0024 | 0.0018 | 0.0028 | 0.0015 | 0.0022 | 0.3723 | 0.6992 |
| TXB2 | 0.0015 | 3.6118 | 2.9670 | 2.9934 | 2.9566 | 2.3535 | 2.3611 | 2.0372 | 5.1732 | 2.8386 | 1.9774 | 0.4744 |
| TXB3 | 0.0015 | 0.0015 | 0.0015 | 0.0015 | 0.0015 | 0.0245 | 0.0553 | 0.0299 | 0.0741 | 0.0353 | 4.6390 | **0.0000** |

| | | | | | | *Y. pestis* infection | | | | | | |
|---|---|---|---|---|---|---|---|---|---|---|---|---|
| | Uninfected (UI) | | | | | 48 hr | | | | | | |
| **Lipid** | **1** | **2** | **3** | **4** | **5** | **1** | **2** | **3** | **4** | **5** | **LogFC** | **p-value** |
| 10-HDoHE | 0.1791 | 0.0015 | 0.2581 | 0.2886 | 0.3397 | 0.8205 | 0.5726 | 0.6726 | 0.5703 | 0.7443 | 2.7791 | **0.0013** |
| 10(11)-EpDPE | 0.0326 | 0.0156 | 0.0317 | 0.0196 | 0.0443 | 0.0437 | 0.0451 | 0.0600 | 0.0514 | 0.0478 | 0.8137 | 0.3125 |
| 10S,17S-DiHDoHE | 0.0015 | 0.0015 | 0.0015 | 0.0015 | 0.0015 | 0.1292 | 0.0624 | 0.0015 | 0.0798 | 0.0912 | 4.6353 | **0.0227** |
| 11-HDoHE | 0.0015 | 0.0015 | 0.4672 | 0.0015 | 0.0015 | 0.0015 | 0.0015 | 0.0015 | 0.0015 | 0.0015 | -1.6280 | 0.5419 |
| 11-HEPE | 0.3896 | 0.2435 | 0.3743 | 0.3234 | 0.3701 | 0.9958 | 0.5170 | 0.7210 | 0.3430 | 0.5873 | 0.7500 | 0.4702 |
| 11-HETE | 79.7221 | 93.6908 | 66.3016 | 71.2922 | 70.8498 | 81.1881 | 45.0465 | 60.0267 | 42.2744 | 58.0212 | -0.4267 | **0.0168** |
| 11,12-DiHETrE | 0.3019 | 0.3424 | 0.2642 | 0.3698 | 0.1507 | 0.2553 | 0.1832 | 0.2634 | 0.1437 | 0.3141 | -0.2416 | 0.5566 |
| 11(12)-EpETrE | 0.0782 | 0.0015 | 0.1706 | 0.1312 | 0.1970 | 0.1519 | 0.1614 | 0.2026 | 0.1858 | 0.0779 | 1.3875 | 0.4395 |
| 11(R)-HEDE | 1.7474 | 1.6548 | 1.4651 | 1.4726 | 1.8574 | 3.5169 | 2.3050 | 2.7873 | 1.4814 | 3.0329 | 0.5151 | 0.2674 |
| 11dh-2,3-dinor TXB2 | 0.0108 | 0.0148 | 0.0071 | 0.0200 | 0.0080 | 0.0204 | 0.0091 | 0.0387 | 0.0154 | 0.0015 | 0.0807 | 0.9579 |
| 11dh-TXB2 | 0.0015 | 0.0015 | 0.0015 | 0.0015 | 0.0015 | 0.0015 | 0.0049 | 0.0015 | 0.0015 | 0.0043 | 0.3862 | 0.6286 |
| 12-HEPE | 2.9162 | 2.2473 | 2.4298 | 3.0685 | 6.7805 | 23.7026 | 11.0465 | 13.7718 | 8.9812 | 19.1773 | 2.0633 | **0.0000** |
| 12-HETE | 72.5816 | 78.9431 | 61.3581 | 78.7440 | 122.5452 | 173.8015 | 103.9258 | 114.2117 | 85.7986 | 140.4699 | 0.5992 | **0.0007** |
| 12,13-DiHOME | 2.1580 | 1.7970 | 1.4632 | 1.5488 | 0.6811 | 0.5544 | 0.6144 | 0.5673 | 0.3745 | 0.8359 | -1.3820 | **0.0007** |
| 12(13)-EpOME | 0.6150 | 0.4682 | 0.4531 | 0.4299 | 0.5792 | 0.7162 | 0.8324 | 0.7426 | 0.4065 | 0.6453 | 0.3316 | 0.3730 |
| 12(S)-HHTrE | 25.4892 | 26.8030 | 23.4114 | 17.5795 | 20.8156 | 11.5452 | 8.2990 | 10.5665 | 3.8862 | 7.2841 | -1.3234 | **0.0000** |
| 13-HDoHE | 1.1767 | 1.5264 | 1.2935 | 1.5491 | 1.4563 | 4.1769 | 2.5265 | 3.1221 | 2.4738 | 3.4850 | 1.0697 | **0.0014** |
| 13-HODE | 102.5982 | 95.7632 | 76.3926 | 74.8717 | 73.3199 | 88.1001 | 57.2060 | 72.2076 | 35.0112 | 64.0209 | -0.5083 | **0.0114** |
| 13-OxoODE | 4.1100 | 3.5354 | 3.4325 | 2.6608 | 4.4553 | 4.2187 | 2.7122 | 3.0183 | 1.7662 | 2.2264 | -0.3143 | 0.3709 |
| 13,14dh-15k-PGD2 | 1.6960 | 1.5422 | 1.2874 | 1.2029 | 1.1678 | 2.2329 | 1.5297 | 1.8663 | 1.1041 | 1.5704 | 0.2189 | 0.5916 |
| 13,14dh-15k-PGE1 | 0.0182 | 0.0099 | 0.0176 | 0.0015 | 0.0170 | 0.0163 | 0.0085 | 0.0045 | 0.0051 | 0.0132 | -0.1173 | 0.9373 |
| 13,14dh-15k-PGE2 | 0.4777 | 0.5916 | 0.5485 | 0.5033 | 0.4110 | 1.0172 | 0.8315 | 0.8628 | 0.7020 | 0.7732 | 0.6701 | 0.0751 |
| 13,14dh-15k-PGF2a | 0.0547 | 0.0785 | 0.0912 | 0.0525 | 0.0810 | 0.0399 | 0.0274 | 0.0384 | 0.0329 | 0.0486 | -0.9138 | 0.3299 |
| 13(14)-EpDPE | 0.0112 | 0.0098 | 0.0015 | 0.0096 | 0.0132 | 0.0120 | 0.0166 | 0.0146 | 0.0164 | 0.0165 | 1.1852 | 0.3915 |
| 13(S)-HOTrE | 1.8809 | 1.0374 | 1.2444 | 1.3337 | 1.1165 | 1.8774 | 0.7916 | 1.2963 | 0.5325 | 1.0254 | -0.3617 | 0.4566 |
| 14-HDoHE | 4.0850 | 3.8589 | 4.0309 | 5.0897 | 5.2854 | 13.2882 | 8.1832 | 9.2808 | 9.0608 | 12.5498 | 1.1475 | **0.0003** |
| 14,15-DiHETrE | 0.4157 | 0.5778 | 0.5527 | 0.4511 | 0.2352 | 0.7161 | 0.7024 | 0.6800 | 0.4925 | 0.9173 | 0.7268 | 0.0569 |
| 14(15)-EpETrE | 0.0015 | 0.0015 | 0.0015 | 0.0015 | 0.0015 | 0.1757 | 0.1851 | 0.2900 | 0.2967 | 0.1574 | 7.2132 | **0.0006** |
| 15-epi LXA4 | 0.0015 | 0.0050 | 0.0015 | 0.0015 | 0.0025 | 0.0025 | 0.0016 | 0.0014 | 0.0016 | 0.0010 | -0.2018 | 0.6521 |
| 15-HETE | 20.1300 | 23.4669 | 18.4581 | 17.9891 | 21.4737 | 21.3253 | 14.1885 | 16.6926 | 10.1328 | 13.5483 | -0.5424 | **0.0024** |
| 15-keto PGE1 | 0.0015 | 0.0015 | 0.0015 | 0.0015 | 0.0015 | 0.0015 | 0.0015 | 0.0015 | 0.0015 | 0.0015 | 0.0000 | 1.0000 |
| 15-keto PGE2 | 0.2065 | 0.4942 | 0.4060 | 0.4265 | 0.3602 | 0.3792 | 0.1497 | 0.1910 | 0.1270 | 0.1388 | -1.0358 | **0.0428** |
| 15-keto PGF2a | 0.5871 | 0.6055 | 0.5364 | 0.5491 | 0.4648 | 1.1756 | 0.9245 | 0.9055 | 0.6960 | 0.8797 | 0.7261 | **0.0406** |
| 15-OxoETE | 0.0015 | 0.4128 | 0.5018 | 0.0015 | 0.4084 | 1.0508 | 0.0015 | 0.0015 | 0.0015 | 0.7181 | -1.3552 | 0.6702 |
| 15(R)-PGE1 | 0.0959 | 0.1149 | 0.0778 | 0.0793 | 0.0015 | 0.1613 | 0.1550 | 0.1490 | 0.1048 | 0.1301 | 1.6864 | 0.3975 |
| 15(S)-HEDE | 0.1069 | 0.0890 | 0.1130 | 0.1090 | 0.1254 | 0.2637 | 0.1681 | 0.1839 | 0.1376 | 0.2383 | 0.8407 | 0.4566 |
| 15(S)-HEPE | 0.4564 | 0.0015 | 0.2618 | 0.2662 | 0.2317 | 0.8100 | 0.4595 | 0.4436 | 0.4049 | 0.5041 | 2.4807 | 0.0859 |
| 15d-D12,14-PGJ2 | 0.0519 | 0.0727 | 0.0757 | 0.0773 | 0.0691 | 0.0656 | 0.0365 | 0.0580 | 0.0492 | 0.0430 | -0.4185 | 0.3548 |
| 16-HDoHE | 0.4735 | 0.3834 | 0.4376 | 0.4385 | 0.5883 | 1.0466 | 0.8216 | 0.7498 | 0.6750 | 0.8657 | 0.7657 | **0.0032** |
| 16(17)-EpDPE | 0.0097 | 0.0126 | 0.0015 | 0.0080 | 0.0183 | 0.0015 | 0.0168 | 0.0176 | 0.0112 | 0.0111 | 0.0931 | 0.9567 |
| 17-HDoHE | 0.3356 | 0.1855 | 0.1926 | 0.2292 | 0.2906 | 1.4160 | 0.8540 | 0.7544 | 0.7190 | 1.0134 | 2.0075 | 0.0569 |
| 17(18)-EpETE | 0.0015 | 0.0015 | 0.0015 | 0.0052 | 0.0015 | 0.0015 | 0.0015 | 0.0143 | 0.0095 | 0.0015 | 0.8047 | 0.3915 |
| 18-carboxy dinor LTB4 | 0.0015 | 0.0015 | 0.0015 | 0.0015 | 0.0015 | 0.0015 | 0.0015 | 0.0035 | 0.0033 | 0.0015 | 0.4784 | 0.7164 |
| 18-HEPE | 0.0015 | 0.0015 | 0.0485 | 0.0015 | 0.0444 | 0.1355 | 0.0630 | 0.0540 | 0.0358 | 0.0956 | 3.7831 | **0.0227** |
| 19,20-DiHDoPE | 0.1499 | 0.2146 | 0.1943 | 0.2219 | 0.0830 | 0.2766 | 0.2833 | 0.2678 | 0.2857 | 0.3445 | 0.8160 | 0.3247 |
| 19(20)-EpDPE | 0.0298 | 0.0203 | 0.0284 | 0.0189 | 0.0378 | 0.0589 | 0.0572 | 0.0596 | 0.0581 | 0.0828 | 1.3371 | **0.0344** |
| 19(R)-OH PGF2a & 20-OH PGF2a | 0.0015 | 0.0015 | 0.0015 | 0.0015 | 0.0015 | 0.0015 | 0.0015 | 0.0015 | 0.0015 | 0.0042 | 0.1471 | 0.8619 |
| 20-HDoHE | 0.4596 | 0.5278 | 0.4812 | 0.5438 | 0.5025 | 1.0352 | 0.6613 | 0.6873 | 0.5496 | 0.7666 | 0.5077 | 0.6206 |
| 20-HETE | 0.0015 | 0.7678 | 0.8797 | 0.7748 | 1.0269 | 0.7847 | 0.5612 | 0.0015 | 0.0015 | 0.6713 | -2.0767 | 0.5743 |
| 20-hydroxy LTB4 | 0.0015 | 0.0015 | 0.0015 | 0.0015 | 0.0015 | 0.0060 | 0.0045 | 0.0068 | 0.0056 | 0.0052 | 1.8871 | **0.0000** |
| 4-HDoHE | 0.1009 | 0.1166 | 0.1178 | 0.1438 | 0.2012 | 0.3465 | 0.2442 | 0.3410 | 0.2387 | 0.3069 | 1.1445 | 0.2127 |
| 5-HEPE | 0.0015 | 0.0015 | 0.0015 | 0.0754 | 0.0854 | 0.6032 | 0.2281 | 0.3129 | 0.2129 | 0.3687 | 5.5169 | **0.0012** |
| 5-HETE | 1.1215 | 1.3183 | 1.0202 | 1.3526 | 1.6977 | 7.6603 | 4.6261 | 5.5748 | 3.2233 | 4.1028 | 1.8673 | **0.0000** |
| 5-oxoETE | 0.0881 | 0.0988 | 0.1752 | 0.1365 | 0.2091 | 0.2897 | 0.1589 | 0.1445 | 0.1171 | 0.1089 | 0.1396 | 0.9276 |
| 5,6-DiHETE(EPA) | 0.0015 | 0.0015 | 0.0015 | 0.0151 | 0.0015 | 0.0060 | 0.0064 | 0.0040 | 0.0015 | 0.0039 | 0.3693 | 0.5566 |
| 5,6-DiHETrE | 0.0116 | 0.0015 | 0.0015 | 0.0144 | 0.0052 | 0.0100 | 0.0155 | 0.0122 | 0.0106 | 0.0146 | 1.5328 | 0.0635 |
| 5(6)-EpETrE | 0.1433 | 0.1314 | 0.1363 | 0.1291 | 0.1562 | 0.0213 | 0.0206 | 0.0149 | 0.0145 | 0.0153 | -3.0064 | **0.0000** |
| 5(S)-HETrE | 0.0015 | 0.0089 | 0.0072 | 0.0015 | 0.0178 | 0.0373 | 0.0261 | 0.0200 | 0.0227 | 0.0159 | 2.6788 | **0.0001** |
| 5(S),12(S)-DiHETE | 0.1200 | 0.2146 | 0.1380 | 0.1362 | 0.1033 | 0.1249 | 0.0849 | 0.0582 | 0.0314 | 0.0868 | -1.0264 | 0.2599 |
| 5(S),15(S)-DiHEPE | 0.0015 | 0.0954 | 0.0015 | 0.0015 | 0.0350 | 0.1329 | 0.0300 | 0.0996 | 0.0238 | 0.1302 | 3.5506 | **0.0169** |
| 5(S),15(S)-DiHETE | 0.0015 | 0.0015 | 0.0015 | 0.0015 | 0.0015 | 0.0015 | 0.0015 | 0.0053 | 0.0015 | 0.0015 | 0.4188 | 0.5775 |
| 6-keto PGE1 | 0.0015 | 0.0172 | 0.0149 | 0.0154 | 0.0136 | 0.0015 | 0.0015 | 0.0015 | 0.0015 | 0.0045 | -1.9056 | 0.1313 |
| 6kPGF1a | 3.6156 | 6.1570 | 5.2604 | 5.9817 | 6.4715 | 0.0015 | 1.7440 | 5.9142 | 2.4927 | 0.0015 | -5.0720 | 0.1529 |
| 7-HDoHE | 0.0884 | 0.0780 | 0.0788 | 0.1264 | 0.1118 | 0.7193 | 0.4118 | 0.4132 | 0.4009 | 0.5177 | 2.4276 | **0.0000** |
| 7(8)-EpDPE | 0.0033 | 0.0054 | 0.0054 | 0.0074 | 0.0108 | 0.0088 | 0.0108 | 0.0103 | 0.0074 | 0.0061 | 0.5877 | 0.5061 |
| 8-HDoHE | 0.0938 | 0.1141 | 0.1405 | 0.0758 | 0.1676 | 0.2841 | 0.2376 | 0.2664 | 0.2122 | 0.2397 | 1.1040 | 0.2127 |
| 8-HEPE | 0.0015 | 0.0015 | 0.0015 | 0.0015 | 0.0498 | 0.0964 | 0.0731 | 0.0571 | 0.0464 | 0.1266 | 4.6703 | **0.0007** |
| 8-HETE | 1.0683 | 0.7753 | 0.9253 | 1.0993 | 0.9928 | 1.5678 | 1.3922 | 1.6630 | 1.1342 | 1.2788 | 0.6531 | **0.0107** |
| 8-isoPGF2a & 11bPGF2a | 0.0015 | 0.1033 | 0.0638 | 0.0015 | 0.0970 | 0.0015 | 0.0604 | 0.0015 | 0.0511 | 0.0015 | -1.2963 | 0.5674 |
| 8,9-DiHETrE | 0.0321 | 0.0314 | 0.0422 | 0.0336 | 0.0253 | 0.0356 | 0.0365 | 0.0381 | 0.0248 | 0.0404 | 0.1888 | 0.6889 |
| 8(9)-EpETrE | 0.0015 | 0.0015 | 0.0395 | 0.0015 | 0.0015 | 0.0015 | 0.0015 | 0.0015 | 0.0015 | 0.0015 | -0.7912 | 0.5305 |
| 8(S)-HETrE | 0.1078 | 0.1475 | 0.1140 | 0.1546 | 0.1888 | 0.4634 | 0.3899 | 0.3110 | 0.2754 | 0.3071 | 1.2792 | 0.1313 |
| 9-HEPE | 0.1265 | 0.0015 | 0.1298 | 0.1464 | 0.2553 | 0.9597 | 0.4311 | 0.0015 | 0.4201 | 0.7963 | 1.5886 | 0.4008 |
| 9-HETE | 0.0015 | 0.0015 | 0.0015 | 0.0015 | 0.0015 | 0.0015 | 0.0015 | 0.0015 | 0.0015 | 0.0015 | 0.0000 | 1.0000 |
| 9-HODE | 13.1826 | 17.9999 | 14.7776 | 15.0953 | 0.0015 | 0.0015 | 0.0015 | 0.0015 | 0.0015 | 0.0015 | -10.5488 | **0.0038** |
| 9-OxoODE | 4.1273 | 3.4742 | 3.2389 | 2.9265 | 3.3894 | 3.9542 | 2.6401 | 2.9667 | 1.4508 | 2.1740 | -0.4944 | 0.0751 |
| 9-OxoOTrE | 0.0664 | 0.0015 | 0.0438 | 0.0509 | 0.0824 | 0.1056 | 0.0609 | 0.0389 | 0.0122 | 0.0345 | 0.5596 | 0.7164 |
| 9,10-DiHOME | 2.3010 | 1.1255 | 1.1798 | 1.2964 | 0.5984 | 0.6614 | 0.6703 | 0.6431 | 0.4309 | 1.0578 | -0.7819 | **0.0453** |
| 9(10)-EpOME | 1.2526 | 0.9361 | 1.0894 | 0.7780 | 1.2517 | 1.6305 | 1.6015 | 1.6141 | 0.9926 | 1.6270 | 0.5808 | 0.6056 |
| 9(S)-HOTrE | 0.3026 | 0.1751 | 0.2697 | 0.2057 | 0.4403 | 0.4527 | 0.2916 | 0.3535 | 0.0015 | 0.2291 | -1.3280 | 0.3125 |
| Bicyclo PGE1 | 3.2853 | 5.6863 | 4.1312 | 3.1560 | 4.1412 | 3.5133 | 1.2590 | 2.1531 | 1.3609 | 1.5707 | -1.1935 | **0.0406** |
| Bicyclo PGE2 | 0.0401 | 0.0476 | 0.0262 | 0.0309 | 0.0386 | 0.1095 | 0.1103 | 0.1019 | 0.0622 | 0.0849 | 1.5213 | 0.0737 |
| LTB4 | 0.0283 | 0.0446 | 0.0495 | 0.0015 | 0.0388 | 0.3353 | 0.1991 | 0.2066 | 0.1534 | 0.1602 | 3.5575 | **0.0036** |
| LXA5 | 0.0015 | 0.0047 | 0.0015 | 0.0015 | 0.0013 | 0.0015 | 0.0005 | 0.0015 | 0.0015 | 0.0015 | -0.5892 | 0.5061 |
| PD1(n-3, DPA) | 3.8907 | 11.0489 | 4.1335 | 6.3073 | 1.6294 | 0.5997 | 0.2012 | 0.7238 | 0.3740 | 0.1925 | -3.5184 | **0.0005** |
| PGA2 | 0.3540 | 0.3827 | 0.3073 | 0.2715 | 0.3636 | 0.9826 | 0.8958 | 0.9887 | 0.5619 | 0.7750 | 1.3229 | **0.0012** |
| PGD2 | 0.0015 | 0.0015 | 0.0015 | 0.0015 | 0.0015 | 0.0015 | 0.3530 | 0.0015 | 0.2585 | 0.0015 | 3.1370 | 0.2876 |
| PGD3 | 0.0258 | 0.0956 | 0.1062 | 0.0015 | 0.0820 | 0.0015 | 0.0015 | 0.0015 | 0.0015 | 0.0015 | -4.2958 | **0.0168** |
| PGE1 | 0.1287 | 0.2363 | 0.1247 | 0.1645 | 0.1673 | 0.6447 | 0.3495 | 0.4746 | 0.3290 | 0.4364 | 1.4395 | **0.0003** |
| PGE2 | 10.9409 | 12.1142 | 10.5898 | 10.3617 | 10.0851 | 22.4021 | 16.6709 | 19.4951 | 13.3961 | 16.0917 | 0.6724 | **0.0344** |
| PGE3 | 0.0314 | 0.0405 | 0.0273 | 0.0380 | 0.0373 | 0.2317 | 0.1030 | 0.1534 | 0.0840 | 0.1314 | 2.2651 | **0.0117** |
| PGF1a | 0.0360 | 0.0483 | 0.0286 | 0.0170 | 0.0389 | 0.0558 | 0.0380 | 0.0292 | 0.0198 | 0.0284 | -0.0311 | 0.9840 |
| PGF2a | 1.3802 | 1.3584 | 1.2208 | 0.6895 | 1.2415 | 1.2546 | 0.8359 | 0.6983 | 0.6011 | 0.7527 | -0.5633 | 0.2366 |
| PGJ2 | 0.1498 | 0.1779 | 0.1303 | 0.1310 | 0.1644 | 0.5114 | 0.4423 | 0.4823 | 0.2810 | 0.3819 | 1.5096 | **0.0030** |
| RvD1 & AT-RvD1 | 0.1682 | 0.0015 | 0.0015 | 0.0015 | 0.1145 | 0.0015 | 0.0252 | 0.0947 | 0.0820 | 0.0491 | 1.5014 | 0.5775 |
| RvD5(n-3DPA) (7,17-DiHDoPE) | 0.0356 | 0.0633 | 0.0591 | 0.0926 | 0.0284 | 0.0015 | 0.0101 | 0.0199 | 0.0159 | 0.0136 | -2.3913 | **0.0390** |
| RvD6 (4,17-DiHDoHE) | 0.0015 | 0.0015 | 0.0015 | 0.0015 | 0.0015 | 0.0155 | 0.0015 | 0.0063 | 0.0050 | 0.0074 | 1.8876 | **0.0080** |
| RvE3 | 0.6231 | 1.9823 | 1.2107 | 1.5691 | 0.3361 | 0.0717 | 0.0423 | 0.1121 | 0.0559 | 0.0661 | -3.8630 | **0.0000** |
| tetranor 12-HETE | 0.0550 | 0.0659 | 0.0563 | 0.0908 | 0.0015 | 0.2502 | 0.2437 | 0.3082 | 0.2500 | 0.7878 | 3.3405 | **0.0114** |
| tetranor PGEM | 0.0022 | 0.0015 | 0.0018 | 0.0015 | 0.0011 | 0.0018 | 0.0010 | 0.0015 | 0.0021 | 0.0021 | -0.1183 | 0.9276 |
| TXB2 | 0.0015 | 3.6118 | 2.9670 | 2.9934 | 2.9566 | 3.2470 | 2.0547 | 3.2387 | 1.9785 | 2.6320 | 1.9204 | 0.4680 |
| TXB3 | 0.0015 | 0.0015 | 0.0015 | 0.0015 | 0.0015 | 0.0469 | 0.0216 | 0.0363 | 0.0015 | 0.0367 | 3.4134 | **0.0007** |

Table 2-1. Changes in inflammatory lipids during first 48h of pneumonic plague

C57BL/6J mice were infected with 10x the $LD_{50}$ of *Y. pestis* KIM5+ and lungs were harvested at 6, 12, 24, 36, and 48 h post-infection (n=5). Total lipids were isolated from homogenized lungs and lipids were quantified by LC-MS. Significant changes in lipid concentrations were observed in at least one time point for 63 lipids. Lipids that were below the limit of detection for all time points were excluded from statistical analysis.

2-2b. BLT1$^{-/-}$ mice are not more susceptible to pneumonic plague than C57BL/6J mice

LTB$_4$ is recognized by the high-affinity G-protein coupled receptor BLT1, which is expressed primarily by innate and adaptive immune cells.[183, 248] LTB$_4$-BLT1 engagement leads to host inflammatory immune responses such as chemotaxis, cytokine release, phagocytosis, and ROS production that contribute to the clearance of pathogens.[150, 249] Mice deficient in the expression of BLT1 cannot effectively respond to LTB$_4$ signaling and are generally more susceptible to infection.[185, 209, 250] Because I did not observe LTB$_4$ synthesis during the early stages of pneumonic plague, I hypothesized that BLT1$^{-/-}$ mice would not be more susceptible to *Y. pestis* infection. To test this hypothesis, I intranasally infected C57BL/6J and BLT1$^{-/-}$ mice with *Y. pestis* KIM5+ and measured bacterial numbers in the lungs at 12 and 24 h post-infection. Bacterial numbers were not significantly higher in BLT1$^{-/-}$ mice than C57BL/6J mice (Fig 2-2A). Furthermore, independent experiments with a *Y. pestis* strain with a luciferase bioreporter (*Y. pestis* CO92 Lux$_{pcysZK}$), which allows for monitoring bacterial proliferation via optical imaging and host survival in the same group,[251] showed no significant differences between the two mouse lines in bacterial proliferation at later time points or in the mean-time to death (Fig 2-2B and C). These data indicate that the loss of LTB$_4$-BLT1 signaling in BLT1$^{-/-}$ mice does not impact the infectivity of *Y. pestis*, further supporting that LTB$_4$ synthesis and signaling is disrupted during pneumonic plague.

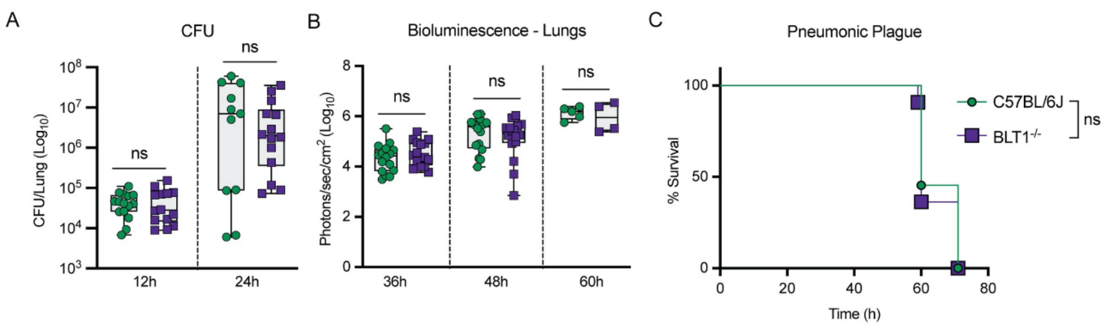


Figure 2-2. BLT1$^{-/-}$ mice are not more susceptible to pneumonic plague than C57BL/6J mice

(A) C57BL/6J (green circles) or BLT1$^{-/-}$ (purple squares) mice were infected intranasally with 10x the $LD_{50}$ of *Y. pestis* KIM5+ and lungs were harvested at 12 and 24 h post-infection. Bacterial proliferation within the lungs was determined by CFU. Each symbol represents an indivdual mouse and the box plot represents the median of the group ± the range. Combined data from two independent experiments. (B-C) C57BL/6J (green circles) or BLT1$^{-/-}$ (purple squares) mice were infected intranasally with 10x the $LD_{50}$ of *Y. pestis* CO92 $LUX_{pcysZK}$. (B) Bacterial proliferation in the lungs as a function of bioluminescence. Each symbol represents an indivdual mouse and the box plot represents the median of the group ± the range. Combined data from two independent experiments. (C) Survival curves of mice from B (n=15). For A and B, T-test with Mann-Whitney's *post hoc* test indicated no statistically significant (ns) differences between C57BL/6J and BLT1$^{-/-}$ groups. For C, Log-Rank anlysis revealed no statistically signficant (ns) differences in surival between the two groups.

## 2-2c. Exogenous $LTB_4$ treatment limits *Y. pestis* proliferation *in vivo*

Because $LTB_4$ synthesis and signaling appears to be disrupted during infection, I next asked if exogenous administration of $LTB_4$ could alter infection. To test this hypothesis, a previously described peritoneal model was used that allows for accurate administration of $LTB_4$ and easy recovery of both elicited leukocytes and bacteria via lavage.[252] As described previously, intraperitoneal administration of $LTB_4$ resulted in an increase in the neutrophil population within the peritoneal cavity in C57BL/6J mice as early as 1 h post-administration (Figs 2-3A and 2-4).[252] When challenged intraperitoneally with *Y. pestis* KIM5+ after $LTB_4$ administration, a significant decrease in the number of viable bacteria was recovered from $LTB_4$-treated animals, approaching the limit of detection, as compared to PBS-treated animals 3 h post-infection (Fig 2-3B; $p \leq 0.0001$). Neutrophil numbers also remained significantly elevated in the $LTB_4$-treated animals at 3 h post-infection compared to PBS-treated animals (Fig 2-3C; $p \leq 0.05$). Moreover, bacterial clearance was dependent on $LTB_4$ signaling, as $LTB_4$ treatment of $BLT1^{-/-}$ mice did not alter bacterial or neutrophil numbers at 3 h post-infection compared to PBS-treated C57BL/6J mice (Fig 2-3B and C). Together, these data indicate that $LTB_4$-mediated recruitment and activation of leukocytes can improve the host response to *Y. pestis*.

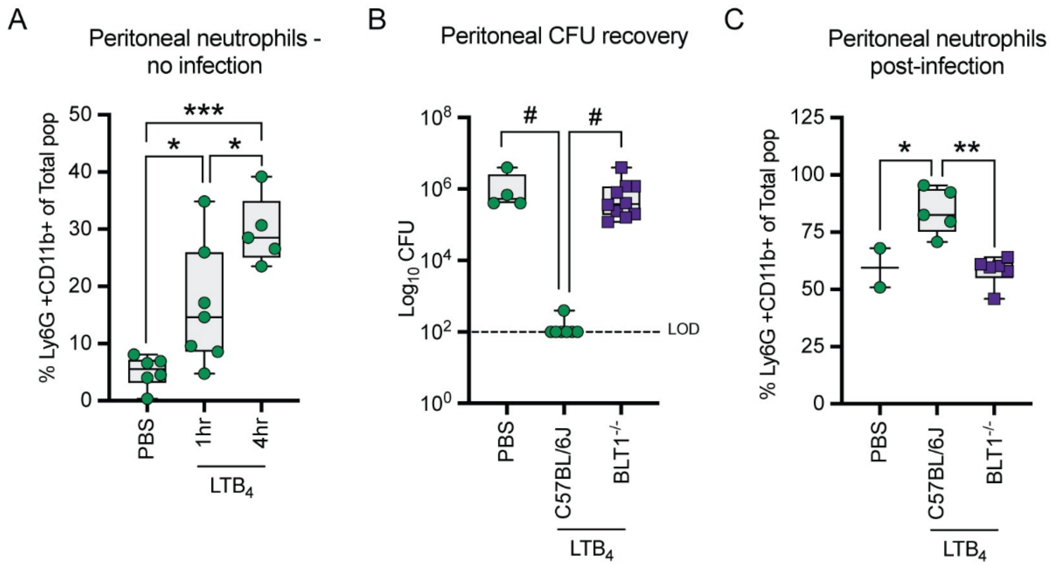


Figure 2-3. $LTB_4$ treatment improves host killing of *Y. pestis*

(A) C57BL/6J mice were administered 1 x DPBS (PBS) or 10 nmol $LTB_4$ intraperitoneally and changes in neutrophil populations (Ly6G+CD11b+) were measured at 1 or 4 h post-treatment. (B) C57BL/6J (green circles) or $BLT1^{-/-}$ (purple squares) mice administered DPBS or 10 nmol $LTB_4$ were infected 1 h later with $10^5$ CFU of *Y. pestis* KIM5+ and bacterial numbers in the peritoneal cavities were enumerated 3 h post-inoculation. LOD = Limit of detection. (C) Neutrophil populations from a subset of animals from B. Each symbol represents an indivdual mouse and the box plot represents the median of the group ± the range. Combined data from three independent experiments. One-way ANOVA with Tukey's *post hoc* test compared to each condition. *=p≤0.05, **=p≤0.01, ***=p≤0.001, #=p≤0.0001.

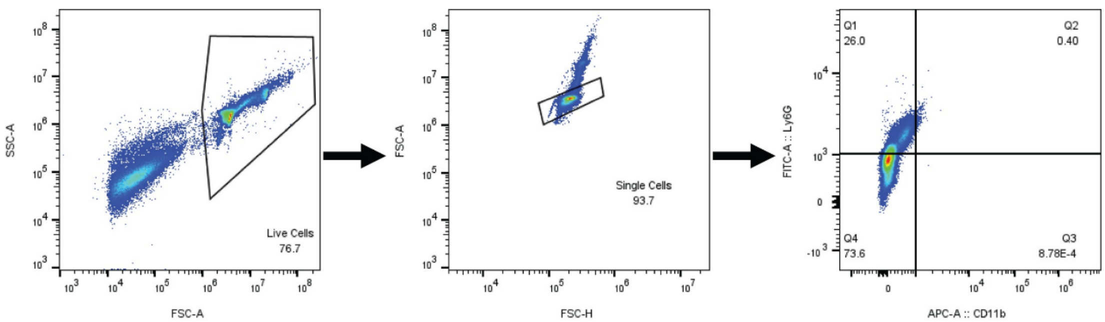


<u>Figure 2-4. Gating strategy for identifying neutrophil populations in the peritoneal cavity</u>

Example gating strategy from the PBS-treated group from Fig 2-3.

2-2d. Neutrophils do not synthesize $LTB_4$ in response to *Y. pestis*

Because neutrophils are robust sources of $LTB_4$,[150] are the primary cells with which *Y. pestis* interacts during the first 24 h of pneumonic plague,[19] and *Y. pestis* inhibits $LTB_4$ synthesis by human neutrophils,[93] I next sought to determine if the $LTB_4$ response by neutrophils differed between *Y. pestis* and other bacteria. When bone marrow-derived neutrophils (BMNs) from C57BL/6J mice were stimulated with *E. coli, S. enterica* Typhimurium, or a *K. pneumoniae manC* mutant (unable to synthesize a capsule), $LTB_4$ synthesis was significantly induced within 1 h of infection (Fig 2-5A; $p \leq 0.0001$). However, infection with *Y. pestis* did not elicit $LTB_4$ synthesis, even when the MOI was increased to 100 bacteria per neutrophil (Fig 2-5B). Similar phenotypes were observed during infection of human peripheral blood neutrophils (hPMNs), recapitulating my lab's previously published data for *Y. pestis* (Fig 2-5C and D).[93] Importantly, the absence of $LTB_4$ synthesis did not appear to be due to *Y. pestis* induced cell death, as no significant changes in cell permeability or cytotoxicity were observed during *Y. pestis* infections at an MOI of 20 when compared to uninfected neutrophils (Fig 2-6A and B). Even at an MOI of 100, while cell permeability appeared slightly elevated in *Y. pestis*-infected murine neutrophils compared to uninfected cells (Fig 2-6C; 9% vs. 28%), overall cytotoxicity was lower in *Y. pestis*-infected cells (Fig 2-6D; 12% vs. 4%). Similarly, *Y. pestis* did not induce elevated permeability or cytotoxicity in human neutrophils (Fig 2-6E and F). These data demonstrate that while neutrophils can rapidly synthesize $LTB_4$ in response to other bacterial pathogens, neither murine nor human neutrophils appear to synthesize $LTB_4$ in response to *Y. pestis.*

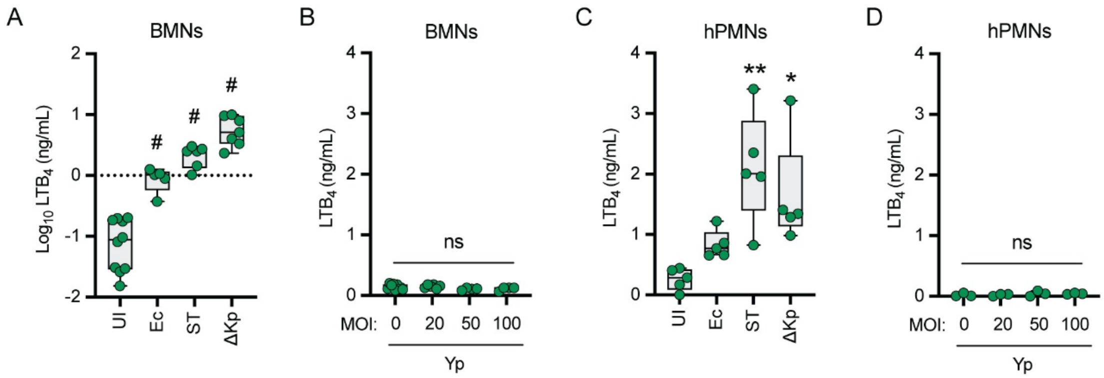


Figure 2-5. Neutrophils do not synthesize LTB$_4$ in response to *Y. pestis*

(A-B) Murine (BMNs) or (C-D) human (hPMNs) neutrophils were infected with *E. coli* DH5α (Ec), *S. enterica* Typhimurium LT2 (ST), or *K. pneumoniae manC* (ΔKp) at an MOI of 20, or with *Y. pestis* (Yp) at increasing MOIs. LTB$_4$ was measured from supernatants 1h post infection by ELISA. Each symbol represents an independent biological infection and the box plot represents the median of the group ± the range. UI or 0 = uninfected. One-way ANOVA with Dunnett's *post hoc* test compared to uninfected. *=p≤0.05, **=p≤0.01, #=p≤0.0001.

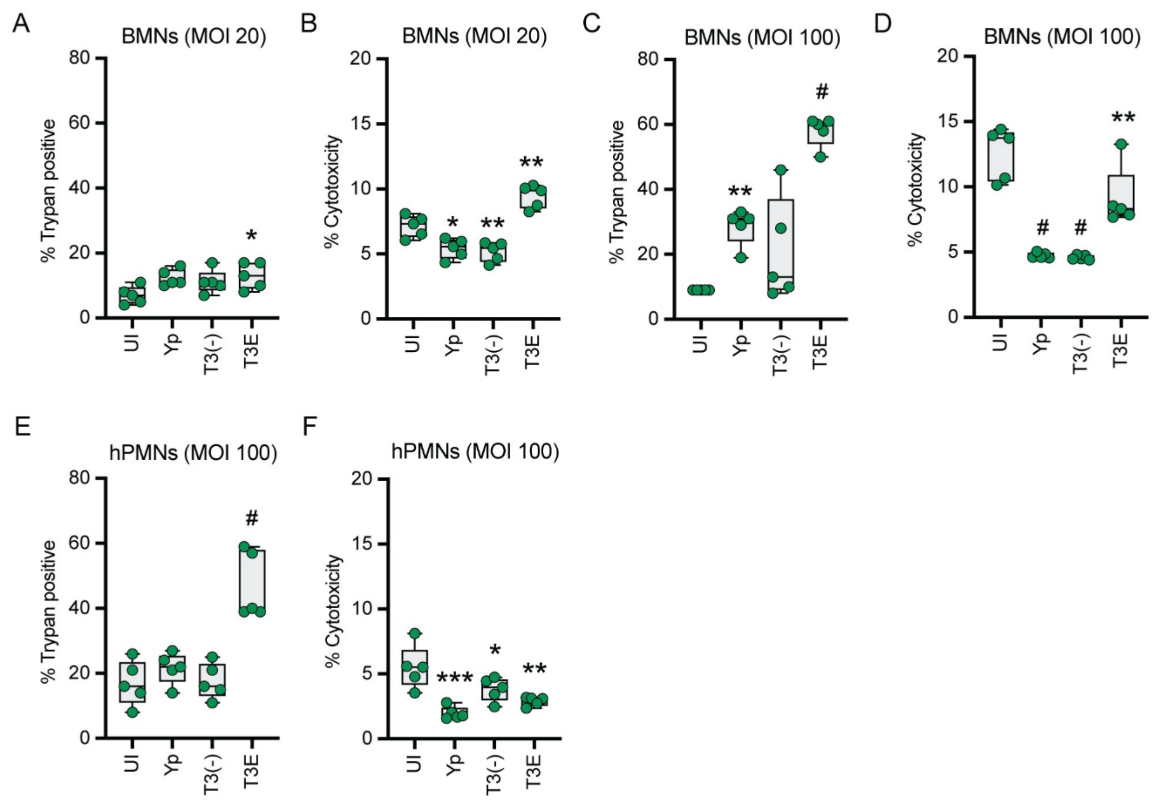


Figure 2-6. Absence of $LTB_4$ response to *Y. pestis* is not due to cell death

(A-D) Murine (BMNs) or (E-F) human (hPMNs) neutrophils were infected with *Y. pestis* (Yp) or mutants that either lacked the Yop effectors (T3E) or lacked the Yop effectors and the T3SS [T3(-)] at the indicated MOIs and cell permeability as a function of trypan exclusion or cytotoxicity as a function of LDH release was measured at 1 h post-infection. Each symbol represents an independent biological infection and the box plot represents the median of the group ± the range. UI = uninfected. One-way ANOVA with Dunnett's *post hoc* test compared to uninfected. *=p≤0.05, **=p≤0.01, ***=p≤0.001, #=p≤0.0001.

2-2e. *Y. pestis* actively inhibits $LTB_4$ synthesis

Seven Yop effectors are secreted via the T3SS,[103, 109, 136, 137] and Pulsifer et al.[93] previously showed Yop effector-mediated inhibition of $LTB_4$ synthesis in human neutrophils by YpkA, YopE, YopJ, YopH, and YopT at an MOI of 100. However, Yop inhibition of $LTB_4$ synthesis by murine neutrophils has not been previously investigated, nor whether the same Yop effectors are sufficient to inhibit $LTB_4$ synthesis at a lower MOI. Therefore, murine and human neutrophils were infected at an MOI of 20 with a *Y. pestis* mutant strain that expresses the T3SS but lacks all seven Yop effectors (*Y. pestis* T3E).[111] In contrast to *Y. pestis* infected cells, I observed a significant increase in $LTB_4$ synthesis in response to the *Y. pestis* T3E strain, indicating that the Yop effectors inhibit synthesis (Fig 2-7A and B; $p \leq 0.0001$). Moreover, when neutrophils were simultaneously infected with *Y. pestis* and the *Y. pestis* T3E mutant or *Y. pestis* and the *K. pneumoniae manC* mutant, $LTB_4$ levels were significantly lower than *Y. pestis* T3E or *K. pneumoniae* only infections (Fig 2-7C-F; $p \leq 0.0001$). To determine if individual Yop effectors were sufficient to inhibit synthesis, murine neutrophils were infected with *Y. pestis* strains that expressed only one Yop effector.[111] $LTB_4$ synthesis was significantly decreased if *Y. pestis* expressed YpkA, YopE, YopH, or YopJ, and an intermediate phenotype was observed during infection with a strain expressing YopT (Fig 2-7G). These phenotypes recapitulated those previously reported for human neutrophils.[93] Together these data confirm that *Y. pestis* is not simply evading immune recognition but is actively inhibiting $LTB_4$ synthesis via the activity of multiple Yop effectors.

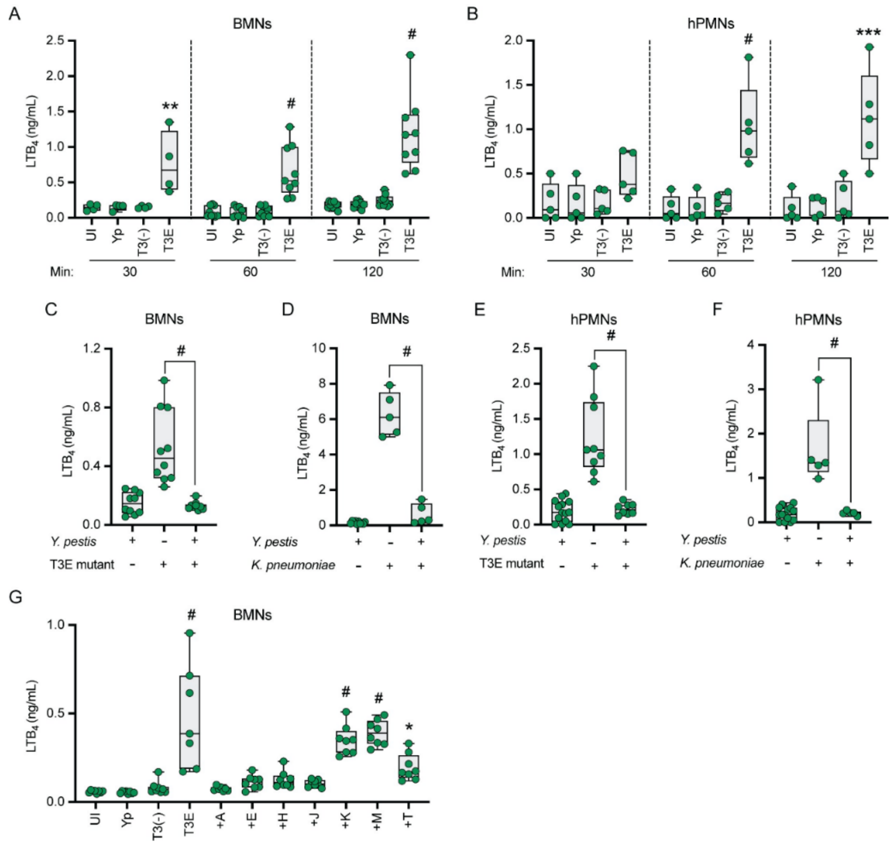


Figure 2-7. *Y. pestis* actively inhibits $LTB_4$ synthesis

(A) Murine (BMNs) or (B) human (hPMNs) neutrophils were infected with *Y. pestis* (Yp) or mutants that either lacked the Yop effectors (T3E) or the Yop effectors and the T3SS [T3(-)] at an MOI of 20 and $LTB_4$ was measured at 30, 60, or 120 min. (C and D) Murine (BMNs) or (E and F) human (hPMNs) neutrophils were co-infected with the indicated bacteria at a combined MOI of 20 and $LTB_4$ was measured at 60 min post-infection. (G) Murine neutrophils (BMNs) were infected with Yp, T3E, T3(-),or *Y. pestis* strains expressing only one Yop effector (+A = YpkA; +E = YopE; +H = YopH; +J = YopJ; +K = YopK; +M = YopM; or +T = YopT) at an MOI of 20 and $LTB_4$ was measured at 60 min post-infection. Each symbol represents an independent biological infection and the box plot represents the median of the group ± the range. UI = uninfected. One-way ANOVA with Dunnett's *post hoc* test compared to uninfected for A, B, and G, or Tukey's *post hoc* test compared to each condition for C, D, E, and F. *=p≤0.05, **=p≤0.01, ***=p≤0.001, #=p≤0.0001.

2-2f. Neutrophils synthesize $LTB_4$ in response to the *Y. pestis* T3SS in the absence of the Yop effectors

Components of the T3SS are pathogen-associated molecular patterns (PAMPs) that are recognized by innate immune cells,[234, 253, 254] suggesting that T3SS interactions with neutrophils may be responsible for the synthesis of $LTB_4$ during infections with the *Y. pestis* T3E strain. To test this hypothesis, I infected murine and human neutrophils with a *Y. pestis* strain lacking the pCD1 plasmid encoding the entire Ysc T3SS [*Y. pestis* $T3^{(-)}$]. Unlike infections with *Y. pestis* T3E, I did not observe an increase in $LTB_4$ synthesis by neutrophils during interactions with *Y. pestis* $T3^{(-)}$ compared to uninfected or *Y. pestis* infected cells, even after 2 h of infection (Fig 2-7A and B). Importantly, *Y. pestis* $T3^{(-)}$ infection did not appear to result in increased neutrophil cell permeability or cytotoxicity (Fig 2-6). To independently test that the T3SS is required to induce $LTB_4$ synthesis, *Y. pestis* T3E was cultured under conditions that alter the expression of the T3SS prior to infection of neutrophils.[4, 26, 56] Measuring expression of the LcrV protein as a proxy for overall T3SS expression confirmed decreased T3SS expression in cultures grown at 26°C compared to 37°C (Figs 2-8A and 2-9A). As predicted by the *Y. pestis* $T3^{(-)}$ data, $LTB_4$ synthesis was not observed from neutrophils infected with *Y. pestis* T3E strains grown at 26°C, while synthesis was induced from bacteria cultured at 37°C (Fig 2-9B). No difference in bacterial viability between any of the *Y. pestis* strains was observed during the time frame of the experiment, diminishing the possibility that differences in neutrophil killing was responsible for these phenotypes (Fig 2-8B). Finally, neutrophils were infected with a *Y. pestis* T3E *yopB* mutant, which retains the other pCD1 encoded genes, but is defective in expression of the translocase that directly interacts with the host cell and is required for injection of the effector proteins.[56, 67, 68, 255, 256] Similar to the *Y. pestis* $T3^{(-)}$ strain, the *Y. pestis* T3E *yopB* mutant did not induce $LTB_4$ synthesis, but synthesis was restored by *yopB* complementation (*yopB*::c*yopB*) (Fig 2-9C). Together, these data indicate that neutrophils recognize components of the *Y. pestis* T3SS as PAMPs, leading to the induction of $LTB_4$ synthesis, but only in the absence of the Yop effectors.

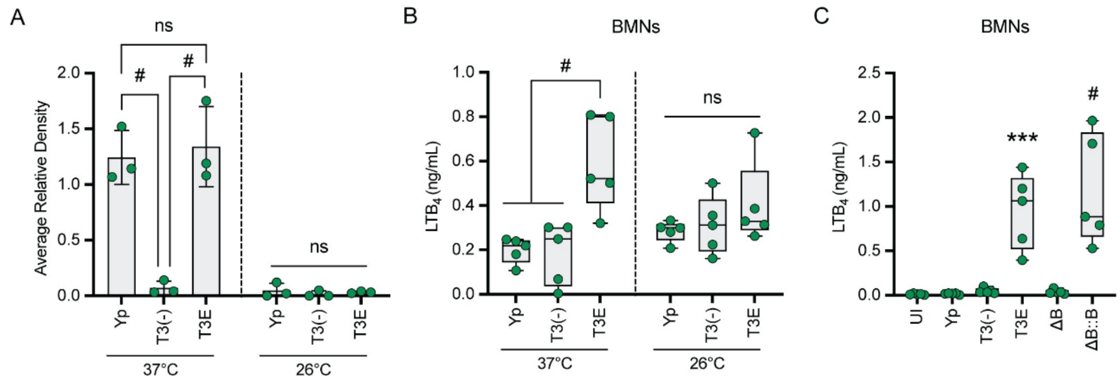


Figure 2-8. Neutrophils synthesize $LTB_4$ in response to the *Y. pestis* T3SS in the absence of the Yop effectors

(A) Relative expression of LcrV based on western blots normalized to total protein loaded from bacteria cultured at 37 or 26$^{o}$C. (B) Murine neutrophils (BMNs) were infected (MOI of 20) with *Y. pestis* (Yp) or mutants that either lacked the Yop effectors (T3E) or the Yop effectors and the T3SS [T3(-)] cultured at 37 or 26$^{o}$C and $LTB_4$ was measured at 60 min post-infection. (C) Murine neutrophils (BMNs) were infected (MOI of 20) with Yp, T3E, T3(-), a *yopB* mutant in the T3E background ($\Delta$B), or $\Delta$B complemented with *yopB* ($\Delta$B::B) cultured at 37$^{o}$C and $LTB_4$ was measured at 60 min post-infection. (A) Each symbol represents an independent biological infection and and the bar graph represents the mean ± the standard deviation. (B-C) Each symbol represents an independent biological infection and the box plot represents the median of the group ± the range. One-way ANOVA with Tukey's *post hoc* test compared to each condition for A and B and Dunnett's *post hoc* test compared to uninfected for C. ns = not significant, ***=p≤0.001, #=p≤0.0001.

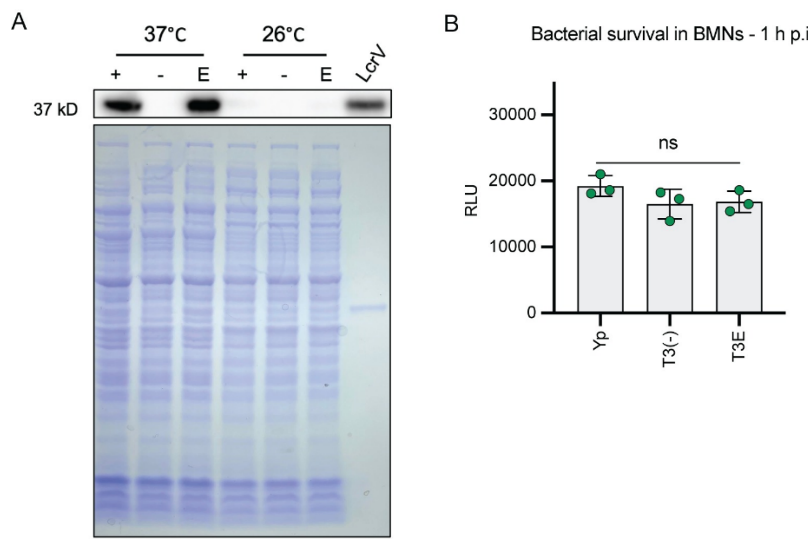


Figure 2-9. Expression of T3SS needle required for $LTB_4$ synthesis in response to *Y. pestis*

(A) Representative western blot and Coomassie images of *Y. pestis* lysates (0.1 OD; 1 OD = 3 x $10^8$ CFU) harvested from cultures grown at 37°C or 26°C used for densitometry reported in Fig 6A. (B) Bacterial viability measured by a function of bioluminescence after 1 h infection of neutrophils. + or Yp = *Y. pestis*, - or T3(-) = *Y. pestis* T3(-); E or T3E = *Y. pestis* T3E; LcrV = 0.2 µg recombinant LcrV protein. Each symbol represents an independent biological infection and and the bar graph represents the mean ± the standard deviation. One-way ANOVA with Tukey's *post hoc* test compared to each condition. ns = not significant.

2-2g. *Y. pestis* inhibition of $LTB_4$ synthesis is conserved during interactions with other leukocytes

In addition to neutrophils, two other lung resident leukocytes that can produce $LTB_4$ are mast cells and macrophages.[242] To determine if *Y. pestis* inhibits $LTB_4$ synthesis by these two cell types, bone marrow-derived mast cells and macrophages were isolated from C57BL/6J mice and infected with *Y. pestis*, *Y. pestis* T3E, or *Y. pestis* $T3^{(-)}$. I observed no synthesis of $LTB_4$ by mast cells, even after 2 h of interacting with *Y. pestis* (Fig 2-10A). However, $LTB_4$ synthesis was significantly elevated in the absence of the Yop effectors (Fig 2-10A; $p \leq 0.01$), reaching levels similar to that of mast cells stimulated with crystalline silica, a potent inducer of $LTB_4$ synthesi.[153, 190] $LTB_4$ synthesis by mast cells was also dependent on the presence of the T3SS, as the *Y. pestis* $T3^{(-)}$ strain did not induce $LTB_4$ synthesis (Fig 2-10A). For macrophages, previous reports indicate that polarization influences the ability to produce $LTB_4$, with M1-polarized macrophages better able to synthesize $LTB_4$ in response to bacterial ligands than M2-polarized cells.[257] Therefore, I measured $LTB_4$ synthesis of both M1- and M2-polarized macrophages (Fig 2-11). Again, I observed no significant synthesis of $LTB_4$ by either macrophage population during interactions with *Y. pestis*, even after 4 h post-infection (Fig 2-10B and C). However, significant synthesis of $LTB_4$ was observed in M1-polarized macrophages in response to the *Y. pestis* T3E strain, which was dependent on the presence of the T3SS (Fig 2-10B; $p \leq 0.0001$). As suggested by previous reports,[258] I did not observe significant changes in $LTB_4$ synthesis by M2-polarized macrophages during interactions with any of the *Y. pestis* strains tested (Fig 2-10C). Together, these data indicate that mast cells and M1-polarized macrophages can synthesize $LTB_4$ in response to the *Y. pestis* T3SS, but the activity of the Yop effectors inhibits this response.

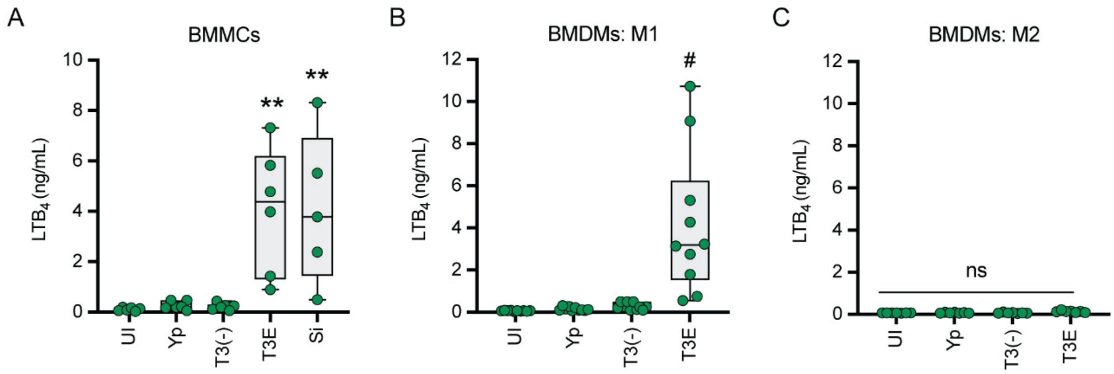


Figure 2-10. Lack of $LTB_4$ response to *Y. pestis* is conserved in other leukocytes

(A) Murine bone-marrow derived mast cells (BMMCs) were infected with *Y. pestis* (Yp) or with mutants that either lacked the Yop effectors (T3E) or the Yop effectors and the T3SS [T3(-)] at an MOI of 20, or treated with 100 mg/cm$^2$ crystalline silica (Si) and $LTB_4$ was measured at 2 h post-infection. (B and C) Murine bone-marrow derived macrophages (BMDMs) differentiated towards (B) M1 or (C) M2 phenotypes were infected with Yp, T3E, or T3(-) at an MOI of 20 and $LTB_4$ was measured at 4 h post-infection. UI = uninfected. Each symbol represents an independent biological infection and the box plot represents the median of the group ± the range. One-way ANOVA with Dunnett's post hoc test compared to uninfected. **=p≤0.01, #=p≤0.0001.

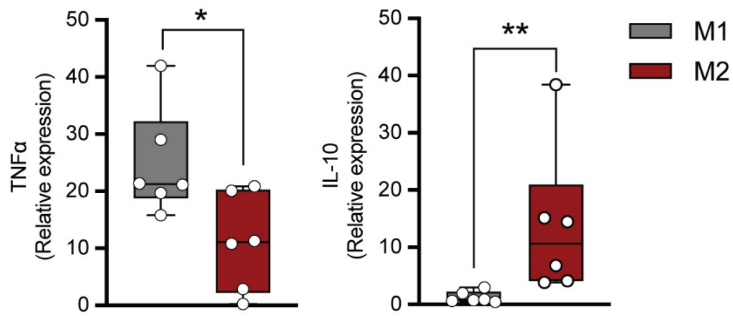


Figure 2-11. M1 polarization required for macrophage synthesis towards *Y. pestis* T3SS

qRT-PCR measurement of TNF-$\alpha$ and IL-10 in murine BMDMs differentiated towards M1 or M2. Each symbol represents an independent biological sample and the box plot represents the median of the group ± the range. T-test with Mann-Whitney's *post hoc* test. *=p≤0.05, **=p≤0.01.

## 2-3. Discussion

A hallmark manifestation of plague is the absence of inflammation during the early stages of infection, which is critical to *Y. pestis* virulence.[31, 236, 238, 254] While *Y. pestis* has been shown to actively dampen the host immune response, there is a gap in our understanding of the role of lipid mediators of inflammation during plague. I sought to better define the host inflammatory lipid mediator response during pneumonic plague and expands our current understanding of how *Y. pestis* manipulates the immune system. During the earliest stages of infection, the host appears unable to initiate a timely $LTB_4$ response (Fig 2-1). Moreover, I demonstrated that exogenous treatment with $LTB_4$ can alter the host response to *Y. pestis* (Fig 2-3), suggesting that $LTB_4$ manipulation by *Y. pestis* contributes to disease outcome. Because $LTB_4$ is a potent chemoattractant crucial for rapid inflammation,[37, 241, 259] a delay in $LTB_4$ synthesis during plague likely has a significant impact on the ability of the host to mount a robust inflammatory response needed to inhibit *Y. pestis* colonization. First, in the absence of $LTB_4$, sentinel leukocytes will not undergo autocrine signaling via $LTB_4$-BLT1. Because $LTB_4$-BLT1 engagement activates antimicrobial programs in leukocytes,[37, 195, 241, 250, 260, 261] the absence of autocrine signaling diminishes the ability of sentinel leukocytes directly interacting with *Y. pestis* to mount an effective antimicrobial response to kill the bacteria. $LTB_4$ synthesis is also regulated by BLT1 signaling, and autocrine signaling is required to amplify the production of $LTB_4$ needed to rapidly recruit additional tissue-resident immune cells to the site of infection.[37, 227, 241, 260, 262] Therefore, the normal feed-forward amplification of $LTB_4$ synthesis, which is key for a rapid response to a bacterial infection, will also be inhibited by *Y. pestis*. Second, because $LTB_4$ is required for neutrophil swarming,[223, 227, 228] *Y. pestis* will also inhibit this key inflammatory mechanism.[21] Neutrophil swarming is required to contain bacteria at initial sites of infection.[225, 226] Thus, while individual neutrophils may migrate towards sites of *Y. pestis* infection, effective neutrophil swarming of large populations of neutrophils will be diminished. Finally, $LTB_4$ is a diffusible molecule that can induce the inflammatory cascade in bystander cells.[37, 263] Thus, while *Y. pestis* can inhibit cytokine and chemokine expression by cells with which it directly interacts,[6, 8] inhibition of $LTB_4$ synthesis likely also delays subsequent release of molecules by cells that do not directly interact with the bacteria. Together with the bacteria's other immune evasion mechanisms, inhibition of $LTB_4$ synthesis is likely another significant contributor to the generation of the non-inflammatory environment associated with the early stages of pneumonic plague.[6, 8, 236] Incorporating these new $LTB_4$ data with published findings from other laboratories,[6, 8, 236] I have updated my lab's working model of *Y. pestis* inhibition of inflammation during pneumonic plague (Fig 2-12).

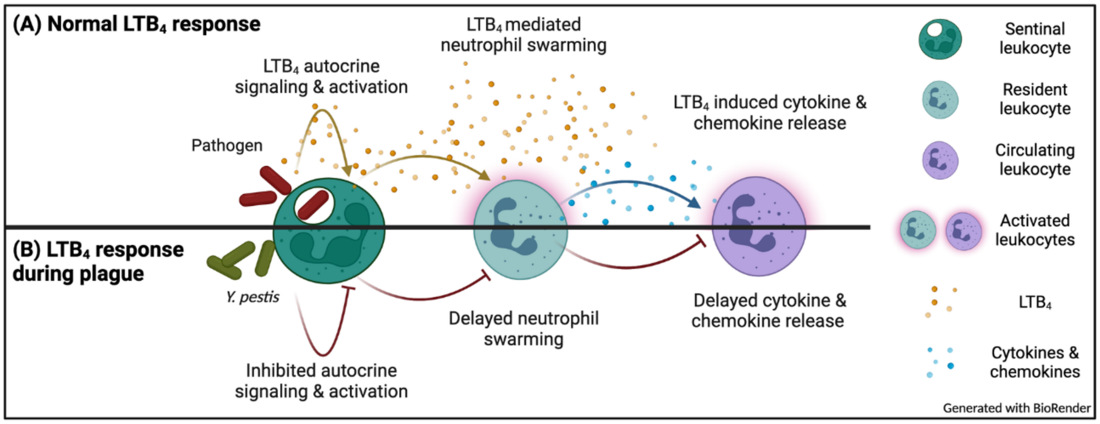


Figure 2-12. Working model for inhibition of the inflammatory cascade during plague

(A) Normal response by sentinel leukocytes results in rapid production of $LTB_4$ that leads to autocrine signaling, neutrophil swarming, and induction of cytokine and chemokine release. (B) *Y. pestis* inhibits the production of $LTB_4$ via the action of the Yop effectors, which delays resident neutrophil recruitment and subsequent production of cytokines and chemokines needed for inflammation.

These studies also revealed that components of the T3SS trigger $LTB_4$ synthesis by leukocytes. Because my lab's previous work with human samples indicated that neutrophils synthesize $LTB_4$ in response to *Y. pestis* in the absence of the T3SS,[93] I was initially surprised that I did not observe $LTB_4$ synthesis by murine neutrophils to the *Y. pestis* $T3^{(-)}$ strain. However, when I infected human neutrophils with lower MOIs, I observed that they also did not synthesize $LTB_4$ in the absence of the T3SS (Fig 2-13). Under these infection conditions, neutrophils from both species only produced $LTB_4$ in response to *Y. pestis* expressing the T3SS but none of the Yop effectors. These data support that components of the T3SS are PAMPs produced by *Y. pestis* that are not only recognized by macrophages[57] but also by neutrophils. While previous studies have indicated that the Yop effectors are PAMPs in neutrophils,[264, 265] to my knowledge the data presented here represent the first example that non-effector components of the *Y. pestis* T3SS can also be recognized as a PAMP by neutrophils. In macrophages, in the absence of the Yop effectors, interactions with the T3SS, notably the translocon proteins YopB and YopD, induce NLRP3-dependent activation of the caspase-1 inflammasome, IL1-$\beta$ secretion, and pyroptosis,[68, 89] suggesting that inflammasome activation may contribute to $LTB_4$ synthesis during interactions with *Y. pestis* T3E. However, whether inflammasome activation is required for the *Y. pestis* T3SS-mediated $LTB_4$ synthesis remains unclear, as $LTB_4$ synthesis in response to other stimuli is not dependent on inflammasome activation.[153, 219, 220] Interestingly, infection of neutrophils with a strain of *Y. pestis* that only expresses YopK, which has been reported to inhibit NLRP3 inflammasome activation in macrophages,[67, 68] does not inhibit $LTB_4$ synthesis (Fig 2-7G),[93] supporting the possibility that $LTB_4$ synthesis may not be dependent on inflammasome activation in neutrophils. Future studies using neutrophils from mice defective in specific NLRs and caspases will allow us to definitively determine if inflammasome activation is required for $LTB_4$ synthesis in response to the *Y. pestis* T3SS. I have also confirmed that four Yop effectors, YpkA, YopE, YopJ, and YopH are sufficient to inhibit $LTB_4$ synthesis by both human and murine neutrophils. Synthesis of $LTB_4$ requires MAPK- and $Ca^{2+}$-dependent activation of $cPLA_2$ and 5-LOX.[152, 266] Previous work, primarily in macrophages, has shown that both of these signaling pathways are efficiently inhibited by these four Yop effectors,[42, 56, 75, 87, 98, 100, 108] suggesting that subversion of MAPK and $Ca^{2+}$ signaling by *Y. pestis* is responsible for inhibition of $LTB_4$ synthesis. Supporting this hypothesis, Pulsifer et al.[93] demonstrated that inhibition of ERK phosphorylation by YopJ is sufficient to inhibit $LTB_4$ synthesis by human neutrophils. Defining the specific molecular mechanisms employed by YpkA, YopE, and YopH to inhibit $LTB_4$ synthesis will be important in better understanding the *Y. pestis* virulence.

One of the key antimicrobial mechanisms inhibited by the Yop effectors is phagocytosis,[4, 26, 41, 44] and Hedge et al.[153] have previously shown that phagocytosis of crystalline silica is required for $LTB_4$ synthesis in that model of sterile inflammation. These data raise the possibility that inhibition of phagocytosis by *Y. pestis* may not only inhibit bacterial killing, but $LTB_4$ synthesis and rapid initiation of inflammatory programing in neutrophils. Studies to delineate the contribution of phagocytosis to $LTB_4$ synthesis are ongoing, but the differences in $LTB_4$ synthesis by cells infected with *Y. pestis* T3E and *Y. pestis* $T3^{(-)}$ suggest that phagocytosis alone is not sufficient to trigger $LTB_4$ synthesis in the absence of proper PAMPs, in this case components of the T3SS. Moreover, the lack of $LTB_4$ synthesis in response to *Y. pestis* $T3^{(-)}$ also differed from what I observed for other gram-negative bacteria without T3SS (*E. coli* and *K. pneumoniae*), indicating that *Y. pestis* may also mask other potential gram-negative PAMPS that would typically be recognized by neutrophils. These data support that *Y. pestis* has evolved both active (via the Yop effectors) and passive mechanisms to evade immune recognition and induction of $LTB_4$ synthesis. It is worth noting that unlike human neutrophils, murine neutrophils did not appear to synthesize $LTB_4$ during infections with the $T3^{(-)}$ strain at high MOIs (Fig 2-13). Differences in neutrophil responses between the two species have been well documented,[267-271] but these observations merit further investigation into

$LTB_4$ responses by human neutrophils using higher MOIs to determine if human neutrophils are able to recognize other PAMPs during *Y. pestis* infection.

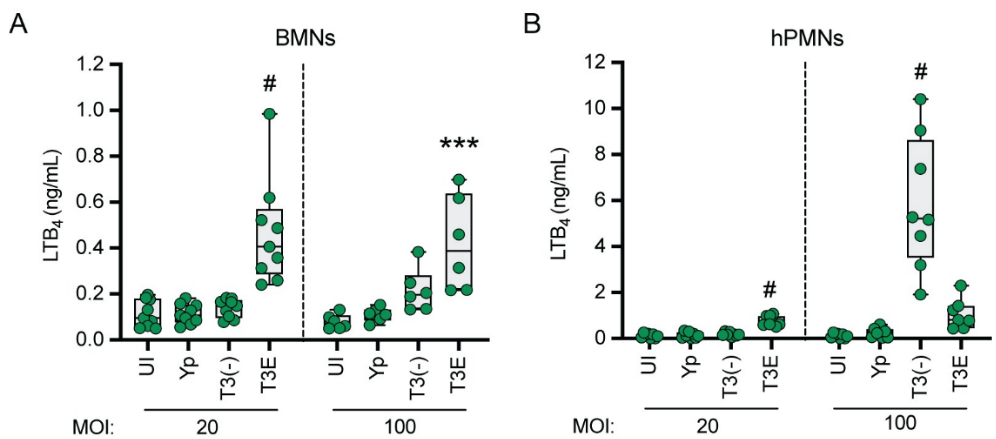


Figure 2-13. Differential recognition of T3$^{(-)}$ *Y. pestis* between human and mice neutrophils

(A) Murine (BMNs) or (B) human (hPMNs) neutrophils were infected with *Y. pestis* (Yp) or mutants that either lacked the Yop effectors (T3E) or lacked the Yop effectors and the T3SS [T3(-)] at the indicated MOIs and $LTB_4$ was measured 1 h post-infection. Each symbol represents an independent biological infection and the box plot represents the median of the group ± the range. UI = uninfected. One-way ANOVA with Dunnett's *post hoc* test compared to uninfected. ***=p≤0.001, #=p≤0.0001.

Finally, while I focused primarily on $LTB_4$ in this chapter, I also observed changes in the synthesis of other lipids during plague that merit future considerations (Table 2-1). The rapid cyclooxygenase response raises questions about whether prostaglandins are protective or detrimental during pneumonic plague. Historically, prostaglandins were thought to promote inflammation, but these mediators appear more nuanced under closer scrutiny and can just as likely inhibit inflammation as well as participate in normal development physiology without eliciting inflammation.[246, 247, 272] The prostaglandins I observed as being significantly elevated during the non-inflammatory stage of pneumonic plague - $PGA_2$, $PGD_2$, $PGE_2$, and $PGJ_2$ - have been shown to inhibit inflammation in various models, especially as concentrations increase.[246, 247, 273-275] $PGE_2$ can inhibit NADPH oxidase activity during infection with *K. pneumoniae,* which suppressed bacterial killing,[276] and directly counteracts the proinflammatory activities of $LTB_4$.[277, 278] The phagocytic index of $LTB_4$-stimulated rat alveolar macrophages (AMs) is reduced when co-stimulated with $PGE_2$.[278] Moreover, AMs treated with $PGE_2$ showed a 40% reduction in $LTB_4$ synthesis when stimulated with an ionophore known to induce a strong $LTB_4$ response.[277] This inhibition of $LTB_4$ by $PGE_2$ is suspected to be via an increase in second messenger cAMP that activates protein kinase A (PKA), which has been shown to inhibit $LTB_4$ synthesis.[277, 279] Together, these data suggest that the elevated levels of prostaglandin synthesis observed during pneumonic plague may contribute to the blunted $LTB_4$ response by the host.

In conclusion, I have defined the kinetics of the key inflammatory lipid mediator $LTB_4$ during pneumonic plague, which revealed a blunted response during the early stages of infection. Furthermore, I have shown that *Y. pestis* actively manipulates $LTB_4$ synthesis by leukocytes via the activity of Yop effectors to generate a beneficial inflammatory outcome to the pathogen. These discoveries warrant further research into the role of lipids, and subsequent manipulation of their synthesis by *Y. pestis*, to fully understand the molecular mechanisms *Y. pestis* has evolved to manipulate the mammalian immune response.

## 2-4. Material and Methods

### 2-4a. Ethics statement

All animal work was approved by the University of Louisville Institutional Animal Care and Use Committee (IACUC Protocol #22157). Use of human neutrophils was approved by the University of Louisville Institutional Review Board guidelines (IRB #96.0191) and written consents for use were obtained.

### 2-4b. Bacterial strains

Bacterial strains used in this chapter are listed in Table 2-2. For mouse infections, *Y. pestis* was grown at 26°C for 6-8 h, diluted to an optical density (OD) (600 nm) of 0.05 in Bacto brain heart infusion (BHI) broth (BD Biosciences Cat. No. 237500) with 2.5 mM $CaCl_2$ and then grown at 37°C with aeration for 15-18 h.[280] For cell culture infections, *Y. pestis* was cultured with BHI broth for 15-18 h at 26°C in aeration. Cultures were then diluted 1:10 in fresh, warmed BHI broth containing 20 mM $MgCl_2$ and 20 mM Na-oxalate and cultured at 37°C for 3 h with aeration to induce expression of the T3SS. Bacterial concentrations were determined using a spectrophotometer and diluted to desired concentrations in 1 × Dulbecco's phosphate-buffered saline (DPBS) for mouse infections or fresh medium for *in vitro* studies. Concentrations of bacterial inoculums for mouse studies were confirmed by serial dilution and enumeration on BHI agar plates.

| Name in manuscript | Genotype | Strain ref. # | Source |
|---|---|---|---|
| **Bacterial Strains** | | | |
| *Y. pestis* KIM5+ | pgm+, pMT1+, pPCP1+, pCD1Ap | X17 | [281] |
| *Y. pestis* CO92 LUX$_{pcysZK}$ | pgm+, pMT1+, pPCP1+, pCD1+, Lux$_{pcysZK}$ | MBLYP043 | [93] |
| *Y. pestis* | KIM1001 pgm-, pMT1+, pPCP1+, pCD1+, pML001+ | JG598 | [111] |
| *Y. pestis* T3$^{(-)}$ | KIM1001 pgm-, pMT1+, pPCP1+, pCD1-, pML001+ | JG597 | [111] |
| *Y. pestis* T3E | KIM1001 pgm-, pMT1+, pPCP1+, pCD1+ (yopH$^{\Delta3-467}$ yopE$^{\Delta40-197}$ yopK$^{\Delta4-181}$ yopM$^{\Delta3-408}$ ypkA$^{\Delta3-731}$ yopJ$^{\Delta4-288}$ yopT$^{\Delta3-320}$), pML001+ | JG715 | [111] |
| *Y. pestis* T3E +ypkA | KIM1001 pgm-, pMT1+, pPCP1+, pCD1+ (yopH$^{\Delta3-467}$ yopE$^{\Delta40-197}$ yopK$^{\Delta4-181}$ yopM$^{\Delta3-408}$ yopJ$^{\Delta4-288}$ yopT$^{\Delta3-320}$), pML001+ | JG684 | [111] |
| *Y. pestis* T3E +yopE | KIM1001 pgm-, pMT1+, pPCP1+, pCD1+ (yopH$^{\Delta3-467}$ yopK$^{\Delta4-181}$ yopM$^{\Delta3-408}$ ypkA$^{\Delta3-731}$ yopJ$^{\Delta4-288}$ yopT$^{\Delta3-320}$), pML001+ | JG681 | [111] |
| *Y. pestis* T3E +yopH | KIM1001 pgm-, pMT1+, pPCP1+, pCD1+ (yopE$^{\Delta40-197}$ yopK$^{\Delta4-181}$ yopM$^{\Delta3-408}$ ypkA$^{\Delta3-731}$ yopJ$^{\Delta4-288}$ yopT$^{\Delta3-320}$), pML001+ | JG680 | [111] |
| *Y. pestis* T3E +yopJ | KIM1001 pgm-, pMT1+, pPCP1+, pCD1+ (yopH$^{\Delta3-467}$ yopE$^{\Delta40-197}$ yopK$^{\Delta4-181}$ yopM$^{\Delta3-408}$ ypkA$^{\Delta3-731}$ yopT$^{\Delta3-320}$), pML001+ | JG686 | This work |
| *Y. pestis* T3E +yopK | KIM1001 pgm-, pMT1+, pPCP1+, pCD1+ (yopH$^{\Delta3-467}$ yopE$^{\Delta40-197}$ yopM$^{\Delta3-408}$ ypkA$^{\Delta3-731}$ yopJ$^{\Delta4-288}$ yopT$^{\Delta3-320}$), pML001+ | JG682 | [111] |
| *Y. pestis* T3E +yopM | KIM1001 pgm-, pMT1+, pPCP1+, pCD1+ (yopH$^{\Delta3-467}$ yopE$^{\Delta40-197}$ yopK$^{\Delta4-181}$ ypkA$^{\Delta3-731}$ yopJ$^{\Delta4-288}$ yopT$^{\Delta3-320}$), pML001+ | JG683 | [111] |
| *Y. pestis* T3E +yopT | KIM1001 pgm-, pMT1+, pPCP1+, pCD1+ (yopH$^{\Delta3-467}$ yopE$^{\Delta40-197}$ yopK$^{\Delta4-181}$ yopM$^{\Delta3-408}$ ypkA$^{\Delta3-731}$ yopJ$^{\Delta4-288}$), pML001+ | JG685 | [111] |
| *Y. pestis* T3E *yopB* | KIM1001 pgm-, pMT1+, pPCP1+, pCD1+ (yopH$^{\Delta3-467}$ yopE$^{\Delta40-197}$ yopK$^{\Delta4-181}$ yopM$^{\Delta3-408}$ ypkA$^{\Delta3-731}$ yopJ$^{\Delta4-288}$ yopT$^{\Delta3-320}$yopB $^{\Delta7-396}$), pML001+ | YPA322 | This work |
| *Y. pestis* *yopB*::*cyopB* | KIM1001 pgm-, pMT1+, pPCP1+, pCD1+ (yopH$^{\Delta3-467}$ yopE$^{\Delta40-197}$ yopK$^{\Delta4-181}$ yopM$^{\Delta3-408}$ ypkA$^{\Delta3-731}$ yopJ$^{\Delta4-288}$ yopT$^{\Delta3-320}$), pML001+ | YPA362 | This work |
| *E. coli* | *E. coli* DH5α pGEN222::mCherry | LOU123 | This work |
| *Salmonella enterica* Typhimurium | *S. enterica* Typhimurium LT2 pGENLux | LOU120 ATCC 14028s | This work |
| *Klebsiella pneumoniae manC* | KPPR1S *ΔmanC* | LOU171 | [282] |
| **Plasmids** | | | |
| pML001 | Luciferase bioreporter | NA | [111] |
| pGENlux | Luciferase bioreporter | MBL343 | [283] |

Table 2-2. Bacterial strains and plasmids used in this chapter

2-4c. Mouse infections

All animal work was performed at least twice to ensure reproducibility. 6-8 week-old C57BL/6J or BLT1$^{-/-}$ [252] male and female mice were infected with *Y. pestis* KIM5+ or *Y. pestis* CO92 LUX$_{\mathrm{p}\textit{cysZK}}$. For lipid measurements, mice were anesthetized with ketamine/xylazine and administered 20 µL of *Y. pestis* KIM5+ suspended in 1× DPBS to the left nare as previously described.[251, 280] Mice were monitored for the development of moribund disease symptoms twice daily and humanely euthanized when they met previously approved end point criteria. At 6, 12, 24, 36, or 48 h, mice were humanely euthanized by $CO_2$ asphyxiation and lungs were harvested and lung masses recorded. Lungs were transferred to a 2 mL tube pre-filled with 2.8 mm ceramic beads (VWR, Cat. No. 10158-612), flash frozen on dry ice, and stored at -80°C until preparation for lipid analysis. For CFU studies, mice were humanely euthanized by $CO_2$ asphyxiation at 12 or 24 h and lungs were harvested. Lungs were transferred to Whirl Pak's containing 1 mL of 1 x DPBS, and gently homogenized using a serological pipette. Homogenized tissues were serial diluted and plated onto BHI agar. After 2 days of incubation at 26°C, bacteria were enumerated. For optical imaging and survival curves, mice were infected with *Y. pestis* CO92 LUX$_{\mathrm{p}\textit{cysZK}}$ and monitored for bacterial proliferation as a function of bioluminescence by optical imaging and for the development of moribund disease. At each time point, mice were anesthetized with isoflurane and imaged using the IVIS Spectrum imaging system (Caliper Life Sciences, Hopkinton, MA). Average radiance (photons/s/cm2) was calculated for the lungs as previously described.[251] For the exogenous $LTB_4$ treatment, mice were intraperitoneally injected with 1 x DPBS or 10 nmol $LTB_4$ (Cayman Chemical Cat. No. 20110). At 1 h post-treatment, mice were administered $10^5$ CFU of *Y. pestis* KIM5+ via intraperitoneal injection. At 3 h post infection, mice were humanely euthanized, and the peritoneal cavity was washed and collected using 2 lavages of 1 mL of 1 x DPBS. Lavages were used for CFU enumeration or neutrophil quantification by flow cytometry.

2-4d. Lipid extraction and quantification by LC-MS

To quantify $LTB_4$ abundance from whole lungs, lungs were thawed with 1.8 mL of ice cold 75% methanol + 0.1% BHT for 3 minutes. Lungs were then homogenized with a Bead Ruptor 4 (OMNI) at speed 5 (5 m/s) for 4 cycles of 45 seconds with 1-minute pauses in which the lungs were placed on ice. Tissue debris was then centrifuged for 10 min at 1,500 x g at 4°C. The supernatant (~1.5 mL) was then transferred to a fresh eppendorf tube, incubated at 4°C for 24 h to inactivate *Y. pestis* and extract lipids. After successful inactivation, samples were removed from BSL3 containment and stored at -80°C. Lipid extraction was then performed as previously described.[284] For the expanded global lipid analysis, lungs were thawed with 1.5 mL of ice cold 1 x DPBS + HALT protease and phosphatase inhibitor cocktail for 3 minutes. Lungs were then homogenized with a Bead Ruptor 4. Tissue debris was then centrifuged for 10 min at 1,500 x g at 4°C. The supernatant (~1.5 mL) was then transferred to a fresh eppendorf tube. From this, 250 µL of supernatant was combined with 750 µL of 100% methanol + 0.1% BHT (final concentration of 75%) and incubated at 4°C for 24 h to inactivate *Y. pestis* and extract lipids. After confirmation of successful inactivation of *Y. pestis*, lipids were extracted and quantified by the Wayne State University Lipidomics Facility as previously described.[285] The extracted samples were analyzed for the fatty acyl lipidome using standardized methods as described previously.[286, 287]

2-4e. Flow cytometry

To quantify the neutrophil population from peritoneal lavages, cells were labeled with anti-Ly6G antibody (1:400; BD Pharminogen Cat. No. 551460) and anti-CD11b antibody (1:600; Biolegend Cat. No. 101212) for 1 h on ice, in the dark. Cells were pelleted and resuspended in 1% PFA. Single cell suspensions were generated by straining with 70 µM mesh prior to analysis on the flow cytometer. Neutrophils were identified as cells with high expression of Ly6G and CD11b and data is represented as the percent of the population that were classified as neutrophils. An example of the gating strategy is shown in Fig 2-4.

2-4f. Cell isolation and cultivation

Human neutrophils were isolated from the peripheral blood of healthy, medication-free donors, as described previously.[288] Briefly, white blood cells were isolated from whole blood using a 6% dextran solution. Neutrophils were then separated from monocytes using a percoll gradient of 42% and 50.5%. RBCs were then lysed from the neutrophil containing layer using 0.2% NaCl for 30 seconds and followed by a quench with 5 mL 1.6% NaCl. Neutrophil isolations yielded ≥ 95% purity and were used within 1 h of isolation. Murine neutrophils were isolated from bone marrow of 7-12-week-old mice using an Anti-Ly-6G Microbeads kit (Miltenyi Biotec Cat. No. 130-120-337) per the manufacturer's instructions. Neutrophil isolations yielded ≥ 95% purity and were used within 1 h of isolation. Macrophages were differentiated from murine bone marrow in DMEM supplemented with 1 mM Na-pyruvate and 10% FBS for 6 days. Macrophages were either polarized with 10 ng/mL of GM-CSF (M1; Kingfisher Biotech Cat. No. RP0407M) or with 30% L929 conditioned media and 10 ng/mL of M-CSF (M2; Kingfisher Biotech Cat. No. RP0462M) throughout the differentiation. The medium was replaced on days 1 and 3 (adapted from [289]). Polarization was confirmed by qRT-PCR, as previously described [290], using markers for M1 and M2 phenotypes, TNF-$\alpha$ and Il-10, respectively (Fig 2-11). Murine mast cells were isolated and differentiated from bone marrow as previously described.[291] Briefly, isolated bone marrow cells were resuspended in BMMC culture medium [DMEM containing 10% FCS, penicillin (100 units/mL), streptomycin (100 mg/mL), 2 mmol/L L-glutamine, and 50 mmol/L β-mercaptoethanol] supplemented with recombinant mouse stem cell factor (SCF) (12.5 ng/mL; R&D Systems Cat. No. 455-MC) and recombinant mouse IL-3 (10 ng/mL; R&D Systems Cat. No. 403-ML). Cells were plated at a density of 1 x $10^6$ cells/mL in a T-75 $cm^2$ flask. Nonadherent cells were transferred after 48 hours into fresh flasks without disturbing the adherent (fibroblast) cells. Mast cells were visible after 4 weeks of culture and propagated further or plated for experiments in DMEM without antibiotics.

2-4g. Leukocyte infections

Human neutrophils were resuspended in Kreb's buffer (w/ $Ca^{2+}$ & $Mg^{2+}$) then adhered to 24-well plates for 30 min that were coated with pooled human serum prior to infection (wells were washed twice with 1 x DPBS prior to plating the cells). Murine bone marrow neutrophils were resuspended in RPMI + 5% FBS then adhered to 24-well plates for 30 min that were coated with FBS prior to infection (wells were washed twice with 1 x DPBS prior to plating the cells). Neutrophils were infected at a multiplicity of infection (MOI) of 20, 50, or 100 and incubated for 1 h in a cell culture incubator at 37°C with a constant rate of 5% $CO_2$. Co-infections were performed at a final MOI of 20 (MOI of 10 for each strain). 1 h post-infection, supernatants were collected, centrifuged for 1 min at 6,000 x g, and supernatants devoid of cells were transferred to a fresh eppendorf tube. Macrophages were adhered to 24-well plates in DMEM + 10% FBS 1 day prior to infection. Macrophages were infected at an MOI of 20. At 4 h post-infection, supernatants were collected, centrifuged for 1 min at 6,000 x g, and supernatants devoid of cells were transferred to a fresh eppendorf tube. Mast cells were adhered to 24-well plates in DMEM only for 1 h prior to infection. Mast cells were infected at an MOI of 20 or treated with crystalline silica (100 mg/$cm^2$). At 2 h post-infection supernatants were collected, centrifuged for 1 min at 6,000 x g, and supernatants devoid of cells were transferred to a fresh eppendorf tube. All infections were synchronized by centrifugation (200 x g for 5 min). All samples were stored at -80°C until ELISA.

2-4h. Measurement of $LTB_4$ by enzyme-linked immunosorbent assay

Supernatants of neutrophils, macrophages, and mast cells were collected and measured for $LTB_4$ by ELISA per manufacturer's instructions (Cayman Chemicals Cat. No. 520111).

2-4i. Cell viability assays

To determine leukocyte permeability, cells were incubated with trypan blue for 5 min and trypan blue exclusion was measured using SD100 counting chambers (VWR Cat. No. MSPP-CHT4SD100) and a cell counter (Nexcelom Cellometer Auto T4). To determine leukocyte cytotoxicity, lactate dehydrogenase (LDH) was measured from leukocyte supernatants using the CytoTox 96 Non-Radioactive Cytotoxicity kit (Promega Cat. No. g1780) per the manufacturer's instructions.

2-4j. Bacterial viability assays

To measure bacterial viability during interactions with neutrophils, murine neutrophils were resuspended in RPMI + 5% FBS then adhered to 96-well white bottom plates for 30 min coated with FBS prior to infection (wells were washed twice with 1 x DPBS prior to plating the cells). Neutrophils were infected at an MOI of 20, centrifuged for 5 min at 200 x g, and bacterial viability was measured as a function of bioluminescence using a plate reader (BioTek Cytation 1 imaging reader).

2-4k. Measurement of LcrV by western blot

Bacterial strains were cultured with BHI broth for 15-18 h at 26°C in aeration. Cultures were then diluted 1:10 in fresh warmed BHI broth containing 20 mM $MgCl_2$ and 20 mM Na-oxalate and cultured at 37 or 26°C for 3 h. 1 $OD_{600}$ of bacterial pellets were collected and resuspended in 1 x SDS-PAGE loading buffer, boiled for 10 min, and 0.1 $OD_{600}$ was separated on a 10% SDS-PAGE gel. As a positive control, 0.2 g of recombinant LcrV protein was used (BEI resources Cat. No. NR-32875). Samples were immunoblotted with polyclonal anti-LcrV antibody diluted to 1:4,000 (BEI Resources Cat. No. NR-31022). Anti-goat IgG HRP secondary antibody was diluted to 1:5,000 (Bio-Techne Cat. No. HAF017). Densitometry was performed using ImageJ software to compare LcrV bands between samples.[292]

2-4l. Statistics

For all studies, male and female mice or human donors were used and no sex biases were observed for any phenotype. All *in vivo* experiments were repeated at least twice and *in vitro* experiments at least 5 times. Where noted in the figure legends, figures may represent the combined data from multiple biologically independent experiments. For *in vitro* experiments, each data point represents data from biologically independent experiments performed on different days. Where appropriate and as indicated in the figure legends, statistical comparisons were performed with Prism (GraphPad) using one-way analysis of variance (ANOVA) with Dunnett's or Tukey's *post hoc* test, T-test with Mann-Whitney's *post hoc* test, or Log-Rank analysis. P values $\leq$ 0.05 were considered statistically significant and reported. For LC-MS analysis of lipids, a LIMMA - Moderated T-test was performed using a modified version of a previously published protocol using R packages.[293-295] Briefly, raw data were transformed by taking logarithmic base 2 followed by quantile normalization. Missing values were then ascribed using a singular value decomposition method. Lipids missing > 40% of the values were excluded from subsequent analysis. Finally, differentially abundant lipids ($p \leq 0.05$) were further filtered by fold-change (FC) criteria ($1 < \log_2 FC < 1$) and multiple comparisons testing with a false discovery rate.

# CHAPTER 3:

# SIGNALING PATHWAYS REQUIRED FOR $LTB_4$ SYNTHESIS IN RESPONSE TO THE BACTERIAL TYPE 3 SECRETION SYSTEM DIFFERS BETWEEN MACROPHAGES AND NEUTROPHILS

## 3-1. Introduction

A hallmark manifestation of plague is a biphasic inflammatory response, which is critical for the progression of *Yersinia pestis* infection.[31, 236, 238, 254] One of the key virulence determinants for *Y. pestis* to colonize the host is the Ysc type 3 secretion system (T3SS) encoded on the pCD1 plasmid.[4, 234] This secretion system allows direct translocation of bacterial effector proteins, called Yops, through the YopB/D translocon into host cells.[4, 56, 67, 68, 235, 255, 256] The Yops target specific host factors to disrupt normal host cell signaling pathways and functions.[6, 8, 28, 102, 236, 237] During mammalian infection, *Y. pestis* primarily targets neutrophils and macrophages for T3SS-mediated injection of the Yops.[19, 98, 239] The outcomes of Yop injection into these cells include inhibition of phagocytosis, reactive oxygen species (ROS) synthesis, degranulation by neutrophils, and inflammatory cytokine and chemokine release that is required to recruit circulating leukocytes to infection sites.[36, 93, 103, 109, 136, 137] Importantly, previous work suggests that inhibition of neutrophil influx and establishing a non-inflammatory environment is crucial for *Y. pestis* virulence.[31, 240] Therefore, defining the molecular mechanisms used by *Y. pestis* to subvert the host immune response is fundamental to understanding the pathogenesis of this organism. Moreover, defining these mechanisms can also provide novel insights into how the host responds to bacterial pathogens to control infection.

Leukotriene B4 ($LTB_4$), an eicosanoid that is rapidly synthesized by leukocytes, is a potent pro-inflammatory chemoattractant and immune cell activator.[37, 195, 241, 250, 260, 261] $LTB_4$ is derived from arachidonic acid (AA) upon activation of the enzymes 5-lipoxygenase (5-LOX) and cytosolic phospholipase $A_2$ ($cPLA_2$). The enzymes are activated by phosphorylation via MAPK signaling and $Ca^{2+}$ binding.[150, 152, 155, 296] This leads to conformational changes and translocation of the enzymes to the nuclear membrane or a lipidisome, where a complex is formed with 5-LOX activating protein (FLAP).[150, 153, 154, 171, 242] This complex then converts AA to $LTA_4$, and $LTA_4$ hydrolase rapidly converts the molecule to $LTB_4$, followed by $LTB_4$ release from the cell.[150, 152] Upon release, $LTB_4$ is recognized by the high affinity BLT1 receptor on immune cells to promote chemotaxis and initiate the inflammatory cascade leading to the production of pro-inflammatory cytokines and chemokines.[37, 150, 151, 183, 185, 241, 243] In Chapter 2, I showed that *Y. pestis* actively inhibits the synthesis of $LTB_4$ in a T3SS/Yop-dependent manner.[93, 297] Additionally, I demonstrated that an $LTB_4$ response triggered by *Y. pestis* requires bacterial expression of the T3SS and the YopB/D translocase.[297] However, the mechanisms leading to T3SS-dependent $LTB_4$ synthesis by the *Y. pestis* T3E mutant remained undefined.

Previous studies have identified that components of the T3SS are pathogen associated molecular patterns (PAMPs) recognized by macrophages (previously reviewed in [57]). In the absence of the Yops, the T3SS YopB/D translocon proteins induced NLRP3-dependent activation of the caspase 1 inflammasome, IL1-$\beta$ secretion, and pyroptosis.[68, 89] Because expression the T3SS and the YopB/D translocase is required for $LTB_4$ synthesis by leukocytes, it is possible that inflammasome activation may also be required for $LTB_4$ synthesis during interactions with the *Y. pestis* T3E strain. However, $LTB_4$ synthesis in response to other stimuli is not dependent on inflammasome activation.[153, 219, 220] Furthermore, infection of neutrophils with a strain of *Y. pestis* T3E that also expresses YopK, which has been reported to inhibit NLRP3 inflammasome activation in macrophages,[67, 68] does not inhibit $LTB_4$ synthesis in neutrophils,[93, 297] raising an alternative possibility for inflammasome-independent mechanisms leading to $LTB_4$ synthesis.

We have previously shown that four Yop effectors - YpkA, YopE, YopJ, or YopH - are sufficient to independently inhibit $LTB_4$ synthesis by both human and murine neutrophils.[93, 297] The function of these Yop effectors have been well defined,[26, 41, 42, 45, 56, 69, 70, 73-75, 83-85, 95, 96] suggesting that these proteins can serve as powerful tools to elucidate the molecular mechanisms responsible for $LTB_4$ synthesis in response to the *Y. pestis* T3SS. Of these Yop effectors, two are intimately involved in

MAPK and $Ca^{2+}$ signaling. YopJ is an acyltransferase that targets several kinases in the MAPK pathway, and it is a potent inhibitor of signaling through JNK, p38, and ERK in macrophages and neutrophils.[44, 105, 108, 298] Additionally, using a combination of *Y. pestis* mutants and chemical inhibitors, Pulsifer et al.[93] was able to show that YopJ inhibition of ERK phosphorylation is sufficient to inhibit $LTB_4$ synthesis by human neutrophils. YopH is a tyrosine phosphatase that has been shown to target multiple proteins of the focal adhesion complex, including SLP-76, SKAP2, PRAM, Vav, and LCK.[42, 95-98] Studies with *Y. pseudotuberculosis* have demonstrated that YopH is a potent inhibitor of β1-integrin-mediated $Ca^{2+}$ signaling and flux, suggesting YopH inhibition of $Ca^{2+}$ signaling also inhibits $LTB_4$ synthesis.[97, 98] However, studies have also suggested that YopH can inhibit ERK phosphorylation in neutrophils,[97, 98, 100, 103] suggesting that YopH can also inhibit the efficient phosphorylation of the $LTB_4$ synthesis enzymes. In this chapter, I apply our understanding of the functions of the Yop effectors to define the molecular mechanisms responsible for T3SS-dependent $LTB_4$ synthesis by leukocytes. Importantly, by comparing the responses between neutrophils and macrophages, I discovered cell-type specific responses to the T3SS and unique signaling pathways involved between the two cell types.

## 3-2. Results

### 3-2a. $LTB_4$ synthesis in response to *Salmonella enterica* Typhimurium is dependent on SPI-1

I showed in Chapter 2 that $LTB_4$ synthesis in response to *Y. pestis* is dependent on the expression of the T3SS and the YopB/D translocon (Figure 2-8). I also showed that *S. enterica* Typhimurium, which encodes two T3SSs (SPI-1 and SPI-2), induces an $LTB_4$ response in neutrophils, but whether the T3SSs were required for synthesis was not tested. To determine if leukocyte sensing of the T3SSs of *S. enterica* Typhimurium was responsible for $LTB_4$ synthesis, bone marrow derived murine neutrophils (BMNs) were infected with *S. enterica* Typhimurium LT2 (ST+) or an ST null mutant for both the *Salmonella* pathogenicity island 1 (SPI-1; Δ*invA*) and SPI-2 (Δ *ssaK*) encoded type 3 export apparatuses. After 1 h of infection, $LTB_4$ synthesis was significantly elevated in ST infected BMNs (Fig 3-1A, ST+ vs. UI, $p \leq 0.0001$) but it was not elevated in cells infected with the ΔSPI1/2 mutant (Fig 3-1A, $p = 0.1513$). To determine the contribution of individual T3SSs, BMNs were next infected with individual SPI-1 or SPI-2 mutants. No significant differences in recovered $LTB_4$ were observed between cells infected with the SPI-1/2 and SPI-1 mutant strains, but $LTB_4$ concentrations were significantly elevated in the SPI-2 mutant infected cells (Fig 3-1A, $p \leq 0.0001$). Together these data support that neutrophils sense the presence of SPI-1 by *S. enterica* Typhimurium to initiate a robust $LTB_4$ response, suggesting that the T3SS may be a common PAMP recognized by neutrophils to rapidly induce $LTB_4$ synthesis.

3-2b. Phagocytosis is not required for $LTB_4$ synthesis in neutrophils in response to *Y. pestis* or *S. enterica* Typhimurium

One important consequence of Yop intoxication of leukocytes is the inhibition of phagocytosis via the action of YopE and YopT.[26, 41, 42, 86, 129] Moreover, an important function of SPI-1 of *S. enterica* Typhimurium is to induce phagocytosis.[299] Because phagocytosis is required for $LTB_4$ synthesis by leukocytes interacting with crystalline silica,[153] I next asked if phagocytosis of *Y. pestis* T3E or ST+ was required for T3SS-dependent $LTB_4$ synthesis by BMNs. To test this hypothesis, BMNs were treated with the phagocytosis inhibitor cytochalasin D (cytoD) prior to infection with either a *Y. pestis* T3E or ST+. While treatment with cytoD inhibited phagocytosis of *Y. pestis* T3E (Fig. 3-1B-C), it did not alter $LTB_4$ synthesis by uninfected or *Y. pestis* T3E-infected BMNs (Fig 3-1D-E), indicating that Yop-mediated inhibition of phagocytosis is not responsible for the inhibition of T3SS-mediated $LTB_4$ synthesis during *Y. pestis* infection. Moreover, as previously reported by Golenkina et. al,[224] cytoD treatment resulted in an increase in $LTB_4$ synthesis by BMNs infected with ST+ (Fig 3-1F; p $p \leq 0.05$), indicating that induction of phagocytosis by *S. enterica* Typhimurium is not required to induce T3SS-mediated $LTB_4$ synthesis. Together, these data suggest that phagocytosis is not required for T3SS-mediated $LTB_4$ synthesis by neutrophils.

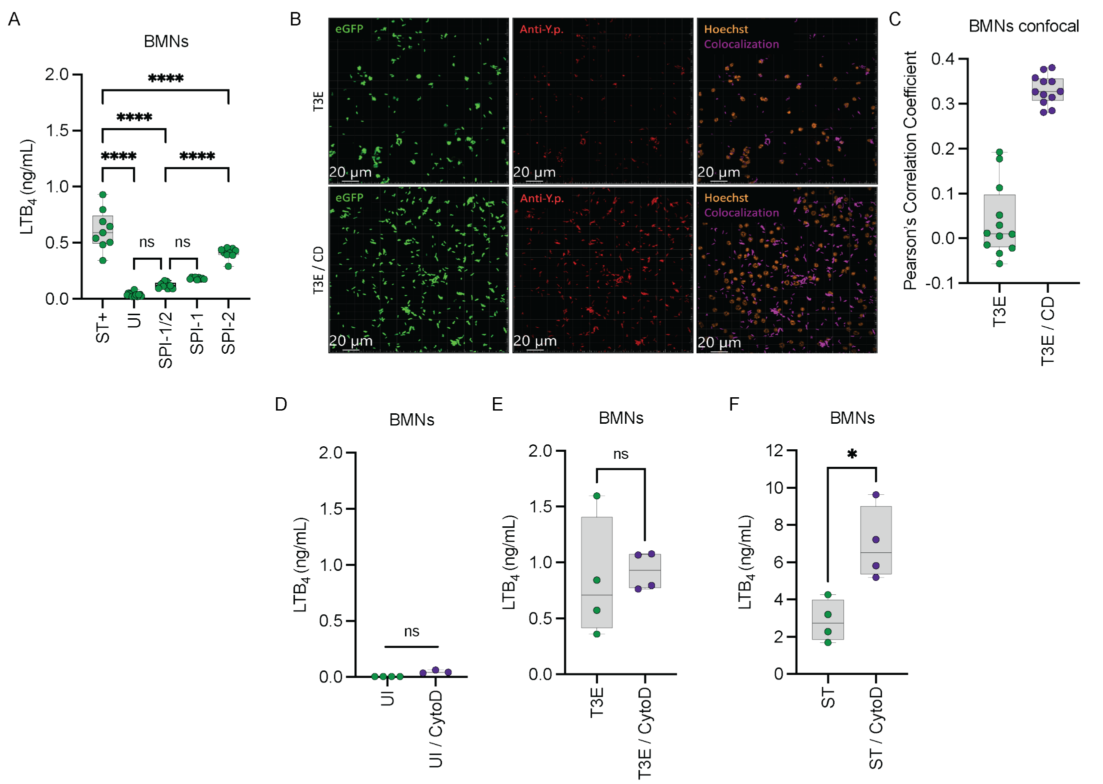


<u>Figure 3-1. Phagocytosis is not triggering $LTB_4$ synthesis in BMNs in response to *Y. pestis*</u>

(A) Murine neutrophils (BMNs) were infected with *S. enterica* Typhimurium LT2 (ST+), mutants that lacked *Salmonella* T3SS SPI-1, SPI-2, or both SPI-1/2 at an MOI of 20. (B-G) BMNs were either left untreated (green circles) or pre-treated with cytochalasin D (10 µM, purple circles) for 30 min. (B) Representative confocal images and (C) Pearson scores of cytochalasin D (10 µM) pre-treated (T3E / CD) or untreated (T3E) BMNs infected with *Y. pestis* T3E at an MOI of 10. BMNs (D) uninfected or infected with (E) *Y. pestis* T3E or (F) ST at an MOI of 20. (A, D-E) $LTB_4$ was measured from supernatants 1h post infection by ELISA. Each symbol represents an independent biological infection, and the box plot represents the median of the group ± the range. (C) Pearson's Correlation Coefficient calculated from three biological independent experiments, four images each (n=12), box plot represents the median of the group ± the range. UI = uninfected. ns = not significant. One-way ANOVA with Tukey's *post hoc* test compared to each condition for A. T-test with Welch's *post hoc* test for B-D. *=p≤0.05, ****=p≤0.0001.

3-2c. T3SS induced $LTB_4$ synthesis is conserved in macrophages

I showed in Chapter 2 that the Yop effectors inhibit $LTB_4$ synthesis triggered by the *Y. pestis* T3SS in neutrophils and M1-polarized macrophages, and that synthesis by neutrophils is dependent on the YopB/D translocase.[297] To determine whether the YopB/D translocase is also required for $LTB_4$ synthesis by macrophages, M1-polarized bone marrow derived macrophages (BMDMs) were infected with *Y. pestis*, *Y. pestis* T3E, a *Y. pestis* strain lacking the pCD1 plasmid encoding the entire Ysc T3SS [*Y. pestis* $T3^{(-)}$], or a *Y. pestis* T3E *yopB* mutant that is defective in expression of the translocase that directly interacts with the host cell plasmid membrane.[56, 67, 68, 255, 256] As previously reported for neutrophils (Fig 2-10B),[297] BMDMs also did not synthesize $LTB_4$ in response to *Y. pestis* $T3^{(-)}$ or *Y. pestis* T3E *yopB* (Fig 3-2A). Normal $LTB_4$ synthesis was restored by *yopB* complementation (*yopB*::c*yopB*) (Fig 3-2A). To confirm that the *S. enterica* Typhimurium SPI-1 is also required for $LTB_4$ synthesis by macrophages, BMDMs were infected with ST or the SPI-1/2, SPI-1, or SPI-2 mutants. As observed for BMNs, BMDM synthesis of $LTB_4$ was dependent on the presence of SPI-1 but not SPI-2 (Fig 3-2B). These data show that like neutrophils, macrophages respond to the T3SS by rapidly synthesizing $LTB_4$.

3-2d. Only YopJ is sufficient to inhibit $LTB_4$ synthesis by macrophages

We have previously shown that YpkA, YopE, YopJ, or YopH are individually sufficient to inhibit $LTB_4$ synthesis in neutrophils (Fig 2-7).[93, 297] To determine if the same individual Yop effectors could inhibit $LTB_4$ synthesis by macrophages, $LTB_4$ was measured from BMDMs infected with *Y. pestis* strains that expressed only one Yop effector. BMDMs infected with strains expressing YpkA, YopE, YopH, YopK, and YopT showed significant decreases in $LTB_4$ compared to those infected with *Y. pestis* T3E, but still produced more $LTB_4$ than uninfected cells (Fig 3-2C). In contrast, BMDMs infected with a strain expressing only YopJ produced the least amount of $LTB_4$, similar to levels recovered from cells infected with *Y. pestis* expressing all of the Yop effectors (Fig 3-2C; Yp). YopM was the only effector that did not appear to impact $LTB_4$ synthesis on its own. Together these data show that *Y. pestis* uses redundant mechanisms to inhibit $LTB_4$ synthesis by macrophages. Moreover, differences in the ability of individual Yop effectors to inhibit $LTB_4$ synthesis between neutrophils and macrophages suggest that different signaling pathways may be activated in each leukocyte.

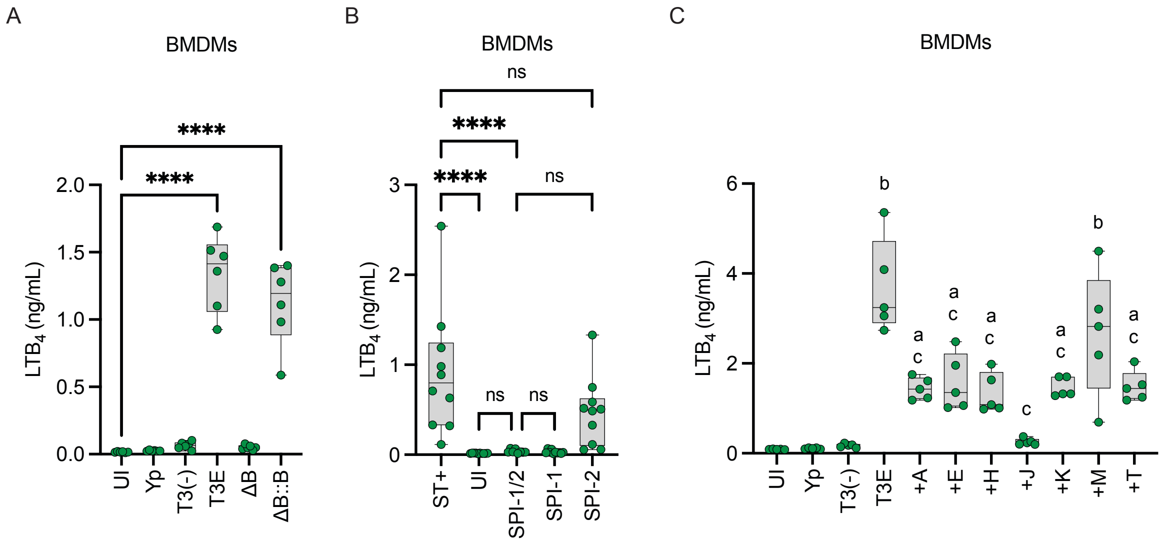


Figure 3-2. Translocase triggered $LTB_4$ synthesis is conserved in BMDMs

(A) Murine macrophages (BMDMs) were infected with *Y. pestis, Y. pestis* T3E, *Y. pestis* T3(-), a yopB mutant in the T3E background (ΔB), or ΔB complemented with yopB (ΔB::B). (B) BMDMs were infected with *S. enterica* Typhimurium LT2 (ST+), mutants that lacked *Salmonella* T3SS SPI-1, SPI-2, or both SPI-1/2 (C) BMDMs infected with *Y. pestis, Y. pestis* T3E, *Y. pestis* T3(-), or *Y. pestis* strains expressing only one Yop (+A = YpkA; +E = YopE; +H = YopH; +J = YopJ; +K = YopK; +M = YopM; or +T = YopT). (A-C) BMDMs were infected at an MOI of 20 or 4 h. $LTB_4$ was measured from supernatants by ELISA. Each symbol represents an independent biological infection, and the box plot represents the median of the group ± the range. UI = uninfected. ns = not significant. One-way ANOVA with Dunnett's *post hoc* test compared to uninfected for A, or Tukey's *post hoc* test compared to each condition for B & C. ****=p≤0.0001. For panel C, p values when compared to uninfected denoted as a=p≤0.05 or b=p≤0.0001, and when compared to *Y. pestis* T3E as c=p≤0.0001.

3-2e. Phagocytosis enhances $LTB_4$ synthesis by macrophages

To determine whether phagocytosis is required for inducing $LTB_4$ synthesis in macrophages, BMDMs were pretreated with cytoD and infected with *Y. pestis* T3E or ST+. Again, cytoD treatment did not alter $LTB_4$ synthesis of uninfected BMDMs (Fig 3-3A). However, in contrast to neutrophils, when phagocytosis was inhibited in BMDMs, $LTB_4$ synthesis was significantly reduced in response to *Y. pestis* T3E (Fig 3-3B) and trending towards reduced for ST+ (Fig 3-3C) compared to untreated infected BMDMs. However, $LTB_4$ levels were still higher in the cytoD infected BMDMs than the uninfected BMDMs (Fig 3-3A), suggesting that phagocytosis is not required for $LTB_4$ but enhances synthesis in macrophages.

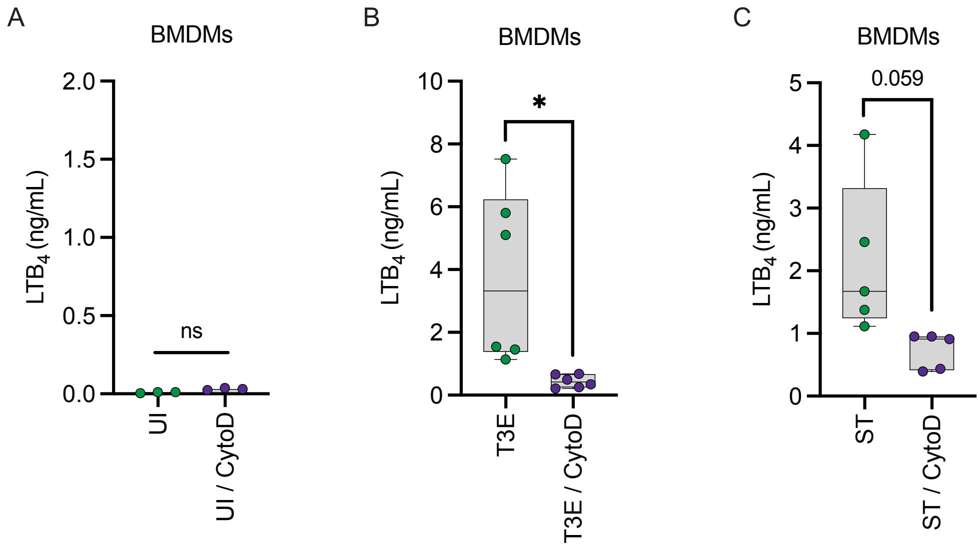


Figure 3-3. Phagocytosis enhances $LTB_4$ synthesis by macrophages

(A) BMDMs were pretreated with cytochalasin D (10 µM; purple circles) for 30 min and were either (A) uninfected or infected with (B) *Y. pestis* T3E or (C) ST. (A-C) BMDMs were infected at an MOI of 20 for 4 h. $LTB_4$ was measured from supernatants by ELISA. Each symbol represents an independent biological infection. ns = not significant. T-test with Welch's *post hoc* test. *=p≤0.05.

3-2f. PLC signaling is required for $LTB_4$ synthesis in neutrophils

$Ca^{2+}$ flux is required for the activation of $cPLA_2$ and 5-LOX.[152, 154] However, it is unclear if the T3SS induces $Ca^{2+}$ flux through $Ca^{2+}$ migration through the YopB/D translocase pore or via conventional $Ca^{2+}$ signaling. Phospholipase C (PLC) is the central mediator of conventional $Ca^{2+}$ signaling in the cell,[300-303] and chemical inhibitors of PLC have been well characterized. Therefore, to determine if $Ca^{2+}$ signaling is required for T3SS-dependent $LTB_4$ synthesis, leukocytes were pretreated with U73122, which inhibits PLC$\beta$ and PLC$\gamma$,[304-306] prior to infection. When PLC signaling was inhibited, BMNs infected with the *Y. pestis* T3E mutant were no longer able to synthesize $LTB_4$ compared to untreated BMNs (Fig 3-4A), suggesting that PLC-mediated $Ca^{2+}$ signaling is required for $LTB_4$ synthesis. To ensure that U73122 treatment did not have off target effects on cPLA or 5-LOX, U73122-treated BMNs were treated with the $Ca^{2+}$ ionophore, A23187, which induces $Ca^{2+}$ flux and $LTB_4$ synthesis independent of PLC signaling.[307] Within 10 min of A23187 treatment, U73122-treated BMNs produced $LTB_4$ at similar levels as untreated cells, supporting that U73122 treatment specifically inhibits PLC and not components of $LTB_4$ synthesis (Fig 3-4A).

Interestingly, U73122 treatment of *Y. pestis* T3E-infected BMDMs only modestly inhibited $LTB_4$ synthesis compared to untreated cells (Fig 3-4B; $p \leq 0.05$), suggesting PLC is not the primary source of $Ca^{2+}$ flux in macrophages. Together, these data suggest that the T3SS activates PLC-mediated $Ca^{2+}$ flux in neutrophils needed for $LTB_4$ synthesis, but additional mechanisms are required for T3SS-induced LTB4 synthesis in macrophages.

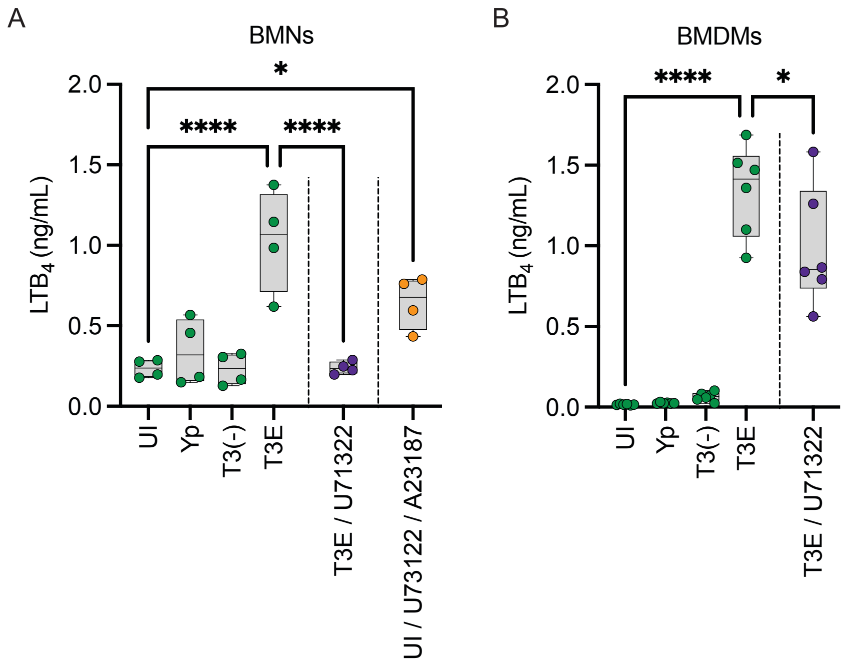


Figure 3-4. PLC signaling is required for $LTB_4$ synthesis in BMNs

(A) BMNs or (B) BMDMs were infected with *Y. pestis, Y. pestis* T3E, or *Y. pestis* T3(-) at an MOI of 20 for (A) 1 h or (B) 4 h. Leukocytes pretreated with PLC inhibitor (U73122; (A) 5 μM or (B) 20 μM) for 30 min (purple circles). (A) BMN supernatants were replaced with fresh media and cells were treated with A23187 (1 μM) for 10 min after treatment with U73122 for 30 min (orange circles). (A-B) $LTB_4$ was measured from supernatants by ELISA. Each symbol represents an independent biological infection, and the box plot represents the median of the group ± the range. UI = uninfected. One-way ANOVA with Tukey's *post hoc* test compared to each condition. *=p≤0.05, ****=p≤0.0001.

3-2g. STIM1-mediated $Ca^{2+}$ flux of extracellular $Ca^{2+}$ is required for *Y. pestis* T3SS-dependent $LTB_4$ synthesis

PLC-mediated $Ca^{2+}$ flux is required for $LTB_4$ synthesis in neutrophils, but PLC signaling can lead to both $Ca^{2+}$ efflux from the ER and influx from the extracellular space.[300-303, 308] To determine if intracellular $Ca^{2+}$ efflux is sufficient to induce T3SS-dependent $LTB_4$ synthesis, BMNs were pre-treated with EGTA to chelate extracellular $Ca^{2+}$ prior to infection with *Y. pestis* T3E – if intracellular efflux is sufficient then EGTA should not inhibit $LTB_4$ synthesis. As observed during PLC inhibition, EGTA chelation of extracellular $Ca^{2+}$ significantly reduced $LTB_4$ production compared to untreated BMNs (Fig 3-5A; $p \leq 0.0001$). Influx of extracellular $Ca^{2+}$ also requires the cell to maintain a membrane potential by efflux of intracellular potassium ($K^+$).[309-311 312-315] Therefore, if extracellular $Ca^{2+}$ is required, disrupting the $K^+$ gradient should also inhibit $LTB_4$ synthesis. As predicted by EGTA treatment, increasing the extracellular $K^+$ concentration significantly inhibited $LTB_4$ synthesis by *Y. pestis* T3E-infected BMNs (Fig 3-5A; $p \leq 0.0001$). Finally, PLC-induced extracellular $Ca^{2+}$ influx can lead to STIM1 activation,[316] and treatment of neutrophils with a pharmacological inhibitor of STIM1 (SKF) also significantly inhibited $LTB_4$ synthesis in BMNs (Fig 3-5A; $p \leq 0.0001$). Together, these data demonstrate that the T3SS induces extracellular $Ca^{2+}$ flux via PLC activation in neutrophils. Interestingly, while PLC does not appear to be required for $LTB_4$ synthesis by macrophages, extracellular $Ca^{2+}$ and STIM1 activation are required (Fig 3-5B), further supporting that alternative pathways are involved in triggering $Ca^{2+}$ flux needed for $LTB_4$ synthesis in macrophages.

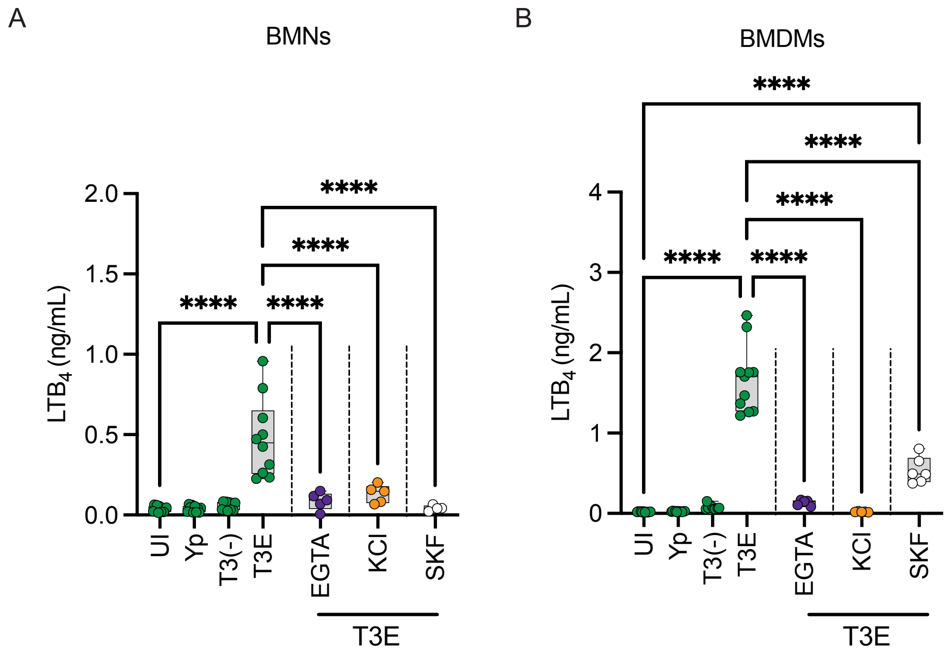


Figure 3-5. Influx of extracellular $Ca^{2+}$ is required for *Y. pestis* T3SS-dependent $LTB_4$ synthesis

(A) BMNs or (B) BMDMs were infected with *Y. pestis, Y. pestis* T3E, or *Y. pestis* T3(-). Leukocytes pretreated with (A-B) EGTA (1 mM; purple circles) for 30 min, with (A) 50 mM or (B) 100 mM KCl (orange circles) for 30 min, or with (A-B) STIM1 inhibitor (SKF, 50 μM; white circles) for 2 min prior to infection with *Y. pestis* T3E. (A-B) Leukocytes were infected at an MOI of 20 for (A) 1 h or (B) 4 h. $LTB_4$ was measured from supernatants by ELISA. Each symbol represents an independent biological infection, and the box plot represents the median of the group ± the range. UI = uninfected. One-way ANOVA with Tukey's *post hoc* test compared to each condition. ****=p≤0.0001.

3-2h. SKAP2 is required for $LTB_4$ synthesis by neutrophils but not macrophages in response to *Y. pestis* T3E

While PLC activation is required for $LTB_4$ synthesis in neutrophils, the molecular mechanisms leading to T3SS-dependent PLC activation are still unknown. However, YopH, which inhibits $LTB_4$ synthesis, also inhibits PLC-mediated $Ca^{2+}$ flux in neutrophils by modifying proteins of the focal adhesion complex,[96-98] suggesting that *Y. pestis* T3E-induced $LTB_4$ synthesis may be mediated via this signaling hub. Moreover, SRC Kinase Adaptor Phosphoprotein 2 (SKAP2) targeting by YopH during *Y. pseudotuberculosis* infection specifically inhibits β1 integrin-induced $Ca^{2+}$ signaling in neutrophils.[97] Therefore, to determine if SKAP2 is required for T3SS-dependent $LTB_4$ synthesis, leukocytes from $SKAP2^{-/-}$ mice were infected with *Y. pestis*, *Y. pestis* T3E, or *Y. pestis* $T3^{(-)}$. Unlike BMNs from parental C57BL/6J mice, $SKAP2^{-/-}$ BMNs did not synthesize $LTB_4$ in response to any of the strains tested (Fig 3-6A). To ensure that $SKAP2^{-/-}$ BMNs were not generally defective in $LTB_4$ synthesis (i.e. unable to synthesize $LTB_4$), BMNs were treated with the $Ca^{2+}$ ionophore A23187, which bypasses PLC signaling but still requires $cPLA_2$, 5-LOX, FLAP, and $LTB_4$ hydrolase to synthesis $LTB_4$, and cells were able to robustly produce $LTB_4$ (Fig 3-6B). Complementing the PLC inhibitor data, $SKAP2^{-/-}$ BMDMs were not impaired in $LTB_4$ synthesis (Fig 3-6C; $p \leq 0.0001$). Together, these data demonstrate that T3SS-inducing $LTB_4$ synthesis requires SKAP2 activation of PLC in neutrophils but not macrophages.

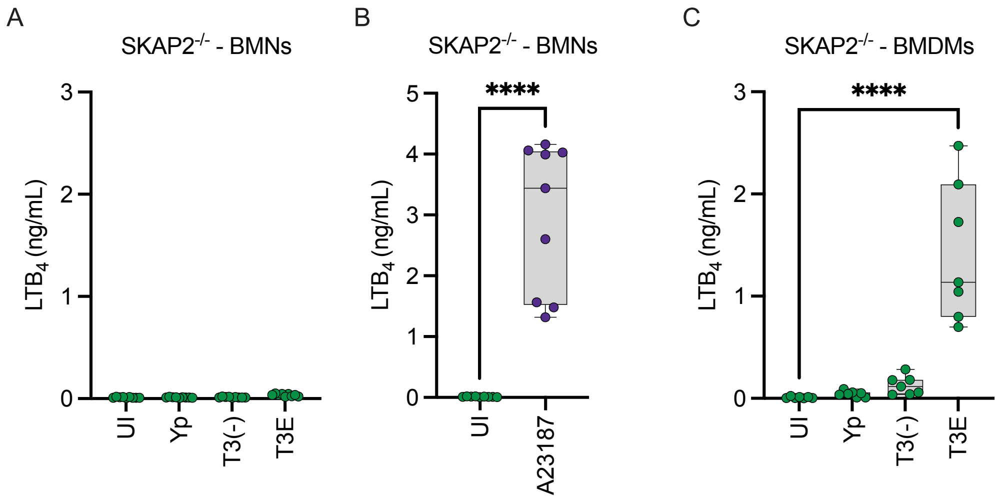


Figure 3-6. SKAP2 signaling required for $LTB_4$ synthesis in BMN

SKAP2$^{-/-}$ (A) BMNs or (C) BMDMs were infected with *Y. pestis, Y. pestis* T3E, or *Y. pestis* T3(-) at an MOI of 20 for (A) 1 h or (C) 4 h. (B) SKAP2$^{-/-}$ BMNs were treated with A23187 (1 μM; purple circles) for 1 h. (A-C) $LTB_4$ was measured from supernatants by ELISA. Each symbol represents an independent biological infection, and the box plot represents the median of the group ± the range. UI = uninfected. One-way ANOVA with Dunnett's *post hoc* test compared to uninfected. ****=p≤0.0001.

3-2i. Activation of MAPK signaling required for $LTB_4$ synthesis is independent of the T3SS

In addition to $Ca^{2+}$ flux, $LTB_4$ synthesis requires MAPK signaling to phosphorylate $cPLA_2$ and 5-LOX.[152, 168, 317-322] While we previously showed that p38 and ERK1/2 are phosphorylated in human neutrophils infected with a high MOI (100 bacteria/cell) of *Y. pestis* T3$^{(-)}$,[93] the MAP kinases responsible for T3SS-dependent $LTB_4$ synthesis have not been defined. Therefore, to determine whether p38 and ERK1/2 are phosphorylated during interactions with *Y. pestis* T3E, leukocytes were infected with *Y. pestis*, *Y. pestis* T3E, or *Y. pestis* T3$^{(-)}$ at an MOI of 20. T3SS-dependent $LTB_4$ production was confirmed (Fig 3-7A and D) and p38 and ERK1/2 phosphorylation from the same samples was determined by western blot. As we previously reported for human PMNs,[93] both p38 and ERK1/2 were phosphorylated in BMNs infected with *Y. pestis* T3E but not *Y. pestis* (Fig 3-7B-C). In the case of the BMDMs, as reported by others,[323-326] we observed elevated basal levels of p38 and ERK1/2 phosphorylation in untreated M1 polarized macrophages, but phosphorylation, especially of p38, was dramatically lower in *Y. pestis* but not *Y. pestis* T3E infected cells (Fig 3-7E-F). Interestingly, regardless of the leukocyte, we observed similar phosphorylation profiles between *Y. pestis* T3E and *Y. pestis* T3$^{(-)}$ infected cells, indicating that MAPK signaling is being triggered by a PAMP unrelated to the T3SS.

3-2j. YopH inhibits ERK phosphorylation in neutrophils and macrophages

We have previously shown that YopJ inhibition of ERK1/2 phosphorylation is sufficient to block $LTB_4$ synthesis,[93] and Shaban et al.[97] previously showed that YopH from *Y. pseudotuberculosis* inhibits ERK1/2 phosphorylation in neutrophils. However, whether YopH can also sufficiently inhibit ERK1/2 phosphorylation in our model has yet to be defined. As expected, phosphorylation of both MAP kinases was inhibited in BMNs infected with a *Y. pestis* T3E strain expressing YopJ (Fig 3-7B, C; +J samples). As predicted by the *Y. pseudotuberculosis* data, infection with *Y. pestis* T3E expressing YopH inhibited ERK1/2 phosphorylation in BMNs (Fig 3-7C; +H samples), YopH was not able to inhibit p38 phosphorylation (Fig 3-7B; +H samples). However, only YopJ appeared able to consistently inhibit p38 and ERK1/2 phosphorylation in BMDMs (Fig 3-7E-F; +H and +J samples). To our knowledge, this is the first time that YopH has been shown to specifically block ERK1/2 but not p38 phosphorylation.

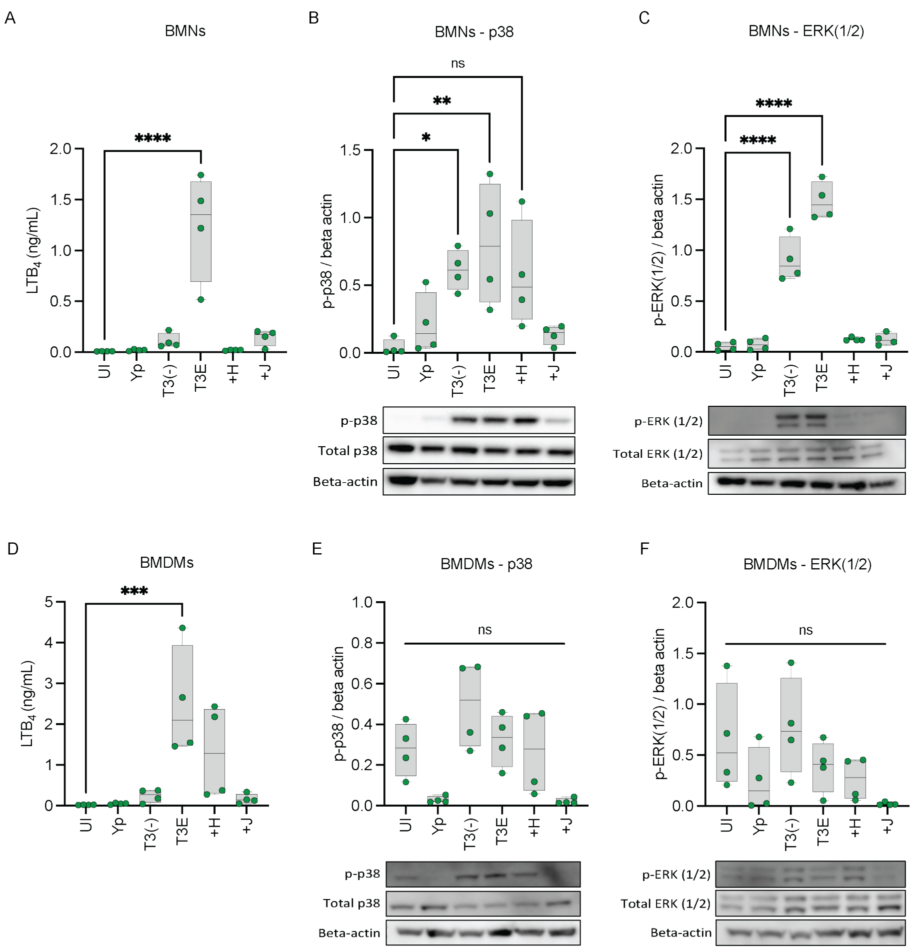


Figure 3-7. p38 and ERK1/2 phosphorylation in neutrophils and macrophages in response to *Y. pestis*

(A-C) BMNs or (D-F) BMDMs were infected with *Y. pestis, Y. pestis* T3E, *Y. pestis* T3(-), or *Y. pestis* TE3 strains expressing only one Yop effector (+H = YopH; +J = YopJ) at an MOI of 20 for 1 h. (A,D) $LTB_4$ measured by ELISA. (B-C, E-F) Densitometry and representative WB images for (B,E) phosphorylated p38 (p-p38) or (C,F) phosphorylated ERK1/2 (p-ERK1/2) from whole cell lysates normalized to beta actin. (A-F) Each symbol represents an independent biological infection, and the box plot represents the median of the group ± the range. UI = uninfected. One-way ANOVA with Dunnett's *post hoc* test compared to uninfected. *=p≤0.05, **=p≤0.01, ***=p≤0.01, ****=p≤0.0001.

3-2k. Inflammasome activation enhances $LTB_4$ synthesis in macrophages but not neutrophils

Previous studies with *Y. pseudotuberculosis* indicate that the T3SS translocase is recognized by NLRP3, leading to activation of the caspase 1 inflammasome and pyroptosis.[68, 90] Inflammasome activation is also required for $LTB_4$ synthesis in response to some PAMPS,[219, 220] but is dispensable for others,[153] raising the question of whether inflammasome activation is required for T3SS-dependent $LTB_4$ synthesis. Therefore, to determine the contribution of the inflammasome to $LTB_4$ synthesis in response to the *Y. pestis* T3SS, leukocytes isolated from $NLRP3^{-/-}$ or $Casp1/11^{-/-}$ mice were infected with *Y. pestis*, *Y. pestis* T3E, or *Y. pestis* $T3^{(-)}$, and $LTB_4$ synthesis was compared to cells isolated from the parental background. Absence of NLRP3 or Casp1/11 did not alter the neutrophil response to *Y. pestis* T3E (Fig 3-8A). Furthermore, treatment with the pan-caspase inhibitor zVAD did not impact the ability of wild type BMNs (Fig 3-8B) or hPMNs (Fig 3-8C) to produce $LTB_4$ in response to infection with *Y. pestis* T3E. In contrast, $LTB_4$ synthesis was significantly lower in both NLRP3 and Casp1/11 deficient BMDMs (Fig 3-8D; $p \leq 0.0001$). However, $LTB_4$ synthesis was still elevated compared to uninfected, *Y. pestis*, or *Y. pestis* $T3^{(-)}$ infected cells ($p \leq 0.0001$ and $p \leq 0.01$, respectively). While treatment of $Casp1/11^{-/-}$ BMDMs with the PLC inhibitor did not dramatically reduce  $LTB_4$ synthesis (Fig 3-8E), treatment with cytoD, or infection with the *Y. pestis* T3E YopE expressing strain, which both disrupt the actin cytoskeleton, reduced $LTB_4$ levels to basal levels (Fig 3-8E; $p \leq 0.0001$), indicating that the residual $LTB_4$ synthesis in CASP1/11-/- BMDMs was not due to PLC signaling. Together, these data indicate that while T3SS-dependent $LTB_4$ synthesis in neutrophils is independent of inflammasome activation, the Casp1/11 inflammasome significantly enhances the $LTB_4$ response by macrophages.

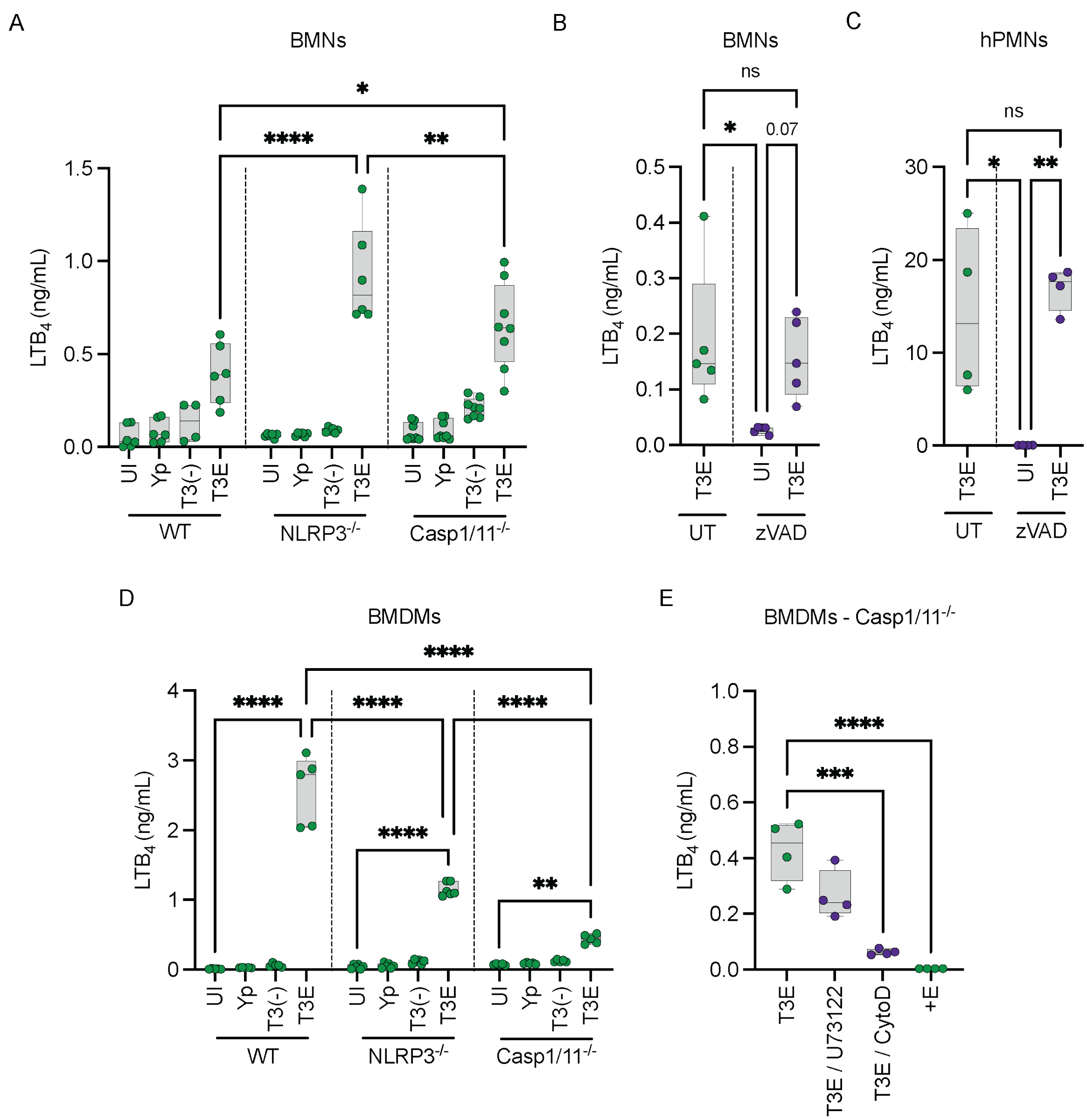


Figure 3-8. Inflammasomes enhance $LTB_4$ synthesis in BMDMs but are dispensable in BMNs

(A) BMNS or (D) BMDMs from WT, NLRP3$^{-/-}$, Casp1/11$^{-/-}$ mice were infected with *Y. pestis, Y. pestis* T3E, or *Y. pestis* T3(-). (B) C57BL/6J BMNs or (C) human PMNs (hPMNs) pretreated with zVAD inhibitor (100 μM; purple circles) for 30 min prior to infection with *Y. pestis* T3E. (E) BMDMs from Casp1/11$^{-/-}$ mice were infected with *Y. pestis* T3E or *Y. pestis* T3E strains expressing only YopE (+E). BMDMs were either left untreated (green circles) or pretreated with PLC inhibitor (U73122, 20 μM; purple circles) or Cytochalasin D (10 μM; purple circles) for 30 min prior to infection with *Y.*

*pestis* T3E. Leukocytes were infected at an MOI of 20 for (A-C) 1 h or (D-E) 4 h. (A-E) $LTB_4$ was measured from supernatants by ELISA. Each symbol represents an independent biological infection, and the box plot represents the median of the group ± the range. UI = uninfected. UT = untreated. ns = not significant. One-way ANOVA with Tukey's *post hoc* test compared to each condition for A-D., or with Dunnett's *post hoc* test compared to untreated/T3E for E. *=p≤0.05, **=p≤0.01, ***=p≤0.001, ****=p≤0.0001.

## 3-3. Discussion

Establishing a non-inflammatory environment during the early stages of plague is crucial for the progression of disease.[31] We and others have shown that *Y. pestis* subverts the host innate immune response by inhibiting leukocyte chemotaxis,[6] phagocytosis,[103, 136] neutrophil degranulation,[36, 93] neutrophil ROS production,[103, 137] and inflammatory lipid, cytokine, and chemokine release.[93, 109, 297] Despite the T3SS being a PAMP,[57] the Yop effectors are highly efficient at preventing immune cell activation, including inhibiting the synthesis of $LTB_4$ needed for a proper inflammatory host response.[93, 297] In this chapter, I sought to understand how the T3SS is recognized by the host, leading to the synthesis of $LTB_4$,and to define how the pathogen uses specific effectors to block this response. Using these data, I have developed a working model showing a differential response to the T3SS between neutrophils and macrophages in both $Ca^{2+}$ signaling and phosphorylation pathways needed for $LTB_4$ synthesis (Fig 3-9).

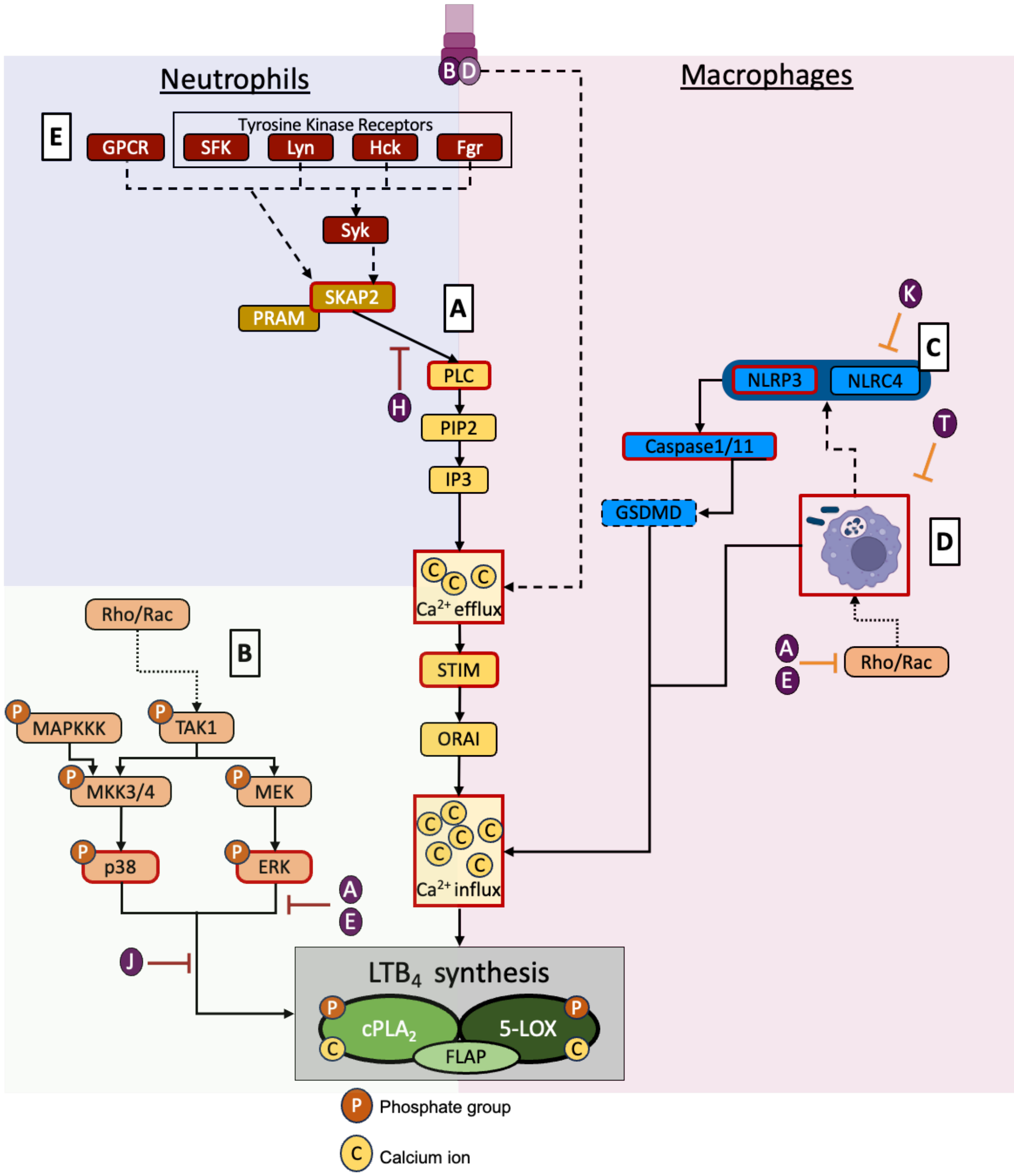


Figure 3-9. T3SS translocase triggered $LTB_4$ synthesis differs between leukocytes

$LTB_4$ synthesis requires (A) an increase in intracellular $Ca^{2+}$ and (B) activation of MAPK signaling. (A) Neutrophils require $Ca^{2+}$ signaling through SKAP2/PLC/STIM1 to produce $LTB_4$, while macrophages show a partial requirement of STIM1 but not SKAP2 or PLC. (B) Activation of MAPK signaling required for $LTB_4$ synthesis appears to be independent of the T3SS, and instead is initiated by a currently unknown PAMP and signaling pathway(s). (C) Inflammasome activation is not required in neutrophils for $LTB_4$ synthesis, but enhances the induction in macrophages, perhaps through GSDMD pore formation increasing $Ca^{2+}$ flux in the cell. (D) Phagocytosis also enhances $LTB_4$ induction in macrophages, but not in neutrophils. (E) Potential receptors contributing to SKAP2 signaling in neutrophils. Purple circles = Yop effectors and either identified or potential target locations of the $LTB_4$ synthesis pathway. Yellow circles = calcium. Orange circles = phosphates. Red bold outlines = locations in the $LTB_4$ synthesis pathway tested in this study. Dotted lines = unknown pathways. Solid lines = known pathways. Red blunted arrows = full inhibition of $LTB_4$ synthesis. Orange blunted arrows = partial inhibition of $LTB_4$ synthesis in WT leukocytes.

One important discovery I report here is that recognition of the T3SS leading to $LTB_4$ synthesis is not specific to the *Y. pestis* T3SS. While the *S. enterica* Typhimurium SPI-1 T3SS varies structurally from the *Y. pestis* secretion system, *S. enterica* Typhimurium still triggers $LTB_4$ in a SPI-1 T3SS-dependent manner. Additionally, $LTB_4$ synthesis by *S. enterica* Typhimurium infected leukocytes appears to be in response to the SPI-1 T3SS and not the SPI-2 system. Like the *Y. pestis* T3SS, the SPI-1 T3SS engages with the host cell through the plasma membrane, while SPI-2 engages through the *Salmonella* containing vacuole,[327, 328] suggesting that the host cells have evolved to sense T3SS interactions across the plasma membrane and respond by synthesizing $LTB_4$. This scenario makes sense, as interactions with the plasma membrane represent the earliest interaction that leukocytes would have with pathogens and allow for rapid synthesis of the lipid. It also appears that unlike *Y. pestis*, *S. enterica* Typhimurium has not evolved effector proteins to inhibit this response, or at minimum not to the degree that the *Y. pestis* Yop effectors can inhibit $LTB_4$ synthesis, as the WT *S. enterica* Typhimurium LT strain produces $LTB_4$ at levels similar to the *Y. pestis* T3E mutant. This difference further supports that the inhibition of $LTB_{4,}$ and initiation of the inflammatory cascade is an important aspect in the virulence and lifestyle of *Y. pestis*.

A key virulence strategy mediated by the T3SSs of both *Y. pestis* and *S. enterica* Typhimurium is the manipulation of phagocytosis.[42, 329] Because phagocytosis of crystalline silica is required for $LTB_4$ synthesis,[153] defining the role of phagocytosis in the $LTB_4$ synthesis was another critical aspect in understanding the leukocyte response to the T3SS. In neutrophils, phagocytosis was clearly not required for $LTB_4$ synthesis, and cytochalasin treatment induced even greater $LTB_4$ synthesis in response to *S. enterica* Typhimurium. However, inhibiting phagocytosis reduced $LTB_4$ synthesis by macrophages, providing the first evidence that host cell signaling leading to $LTB_4$ synthesis may differ between these two cell types. It is important to note that for both bacteria, $LTB_4$ synthesis by macrophages was not completely inhibited by cytochalasin treatment, indicating that synthesis is not wholly dependent on phagocytosis in macrophages. Moreover, data from infections with the *Y. pestis* T3$^{(-)}$ mutant, which is as readily phagocytosed as the *Y. pestis* T3E mutant, indicates that phagocytosis alone is not sufficient to trigger $LTB_4$ synthesis in the absence of the T3SS.

$Ca^{2+}$ flux is a critical step in the enzyme activation required for $LTB_4$ synthesis,[152, 154] and thus understanding the mechanisms leading to $Ca^{2+}$ influx during host cell interactions with the T3SS is key to understanding how the cells are sensing this PAMP. YopB and YopD insert into the plasma membrane to form a pore needed for effector translocation into the host cell.[61, 62] Previous work has shown that the pore formed by the translocase can result in the diffusion of molecules larger than $Ca^{2+}$, but YopN appears to act as a plug to regulate whether diffusion through the YopB/D translocase occurs.[330] While the *Y. pestis* T3E strain retains YopN, it was still possible that $Ca^{2+}$ diffusion through the translocase occurred in infected cells, leading to $Ca^{2+}$ flux. However, using pharmacological inhibitors of $Ca^{2+}$ signaling, I have shown that PLC signaling, and not diffusion of $Ca^{2+}$ through the T3SS, is the primary driver of $Ca^{2+}$ flux needed for $LTB_4$ synthesis in neutrophils. Interestingly, PLC inhibition had little effect on $LTB_4$ synthesis in macrophages, strongly suggesting $Ca^{2+}$ diffusion across the membrane is contributing to the $LTB_4$ synthesis response. This conclusion is further supported by the differential ability of YopH to inhibit $LTB_4$ synthesis in neutrophils but not macrophages. Additionally, work primarily from *Y. pseudotuberculosis* shows that YopH dephosphorylation of SLP-76 and SKAP2 is directly linked to the inhibition of PLC phosphorylation and $Ca^{2+}$ flux in neutrophils,[97, 98] and I have shown here that SKAP2 is also required for $LTB_4$ synthesis in neutrophils. As $LTB_4$ synthesis by macrophages is not dependent on SKAP2 or PLC signaling, it appears STIM1 activation and SOCE in macrophages requires a different signaling pathway. Future work to define this pathway is necessary to understand how macrophages recognize and respond to the T3SS.

While SKAP2 is required for PLC activation and $LTB_4$ synthesis in neutrophils, the receptors and kinases responsible for SKAP2 phosphorylation in response to the T3SS are yet to be identified. Several tyrosine kinase receptors, including LYN, HCK, FGR, FYN, FRK, and YES, have been shown to activate SKAP2.[331] In many cases this is mediated through the kinase Syk. However, Shaban et al.[97] have shown that during neutrophil interactions with *Y. pseudotuberculosis*, ROS production is both Syk-dependent and independent, depending on which receptor is engaged. We are currently using a combination of phosphoproteomics and kinase inhibitor regression to identify other kinases involved in the recognition of the T3SS.

In addition to $Ca^{2+}$ flux, $cPLA_2$ and 5-LOX phosphorylation via MAP kinase signaling is also essential for $LTB_4$ synthesis. Interestingly, while I observed phosphorylation of p38 and ERK1/2 in the leukocytes, MAPK phosphorylation does not appear to be dependent on the T3SS, as the *Y. pestis* $T3^{(-)}$ strain, which lacks the T3SS still induces phosphorylation. These data suggest that the primary signal regulating T3SS-dependent $LTB_4$ synthesis is the $Ca^{2+}$ flux, not the MAP kinase signaling pathway. The PAMP that is responsible for initiating MAPK signaling still remains unknown.

Previous work with *Y. pseudotuberculosis* and *Y. pestis* have significantly contributed to our understanding of inflammasome activation and pyroptosis.[70, 332] Components of the T3SS, including YopB, are recognized by NLRP3 and NLRC4 to activate the caspase 1 inflammasome and pyroptosis by macrophages, but inflammasome activation is limited by YopK.[67, 68] Because the *Y. pestis* T3E strain lacks YopK, I hypothesized that the inflammasome might be activated during interactions with immune cells. However, while BLT1-$LTB_4$ signaling has been shown to enhance inflammasome activation in the gout,[193] asthma,[261] and *Staphylococcus aureus* skin infection models,[218] evidence that inflammasome activation induces $LTB_4$ synthesis is much more limited.[219] Thus, it was unclear if T3SS-induced inflammasome activation contributed to $LTB_4$ synthesis.

Indeed, $LTB_4$ synthesis by neutrophils was not dependent on NLRP3 or Caspase 1/11. However, $LTB_4$ synthesis was significantly reduced in NLRP3$^{-/-}$ and Caspase1/11$^{-/-}$ macrophages. Importantly, expression of YopK in the *Y. pestis* T3E strain also reduced $LTB_4$ synthesis in macrophages (Fig 3-2) but not neutrophils,[93, 297] supporting that T3SS-induced inflammasome activation contributes to $LTB_4$ synthesis in macrophages. To our knowledge, this is the first evidence that inflammasome activation in response to bacterial infection leads to $LTB_4$ synthesis, indicating that in addition to the processing and secretion of protein mediators of inflammation (e.g., IL-1B and IL-18), inflammasome activation in macrophages can also increase the synthesis of lipid mediators of inflammation. It also raises the possibility that Casp1/11 and/or inflammasome activation may contribute to STIM1 activation in macrophages and will be explored in the future.

In conclusion, I have shown that leukocytes have evolved to recognize the T3SS to induce $LTB_4$ synthesis during bacterial interactions. However, the molecular mechanisms of recognition differ between neutrophils and macrophages. Moreover, while others have shown that the T3SS is a PAMP that stimulates the inflammasome in macrophages to induce the production of pro-inflammatory mediators, here I demonstrated for the first time that neutrophils use an inflammasome independent mechanism to sense the T3SS and induce the production of $LTB_4$. Together, these data provide us with a better understanding of the early response of leukocytes to bacterial pathogens.

## 3-4. Material and Methods

### 3-4a. Ethics statement

All animal work was approved by the University of Louisville Institutional Animal Care and Use Committee (IACUC Protocol #22157). Use of human neutrophils was approved by the University of Louisville Institutional Review Board guidelines (IRB #96.0191) and written consents for use were obtained.

### 3-4b. Bacterial strains

Bacterial strains used in this study are listed in Table 3-1. *Y. pestis* was cultured with BHI broth for 15-18 h at 26°C in aeration. Cultures were then diluted 1:10 in fresh, warmed BHI broth containing 20 mM $MgCl_2$ and 20 mM Na-oxalate and cultured at 37°C for 3 h with aeration to induce expression of the T3SS. Bacterial concentrations were determined using a spectrophotometer and diluted to desired concentrations in fresh medium.

| Name in manuscript | Genotype | Strain ref. # | Source |
|---|---|---|---|
| **Bacteria** | | | |
| *Y. pestis* | KIM1001 pgm-, pMT1+, pPCP1+, pCD1+, pML001+ | JG598 | 111 |
| *Y. pestis* T3$^{(-)}$ | KIM1001 pgm-, pMT1+, pPCP1+, pCD1-, pML001+ | JG597 | 111 |
| *Y. pestis* T3E | KIM1001 pgm-, pMT1+, pPCP1+, pCD1+ (yopH$^{\Delta 3\text{-}467}$ yopE$^{\Delta 40\text{-}197}$ yopK$^{\Delta 4\text{-}181}$ yopM$^{\Delta 3\text{-}408}$ ypkA$^{\Delta 3\text{-}731}$ yopJ$^{\Delta 4\text{-}288}$ yopT$^{\Delta 3\text{-}320}$), pGEN222+ | YPA366 | This work |
| *Y. pestis* T3E | KIM1001 pgm-, pMT1+, pPCP1+, pCD1+, (yopH$^{\Delta 3\text{-}467}$ yopE$^{\Delta 40\text{-}197}$ yopK$^{\Delta 4\text{-}181}$ yopM$^{\Delta 3\text{-}408}$ ypkA$^{\Delta 3\text{-}731}$ yopJ$^{\Delta 4\text{-}288}$ yopT$^{\Delta 3\text{-}320}$), pML001+ | JG715 | 111 |
| *Y. pestis* T3E +ypkA | KIM1001 pgm-, pMT1+, pPCP1+, pCD1+ (yopH$^{\Delta 3\text{-}467}$ yopE$^{\Delta 40\text{-}197}$ yopK$^{\Delta 4\text{-}181}$ yopM$^{\Delta 3\text{-}408}$ yopJ$^{\Delta 4\text{-}288}$ yopT$^{\Delta 3\text{-}320}$), pML001+ | JG684 | 111 |
| *Y. pestis* T3E +yopE | KIM1001 pgm-, pMT1+, pPCP1+, pCD1+ (yopH$^{\Delta 3\text{-}467}$ yopK$^{\Delta 4\text{-}181}$ yopM$^{\Delta 3\text{-}408}$ ypkA$^{\Delta 3\text{-}731}$ yopJ$^{\Delta 4\text{-}288}$ yopT$^{\Delta 3\text{-}320}$), pML001+ | JG681 | 111 |
| *Y. pestis* T3E +yopH | KIM1001 pgm-, pMT1+, pPCP1+, pCD1+ (yopE$^{\Delta 40\text{-}197}$ yopK$^{\Delta 4\text{-}181}$ yopM$^{\Delta 3\text{-}408}$ ypkA$^{\Delta 3\text{-}731}$ yopJ$^{\Delta 4\text{-}288}$ yopT$^{\Delta 3\text{-}320}$), pML001+ | JG680 | 111 |
| *Y. pestis* T3E +yopJ | KIM1001 pgm-, pMT1+, pPCP1+, pCD1+ (yopH$^{\Delta 3\text{-}467}$ yopE$^{\Delta 40\text{-}197}$ yopK$^{\Delta 4\text{-}181}$ yopM$^{\Delta 3\text{-}408}$ ypkA$^{\Delta 3\text{-}731}$ yopT$^{\Delta 3\text{-}320}$), pML001+ | JG686 | 297 |
| *Y. pestis* T3E +yopK | KIM1001 pgm-, pMT1+, pPCP1+, pCD1+ (yopH$^{\Delta 3\text{-}467}$ yopE$^{\Delta 40\text{-}197}$ yopM$^{\Delta 3\text{-}408}$ ypkA$^{\Delta 3\text{-}731}$ yopJ$^{\Delta 4\text{-}288}$ yopT$^{\Delta 3\text{-}320}$), pML001+ | JG682 | 111 |
| *Y. pestis* T3E +yopM | KIM1001 pgm-, pMT1+, pPCP1+, pCD1+ (yopH$^{\Delta 3\text{-}467}$ yopE$^{\Delta 40\text{-}197}$ yopK$^{\Delta 4\text{-}181}$ ypkA$^{\Delta 3\text{-}731}$ yopJ$^{\Delta 4\text{-}288}$ yopT$^{\Delta 3\text{-}320}$), pML001+ | JG683 | 111 |
| *Y. pestis* T3E +yopT | KIM1001 pgm-, pMT1+, pPCP1+, pCD1+ (yopH$^{\Delta 3\text{-}467}$ yopE$^{\Delta 40\text{-}197}$ yopK$^{\Delta 4\text{-}181}$ yopM$^{\Delta 3\text{-}408}$ ypkA$^{\Delta 3\text{-}731}$ yopJ$^{\Delta 4\text{-}288}$), pML001+ | JG685 | 111 |
| *Y. pestis* T3E *yopB* | KIM1001 pgm-, pMT1+, pPCP1+, pCD1+ (yopH$^{\Delta 3\text{-}467}$ yopE$^{\Delta 40\text{-}197}$ yopK$^{\Delta 4\text{-}181}$ yopM$^{\Delta 3\text{-}408}$ ypkA$^{\Delta 3\text{-}731}$ yopJ$^{\Delta 4\text{-}288}$ yopT$^{\Delta 3\text{-}320}$yopB $^{\Delta 7\text{-}396}$), pML001+ | YPA322 | 297 |
| *Y. pestis* *yopB*::*cyopB* | KIM1001 pgm-, pMT1+, pPCP1+, pCD1+ (yopH$^{\Delta 3\text{-}467}$ yopE$^{\Delta 40\text{-}197}$ yopK$^{\Delta 4\text{-}181}$ yopM$^{\Delta 3\text{-}408}$ ypkA$^{\Delta 3\text{-}731}$ yopJ$^{\Delta 4\text{-}288}$ yopT$^{\Delta 3\text{-}320}$), pML001+ | YPA362 | 297 |
| *S.* Typhimurium | *Salmonella enterica* Typhimurium LT2 pGENLux - 14028s | LOU120 | 297 |
| *S.* Typhimurium SPI-1 null mutant | *Salmonella enterica* Typhimurium *invA::Km* - 14028s | MJW1301 | 328 |
| *S.* Typhimurium SPI-2 null mutant | *Salmonella enterica* Typhimurium *ssak::Cm* - 14028s | MJW1835 | 333 |
| *S.* Typhimurium SPI-1/2 mutant | *Salmonella enterica* Typhimurium *invA::Km ssak::Cm* - 14028s | MJW1836 | Micah Worley |
| *K. pneumoniae* | *Klebsiella pneumoniae* KPPR1S | VK148 | 334 |
| *K. pneumoniae manC* | *Klebsiella pneumoniae* KPPR1S *ΔmanC* | LOU171 | 282 |
| **Plasmids** | | | |
| pGEN222 | GFP gene | NA | |
| pML001 | Luciferase bioreporter | NA | 111 |

Table 3-1. Bacterial strains and plasmids used in this chapter

3-4c. Cell isolation and cultivation

Leukocytes were isolated from bone marrow of 7-12-week-old mice that were either C57BL/6J, C57BL/6J Tyrosinase$^{-/-}$, C57BL/6J Tyrosinase$^{-/-}$ NLRP3$^{-/-}$, C57BL/6J Tyrosinase$^{-/-}$ Caspase1/11$^{-/-}$, or BALB/c SKAP2$^{-/-}$. Murine neutrophils were isolated using an Anti-Ly-6G Microbeads kit (Miltenyi Biotec Cat. No. 130-120-337) per the manufacturer's instructions. Neutrophil isolations yielded ≥ 95% purity and were used within 1 h of isolation. Macrophages were differentiated from murine bone marrow (BMDMs) in DMEM supplemented with 1 mM Na-pyruvate, and 10% FBS for 6 days. Macrophages were polarized with 20 ng/mL of GM-CSF (M1; Kingfisher Biotech Cat. No. RP0407M) throughout the differentiation. The medium was replaced on days 1 and 3 (adapted from [289]). Use of human neutrophils was approved by the University of Louisville Institutional Review Board (IRB) guidelines (IRB #96.0191) and written consents for use were obtained. Human neutrophils were isolated from the peripheral blood of healthy, medication-free donors, as described previously.[288] Briefly, white blood cells were isolated from whole blood using a 6% dextran solution. Neutrophils were then separated from monocytes using a percoll gradient of 42% and 50.5%. RBCs were then lysed from the neutrophil containing layer using 0.2% NaCl for 30 seconds and followed by a quench with 5 mL 1.6% NaCl. Neutrophil isolations yielded ≥ 95% purity and were used within 1 h of isolation.

3-4d. Leukocyte infections

Neutrophils were cultured in RPMI + 5% FBS and macrophages were cultured in DMEM + 10% FBS. BMNs were adhered to 24-well plates for 30 min that were coated with FBS prior to infection (wells were washed twice with 1 x DPBS prior to plating the cells). BMDMs were adhered to 24-well plates 1 day prior to infection. Human neutrophils were resuspended in Kreb's buffer (w/ $Ca^{2+}$ & Mg) then adhered to 24-well plates for 30 min that were coated with pooled human serum prior to infection (wells were washed twice with 1 x DPBS prior to plating the cells). Leukocytes were infected at a multiplicity of infection (MOI) of 20 and incubated for 1 h or 4 h in a cell culture incubator at 37°C with a constant rate of 5% $CO_2$. Supernatants or pellets were then collected, centrifuged for 1 min at 6,000 x g, and supernatants devoid of cells were transferred to a fresh eppendorf tube and stored at -80°C until ELISA and pellets were prepped for western blot analysis. All infections were synchronized by centrifugation (200 x g for 5 min).

3-4e. Treatments and inhibitors

Prior to infection, leukocytes were treated with the following for the times and concentrations indicated in the figure legends: phagocytosis inhibitor cytochalasin D (VWR; Cat. No. 100507-376), calcium ionophore A23187 (Sigma-Aldrich; Cat. No. C7522), PLC inhibitor U73122 (Abcam; Cat. No. ab120998), STIM1 inhibitor SKF-96365 (VWR; Cat. No. 89156-792), extracellular calcium chelator EGTA, KCl, or pan-caspase inhibitor Z-Vad-FMK (Enzo; Cat. No. ALX-260-020). At the time of infection, bacteria were added for a 500 μL final volume.

3-4f. Measurement of $LTB_4$ by enzyme-linked immunosorbent assay

Supernatants of neutrophils and macrophages were collected and measured for $LTB_4$ by ELISA per manufacturer's instructions (Cayman Chemicals; Cat. No. 520111).

3-4g. Western blots

Pellets were lysed over ice in 1x Novex lysis buffer and processed through Qiashredders (Qiagen, Cat. No. 79654). Samples were boiled for 10 min, and 10 μL was separated on a 10% SDS-PAGE gel. Samples were immunoblotted with polyclonal anti-p-p38 antibody (Cell Signaling; Cat. No. 9211S), anti-p38 antibody (Cell Signaling; Cat. No. 9228), anti-p-p44/42 (ERK1/2) antibody (Cell Signaling; Cat. No. 9101s), anti-beta-actin antibody (Cell Signaling; Cat. No. 3700s) diluted to 1:1000 or anti-p44/42 antibody (Cell Signaling; Cat. No. 4696) diluted to 1:2,000. Anti-rabbit (Sigma-Aldrich; Cat. No. A9169) or anti-mouse (ThermoFisher Scientific; Cat. No. 31430) IgG HRP secondary antibodies were diluted to 1:20,000. SuperSignal West Femto maximum-sensitivity substrate (ThermoFisher Scientific; cat. no. 34095) was used to detect antigen-antibody binding. Densitometry was performed using ImageJ software to quantify bands, normalized to total protein.

3-4h. Confocal

BMNs infected at an MOI of 10 with a GFP expressing *Y. pestis* T3E strain were pretreated with 10 µM cytochalasin D or DPBS. After 1 h of infection, cells were then fixed with 4% PFA (Sigma Aldrich: P6148-500G), blocked with 3% BSA-PBS (Sigma: A4503-100G), stained with primary antibody, rabbit anti-*Yersinia pestis* sera (1:1,000; lot UL25, 9/14/2013) overnight at 4°C, followed by secondary antibody, donkey anti-rabbit Alexa Fluor 647 (1:1,000; JacksonImmuno Research: 711-605-152) for 2 hours at room temperature, and finally with Hoechst (1:350; ThermoScientific: 62249) at room temperature for 15 minutes. Cells were then mounted in Prolong Gold (Invitrogen: P36980) and visualized with z-stack images using a confocal Olympus Fluoview FV3000 UPlanxApo. To quantify the rates at which bacteria were phagocytosed, 3D volume Pearson correlation coefficients were calculated for eGFP and Alexa647.

3-4i. Statistics

For all studies, male and female mice or human donors were used and no sex biases were observed for any phenotype. For all experiments, each data point represents data from biologically independent experiments performed on different days. Where appropriate and as indicated in the figure legends, statistical comparisons were performed with Prism (GraphPad) using one-way analysis of variance (ANOVA) with Dunnett's or Tukey's *post hoc* test, or T-test with Mann-Whitney's *post hoc* test. P values ≤ 0.05 were considered statistically significant and reported.

# CHAPTER 4:

# SUMMARY OF MY DISCOVERIES, SIGNIFICANCE OF MY DISCOVERIES, QUESTIONS, QUESTIONS THAT NEED ANSWERING, & CONCLUSIONS

## 4-1. Summary of my discoveries

My lab discovered that a *Y. pestis* strain that is missing the pCD1 plasmid ($T3^{(-)}$) can induce an $LTB_4$ response in human neutrophils, and that five Yop effectors can then independently inhibit $LTB_4$ synthesis.[93] I decided to explore this phenotype further and made quite a few discoveries of my own.

My first discovery was that the human neutrophil $LTB_4$ response to the $T3^{(-)}$ strain only occurs at high MOIs, e.g., at MOIs of ≥50, which differs from mouse neutrophils, in which the $T3^{(-)}$ strain never triggers an $LTB_4$ response. Because the mouse neutrophils were non-responsive, I pivoted and infected the cells with a *Y. pestis* strain which still expressed the T3SS but lacked the seven Yop effectors. This is when I discovered both mouse and human neutrophils recognize the T3SS needle of *Y. pestis* triggering an $LTB_4$ response at low MOIs. Specifically, the YopB/D translocase of the T3SS is required for this response, whether it be the translocase itself or the non-effector proteins, the translocase allows to pass through into the cell is still unclear. Next, I showed the same phenotype in macrophages and mast cells. I further showed the Yop effectors can actively inhibit $LTB_4$ synthesis, even when triggered by other PAMPs. Within macrophages, I showed that only one Yop effector can independently inhibit $LTB_4$ synthesis, while another five may work cooperatively to inhibit $LTB_4$.

Having found the needle as the required PAMP for $LTB_4$ synthesis in response to *Y. pestis*, I next determined the mechanism in which the needle is triggering the synthesis in neutrophils and macrophages. Neutrophils recognize the needle in a SKAP2/PLC/STIM1-dependent $Ca^{2+}$ signaling pathway. In contrast, macrophages T3SS-induction of $Ca^{2+}$ flux required for $LTB_4$ synthesis appears to occur through additional pathways. I also found that the needle doesn't induce ERK1/2 phosphorylation in macrophages but does in neutrophils. Surprisingly, while neutrophils do not require phagocytosis of *Y. pestis* to trigger $LTB_4$ synthesis, macrophages have a heightened $LTB_4$

response when the bacteria are phagocytosed. Additionally, I found that in neutrophils, the T3SS triggered an inflammasome-independent pathway that induces $LTB_4$ synthesis, but in macrophages, inflammasome activation enhances $LTB_4$ synthesis.

**4-2. Significance of my discoveries**

The first novelty of my research is in exploring the global lipid mediator response during plague. Previous research focused on the protein mediator response during *Yersinia* infections, despite lipid mediators playing a pivotal role in inducing a rapid inflammatory response to pathogens. By performing a lipidomic analysis, I have contributed to the *Yersinia* field by revealing an additional mechanism of how *Y. pestis* induces a biphasic inflammatory response during plague, in which the initial target may not be protein mediators directly, but rather the rapid synthesis of lipid mediators which are required for timely protein-mediated responses.

To my knowledge, my data also represents the first example that non-effector components of the *Y. pestis* T3SS can also be recognized as a PAMP by neutrophils, as previous studies showed that only the Yop effectors themselves were recognized.[264, 265] Additionally, I identified a previously undescribed inflammasome-independent mechanism that neutrophils use to sense and respond to the bacterial T3SS to rapidly produce $LTB_4$. Furthermore, in macrophages, my work is the first evidence that inflammasome activation in response to a bacterial infection leads to $LTB_4$ synthesis, indicating inflammasome activation in macrophages can also increase the synthesis of lipid mediators of inflammation. This response is especially important during a *Yersinia* infection in which induction of inflammation in the first 36 h of colonization is critical for survival.

By exploring both neutrophils and macrophages, I not only revealed two separate mechanisms that the host has developed to recognize the *Y. pestis* T3SS, but more importantly, I discovered *Y. pestis* has evolved virulence mechanisms to counteract both signaling pathways to inhibit $LTB_4$ synthesis, further highlighting the importance and significance of $LTB_4$ during a *Yersinia* infection.

I also showed that the sensing of the T3SS across the plasma membrane is responsible for triggering the rapid $LTB_4$ response, and this response is conserved against other T3SS. Importantly, *Y. pestis* has evolved effector proteins to inhibit this response, while *Salmonella*, and perhaps other pathogens, do not produce proteins which directly target $LTB_4$ synthesis.

Previous studies have used exogenous treatment of $LTB_4$ to show an increase in antimicrobial responses or the detrimental effects of $LTB_4$ in sterile inflammation. My work implemented a simple infection model to explore the interplay of the significance of $LTB_4$ during the host-pathogen interaction during *Yersinia* infection. A model that can be applied to other pathogens, in which inflammation plays a major role.

Overall, my research has improved our understanding of the early leukocyte responses to bacterial pathogens and how *Y. pestis* alters the host response to generate a beneficial non-inflammatory environment for the pathogen.

## 4-3. Questions, questions that need answering

### 4-3a. What are the consequences of $LTB_4$ inhibition on plague?

While I have shown that $LTB_4$ synthesis is inhibited during plague, ultimately, we still don't completely understand the impact of this inhibition on disease and if targeting $LTB_4$ could alter the course of infection. However, data from our lab supports that inhibition of $LTB_4$ is beneficial to the bacteria. First, exogenous $LTB_4$ treatment in the intraperitoneal model of infection showed an increase in neutrophil influx and a decrease in bacterial survival (Fig 2-3). Moreover, I have also shown that $LTB_4$ treatment of macrophages increases bacterial killing to the same level as treatment with IFN-$\gamma$ (Fig 4-1). However, the impact of $LTB_4$ on pneumonic and bubonic plague has not been directly tested. Thus, it would be prudent to determine what the consequences are to treating mice with $LTB_4$ during pneumonic and bubonic plague. To do this, C57BL/6J and BLT1$^{-/-}$ mice could be treated with $LTB_4$ 1 h prior to, or at the time of, infection with *Y. pestis* and changes in leukocyte influx, cytokine and chemokine levels, bacterial proliferation, and host survival could be measured. If $LTB_4$ inhibition is important to establish the non-inflammatory environment during plague, then I would expect for the C57BL/6J mice to show an increase of leukocyte influx and cytokine/chemokine levels earlier in the infection, during the non-inflammatory phase of infection. This would be accompanied by a decrease in bacterial replication and host survival. The $BLT1^{-/-}$ mice would show no change in phenotype, even with treatment.

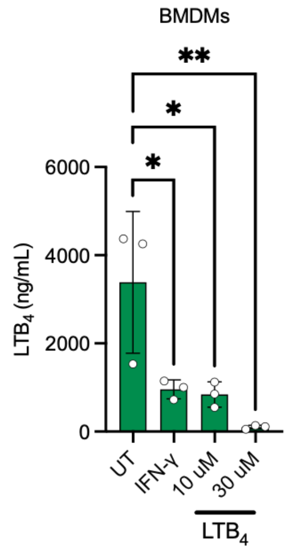


<u>Figure 4-1. $LTB_4$ treatment improves host killing of *Y. pestis*</u>

Murine bone-marrow derived macrophages (BMDM) differentiated towards M2 phenotypes, were pre-treated with either IFN-γ (5 ng/mL) or $LTB_4$ for a total of 4 h. 3 h into treatment, macrophages were infected with *Y. pestis* (*Y. pestis* KIM1001 pML001 (Lux plasmid)) that expressed the T3SS (Yp) and bacterial survival was measured at 8 h (MOI 5). Each symbol represents the average of three technical replicates from independent biological replicates and the bar graph represents the mean ± the standard deviation. UT=untreated infected macrophages. One-way ANOVA with Dunnett's *post hoc* test comparing to the UI sample. *=p≤0.05, **=p≤0.01.

4-3b. How are YpkA and YopE inhibiting $LTB_4$ synthesis in neutrophils?

In BMNs, YpkA and YopE can also independently inhibit $LTB_4$ synthesis. While these proteins are known to limit phagocytosis, this is likely not contributing to $LTB_4$ inhibition. Therefore, I would also like to determine whether these effectors are inhibiting MAPK phosphorylation or $Ca^{2+}$ influx needed for $LTB_4$ synthesis. To determine this, I would infect BMNs with the single add back mutants, and measure p38 and ERK phosphorylation. Based on what each of these effectors target within the host, I suspect both would inhibit the phosphorylation pathways. Alternatively, YpkA has also been shown to target $Ca^{2+}$ signaling, so I may not see phosphorylation of one or both pathways, showing the same phenotype seen with YopH. $Ca^{2+}$ flux could then be directly measured.

4-3c. Which PRR is the T3SS needle activating in neutrophils?

I have identified the $Ca^{2+}$ and phosphorylation pathways triggered by the T3SS in neutrophils. Using this information, I could determine the upstream kinases that directly activate these pathways. I would start by doing a tyrosine kinase inhibitor screen, which would utilize machine learning to identify the phospho-signaling pathways activated by the T3SS.[335] Using a PLC inhibitor as a positive control, a 96-well plate worth of neutrophils treated with tyrosine kinase inhibitors would be infected with the *Y. pestis* T3E strain and $LTB_4$ would be measured after an hour. The inhibitor for the kinase(s) responsible recognizing the needle would result in a decrease or abrogation of $LTB_4$ synthesis.

4-3d. What is the role of prostaglandins during plague?

The results from my lipidomic analysis showed that unlike $LTB_4$, the cyclooxygenase pathway appears to be induced during pneumonic plague (Fig 2-1), suggesting that *Y. pestis* is unable to inhibit prostaglandin synthesis by leukocytes. Therefore, using $PGE_2$ as a representative prostaglandin, I examined the ability of murine neutrophils, macrophages, and mast cells to release prostaglandins in response to *Y. pestis*. Like $LTB_4$, neutrophils, and M1-polarized macrophages produce $PGE_2$ in response to the T3SS, but release is inhibited by secretion of the Yop effectors (Fig 4-2A and B; $p \leq 0.0001$). However, mast cells appeared to produce equivalent amounts of $PGE_2$ in response to all three strains of *Y. pestis*, indicating that *Y. pestis* is not able to inhibit $PGE_2$ synthesis in mast cells (Fig 4-2C; $p \leq 0.05$). These data suggest that signals leading to cyclooxygenase activity in mast cells differ from those in other leukocytes. Additionally, these data and the mouse lipidomic data suggest that mast cells may be a primary source of $PGE_2$, and potentially other prostaglandins, in response to *Y. pestis* infection of the lungs. To test this hypothesis, I would measure the prostaglandin response in mast cell KO mice. I would also infect $COX^{-/-}$ mice and see how pneumonic plague progresses.

The other question these data raise is whether PG synthesis is protective or detrimental to the host. $PGE_2$ has been shown to inhibit NADPH oxidase activity during infection with *K. pneumoniae,* which directly counteracts the proinflammatory activities of $LTB_4$.[277, 278] The phagocytic index of $LTB_4$-stimulated rat alveolar macrophages (AMs) is reduced when co-stimulated with $PGE_2$.[278] Moreover, AMs treated with $PGE_2$ showed a 40% reduction in $LTB_4$ synthesis when stimulated with an ionophore known to induce a strong $LTB_4$ response.[277] These data suggest that the elevated levels of prostaglandin synthesis observed during pneumonic plague may contribute to the blunted $LTB_4$ response by the host.

As an important side note, when I measured $PGE_2$ as a function of synthesis vs. release in human neutrophils, I found that while prostaglandins were not being released, they were still being synthesized (Fig 4-3). This was different than what we observed for $LTB_4$ in which synthesis and release were inhibited by the Yop effectors (Fig 4-3 and [93]). Together these data warrant future studies to better define if synthesis or release of $PGE_2$ is being targeted by the Yop effectors.

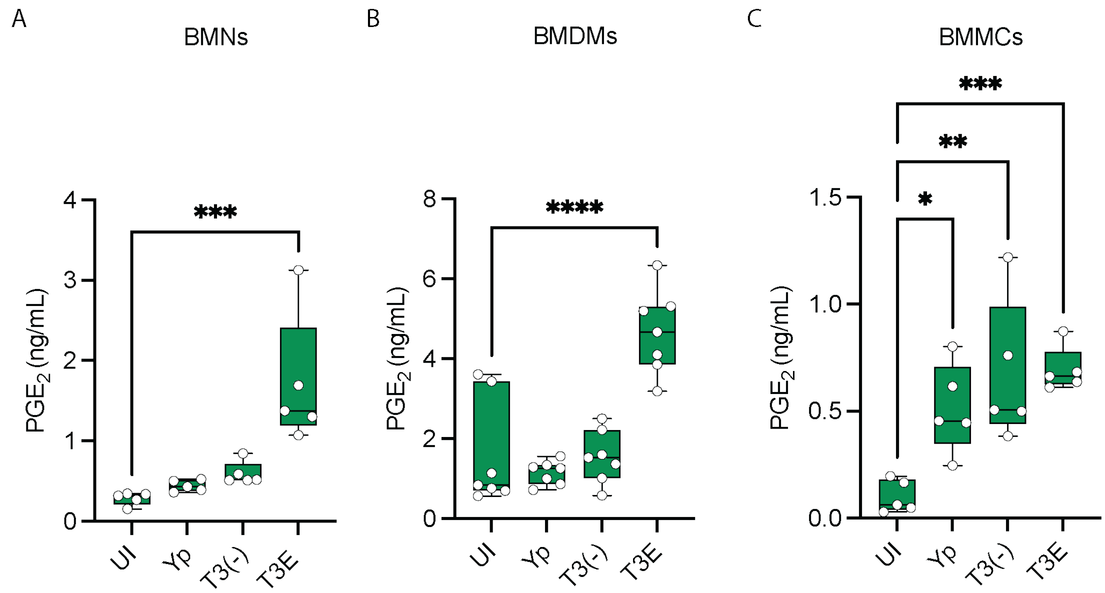


Figure 4-2. *Y. pestis* inhibits $PGE_2$ synthesis in BMNs, BMDMs, but not BMMCs

(A) Neutrophils isolated from bone-marrow using an Anti-Ly-6G MicroBeads UltraPure kit (B) BMDMs differentiated towards M1 or (C) BMMCs were infected at an MOI of 20 with *Y. pestis*, *Y. pestis* T3E, or *Y. pestis* T3(-). $PGE_2$ measured by ELISA after 1 h of incubation at 37°C. UI=uninfected. Each symbol represents an independent biological sample and the box plot represents the median of the group ± the range. One-way ANOVA with Dunnett's *post hoc* test comparing to the UI sample. *=p≤0.05, *=p≤0.01, ***=p≤0.001, ****=p≤0.0001.

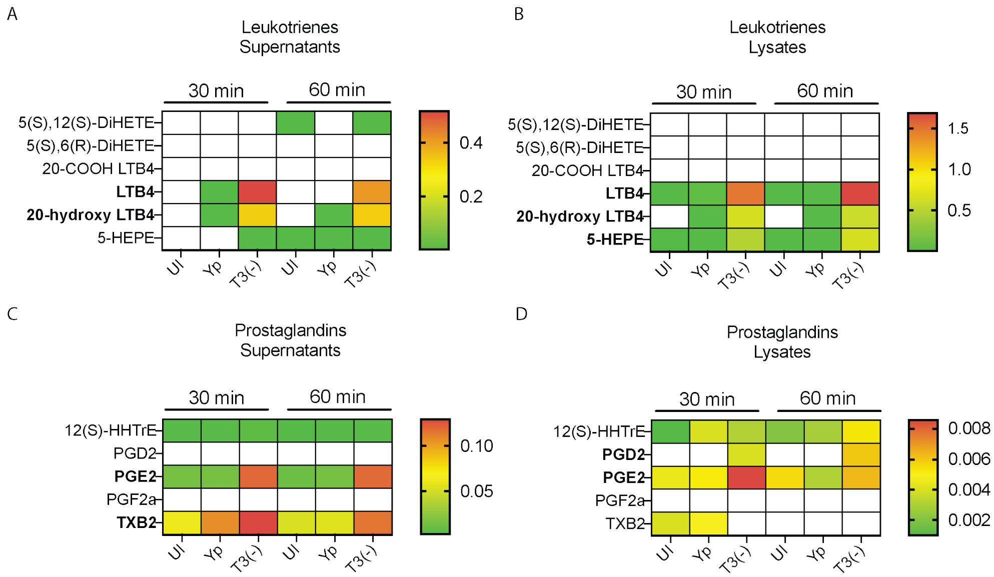


<u>Figure 4-3. Lipidomic analysis of human neutrophils after *Y. pestis* infection</u>

Human neutrophils isolated from whole blood were infected at an MOI of 100 with *Y. pestis* or a *Y. pestis* T3(-) mutant. At 30- and 60-min post infection, cells were pelleted, and supernatants were transferred to a fresh eppendorf tube. Cells were then lysed with miliQ water. Lysates and supernatants were spiked with protease and phosphatase inhibitors. Samples were frozen and lipids were quantified by LC-MS. Results were reported as ng per sample. Changes in leukotriene synthesis from (A) supernatants and (B) lysates. Changes in prostaglandin synthesis from (C) supernatants and (D) lysates. Bolded letters indicate significant increase in T3(-) infected compared to uninfected and Yp. UI = uninfected.

4-3e. How do hPMNs respond to a high MOI of T3$^{(-)}$ and synthesize $LTB_4$ but BMNs can't?

One of my early discoveries was that mouse neutrophils were unable to synthesize $LTB_4$ in response to the *Y. pestis* T3$^{(-)}$ strain, even at high MOIs, while human neutrophils can. Although initially perplexing (and for a short time, very inconvenient), differences in the abilities of human and murine neutrophils have been well documented.[267-271] For example, there are PAMPS not recognized by the mouse but can be recognized by humans. TLR2 and TLR4 activation also differ between the two species.[336, 337] Another study showed that while both species express PAR4, activation of the receptor results in a different host response between the two species.[338] Human PAR4 activation has a stronger $Ca^{2+}$ influx response than the mouse PAR4. Therefore, multiple host responses could be responsible for the difference in this phenotype.

4-3f. Do the other *Yersinia* inhibit $LTB_4$?

*Y. pseudotuberculosis* and *Y. enterocolitica* are both enteric pathogens closely related to *Y. pestis* and encode the Ycs T3SS and Yop effectors. However, *Y. pseudotuberculosis* and *Y. enterocolitica* both express integrin binding proteins as well as lack other virulence determinants elicited by *Y. pestis*. Due to these differences, I wanted to determine whether the $LTB_4$ response differed between the *Yersinia* species. To determine this, I infected BMNs with strains of all three *Yersinia* species that expressed the T3SS or were missing the pCD1 plasmid or with *E. coli* as a positive control. As expected, all three WT strains inhibited $LTB_4$ synthesis in the presence of the Yop effectors (Fig 4-4). Also as expected, the *Y. pestis* T3$^{(-)}$ strain did not induce an $LTB_4$ response in the mouse neutrophils. While I also observed no $LTB_4$ from the *Y. pseudotuberculosis* T3$^{(-)}$ infected BMNs, surprisingly there was a robust $LTB_4$ response to the *Y. enterocolitica* T3$^{(-)}$ strain (Fig 4-4). This provides evidence that PAMPs that trigger $LTB_4$ synthesis were lost during the divergence of *Y. pseudotuberculosis* from *Y. enterocolitica*, and these may have contributed to predispose the evolution of *Y. pestis* to a vector- and blood-borne pathogen.

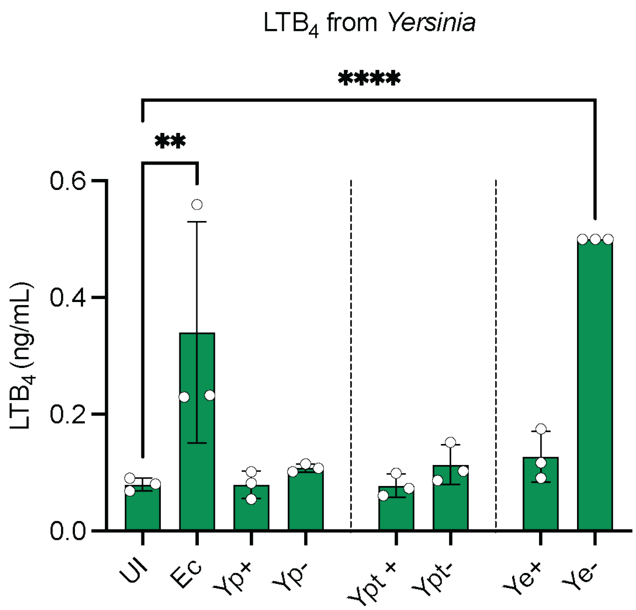


Figure 4-4. *Y. enterocolitica* does not require the T3SS needle to trigger $LTB_4$ synthesis, when Yop effectors are absent

Neutrophils isolated from bone-marrow using a Percoll Plus gradient (Percoll) (Cytiva, Cat. No. 17-5445-02) were infected at an MOI of 10 with *Y. pestis* with or without the T3SS (Yp+ or Yp-), *Y. pseudotuberculosis* with or without the T3SS (Ypt+ or Ypt-), *Y. enterocolitica* with or without the T3SS (Ye+ or Ye-), or *E. coli* (Ec). $LTB_4$ measured by ELISA after 1 h of incubation at 37°C. UI=uninfected. Each symbol represents an independent biological sample and the bar graph represents the mean ± the standard deviation. One-way ANOVA with Dunnett's *post hoc* test comparing to the UI sample. **=p≤0.01, ****=p≤0.0001.

4-4g. Do other bacteria inhibit an $LTB_4$ response?

My dissertation shows that *Y. pestis* effectively limits the synthesis of $LTB_4$ during pneumonic plague through a T3SS/Yop-dependent manner. While this may be a *Y. pestis* specific virulence mechanism, it is likely that other bacteria have also evolved virulence strategies to inhibit this important immune mediator. Case in point, during my global lipidomics screen of pneumonic plague, I also examined the induction of inflammatory lipids during pulmonary infection with *Klebsiella pneumoniae*. Like *Y. pestis* infected mice, I observed a delay in $LTB_4$ synthesis by *K. pneumoniae* infection (Fig 4-5A-B and 2-1, Table 5-1). Because *K. pneumoniae* induces inflammation much quicker than *Y. pestis*, I did not expect the same phenotype and this data was initially perplexing. However, when I challenged neutrophils with *K. pneumoniae in vitro*, I observed that they did not produce $LTB_4$ (Fig 4-5C), even when I increased the MOI to 100 (data not shown). However, if I infected neutrophils with a *K. pneumoniae manC* mutant, which does not synthesize the capsule, neutrophils generated a robust $LTB_4$ response (Fig 2-5).[297] Because the capsule inhibits phagocytosis, these data suggest phagocytosis of the bacterium is required to synthesize $LTB_4$ in the *K. pneumoniae* model within neutrophils. To test this hypothesis, I infected BMNs that were pretreated with cytoD with the *K. pneumoniae manC* mutant. Inhibiting phagocytosis completely abrogated the $LTB_4$ response to the capsule mutant (Fig 4-5D, $p \leq 0.001$), validating that phagocytosis is required for the $LTB_4$ response triggered by *K. pneumoniae*. Previous studies have shown opsonized *K. pneumoniae* induces $LTB_4$ in alveolar macrophages.[198] In my experiment, the bacteria were not opsonized. Therefore, I would be inclined to repeat this experiment and see how the host responds when WT *K. pneumoniae* is opsonized prior to infection or when infected with the *K. pneumoniae* $\Delta$*manC* mutant. Overall, these data support that my work with *Y. pestis* will have a broader impact on the effect pathogens may have on inflammatory lipids.

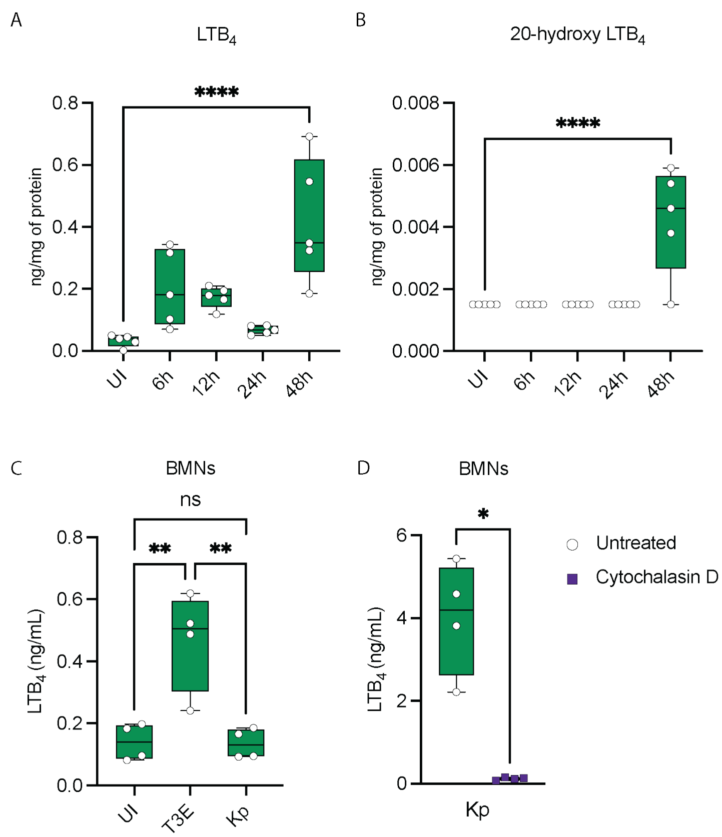


<u>Figure 4-5. Lipid mediator response to *K. pneumoniae*</u>

(A-D) C57BL/6J mice were infected with 10x the $LD_{50}$ of WT *K. pneumoniae*. Lungs were harvested at the indicated times (n=5) to measure host lipids by LC-MS. (A) $LTB_4$ concentrations. (B) 20-hydroxy $LTB_4$ concentrations. (C-D) Murine neutrophils (BMNs) were infected with *Y. pestis* mutant that lacked the Yop effectors (T3E) or WT *K. pneumoniae* (Kp) at an MOI of 20 for 1 h. (D) BMNs were pre-treated with cytochalasin D (10 μM) for 30 min prior to infection. (A-D) Each symbol represents an individual mouse, or an independent biological infection and the box plot represents the median of the group ± the range. UI=uninfected. ns=not significant. One-way ANOVA with Dunnett's *post hoc* test comparing to the UI samples for A thru D or Tukey's *post hoc* test compared to each condition for E. T-test with Welch's *post hoc* test for F. *=p≤0.05, **=p≤0.01, ****=p≤0.0001.

**4-5. Conclusions**

The culmination of the work I have completed in this dissertation has provided a sturdy base in the understanding of $LTB_4$ during plague. My findings have also unveiled more questions in the context of other lipid mediators, other pathogens, and different host responses during plague, including the host-pathogen interactions between mast cells and *Y. pestis*.

# CHAPTER 5:

# APPROACHES FOR THE INACTIVATION OF *YERSINIA PESTIS*[1]

[1]Brady A, Tomaszewski M, Garrison TM, Lawrenz MB. Approaches for the inactivation of *Yersinia pestis*. 2024. Applied Biosafety. 2024; doi: 10.1089/apb.2023.0022

## **5-1. Introduction**

*Yersinia pestis* is the gram-negative, facultative intracellular bacterium that causes the disease known as plague. Historically, there have been three plague pandemics. While the last plague pandemic officially ended in 1945, *Y. pestis* became endemic in rodent populations throughout the world.[231] Within these endemic locations, there is still the potential for spillover events to occur when fleas transfer *Y. pestis* to humans, highlighted by the 2017 Madagascar and 2022 Democratic Republic of Congo human plague outbreaks.[339, 340] Mathematical modeling of the impact of climate change on the spread of *Y. pestis* suggests that the frequency of spillovers is likely to increase - warmer temperatures lead to higher rodent densities and increases in flea populations, which in turn increases the likelihood that humans will come in contact with the infected vectors.[341] While *Y. pestis* is considered a vector-borne disease, there has been recent evidence towards *Y. pestis* thriving in soil, further increasing the possibility of spillover events.[342] Considering these risks, research on plague is still necessary. To ensure laboratorian safety, *Y. pestis* research is conducted at biosafety level 3 (BSL-3) facilities, which provide the appropriate safeguards to minimize accidental exposures and environmental release.

The Federal Select Agent Program (FSAP) was established in 1996 and supervises the possession, use, and transfer of select agents. Select agents are pathogens or toxins determined to have the potential to pose a severe threat to public health and safety. To be considered a select agent, the danger to human health, speed of transmission, and the availability and effectiveness of treatment and/or prevention are all considered. In addition to the acute progression of the plague, *Y. pestis* also has a history of misuse as a biological weapon.[9, 10] Because of the rapid nature of plague infection, potential for aerosols and person-to-person transmission, and its risk of deliberate misuse, the FSAP has categorized *Y. pestis* as a Tier 1 select agent. This designation limits access to government vetted entities and individuals and ensures an increased level of biosecurity to protect the public from accidental or intentional release.

While research with *Y. pestis* requires work within BSL-3 laboratories to minimize risks to laboratorians and potential release, inactivation of the bacterium (i.e. rendering it non-viable and unable to cause infection) can generate products that can be safely handled at lower containment. However, after the shipment of anthrax spores that were not successfully inactivated, the FSAP has increased safeguards to prevent similar accidents.[343] These procedures include the development of standardized inactivation protocols that are validated prior to use, which includes documentation demonstrating that an inactivation protocol successfully inactivates the sample. Important considerations for validation can include kill curves, which identify either minimal concentrations or times required for an inactivation agent to fully inactivate the organism. Furthermore, each validated protocol needs to include an inactivation verification step, which provides proof of successful inactivation each time a protocol is performed prior to removal of the sample from the BSL-3 laboratory. To aid in developing effective inactivation protocols, the FSAP allows the use of surrogate organisms that can be handled at BSL-2 for the validation of these procedures.[343] While commonly used inactivation methods have been published for various select agents, there is an absence in the literature of a single source providing data supporting inactivation methods that can be used for *Y. pestis* while still providing downstream applications.[344, 345] Albeit not all inclusive, my purpose here is to provide the community with examples of several common inactivation approaches used with *Y. pestis* that can serve as a foundation for their own in-house development of validated inactivation protocols.

**5-2. Results**

5-2a. Heat inactivation of *Y. pestis*

To determine the impact of elevated temperature on the survival of *Y. pestis*, I examined two conditions, extended incubation at 50$^{o}$C and boiling bacteria with and without Laemli buffer, a buffer commonly used for protein analyses. To determine the viability of *Y. pestis* at 50$^{o}$C, bacteria were incubated at the elevated temperature for 60 min and recovery of viable bacteria was determined by enumeration. By as early as 10 min, I observed a 10-fold decrease in viability, which continued to decrease over the next 50 min. By 60 min, bacterial viability decreased by >5 orders of magnitude, with one sample below the limit of detection (Fig 5-3A). Using these data, I calculated that *Y. pestis* should be completely inactivated after 81 min when incubated at 50$^{o}$C. Based on this prediction, I incubated a separate group of samples at 50$^{o}$C for 120 min (a time frame exceeding the minimum inactivation calculated above to ensure complete inactivation of the bacteria). No viable bacteria were recovered from the 120 min samples (Fig 5-3B; $p \leq 0.0001$). Together these data indicate that complete inactivation of *Y. pestis* can be achieved by incubating the bacteria at 50$^{o}$C for ≥120 min.

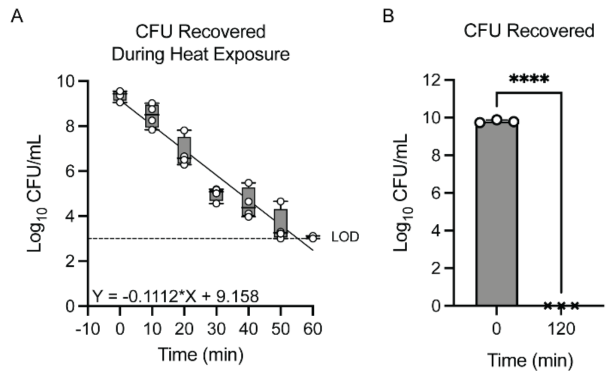


Figure 5-1. Heat shock at 50°C inactivates *Y. pestis* within 2 h

*Y. pestis* was incubated at 50°C. (A) Enumeration of viable bacteria at 10 min intervals for 60 min. The limit of detection was $10^3$ CFU, indicated by the dotted line. Each symbol represents an independent biological experiment, and the box plot represents the median of the group ± the range. The equation represents the linear regression analysis of the data used to predict how much time would be required for complete in activation. (B) Enumeration of bacteria from a sample before (0 min) or after incubation at 50°C (120 min). The limit of detection was 1 CFU. Each symbol represents an independent biological experiment, and the bars represent the mean of the group ± the standard deviation. Two-tailed unpaired T-test. ****=p≤0.0001.

Samples are often prepared for SDS-page analysis by adding Laemli buffer and boiling. To determine if incubation with Laemli buffer inactivated *Y. pestis*, bacteria were resuspended in the buffer with and without boiling. Incubation of *Y. pestis* at room temperature with Laemli buffer significantly reduced bacterial viability compared to samples without Laemli buffer (Fig 5-4; Laemli-RT vs. PBS-RT, respectively; $p \leq 0.0001$). However, boiling the bacteria for 10 min with or without Laemli buffer resulted in no recovery of viable bacteria (Fig 5-4; PBS-Boil and Laemli-Boil vs. PBS-RT; $p \leq 0.0001$). Together, these data demonstrate that boiling samples for 10 min, with or without Laemli buffer, is sufficient to inactive *Y. pestis*.

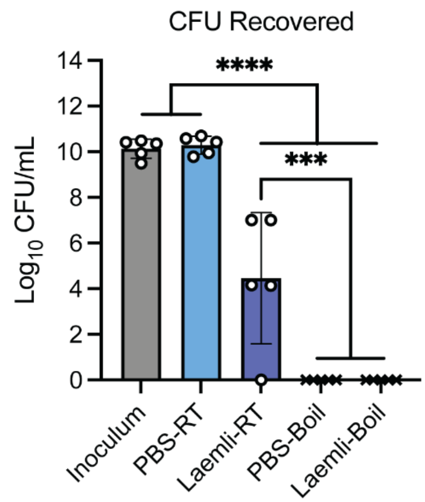


Figure 5-2. *Y. pestis* is inactivated by boiling for 10 min

*Y. pestis* was incubated at room temperature in 1X PBS for 15 min (PBS-RT), in 1X Laemli buffer for 5 min (Laemli-RT), or in a boiling water in 1X PBS (PBS-Boil) or in 1X Laemli Buffer for 10 min (Laemli-Boil). After incubation, viable bacteria were enumerated. The limit of detection was determined as 1 CFU. Each symbol represents an independent biological experiment, and the bars represent the mean of the group ± the standard deviation. One-way ANOVA with Tukey's *post hoc* test. ***=p≤0.001. ****=p≤0.0001. PBS, phosphate-buffered saline; RT, room temperature.

5-2b. Paraformaldehyde and formalin inactivation of *Y. pestis*

Paraformaldehyde (PFA) and neutral-buffered formalin (NBF) inactivate biological samples by covalent crosslinking amines between proteins and nucleic acids.[346] Typical protocols for microscopy and flow cytometry applications include incubation with 4-10% of fixative for 15-30 mins.[139] To define the kinetics of PFA inactivation, *Y. pestis* was incubated with 0.5, 1, 2, or 4% PFA (final concentration) and CFU were enumerated every 15 min for 60 min. I observed a >6 log decrease within 15 min with all PFA-treated samples, below the limit of detection of this experiment (Fig 5-5A; $p \leq 0.001$). In a separate experiment, *Y. pestis* was incubated with 1% PFA for 15 min and the entire sample was transferred to an agar plate to determine if any viable bacteria were present. No viable bacteria were recovered (Fig 5-5B; $p \leq 0.0001$). For NBF, bacteria were incubated with 1.25, 2.5, 5, or 10% (final concentration). As observed for PFA, viable bacteria were below the limit of detection for all concentrations within 30 min of incubation (Fig 5-5C; $p \leq 0.0001$), and all concentrations >1.25% were below the limit of detection within 15 min (Fig 5-5C; $p \leq 0.0001$). To determine in a separate experiment if any viable bacteria were present at this concentration, bacteria were incubated for 15 min in 2.5% NBF and the entire sample was transferred to an agar plate. No viable bacteria were recovered (Fig 5-5D; $p \leq 0.0001$). Together these data indicate that incubation with ≥1% PFA or ≥2.5% NBF for 15 min is sufficient to inactive *Y. pestis.*

Formalin is also commonly used as a fixative for tissues for histological examination. To demonstrate that 10% NBF can inactive *Y. pestis* in tissues, mice were intranasally infected with fully virulent *Y. pestis*. 48 h post-infection, bacterial numbers in the lungs were $7.12 \times 10^9 \pm 2.76 \times 10^9$ per tissue, in the spleens were $9.68 \times 10^4 \pm 1.59 \times 10^4$ per tissue, and the in the livers were $2.55 \times 10^5 \pm 8.36 \times 10^4$ per tissue (Fig 5-5E). After 24 h incubation with 10% NBF, tissues were cultured in BHI broth for 48 h. Cultures were not turbid after incubation, indicating the absence of viable bacteria. Sterility was confirmed by plating a portion of the broth on BHI agar plates. Again, no viable bacteria were recovered (Fig 5-5E). Together, these data demonstrate that 24 h incubation with 10% NBF can effectively inactivate *Y. pestis* in murine tissues.

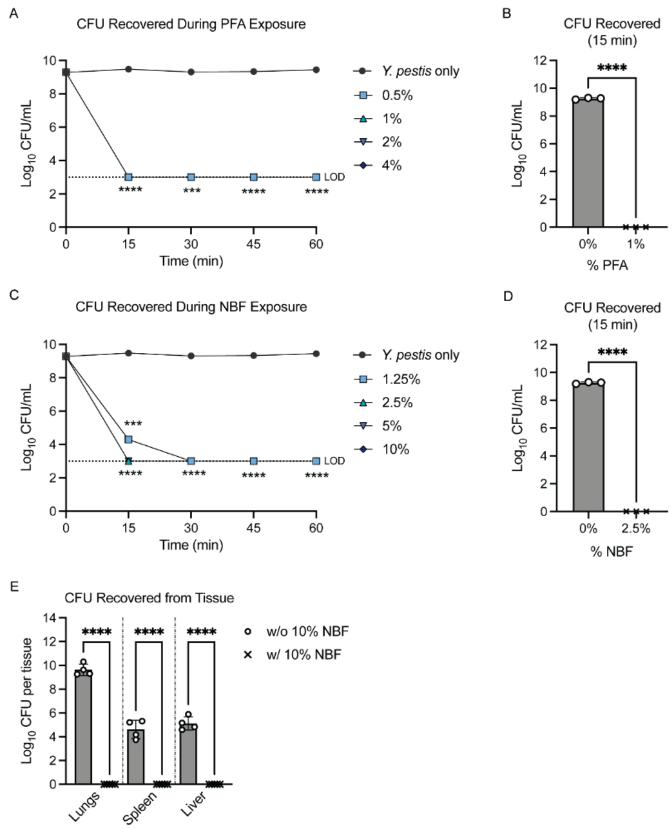


<u>Figure 5-3. Low concentrations of PFA and NBF inactivate *Y. pestis*</u>

*Y. pestis* was incubated with indicated concentrations of (A,B) PFA or (C, D) NBF and bacterial survival was measured by CFU from (A,C) 10 μL aliquots every 15 min or (B, D) the whole sample at 15 min. Limit of detection was determined as (A,C) $10^3$ or (B,D) 1 CFU. (E) C57BL6/J mice were infected intranasally with 10x the $LD_{50}$ of *Y. pestis* KIM5+ and lungs, spleen, and liver were harvested 48 h post-infection. Incubated with 10% NBF for 24 h. (A,C) Symbols represent the mean of 3 biological replicates and the error bars represent ± the standard deviation. Two-way ANOVA with Dunnett's *post hoc* test comparing to untreated. ***=p≤0.001, ****=p≤0.0001. (B,D) Each symbol represents an independent biological experiment and the bars represent the mean of the group ± the standard deviation. Two-tailed unpaired T-test. ****=p≤0.0001. (E) Each symbol represents tissues from an individual mouse, and the bars represent the mean of the group ± the standard deviation. Two-tailed unpaired T-test within each tissue group. ****=p≤0.0001.

5-2c. Methanol inactivation of *Y. pestis*

Methanol (MeOH) can be used to permeabilize and fix samples for microscopy and to extract lipids from biological samples for subsequent lipid identification by Liquid Chromatography Tandem Mass Spectrometry (LC-MS/MS).[347-349] To determine if MeOH inactivates *Y. pestis*, bacteria were treated with increasing concentrations of MeOH and bacterial viability was determined every 15 min for 60 min by enumeration. *Y. pestis* appeared relatively resistant to 25% MeOH but was sensitive to inactivation at concentrations ≥50% (Fig 5-6A). In a separate experiment, bacteria were incubated with 50% MeOH and the entire sample was plated at 15, 30, and 60 min (Fig 5-6B). In this experiment, incubation for 1 h was required to completely inactivate $>10^8$ CFU of bacteria ($p \leq 0.0001$).

To determine the ability of MeOH to inactivate *Y. pestis* in the presence of host tissue, mouse lungs were transferred to a 2 ml tube and a known concentration of bacteria ($5.4 \times 10^9$ CFU/mL) was added to the tissues. The tissues + bacteria were resuspended in 1X PBS with ceramic beads for homogenization. Following tissue homogenization, bacterial viability decreased by ~3-logs (Fig 5-6C; 'After homogenization' vs. 'Inoculum'; $p \leq 0.0001$). Viability decreased slightly if the samples were further incubated at 4°C for 24 h (Fig 5-6; '24 h PBS'). However, no viable bacteria were recovered from homogenized samples after 24 h of incubation in 75% MeOH + 0.1% BHT, final concentration (75% was chosen as this is a concentration applicable to lipid extraction) (Fig 5-6C; '24 h 75% MeOH'). Based on these results, lungs were isolated from mice intranasally infected with fully virulent *Y. pestis* at 6, 12, 24, 36, and 48 h post-infection, and the tissues were homogenized. Prior to addition of MeOH, bacterial numbers were enumerated, and then samples were incubated with 75% MeOH + 0.1% BHT for 24 h. Inactivation was verified by plating 5% of the sample, of which no viable bacteria were recovered (Fig 5-6D; $p \leq 0.0001$). Together, these data demonstrate that 75% MeOH can effectively inactivate *Y. pestis*, even in the presence of host tissues.

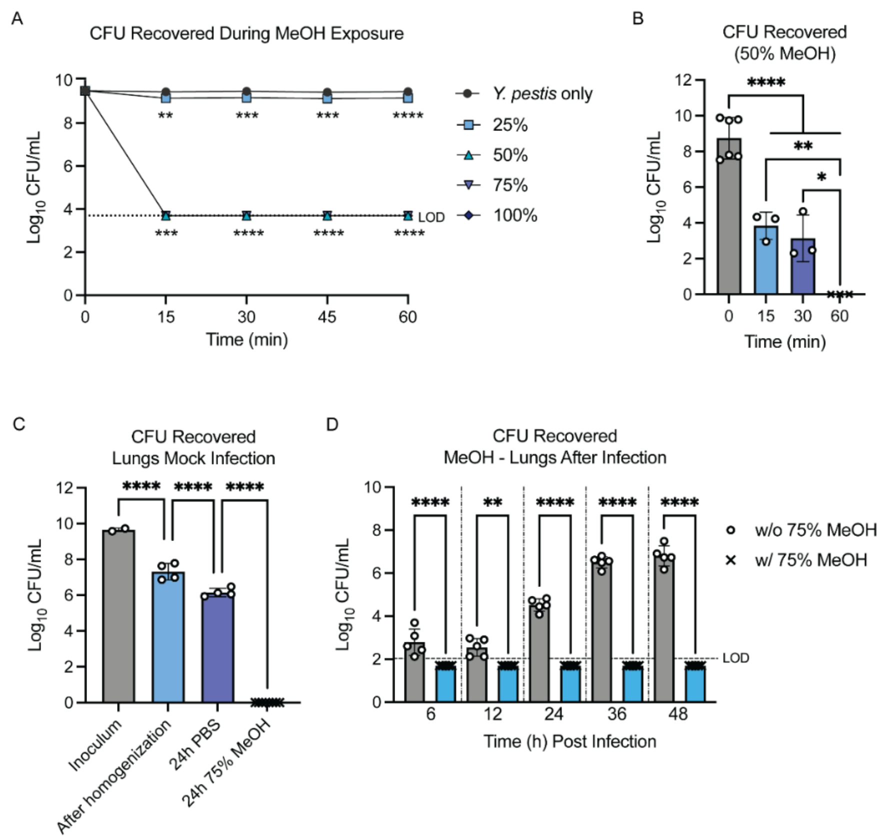


<u>Figure 5-4. Methanol inactivation of *Y. pestis*</u>

(A,B) *Y. pestis* was incubated with indicated concentrations of MeOH and bacterial survival was measured by CFU from (A) 10 μL aliquots every 15 min or (B) the whole sample at 15, 30, or 60 min. Limit of detection was determined as (A) $10^3$ or (B) 1 CFU. (C) Enumeration of the bacteria recovered after lungs + *Y. pestis* were incubated with 75% MeOH + 0.1% BHT. Limit of detection was calculated as 1 CFU. (D) Enumeration of bacteria recovered after lungs from *Y. pestis* infected animals were incubated with 75% MeOH + 0.1% BHT. Limit of detection was calculated as 50 CFU. (A) Symbols represent the mean of 3 biological replicates and the error bars represent ± the standard deviation. Two-way ANOVA with Dunnett's *post hoc* test. **=p≤0.01, ***=p≤0.001, ****=p≤0.0001. (B-D) Each symbol represents an independent biological experiment, and the bars represent the mean of the group ± the standard deviation. One-way ANOVA with Tukey's *post hoc* test. *=p≤0.05, **=p≤0.01, ****=p≤0.0001.

5-2d. Nucleic acid extraction inactivates *Y. pestis*

There are a variety of approaches to isolate nucleic acids from bacteria. Here, I chose two common approaches used to isolate genomic DNA or RNA from bacterial cultures. For DNA isolation, I used a commercial alkaline lysis approach following the manufacturer's protocol for gram-negative bacteria. No viable bacteria were recovered in the elution after extraction, indicating that this commercial kit completely inactivated the bacteria (Fig 5-7A). For RNA extraction, I used a TRIzol extraction approach and plated the entire aqueous phase after chloroform extraction. No viable bacteria were recovered from the aqueous phase, indicating that TRIzol/chloroform extraction completely inactivates *Y. pestis* (Fig 5-7B).

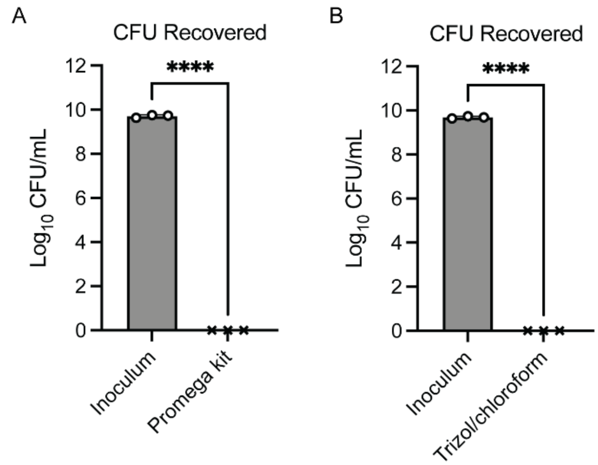


Figure 5-5. Alkaline lysis and TRIzol/chloroform extraction successfully inactivate *Y. pestis*

*Y. pestis* was treated for nucleic acid extraction using the (A) Promega Wizard Genomic DNA Purification Kit or (B) TRIzol/chloroform extraction. The limit of detection was determined as 1 CFU. Each symbol represents an independent biological experiment, and the bars represent the mean of the group ± the standard deviation. Two-tailed unpaired T-test. ****=p≤0.0001.

## 5-3. Discussion

BSL-3 containment facilities and procedures protect laboratorians from accidental exposure and infection by *Y. pestis*. However, many pieces of equipment needed for research may not be available or amenable to use within the BSL-3 laboratory. Thus, samples need to be inactivated, and confirmed for inactivation, for them to be safely removed from BSL-3 for downstream experimentation. As such, the development of validated inactivation protocols is required to ensure samples can be safely handled at lower containment. For *Y. pestis*, there have been several studies published demonstrating the efficacy of common disinfectants[350, 351], gas decontamination (both hydrogen peroxide and chlorine dioxide) [352-356], and UV radiation.[357-362] However, published data related to inactivation methods more amenable to research applications are limited.[361, 363-365] Here I built upon these studies to provide a systematic analysis of several inactivation methods commonly used within the research field. My goal was to provide others with approaches and data that can serve as the foundation for the development of in-house validated inactivation protocols.

*Y. pestis* is a mesophilic bacterium that thrives in a temperature range from 20-40°C, temperatures of its native insect and mammalian hosts, but it can also grow efficiently at 4°C.[366] Temperatures >45°C can negatively impact many cellular processes for mesophilic bacteria, including protein stability, membrane structure, metabolic activity, and DNA repair.[365, 367-369] Therefore, exposure to elevated temperatures can result in loss of viability over time.[367] Wang et al. reported previously that incubation at 68°C for 10 h completely inactivated *Y. pestis,* but also briefly mentioned that one CFU was recovered from treatments at lower temperatures for shorter periods of time.[361] In my hands performing multiple biologically independent experiments, I was unable to recover viable bacteria from samples at a starting concentration of ~2.65 x $10^9$ CFU/ml when the bacteria were incubated at 55°C for 2 hours. Because specific details on the bacterial concentration of the samples, how many times the inactivation was performed, the amount of sample enumerated, and whether the single colony recovered was verified as *Y. pestis* were not provided by Wang et al., it is difficult determine why I observed differences in my evaluations. However, simple differences in the validation of the temperature of the heating elements or sample diluent (e.g., PBS vs. water) could explain the differences and highlight the need to have in-house validation of inactivation procedures.

Wang et al. also reported that incubation with 4% PFA at 4°C overnight inactivated *Y. pestis*.[361] By applying both time- and dose-dependent kill curve analysis, I expanded on these data to show that concentrations of 1% PFA or 2.5% NBF can fully inactivate *Y. pestis* within 15 min when incubated at room temperature (Fig 5-5). These data support that standard treatments with formaldehyde that conserve cell morphology and retaining fluorophore activity for confocal imaging and flow cytometry should be sufficient to inactivate *Y. pestis*.[370-374] In the context of formaldehyde fixation of infected tissues, Chua et al.[363] previously reported that incubation of tissues from *Y. pestis* infected rabbits and guinea pigs with glutaraldehyde or formaldehyde fixatives for 6 or 13 days, respectively, resulted in bacterial inactivation. However, whether shorter incubation periods were sufficient was not reported. As tissues from mice are significantly smaller than those from rabbits or guinea pigs, I hypothesized that shorter incubation times would be sufficient to perfuse the tissues, and as predicted, incubation with 10% NBF for 24 h was sufficient to inactivate *Y. pestis* in murine tissues of different densities (lungs, spleens, and livers). However, as indicated by Chua et al.[363] and Buesa and Peshkov[375], the time required for sufficient perfusion of tissues and bacterial inactivation may differ for other tissues like the skin. Therefore, fixation of tissues other than the ones tested here may require different incubation periods that will need to be empirically determined.

In addition to formaldehyde, alcohols are also commonly used to inactivate and fix biological samples for imaging.[365, 376-379] Moreover, these chemical fixatives are amenable to both lipid and proteomic analysis by LC-MS/MS.[297] Lin et al. previously reported that incubation of *Y. pestis* with 40% ethanol for 30 min was sufficient to inactivate the bacteria without significantly impacting proteomic data quality.[365] Wang et al. also reported that incubation with 100% methanol at 4$^{o}$C for 10 min inactivated *Y. pestis* while retaining cell morphology as assessed by atomic force microscopy.[361] However, for both studies, bacterial concentrations were not reported and only a portion of the inactivated cultures were plated for viability (10% and 1%, respectively). I have expanded on these studies to show that while methanol can rapidly inactive *Y. pestis*, at a concentration of 50%, incubation for 1 h was required to completely inactivate ~3.2 x $10^9$ CFU. I did not determine if shorter periods of time were required for 100% methanol, but this time frame could easily be determined following a similar protocol. I also showed that incubation with 75% methanol for 24 h in the presence of host tissue lysates was sufficient to inactivate *Y. pestis*. Moreover, I show inactivation in the presence of BHT, an antioxidant that prevents oxidation of lipids for downstream lipid analysis.[380, 381]

Together these studies provide other researchers with a foundation as they develop their own in-house inactivation procedures. As protocols are being developed, careful considerations need to be made regarding the bacterial concentrations used in the validation process to ensure that protocols will not be applied later to experimental situations in which the bacterial concentrations are greater than the concentrations for which the protocols were validated. Moreover, as recommended by the CDC, protocols should also include a verification step to ensure inactivation was achieved each time the protocol is performed.

## 5-4. Methods and Materials

### 5-4a. Bacteria

For *in vitro* studies, I used attenuated derivatives of the *Y. pestis* KIM biovar missing the high pathogenesis island (pgm) and the large virulence plasmid (pCD1), which are exempt from Select Agent regulation.[382] These strains also harbored bioluminescent bioreporters (pLUX or $Lux_{ptolC}$) to monitor bacterial viability as a function of bioluminescence.[111, 251] These strains represents a surrogate for fully virulent *Y. pestis* that can be handled safely at BSL-2 to develop and validate inactivation procedures .[343, 382] Bacteria were routinely cultured for 15 to 18 h at 26°C in Bacto brain heart infusion (BHI) broth (BD Biosciences; Cat. No. 237500) on a roller drum. Optical densities at 600nm ($OD_{600}$) were determined with a spectrophotometer and used as a reference to dilute samples to the desired bacterial concentrations. Final bacterial concentrations were enumerated by serial dilutions of samples and growth on Diffco BHI agar plates (BD Biosciences; Cat. No. 241830) for two days at 26°C. Data is reported as colony forming units (CFU) per mL.

### 5-4b. Heat inactivation of *Y. pestis*

Approximately 2.65 x $10^9$ CFU of bacteria were resuspended in 1 mL of phosphate buffered saline (1X PBS) in 1.5 mL eppendorf tubes and placed in a heating block that was pre-heated to 50°C. For one hour, 10 µL aliquots were removed every 10 min and bacterial numbers were enumerated. Enumeration was performed with three technical replicates for each biological replicate at each time point. The limit of detection was determined as $10^3$ CFU. In a separate experiment, samples (n = 3 biological replicates) were incubated for two hours, pelleted for 1 min at 16,000 x g, and resuspended in 100 µL 1X PBS. The entire 100 µL sample was plated onto BHI agar and incubated for 2 days at 26°C. The limit of detection was determined as 1 CFU. The inactivation was performed 4 times.

### 5-4c. Laemli buffer and boiling inactivation of *Y. pestis*

Approximately 2 x $10^{10}$ CFU of bacteria were resuspended in 200 µL of 1X PBS. Samples were either incubated at room temperature in 1X PBS for 15 min, in 1X Laemli buffer (6X Laemli buffer is 5% 2-mercaptoethanol, 2% SDS, 10% glycerol, 0.012% bromophenol blue, and 0.375M Tris-HCl) for 5 min, in 1X PBS in a boiling water bath for 10 min, or in 1X Laemli Buffer for 5 min at room temperature followed by boiling for 10 min. After each condition, the entire sample was inoculated onto BHI agar and incubated for 2 days at 26°C. The limit of detection was determined as 1 CFU. The inactivation was performed 5 times.

5-4d. Paraformaldehyde and formalin inactivation of *Y. pestis*

Approximately 1.95 x $10^9$ CFU of bacteria were resuspended in 1X PBS. Freshly prepared 4% paraformaldehyde (PFA; Sigma-Aldrich, Cat. No. P6148) was added at final concentrations of 0.5, 1, 2, or 4% (n=3). Neutral-buffered formalin (NBF; VWR, Cat. No. 89370) was added at final concentrations of 1.25, 2.5, 5, or 10% (n=3). Final volumes were 1 mL for each condition. As a growth control, 1 mL of 1X PBS was added to a separate sample. Samples were then mixed by pipetting and incubated at 4°C. Every 15 min for 60 min, 10 µL aliquots were removed to measure bacterial concentration. To confirm starting concentrations, untreated bacteria incubated in 1 mL of 1X PBS were serially diluted and plated on BHI agar. The limit of detection was determined as $10^3$ CFU. Inactivation was performed 3 times.

Approximately 1.8 x $10^9$ CFU of bacteria were resuspended in 1 mL of freshly prepared 1% paraformaldehyde or 2.5% NBF. Samples were then mixed by pipetting and incubated at 4°C. At 30 min, samples were centrifuged for 1 min at 16,000 x g, washed once with 1X PBS, and then resuspended in 100 µL of 1X PBS. The entire sample was transferred to a BHI agar plate and incubated for 2 days at 26°C. To confirm starting concentrations, untreated bacteria incubated in 1 mL of 1X PBS were serially diluted and plated on BHI agar. The limit of detection was determined as 1 CFU. The inactivation was performed 3 times.

5-4e. Formalin inactivation of *Y. pestis* in the presence of tissues

*Y. pestis* was grown at 26°C for 6-8 h, diluted to an optical density (OD) (600 nm) of 0.05 in Bacto brain heart infusion (BHI) broth (BD Biosciences Cat. No. 237500) with 2.5 mM $CaCl_2$ and then grown at 37°C with aeration for 15-18 h.[280] C57BL/6J mice (University of Louisville IACUC approval # 22157) were anesthetized with ketamine/xylazine and administered 20 µL of fully virulent *Y. pestis* suspended in 1X Dulbecco's PBS (DPBS) to the left nare as previously described.[251, 280] At 48 h post infection, lungs, spleen, and liver were removed by sterile necropsy. Tissues from 5 mice were cut in half, prior to adding to tissue cassettes, and submerged in 10% NBF for 24 h, 12 mL per tissue. Untreated tissues from 4 mice were macerated, and bacterial numbers were enumerated by serial dilution and plated on BHI agar. After 24 h, tissues were removed from the 10% NBF and washed with 1X PBS. The NBF-treated tissues were transferred to 3 ml of BHI and incubated for 2 days at 26°C. Cultures were visually inspected for turbidity as a sign of bacterial growth, and 150 µL (5%) were plated on BHI agar to confirm absence of growth.

5-4f. Methanol inactivation of *Y. pestis*

Approximately 3.2 x $10^9$ CFU of bacteria were resuspended in 1 mL of 1X PBS + methanol (MeOH; Fisher Chemical, Cat. No. A412) at final concentrations of 0, 25, 50, 75, and 100% methanol. Samples were mixed by pipetting and incubated at 4°C. Every 15 min for 60 min, 10 µL aliquots were removed to enumerate bacterial numbers. To confirm starting concentrations, untreated bacteria incubated in 1X PBS were serially diluted and plated on BHI agar. The limit of detection was determined as 5 x $10^3$ CFU. The inactivation was performed 3 times.

Approximately 3.22 x $10^9$ CFU of bacteria were resuspended in 1 mL of 50% MeOH. Samples were mixed by pipetting and incubated at 4°C. At 15, 30, and 60 min, samples were centrifuged for 1 min at 16,000 x g, washed once with 1X PBS, and resuspended in 100 µL of 1X PBS. The entire sample was transferred to BHI agar and incubated for 2 days at 26°C. To confirm starting concentrations, untreated bacteria incubated in 1X PBS were serially diluted and plated on BHI agar. The limit of detection was determined as 1 CFU. The inactivation was performed 3 times.

5-4g. Methanol inactivation of *Y. pestis* in tissues

Lungs from C57BL/6J mice (University of Louisville IACUC approval # 22157) were removed by sterile necropsy and immediately frozen in a 2 mL tube pre-filled with 2.8 mm ceramic beads (VWR, Cat. No. 10158-612). Lungs were thawed and ~5 x $10^9$ CFU of bacteria in 1X PBS were added. Additional 1X PBS was added to fill the remaining air space within the tube. Tissues were homogenized with an Omni Bead Ruptor 4 at speed 5 (5 m/s) for 3 cycles of 30 seconds with 1-minute pauses in which the lungs were placed on ice to prevent samples from overheating. Bacterial CFU were enumerated by serial dilution of 100 µL of the homogenized samples to determine the effects of the homogenization process on bacterial survival. Tissue debris was then centrifuged for 10 min at 1,500 x g. The supernatants (~1.5 mL) were then transferred to a fresh Eppendorf tube. From this, 250 µL aliquots were added to methanol + butylated hydroxy toluene (BHT) (75% + 0.1% final concentration, respectively) and incubated at 4°C for 24 h. After incubation, samples were pelleted for 1 min at 16,000 x g. Methanol + BHT was removed, and pellets were washed 3 times with 1X PBS. Samples were then resuspended in 250 µL of 1X PBS and the entire sample was transferred to BHI agar supplemented with irgasan (1 µg/ml) and polymyxin B (12.5 µg/ml) (the *Y. pestis* strain used is resistant to these antibiotics and allows for differentiation from potential contamination by the host microbiota) and incubated for 2 days at 26°C. The limit of detection was determined as 1 CFU. The inactivation was performed 4 times.

C57BL/6J mice were anesthetized with ketamine/xylazine and administered 20 µL of fully virulent *Y. pestis* as previously described.[251, 280] At 6, 12, 24, 36, and 48 h post infection, whole lungs were necropsied and homogenized as described above. Bacterial CFU were enumerated from each sample by serial dilution of 100 µL of the homogenized samples to determine the bacterial concentration prior to inactivation. 250 µL aliquots from the fresh Eppendorf tube were added to methanol + butylated hydroxy toluene (BHT) (75% + 0.1% final concentration, respectively) and incubated at 4°C for 24 h. After incubation, 50 µL from each sample was transferred to a BHI agar plate supplemented with irgasan (1 µg/ml) and polymyxin B (12.5 µg/ml) then incubated for 2 days at 26°C. The limit of detection was determined as 50 CFU. The inactivation included 5 biological replicates.

5-4h. *Y. pestis* inactivation with Promega Wizard Genomic DNA Purification kit

Approximately 5.7 x $10^9$ CFU of bacteria were collected into 1.5 mL Eppendorf tubes. Bacteria were pelleted for 1 min at 12,000 x g and DNA extraction was performed per manufacturer's instructions (Promega; Cat. No. A1120). The entire elution after purification was transferred to BHI agar and incubated for 2 days at 26°C. The limit of detection was determined as 1 CFU. The inactivation was performed 3 times.

5-4i. *Y. pestis* inactivation with TRIzol and chloroform

Approximately 5.4 x $10^9$ CFU of bacteria were collected into a 1.5 mL RNase free Eppendorf tube. Bacteria were pelleted for 1 min at 10,000 x g and gently resuspended in 1 mL TRIzol reagent (Thermo Scientific; Cat. No. 15596026) and incubated for 5 min at room temperature. 200 µL of chloroform (Fisher Chemical; Cat. No. 513-35-9) was added, followed by 15 seconds of vigorous shaking and a 3 min incubation at room temperature. Samples were then centrifuged for 15 min at 12,000 x g at 4°C. The aqueous phase was transferred to BHI agar and incubated for 2 days at 26°C. The limit of detection was determined as 1 CFU. Inactivation was performed 3 times.

5-4j. Statistics

Prior to statistical analysis, values for samples that were below the limit of detection were converted to the limit of detection and log transformed. All statistical calculations were performed using GraphPad Prism and the tests used for comparison are reported in the figure legends. When comparing groups to untreated samples, a One-way ANOVA with Dunnett's post hoc test was used. For comparing multiple groups to each other, a One-way ANOVA with Tukey's post hoc test was used. When there were only two groups in the experiment, a Two-tailed unpaired T-test was used.

## REFERENCES


1. Fukushima H, Shimizu S, Inatsu Y. Yersinia enterocolitica and Yersinia pseudotuberculosis Detection in Foods. J Pathog. 2011;2011:735308. doi:10.4061/2011/735308.
2. Galindo CL, Rosenzweig JA, Kirtley ML, Chopra AK. Pathogenesis of Y. enterocolitica and Y. pseudotuberculosis in Human Yersiniosis. J Pathog. 2011;2011:182051. doi:10.4061/2011/182051.
3. Gage KL, Kosoy MY. Natural history of plague: Perspectives from more than a century of research. Annu Rev Entomol. 2005;50:505-28. doi:10.1146/annurev.ento.50.071803.130337.
4. Perry RD, Fetherston JD. *Yersinia pestis*—Etiologic agent of plague. Clinical Microbiology Reviews. 1997;10(1):35-66. doi:10.1128/cmr.10.1.35.
5. Nelson CA, Meaney-Delman D, Fleck-Derderian S, Cooley KM, Yu PA, Mead PS. Antimicrobial treatment and prophylaxis of plague: recommendations for naturally acquired infections and bioterrorism response. Morb Mortal Weekly Rep. 2021;70(3).
6. Lathem WW, Crosby SD, Miller VL, Goldman WE. Progression of primary pneumonic plague A mouse model of infection, pathology, and bacterial transcriptional activity. PNAS. 2005;102(49):17786-91. doi:10.1073/pnas.0506840102.
7. Price PA, Jin J, Goldman WE. Pulmonary infection by Yersinia pestis rapidly establishes a permissive environment for microbial proliferation. Proc Natl Acad Sci U S A. 2012;109(8):3083-8. doi:10.1073/pnas.1112729109.
8. Bubeck SS, Cantwell AM, Dube PH. Delayed inflammatory response to primary pneumonic plague occurs in both outbred and inbred mice. Infect Immun. 2007;75(2):697-705. doi:10.1128/IAI.00403-06.
9. Wheelis M. Biological warfare at the 1346 siege of Caffa. Emerg Infect Dis. 2002;8(9):971–5. doi:10.3201/eid0809.010536.
10. Riedel S. Plague: from natural disease to bioterrorism. BUMC Proceed. 2005;18(2):116-24. doi:10.1080/08998280.2005.11928049.
11. Bevins SN, Baroch JA, Nolte DL, Zhang M, He H. Yersinia pestis: examining wildlife plague surveillance in China and the USA. Integr Zool. 2012;7(1):99-109. doi:10.1111/j.1749-4877.2011.00277.x.
12. Vadyvaloo V, Jarrett C, Sturdevant DE, Sebbane F, Hinnebusch BJ. Transit through the flea vector induces a pretransmission innate immunity resistance phenotype in Yersinia pestis. PLoS Pathog. 2010;6(2):e1000783. doi:10.1371/journal.ppat.1000783.
13. Dewitte A, Bouvenot T, Pierre F, Ricard I, Pradel E, Barois N, et al. A refined model of how *Yersinia pestis* produces a transmissible infection in its flea vector. PLoS Pathogens. 2020;16(4):e1008440. doi:10.1371/journal.ppat.1008440.
14. Jarrett CO, Deak E, Isherwood KE, Oyston PC, Fischer ER, Whitney AR, et al. Transmission of *Yersinia pestis* from an infectious biofilm in the flea vector. J Infect Dis. 2004;190(4):783-92. doi:10.1086/422695.
15. Hinnebusch BJ, Perry RD, Schwan TG. Role of the *Yersinia pestis* hemin storage (hms) locus in the transmission of plague by fleas. Science. 1996;273(5273).
16. Hinnebusch BJ, Rudolph AE, Cherepanov P, Dixon JE, Schwan TG, Forsberg Å. Role of *Yersinia* murine toxin in survival of *Yersinia pestis* in the midgut of the flea vector. Science. 2002;296(5568).
17. Pujol C, Klein KA, Romanov GA, Palmer LE, Cirota C, Zhao Z, et al. Yersinia pestis can reside in autophagosomes and avoid xenophagy in murine macrophages by preventing vacuole acidification. Infect Immun. 2009;77(6):2251-61. doi:10.1128/IAI.00068-09.

18. Shannon JG, Bosio CF, Hinnebusch BJ. Dermal neutrophil, macrophage and dendritic cell responses to Yersinia pestis transmitted by fleas. PLoS Pathog. 2015;11(3):e1004734. doi:10.1371/journal.ppat.1004734.
19. Pechous RD, Sivaraman V, Price PA, Stasulli NM, Goldman WE. Early host cell targets of *Yersinia pestis* during primary pneumonic plague. PLoS Pathogens. 2013;9(10):e1003679. doi:10.1371/journal.ppat.1003679.
20. Ge Y, Huang M, Yao YM. Efferocytosis and Its Role in Inflammatory Disorders. Front Cell Dev Biol. 2022;10:839248. doi:10.3389/fcell.2022.839248.
21. Shannon JG, Hasenkrug AM, Dorward DW, Nair V, Carmody AB, Hinnebusch BJ. *Yersinia pestis* subverts the dermal neutrophil response in a mouse model of bubonic plague. mBio. 2013;4(5):e00170-13. doi:10.1128/mBio.00170-13.
22. Spinner JL, Winfree S, Starr T, Shannon JG, Nair V, Steele-Mortimer O, et al. Yersinia pestis survival and replication within human neutrophil phagosomes and uptake of infected neutrophils by macrophages. J Leukoc Biol. 2014;95(3):389-98. doi:10.1189/jlb.1112551.
23. Ke Y, Chen Z, Yang R. Yersinia pestis: mechanisms of entry into and resistance to the host cell. Front Cell Infect Microbiol. 2013;3:106. doi:10.3389/fcimb.2013.00106.
24. Gonzalez RJ, Weening EH, Frothingham R, Sempowski GD, Miller VL. Bioluminescence imaging to track bacterial dissemination of Yersinia pestis using different routes of infection in mice. BMC Microbiol. 2012;12:147. doi:10.1186/1471-2180-12-147.
25. Demeure CE, Dussurget O, Mas Fiol G, Le Guern AS, Savin C, Pizarro-Cerda J. *Yersinia pestis* and plague: an updated view on evolution, virulence determinants, immune subversion, vaccination, and diagnostics. Genes & Immunity. 2019;20(5):357-70. doi:10.1038/s41435-019-0065-0.
26. Plano GV, Schesser K. The *Yersinia pestis* type III secretion system: expression, assembly and role in the evasion of host defenses. Immunol Res. 2013;57(1-3):237-45. doi:10.1007/s12026-013-8454-3.
27. Sebbane F, Gardner D, Long D, Gowen BB, Hinnebusch BJ. Kinetics of Disease Progression and Host Response in a Rat Model of Bubonic Plague. The American Journal of Pathology. 2005;166(5):1427-39. doi:10.1016/s0002-9440(10)62360-7.
28. Peters KN, Dhariwala MO, Hughes Hanks JM, Brown CR, Anderson DM. Early apoptosis of macrophages modulated by injection of *Yersinia pestis* YopK promotes progression of primary pneumonic plague. PLoS Pathog. 2013;9(4):e1003324. doi:10.1371/journal.ppat.1003324.
29. Bergsbaken T, Cookson BT. Innate immune response during Yersinia infection: critical modulation of cell death mechanisms through phagocyte activation. J Leukoc Biol. 2009;86(5):1153-8. doi:10.1189/jlb.0309146.
30. Olson RM, Anderson DM. Shift from primary pneumonic to secondary septicemic plague by decreasing the volume of intranasal challenge with Yersinia pestis in the murine model. PLoS ONE. 2019;14(5):e0217440. doi:10.1371/journal.pone.0217440.
31. Vagima Y, Zauberman A, Levy Y, Gur D, Tidhar A, Aftalion M, et al. Circumventing *Y. pestis* virulence by early recruitment of neutrophils to the lungs during pneumonic plague. PLoS Pathog. 2015;11(5):e1004893. doi:10.1371/journal.ppat.1004893.
32. Zhang Y, Ying X, He Y, Jiang L, Zhang S, Bartra SS, et al. Invasiveness of the Yersinia pestis ail protein contributes to host dissemination in pneumonic and oral plague. Microb Pathog. 2020;141:103993. doi:10.1016/j.micpath.2020.103993.
33. Laws TR, Davey MS, Titball RW, Lukaszewski R. Neutrophils are important in early control of lung infection by Yersinia pestis. Microbes Infect. 2010;12(4):331-5. doi:10.1016/j.micinf.2010.01.007.

34. Merritt PM, Nero T, Bohman L, Felek S, Krukonis ES, Marketon MM. Yersinia pestis targets neutrophils via complement receptor 3. Cell Microbiol. 2015;17(5):666-87. doi:10.1111/cmi.12391.
35. Stasulli NM, Eichelberger KR, Price PA, Pechous RD, Montgomery SA, Parker JS, et al. Spatially distinct neutrophil responses within the inflammatory lesions of pneumonic plague. mBio. 2015;6(5):e01530-15. doi:10.1128/mBio.01530-15.
36. Eichelberger KR, Jones GS, Goldman WE. Inhibition of Neutrophil Primary Granule Release during Yersinia pestis Pulmonary Infection. mBio. 2019;10(6). doi:10.1128/mBio.02759-19.
37. Sadik CD, Luster AD. Lipid-cytokine-chemokine cascades orchestrate leukocyte recruitment in inflammation. J Leukoc Biol. 2012;91(2):207-15. doi:10.1189/jlb.0811402.
38. Bennett M, Gilroy DW. Lipid mediators in inflammation. Microbiol Spectr. 2016;4(6). doi:10.1128/microbiolspec.MCHD-0035-2016.
39. Chen L, Deng H, Cui H, Fang J, Zuo Z, Deng J, et al. Inflammatory responses and inflammation-associated diseases in organs. Oncotarget. 2018;9(6).
40. Varela ML, Mogildea M, Moreno I, Lopes A. Acute Inflammation and Metabolism. Inflammation. 2018;41(4):1115-27. doi:10.1007/s10753-018-0739-1.
41. Aepfelbacher M, Trasak C, Ruckdeschel K. Effector functions of pathogenic *Yersinia* species. Thrombosis and Haemostasis. 2007;98(09):521-9. doi:10.1160/th07-03-0173.
42. Grabowski B, Schmidt MA, Ruter C. Immunomodulatory *Yersinia* outer proteins (Yops): Useful tools for bacteria and humans alike. Virulence. 2017;8(7):1124-47. doi:10.1080/21505594.2017.1303588.
43. Plano GV, Barve SS, Straley SC. LcrD, a Membrane-Bound Regulator of the Yersinia pestis Low-Calcium Response. J Bacteriol. 1991;173(22):7293-303.
44. Viboud GI, Bliska JB. *Yersinia* outer proteins: role in modulation of host cell signaling responses and pathogenesis. Annu Rev Microbiol. 2005;59:69-89. doi:10.1146/annurev.micro.59.030804.121320.
45. Matsumoto H, Young GM. Translocated effectors of Yersinia. Curr Opin Microbiol. 2009;12(1):94-100. doi:10.1016/j.mib.2008.12.005.
46. Schwiesow L, Lam H, Dersch P, Auerbuch V. Yersinia Type III Secretion System Master Regulator LcrF. J Bacteriol. 2015;198(4):604-14. doi:10.1128/JB.00686-15.
47. Yother J, Chamness TW, Goguen JD. Temperature-controlled plasmid regulon associated with low calcium response in *Yersinia pestis*. J Bacteriol. 1986;165(2):443-7. doi:10.1128/jb.165.2.443-447.1986.
48. Hooker-Romero D, Mettert E, Schwiesow L, Balderas D, Alvarez PA, Kicin A, et al. Iron availability and oxygen tension regulate the Yersinia Ysc type III secretion system to enable disseminated infection. PLoS Pathog. 2019;15(12):e1008001. doi:10.1371/journal.ppat.1008001.
49. Pan NJ, Brady MJ, Leong JM, Goguen JD. Targeting type III secretion in Yersinia pestis. Antimicrob Agents Chemother. 2009;53(2):385-92. doi:10.1128/AAC.00670-08.
50. Michiels T, Wattiau P, Brasseur R, Ruysschaert JM, Cornelis G. Secretion of Yop proteins by Yersiniae. Infect Immun. 1990;58(9):2840-9. doi:10.1128/iai.58.9.2840-2849.1990.
51. Fields KA, Straley SC. LcrV of Yersinia pestis enters infected eukaryotic cells by a virulence plasmid-independent mechanism. Infect Immun. 1999;67(9):4801-13. doi:10.1128/iai.67.9.4801-4813.1999.
52. Fields KA, Plano GV, Straley SC. A Low-Ca2+ Response (LCR) Secretion (ysc) Locus Lies within the lcrB Region of the LCR Plasmid in Yersinia pestis. J Bacteriol. 1994;176(3):569-79.

53. Cornelis GR, Biot T, Rouvroit CL, Michiels T, Mulder B, Sluiters C, et al. The Yersina yop regulon. Mol Microbiol. 1989;3(10):1455-9.
54. Sarker MR, Neyt C, Stainier I, Cornelis GR. The Yersinia Yop virulon: LcrV is required for extrusion of the translocators YopB and YopD. J Bacteriol. 1998;180(5):1207-14. doi:10.1128/jb.180.5.1207-1214.1998.
55. Cornelis GR. The *Yersinia* deadly kiss. J Bacteriol. 1998;180(21):5495-504. doi:10.1128/JB.180.21.5495-5504.1998.
56. Dewoody RS, Merritt PM, Marketon MM. Regulation of the *Yersinia* type III secretion system: traffic control. Front Cell Infect Microbiol. 2013;3:4. doi:10.3389/fcimb.2013.00004.
57. Bliska JB, Wang X, Viboud GI, Brodsky IE. Modulation of innate immune responses by *Yersinia* type III secretion system translocators and effectors. Cell Microbiol. 2013;15(10):1622-31. doi:10.1111/cmi.12164.
58. Rosqvist R, Magnusson KE, Wolf-Watz H. Target cell contact triggers expression and polarized transfer of Yersinia YopE cytotoxin into mammalian cells. EMBO J. 1994;13(4):964-72. doi:10.1002/j.1460-2075.1994.tb06341.x.
59. Coleman MA, Cappuccio JA, Blanchette CD, Gao T, Arroyo ES, Hinz AK, et al. Expression and Association of the Yersinia pestis Translocon Proteins, YopB and YopD, Are Facilitated by Nanolipoprotein Particles. PLoS ONE. 2016;11(3):e0150166. doi:10.1371/journal.pone.0150166.
60. Håkansson S, Bergman T, Vanooteghem JC, Cornelis G, Wolf-Watz H. YopB and YopD constitute a novel class of Yersinia Yop proteins. Infect Immun. 1993;61(1):71-80. doi:10.1128/iai.61.1.71-80.1993.
61. Montagner C, Arquint C, Cornelis GR. Translocators YopB and YopD from Yersinia enterocolitica form a multimeric integral membrane complex in eukaryotic cell membranes. J Bacteriol. 2011;193(24):6923-8. doi:10.1128/JB.05555-11.
62. Costa TR, Edqvist PJ, Broms JE, Ahlund MK, Forsberg A, Francis MS. YopD self-assembly and binding to LcrV facilitate type III secretion activity by Yersinia pseudotuberculosis. J Biol Chem. 2010;285(33):25269-84. doi:10.1074/jbc.M110.144311.
63. Viboud GI, So SS, Ryndak MB, Bliska JB. Proinflammatory signalling stimulated by the type III translocation factor YopB is counteracted by multiple effectors in epithelial cells infected with Yersinia pseudotuberculosis. Mol Microbiol. 2003;47(5):1305-15. doi:10.1046/j.1365-2958.2003.03350.x.
64. Francis MS, Aili M, Wiklund ML, Wolf-Watz H. A study of the YopD-lcrH interaction from Yersinia pseudotuberculosis reveals a role for hydrophobic residues within the amphipathic domain of YopD. Mol Microbiol. 2000;38(1):85-102. doi:10.1046/j.1365-2958.2000.02112.x.
65. Francis MS, Wolf-Watz H. YopD of Yersinia pseudotuberculosis is translocated into the cytosol of HeLa epithelial cells: evidence of a structural domain necessary for translocation. Mol Microbiol. 1998;29(3):799-813. doi:10.1046/j.1365-2958.1998.00973.x.
66. Olsson J, Edqvist PJ, Broms JE, Forsberg A, Wolf-Watz H, Francis MS. The YopD translocator of Yersinia pseudotuberculosis is a multifunctional protein comprised of discrete domains. J Bacteriol. 2004;186(13):4110-23. doi:10.1128/JB.186.13.4110-4123.2004.
67. Zwack EE, Snyder AG, Wynosky-Dolfi MA, Ruthel G, Philip NH, Marketon MM, et al. Inflammasome activation in response to the *Yersinia* type III secretion system requires

hyperinjection of translocon proteins YopB and YopD. mBio. 2015;6(1):e02095-14. doi:10.1128/mBio.02095-14.
68. Brodsky IE, Palm NW, Sadanand S, Ryndak MB, Sutterwala FS, Flavell RA, et al. A *Yersinia* effector protein promotes virulence by preventing inflammasome recognition of the type III secretion system. Cell Host Microbe. 2010;7(5):376-87. doi:10.1016/j.chom.2010.04.009.
69. Cornelis GR. *Yersinia* type III secretion: send in the effectors. J Cell Biol. 2002;158(3):401-8. doi:10.1083/jcb.200205077.
70. Schubert KA, Xu Y, Shao F, Auerbuch V. The *Yersinia* type III secretion system as a tool for studying cytosolic innate immune surveillance. Annu Rev Microbiol. 2020;74:221-45. doi:10.1146/annurev-micro-020518-120221.
71. Barz C, Abahji TN, Trulzsch K, Heesemann J. The Yersinia Ser/Thr protein kinase YpkA/YopO directly interacts with the small GTPases RhoA and Rac-1. FEBS Lett. 2000;482(1-2):139-43. doi:10.1016/s0014-5793(00)02045-7.
72. Prehna G, Ivanov MI, Bliska JB, Stebbins CE. Yersinia virulence depends on mimicry of host Rho-family nucleotide dissociation inhibitors. Cell. 2006;126(5):869-80. doi:10.1016/j.cell.2006.06.056.
73. Navarro L, Koller A, Nordfelth R, Wolf-Watz H, Taylor S, Dixon JE. Identification of a molecular target for the *Yersinia* protein kinase A. Mol Cell. 2007;26(4):465-77. doi:10.1016/j.molcel.2007.04.025.
74. Dukuzumuremyi JM, Rosqvist R, Hallberg B, Akerstrom B, Wolf-Watz H, Schesser K. The Yersinia protein kinase A is a host factor inducible RhoA/Rac-binding virulence factor. J Biol Chem. 2000;275(45):35281-90. doi:10.1074/jbc.M003009200.
75. Pha K, Wright ME, Barr TM, Eigenheer RA, Navarro L. Regulation of Yersinia protein kinase A (YpkA) kinase activity by multisite autophosphorylation and identification of an N-terminal substrate-binding domain in YpkA. J Biol Chem. 2014;289(38):26167-77. doi:10.1074/jbc.M114.601153.
76. Juris SJ, Rudolph AE, Huddler D, Orth K, Dixon JE. A distinctive role for the Yersinia protein kinase: actin binding, kinase activation, and cytoskeleton disruption. Proc Natl Acad Sci U S A. 2000;97(17):9431-6. doi:10.1073/pnas.170281997.
77. Kim MJ, Byun JY, Yun CH, Park IC, Lee KH, Lee SJ. c-Src-p38 mitogen-activated protein kinase signaling is required for Akt activation in response to ionizing radiation. Mol Cancer Res. 2008;6(12):1872-80. doi:10.1158/1541-7786.MCR-08-0084.
78. Schmidt SI, Blaabjerg M, Freude K, Meyer M. RhoA Signaling in Neurodegenerative Diseases. Cells. 2022;11(9). doi:10.3390/cells11091520.
79. Coso OA, Chiariello M, Yu JC, Teramoto H, Crespo P, Xu N, et al. The small GTP-binding proteins Rac1 and Cdc42 regulate the activity of the JNK/SAPK signaling pathway. Cell. 1995;81(7):1137-46. doi:10.1016/s0092-8674(05)80018-2.
80. Kamato D, Thach L, Bernard R, Chan V, Zheng W, Kaur H, et al. Structure, Function, Pharmacology, and Therapeutic Potential of the G Protein, Galpha/q,11. Front Cardiovasc Med. 2015;2:14. doi:10.3389/fcvm.2015.00014.
81. Cheng Z, Garvin D, Paguio A, Stecha P, Wood K, Fan F. Luciferase Reporter Assay System for Deciphering GPCR Pathways. Curr Chem Genomics. 2010;4:84-91. doi:10.2174/1875397301004010084.
82. Park H, Teja K, O'Shea JJ, Siegel RM. The Yersinia effector protein YpkA induces apoptosis independently of actin depolymerization. J Immunol. 2007;178(10):6426-34. doi:10.4049/jimmunol.178.10.6426.

83. Coso OA, Chiariello M, Yu J-C, Teramoto H, Crespo P, Xu N, et al. The small GTP-binding proteins Rac1 and Cdc42 regulate the activity of the JNK/SAPK signaling pathway. Cell. 1995;81(7):1137-46. doi:10.1016/s0092-8674(05)80018-2.
84. Frost JA, Swantek JL, Stippec S, Yin MJ, Gaynor R, Cobb MH. Stimulation of NFkappa B activity by multiple signaling pathways requires PAK1. J Biol Chem. 2000;275(26):19693-9. doi:10.1074/jbc.M909860199.
85. Nobes CD, Hall A. Rho, rac, and cdc42 GTPases regulate the assembly of multimolecular focal complexes associated with actin stress fibers, lamellipodia, and filopodia. Cell. 1995;81(1):53-62. doi:10.1016/0092-8674(95)90370-4.
86. Andor A, Trulzsch K, Essler M, Roggenkamp A, Wiedemann A, Heesemann J, et al. YopE of Yersinia, a GAP for Rho GTPases, selectively modulates Rac-dependent actin structures in endothelial cells. Cell Microbiol. 2001;3(5):301-10. doi:10.1046/j.1462-5822.2001.00114.x.
87. Viboud GI, Mejia E, Bliska JB. Comparison of YopE and YopT activities in counteracting host signalling responses to Yersinia pseudotuberculosis infection. Cell Microbiol. 2006;8(9):1504-15. doi:10.1111/j.1462-5822.2006.00729.x.
88. Medici NP, Rashid M, Bliska JB. Characterization of pyrin dephosphorylation and inflammasome activation in macrophages as triggered by the *Yersinia* effectors YopE and YopT. Infect Immun. 2019;87(3). doi:10.1128/IAI.00822-18.
89. Chung LK, Park YH, Zheng Y, Brodsky IE, Hearing P, Kastner DL, et al. The *Yersinia* virulence factor YopM hijacks host kinases to inhibit type III effector-triggered activation of the pyrin inflammasome. Cell Host Microbe. 2016;20(3):296-306. doi:10.1016/j.chom.2016.07.018.
90. Ratner D, Orning MP, Proulx MK, Wang D, Gavrilin MA, Wewers MD, et al. The *Yersinia pestis* effector YopM inhibits pyrin inflammasome activation. PLoS Pathog. 2016;12(12):e1006035. doi:10.1371/journal.ppat.1006035.
91. Wang X, Parashar K, Sitaram A, Bliska JB. The GAP activity of type III effector YopE triggers killing of Yersinia in macrophages. PLoS Pathog. 2014;10(8):e1004346. doi:10.1371/journal.ppat.1004346.
92. Bartra S, Cherepanov P, Forsberg Ak, Schess K. The *Yersinia* YopE and YopH type III effector proteins enhance bacterial proliferation following contact with eukaryotic cells. BMC Microbiol. 2001;1(22). doi:10.1186/1471-2180-1-22.
93. Pulsifer AR, Vashishta A, Reeves SA, Wolfe JK, Palace SG, Prouix MK, et al. Redundant and cooperative roles for *Yersinia pestis* yop effectors in the inhibition of human neutrophil exocytic responses revealed by gain-of-function approach. Infection and Immunity. 2020;88(3):1-16. doi:10.1128/IAI.00909-19.
94. Taheri N, Fahlgren A, Fallman M. Yersinia pseudotuberculosis Blocks Neutrophil Degranulation. Infect Immun. 2016;84(12):3369-78. doi:10.1128/IAI.00760-16.
95. de la Puerta ML, Trinidad AG, del Carmen Rodriguez M, Bogetz J, Sanchez Crespo M, Mustelin T, et al. Characterization of new substrates targeted by Yersinia tyrosine phosphatase YopH. PLoS One. 2009;4(2):e4431. doi:10.1371/journal.pone.0004431.
96. Black DS, Marie-Cardine A, Schraven B, Bliska JB. The Yersinia tyrosine phosphatase YopH targets a novel adhesion-regulated signalling complex in macrophages. Cell Microbiol. 2000;2(5):401-14. doi:10.1046/j.1462-5822.2000.00061.x.
97. Shaban L, Nguyen GT, Mecsas-Faxon BD, Swanson KD, Tan S, Mecsas J. Yersinia pseudotuberculosis YopH targets SKAP2-dependent and independent signaling pathways to block neutrophil antimicrobial mechanisms during infection. PLoS Pathog. 2020;16(5):e1008576. doi:10.1371/journal.ppat.1008576.

98. Rolan HG, Durand EA, Mecsas J. Identifying *Yersinia* YopH-targeted signal transduction pathways that impair neutrophil responses during *in vivo* murine infection. Cell Host Microbe. 2013;14(3):306-17. doi:10.1016/j.chom.2013.08.013.
99. Hamid N, Gustavsson A, Andersson K, McGee K, Persson C, Rudd CE, et al. YopH dephosphorylates Cas and Fyn-binding protein in macrophages. Microbial Pathogensis. 1999;27(4):231-42. doi:10.1006/mpat.1999.0301.
100. Andersson K, Magnusson K, Majeed M, Stendahl O, Fallman M. Yersinia pseudotuberculosis-Induced Calcium Signaling in Neutrophils Is Blocked by the Virulence Effector YopH. Infection and Immunity. 1999;67(5).
101. Alonso A, Bottini N, Bruckner S, Rahmouni S, Williams S, Schoenberger SP, et al. Lck dephosphorylation at Tyr-394 and inhibition of T cell antigen receptor signaling by Yersinia phosphatase YopH. J Biol Chem. 2004;279(6):4922-8. doi:10.1074/jbc.M308978200.
102. Cantwell AM, Bubeck SS, Dube PH. YopH inhibits early pro-inflammatory cytokine responses during plague pneumonia. BMC Immunology. 2010;11(29). doi:10.1186/1471-2172-11-29.
103. Spinner JL, Cundiff JA, Kobayashi SD. *Yersinia pestis* type III secretion system-dependent inhibition of human polymorphonuclear leukocyte function. Infect Immun. 2008;76(8):3754-60. doi:10.1128/IAI.00385-08.
104. Bubeck SS, Dube PH. Yersinia pestis CO92 delta yopH is a potent live, attenuated plague vaccine. Clin Vaccine Immunol. 2007;14(9):1235-8. doi:10.1128/CVI.00137-07.
105. Paquette N, Conlon J, Sweet C, Rus F, Wilson L, Pereira A, et al. Serine/threonine acetylation of TGFbeta-activated kinase (TAK1) by Yersinia pestis YopJ inhibits innate immune signaling. Proc Natl Acad Sci U S A. 2012;109(31):12710-5. doi:10.1073/pnas.1008203109.
106. Zhang L, Mei M, Yu C, Shen W, Ma L, He J, et al. The functions of effector proteins in *Yersinia* virulence. Polish Journal of Microbiology. 2016;65(1):5-12.
107. Zhou H, Monack DM, Kayagaki N, Wertz I, Yin J, Wolf B, et al. Yersinia virulence factor YopJ acts as a deubiquitinase to inhibit NF-kappa B activation. J Exp Med. 2005;202(10):1327-32. doi:10.1084/jem.20051194.
108. Palmer LE, Hobbie S, Galan JE, Bliska JB. YopJ of *Yersinia pseudotuberculosis* is required for the inhibition of macrophage TNF-a production and downregulation of the MAP kinases p38 and JNK. Molecular Microbiology. 1998;27(5):953-65.
109. Spinner JL, Hasenkrug AM, Shannon JG, Kobayashi SD, Hinnebusch BJ. Role of the *Yersinia* YopJ protein in suppressing interleukin-8 secretion by human polymorphonuclear leukocytes. Microbes Infect. 2016;18(1):21-9. doi:10.1016/j.micinf.2015.08.015.
110. Ratner D, Orning MP, Starheim KK, Marty-Roix R, Proulx MK, Goguen JD, et al. Manipulation of Interleukin-1beta and Interleukin-18 Production by Yersinia pestis Effectors YopJ and YopM and Redundant Impact on Virulence. J Biol Chem. 2016;291(19):9894-905. doi:10.1074/jbc.M115.697698.
111. Palace SG, Proulx MK, Szabady RL, Goguen JD. Gain-of-function analysis reveals important virulence roles for the *Yersinia pestis* type III secretion system effectors YopJ, YopT, and YpkA. Infection and Immunity. 2018;86(9):1-11. doi:10.1128/IAI.
112. Monack DMM, J. Ghori, N. & Falkow, S. Yersinia signals macrophages to undergo apoptosis and YopJ is necessary for this cell death. Proc Natl Acad Sci U S A. 1997;94:10385–90.
113. Philip NH, Brodsky IE. Cell death programs in Yersinia immunity and pathogenesis. Front Cell Infect Microbiol. 2012;2:149. doi:10.3389/fcimb.2012.00149.

114. Chung LK, Philip NH, Schmidt VA, Koller A, Strowig T, Flavell RA, et al. IQGAP1 is important for activation of caspase-1 in macrophages and is targeted by Yersinia pestis type III effector YopM. mBio. 2014;5(4):e01402-14. doi:10.1128/mBio.01402-14.
115. LaRock CN, Cookson BT. The *Yersinia* virulence effector YopM binds caspase-1 to arrest inflammasome assembly and processing. Cell Host Microbe. 2012;12(6):799-805. doi:10.1016/j.chom.2012.10.020.
116. Lilo S, Zheng Y, Bliska JB. Caspase-1 activation in macrophages infected with Yersinia pestis KIM requires the type III secretion system effector YopJ. Infect Immun. 2008;76(9):3911-23. doi:10.1128/IAI.01695-07.
117. Schoberle TJ, Chung LK, McPhee JB, Bogin B, Bliska JB. Uncovering an important role for YopJ in the inhibition of caspase-1 in activated macrophages and promoting *Yersinia pseudotuberculosis* virulence. Infect Immun. 2016;84(4):1062-72. doi:10.1128/IAI.00843-15.
118. Montminy SW, Khan N, McGrath S, Walkowicz MJ, Sharp F, Conlon JE, et al. Virulence factors of Yersinia pestis are overcome by a strong lipopolysaccharide response. Nat Immunol. 2006;7(10):1066-73. doi:10.1038/ni1386.
119. Vladimer GI, Weng D, Paquette SW, Vanaja SK, Rathinam VA, Aune MH, et al. The NLRP12 inflammasome recognizes Yersinia pestis. Immunity. 2012;37(1):96-107. doi:10.1016/j.immuni.2012.07.006.
120. Thorslund SE, Edgren T, Pettersson J, Nordfelth R, Sellin ME, Ivanova E, et al. The RACK1 signaling scaffold protein selectively interacts with Yersinia pseudotuberculosis virulence function. PLoS ONE. 2011;6(2):e16784. doi:10.1371/journal.pone.0016784.
121. Tan Y, Liu W, Zhang Q, Cao S, Zhao H, Wang T, et al. Yersinia pestis YopK Inhibits Bacterial Adhesion to Host Cells by Binding to the Extracellular Matrix Adaptor Protein Matrilin-2. Infect Immun. 2017;85(8). doi:10.1128/IAI.01069-16.
122. Thorslund SE, Ermert D, Fahlgren A, Erttmann SF, Nilsson K, Hosseinzadeh A, et al. Role of YopK in Yersinia pseudotuberculosis resistance against polymorphonuclear leukocyte defense. Infect Immun. 2013;81(1):11-22. doi:10.1128/IAI.00650-12.
123. McDonald C, Vacratsis PO, Bliska JB, Dixon JE. The yersinia virulence factor YopM forms a novel protein complex with two cellular kinases. J Biol Chem. 2003;278(20):18514-23. doi:10.1074/jbc.M301226200.
124. Anjum R, Blenis J. The RSK family of kinases: emerging roles in cellular signalling. Nat Rev Mol Cell Biol. 2008;9(10):747-58. doi:10.1038/nrm2509.
125. Carriere A, Ray H, Blenis J, Roux PP. The RSK factors of activating the Ras/MAPK signaling cascade. Front Biosci. 2008;13:4258-75. doi:10.2741/3003.
126. Lim PS, Sutton CR, Rao S. Protein kinase C in the immune system: from signalling to chromatin regulation. Immunology. 2015;146(4):508-22. doi:10.1111/imm.12510.
127. Ye Z, Gorman AA, Uittenbogaard AM, Myers-Morales T, Kaplan AM, Cohen DA, et al. Caspase-3 mediates the pathogenic effect of Yersinia pestis YopM in liver of C57BL/6 mice and contributes to YopM's function in spleen. PLoS ONE. 2014;9(11):e110956. doi:10.1371/journal.pone.0110956.
128. Shao F, Vacratsis PO, Bao Z, Bowers KE, Fierke CA, Dixon JE. Biochemical characterization of the *Yersinia* YopT protease: Cleavage site and recognition elements in Rho GTPases. PNAS. 2003;100(3). doi:10.1073/pnas.252770599.
129. Aepfelbacher M, Trasak C, Wilharm G, Wiedemann A, Trulzsch K, Krauss K, et al. Characterization of YopT effects on Rho GTPases in Yersinia enterocolitica-infected cells. J Biol Chem. 2003;278(35):33217-23. doi:10.1074/jbc.M303349200.

130. Chandler CE, Harberts EM, Pelletier MR, Thaipisuttikul I, Jones JW, Hajjar AM, et al. Early evolutionary loss of the lipid A modifying enzyme PagP resulting in innate immune evasion in Yersinia pestis. Proc Natl Acad Sci U S A. 2020;117(37):22984-91. doi:10.1073/pnas.1917504117.
131. Martinez-Chavarria LC, Vadyvaloo V. Yersinia pestis and Yersinia pseudotuberculosis infection: a regulatory RNA perspective. Front Microbiol. 2015;6:956. doi:10.3389/fmicb.2015.00956.
132. Chauvaux S, Dillies MA, Marceau M, Rosso ML, Rousseau S, Moszer I, et al. In silico comparison of Yersinia pestis and Yersinia pseudotuberculosis transcriptomes reveals a higher expression level of crucial virulence determinants in the plague bacillus. Int J Med Microbiol. 2011;301(2):105-16. doi:10.1016/j.ijmm.2010.08.013.
133. Bi Y, Wang X, Han Y, Guo Z, Yang R. Yersinia pestis versus Yersinia pseudotuberculosis: effects on host macrophages. Scand J Immunol. 2012;76(6):541-51. doi:10.1111/j.1365-3083.2012.02767.x.
134. Mecsas J. Unraveling neutrophil- Yersinia interactions during tissue infection. F1000Res. 2019;8. doi:10.12688/f1000research.18940.1.
135. Janssen WA, Surgalla MJ. Plague Bacillus: Survival within Host Phagocytes. Science. 1969;163(3870):950-2. doi:10.1126/science.163.3870.950.
136. Dudte SC, Hinnebusch BJ, Shannon JG. Characterization of *Yersinia pestis* interactions with human neutrophils *In vitro*. Front Cell Infect Microbiol. 2017;7:358. doi:10.3389/fcimb.2017.00358.
137. Spinner JL, Seo KS, O'Loughlin JL, Cundiff JA, Minnich SA, Bohach GA, et al. Neutrophils are resistant to *Yersinia* YopJ/P-induced apoptosis and are protected from ROS-mediated cell death by the type III secretion system. PLoS One. 2010;5(2):e9279. doi:10.1371/journal.pone.0009279.
138. O'Loughlin JL, Spinner JL, Minnich SA, Kobayashi SD. Yersinia pestis two-component gene regulatory systems promote survival in human neutrophils. Infect Immun. 2010;78(2):773-82. doi:10.1128/IAI.00718-09.
139. Connor MG, Pulsifer AR, Chung D, Rouchka EC, Ceresa BK, Lawrenz MB. *Yersinia pestis* targets the host endosome recycling pathway during the biogenesis of the *Yersinia*-containing vacuole to avoid killing by macrophages. mBio. 2018;9(1). doi:10.1128/mBio.01800-17.
140. Connor MG, Pulsifer AR, Price CT, Abu Kwaik Y, Lawrenz MB. *Yersinia pestis* requires host Rab1b for survival in macrophages. PLoS Pathogens. 2015;11(10):e1005241. doi:10.1371/journal.ppat.1005241.
141. Du Y, Rosqvist R, Forsberg A. Role of fraction 1 antigen of Yersinia pestis in inhibition of phagocytosis. Infect Immun. 2002;70(3):1453-60. doi:10.1128/iai.70.3.1453-1460.2002.
142. Rosqvist R, Forsberg A, Rimpilainen M, Bergman T, Wolf-Watz H. The cytotoxic protein YopE of Yersinia obstructs the primary host defence. Mol Microbiol. 1990;4(4):657-67. doi:10.1111/j.1365-2958.1990.tb00635.x.
143. Lukaszewski RA, Kenny DJ, Taylor R, Rees DG, Hartley MG, Oyston PC. Pathogenesis of Yersinia pestis infection in BALB/c mice: effects on host macrophages and neutrophils. Infect Immun. 2005;73(11):7142-50. doi:10.1128/IAI.73.11.7142-7150.2005.
144. Arifuzzaman M, Ang WXG, Choi HW, Nilles ML, St John AL, Abraham SN. Necroptosis of infiltrated macrophages drives Yersinia pestis dispersal within buboes. JCI Insight. 2018;3(18). doi:10.1172/jci.insight.122188.

145. Kerschen EJ, Cohen DA, Kaplan AM, Straley SC. The plague virulence protein YopM targets the innate immune response by causing a global depletion of NK cells. Infect Immun. 2004;72(8):4589-602. doi:10.1128/IAI.72.8.4589-4602.2004.
146. Bi Y, Du Z, Han Y, Guo Z, Tan Y, Zhu Z, et al. Yersinia pestis and host macrophages: immunodeficiency of mouse macrophages induced by YscW. Immunology. 2009;128(1 Suppl):e406-17. doi:10.1111/j.1365-2567.2008.02990.x.
147. Choi HW, Brooking-Dixon R, Neupane S, Lee CJ, Miao EA, Staats HF, et al. *Salmonella typhimurium* impedes innate immunity with a mast-cell-suppressing protein tyrosine phosphatase, SptP. Immunity. 2013;39(6):1108-20. doi:10.1016/j.immuni.2013.11.009.
148. de Paula Rogerio A, Sorgi CA, Sadikot R, Carlo T. The role of lipids mediators in inflammation and resolution. Biomed Res Int. 2015;2015:605959. doi:10.1155/2015/605959.
149. Calder P. Polyunsaturated fatty acids and inflammation: Therapeutic potential in rheumatoid arthritis. Current Rheumatology Reviews. 2009;5(4):214-25. doi:10.2174/157339709790192558.
150. Crooks SW, Stockley RA. Leukotriene B4. The International Journal of Biochemistry and Cell Biology. 1998;30(2):173-8. doi:10.1016/s1357-2725(97)00123-4.
151. Woo CH, You HJ, Cho SH, Eom YW, Chun JS, Yoo YJ, et al. Leukotriene $B_4$ stimulates Rac-ERK cascade to generate reactive oxygen species that mediates chemotaxis. J Biol Chem. 2002;277(10):8572-8. doi:10.1074/jbc.M104766200.
152. Wan M, Tang X, Stsiapanava A, Haeggstrom JZ. Biosynthesis of leukotriene $B_4$. Semin Immunol. 2017;33:3-15. doi:10.1016/j.smim.2017.07.012.
153. Hegde B, Bodduluri SR, Satpathy SR, Alghsham RS, Jala VR, Uriarte SM, et al. Inflammasome-independent leukotriene $B_4$ production drives crystalline silica-induced sterile inflammation. J Immunol. 2018;200(10):3556-67. doi:10.4049/jimmunol.1701504.
154. Peters-Golden M, Song K, Marshall T, Brock T. Translocation of cytosolic phospholipase A2 topographically localized phospholipid hydrolysis. Biochemical Journal. 1996;318:797-803.
155. Hanna VS, Hafez EAA. Synopsis of arachidonic acid metabolism: A review. J Adv Res. 2018;11:23-32. doi:10.1016/j.jare.2018.03.005.
156. Hirabayashi T, Kume K, Hirose K, Yokomizo T, Iino M, Itoh H, et al. Critical Duration of Intracellular $Ca2^+$ Response Required for Continuous Translocation and Activation of Cytosolic Phospholipase $A_2$. The Journal of Biological Chemistry. 1999;274(8):5163–9.
157. Lin LL, Wartmann M, Knopf JL, Lin AY, Seth A, Davis RJ. cPLA2 is phosphorylated and activated by MAP kinase. Cell. 1993;72:269-78.
158. Dulin NO, Sorokin A, Douglas JG. Arachidonate-induced tyrosine phosphorylation of epidermal growth factor receptor and Shc-Grb2-Sos association. Hypertension. 1998;32(6):1089-93. doi:10.1161/01.hyp.32.6.1089.
159. Peppelenbosch MP, Qiu RG, de Vries-Smits AM, Tertoolen LG, de Laat SW, McCormick F, et al. Rac mediates growth factor-induced arachidonic acid release. Cell. 1995;81(6):849-56. doi:10.1016/0092-8674(95)90005-5.
160. Huang XL, Pawliczak R, Cowan MJ, Gladwin MT, Madara P, Logun C, et al. Epidermal growth factor induces p11 gene and protein expression and down-regulates calcium ionophore-induced arachidonic acid release in human epithelial cells. J Biol Chem. 2002;277(41):38431-40. doi:10.1074/jbc.M207406200.
161. Wu T, Angus CW, Yao XL, Logun C, Shelhamer JH. p11, a Unique Member of the S100 Family of Calcium-binding Proteins, Interacts with and Inhibits the Activity of the 85-kDa Cytosolic Phospholipase A2. The Journal of Biological Chemistry. 1997;272(27):17145–53.

162. Li B, Xia L, Krantz A, Yuan Z. Site-Directed Mutagenesis of Cys324 and Cys331 in Human Cytosolic Phospholipase A2 Locus of Action of Thiol Modification Reagents Leading to Inactivation of cPLA2. Biochemistry (Mosc). 1996;35:3156-61.
163. Rosse C, Linch M, Kermorgant S, Cameron AJ, Boeckeler K, Parker PJ. PKC and the control of localized signal dynamics. Nat Rev Mol Cell Biol. 2010;11(2):103-12. doi:10.1038/nrm2847.
164. Sun MK, Alkon DL. Pharmacology of protein kinase C activators: cognition-enhancing and antidementic therapeutics. Pharmacol Ther. 2010;127(1):66-77. doi:10.1016/j.pharmthera.2010.03.001.
165. Chilton FH, Fonteh AN, Surette ME, Triggiani M, Winkler JD. Control of arachidonate levels within inflammatory cells. 1996.
166. Perez-Chacon G, Astudillo AM, Ruiperez V, Balboa MA, Balsinde J. Signaling role for lysophosphatidylcholine acyltransferase 3 in receptor-regulated arachidonic acid reacylation reactions in human monocytes. J Immunol. 2010;184(2):1071-8. doi:10.4049/jimmunol.0902257.
167. Werz O, Klemm J, Samuelsson B, Rådmark O. 5-Lipoxygenase is phosphorylated by p38 kinase-dependent MAPKAP kinases. PNAS. 2000;97(10):5261-6. doi:10.1073/pnas.050588997.
168. Werz O, Szellas D, Steinhilber D, Radmark O. Arachidonic acid promotes phosphorylation of 5-lipoxygenase at Ser-271 by MAPK-activated protein kinase 2 (MK2). J Biol Chem. 2002;277(17):14793-800. doi:10.1074/jbc.M111945200.
169. Radmark O, Samuelsson B. Regulation of 5-lipoxygenase enzyme activity. Biochem Biophys Res Commun. 2005;338(1):102-10. doi:10.1016/j.bbrc.2005.08.013.
170. Radmark O, Werz O, Steinhilber D, Samuelsson B. 5-Lipoxygenase: regulation of expression and enzyme activity. Trends Biochem Sci. 2007;32(7):332-41. doi:10.1016/j.tibs.2007.06.002.
171. Peters-Golden M, Brock TG. 5-Lipoxygenase and FLAP. Prostaglandins, Leukotrienes and Essential Fatty Acids. 2003;69(2-3):99-109. doi:10.1016/s0952-3278(03)00070-x.
172. Brock TG. Regulating leukotriene synthesis: the role of nuclear 5-lipoxygenase. J Cell Biochem. 2005;96(6):1203-11. doi:10.1002/jcb.20662.
173. Cowburn AS, Holgate ST, Sampson AP. IL-5 Increases Expression of 5-Lipoxygenase-Activating Protein and Translocates 5-Lipoxygenase to the Nucleus in Human Blood Eosinophils. The Journal of Immunology. 1999;163(1):456-65. doi:10.4049/jimmunol.163.1.456.
174. Reddy KV, Serio KJ, Hodulik CR, Bigby TD. 5-lipoxygenase-activating protein gene expression. Key role of CCAAT/enhancer-binding proteins (C/EBP) in constitutive and tumor necrosis factor (TNF) alpha-induced expression in THP-1 cells. J Biol Chem. 2003;278(16):13810-8. doi:10.1074/jbc.M211102200.
175. Riddick CA, Ring WL, Baker JR, Hodulik CR, Bigby TD. Dexamethasone increases expression of 5-lipoxygenase and its activating protein in human monocytes and THP-1 cells. Eur J Biochem. 1997;246(1):112-8. doi:10.1111/j.1432-1033.1997.00112.x.
176. Serio KJ, Reddy KV, Bigby TD. Lipopolysaccharide induces 5-lipoxygenase-activating protein gene expression in THP-1 cells via a NF-kappaB and C/EBP-mediated mechanism. Am J Physiol Cell Physiol. 2005;288(5):C1125-33. doi:10.1152/ajpcell.00296.2004.
177. Ring WL, Riddick CA, Baker JR, Munafo DA, Bigby TD. Lymphocytes stimulate expression of 5-lipoxygenase and its activating protein in monocytes in vitro via granulocyte macrophage colony-stimulating factor and interleukin 3. J Clin Invest. 1996;97(5):1293-301. doi:10.1172/jci118545.

178. Miller DK, Gillard JW, Vickers PJ, Sadowski S, Léveillé C, Mancini JA, et al. Identification and isolation of a membrane protein necessary for leukotriene production. Nature. 1990;343(6255):278-81. doi:10.1038/343278a0.
179. Haeggstrom JZ. Structure, Function, and Regulation of Leukotriene A 4 Hydrolase. American Journal of Respiratory Critical Care Medicine. 2000;161:S25-S31.
180. Rudberg PC, Tholander F, Thunnissen MM, Haeggstrom JZ. Leukotriene A4 hydrolase/aminopeptidase. Glutamate 271 is a catalytic residue with specific roles in two distinct enzyme mechanisms. J Biol Chem. 2002;277(2):1398-404. doi:10.1074/jbc.M106577200.
181. Haeggstrom JZ. Leukotriene A4 hydrolase/aminopeptidase, the gatekeeper of chemotactic leukotriene B4 biosynthesis. J Biol Chem. 2004;279(49):50639-42. doi:10.1074/jbc.R400027200.
182. Tager AM, Luster AD. BLT1 and BLT2: the leukotriene B(4) receptors. Prostaglandins Leukot Essent Fatty Acids. 2003;69(2-3):123-34. doi:10.1016/s0952-3278(03)00073-5.
183. Yokomizo T. Two distinct leukotriene $B_4$ receptors, BLT1 and BLT2. J Biochem. 2015;157(2):65-71. doi:10.1093/jb/mvu078.
184. Yokomizo T, Kato K, Terawaki K, Izumi T, Shimizu T. A Second Leukotriene B4 Receptor, BLT2: A New Therapeutic Target in Inflammation and Immunological Disorders. J Exp Med. 2000;192(3).
185. He R, Chen Y, Cai Q. The role of the LTB4-BLT1 axis in health and disease. Pharmacol Res. 2020;158:104857. doi:10.1016/j.phrs.2020.104857.
186. Spite M, Hellmann J, Tang Y, Mathis SP, Kosuri M, Bhatnagar A, et al. Deficiency of the leukotriene B4 receptor, BLT-1, protects against systemic insulin resistance in diet-induced obesity. J Immunol. 2011;187(4):1942-9. doi:10.4049/jimmunol.1100196.
187. Terawaki K, Yokomizo T, Nagase T, Toda A, Taniguchi M, Hashizume K, et al. Absence of leukotriene B4 receptor 1 confers resistance to airway hyperresponsiveness and Th2-type immune responses. J Immunol. 2005;175(7):4217-25. doi:10.4049/jimmunol.175.7.4217.
188. Li K, Zheng L, Guo H, Hong F, Yang S. LTB4-induced anti-apoptosis and infiltration of neutrophils in rheumatoid arthritis. Clin Exp Rheumatol. 2020;38.
189. Ramalho T, Ramalingam L, Filgueiras L, Festuccia W, Jancar S, Moustaid-Moussa N. Leukotriene-B4 modulates macrophage metabolism and fat loss in type 1 diabetic mice. J Leukoc Biol. 2019;106(3):665-75. doi:10.1002/JLB.MA1218-477RR.
190. Satpathy SR, Jala VR, Bodduluri SR, Krishnan E, Hegde B, Hoyle GW, et al. Crystalline silica-induced leukotriene $B_4$-dependent inflammation promotes lung tumour growth. Nat Commun. 2015;6:7064. doi:10.1038/ncomms8064.
191. Wilborn J, Bailie M, Coffey M, Burdick M, Strieter R, Peters-Golden M. Constitutive Activation of 5-Lipoxygenase in the Lungs of Patients with Idiopathic Pulmonary Fibrosis. J Clin Invest. 1996;97(8).
192. Alvarez K, Villar-Vesga J, Ortiz-Reyes B, Vanegas-Garcia A, Castano D, Rojas M, et al. Induction of NF-kappaB inflammatory pathway in monocytes by microparticles from patients with systemic lupus erythematosus. Heliyon. 2020;6(12):e05815. doi:10.1016/j.heliyon.2020.e05815.
193. Amaral FA, Costa VV, Tavares LD, Sachs D, Coelho FM, Fagundes CT, et al. NLRP3 inflammasome-mediated neutrophil recruitment and hypernociception depend on leukotriene B(4) in a murine model of gout. Arthritis Rheum. 2012;64(2):474-84. doi:10.1002/art.33355.

194. Horii Y, Nakaya M, Ohara H, Nishihara H, Watari K, Nagasaka A, et al. Leukotriene B4 receptor 1 exacerbates inflammation following myocardial infarction. FASEB J. 2020;34(6):8749-63. doi:10.1096/fj.202000041R.
195. Peters-Golden M, Canetti C, Mancuso P, Coffey MJ. Leukotrienes: Underappreciated mediators of innate immune responses. J Immunol. 2005;174(2):589-94. doi:10.4049/jimmunol.174.2.589.
196. Le Bel M, Brunet A, Gosselin J. Leukotriene B4, an endogenous stimulator of the innate immune response against pathogens. J Innate Immun. 2014;6(2):159-68. doi:10.1159/000353694.
197. Flamand L, Tremblay MJ, Borgeat P. Leukotriene B4 triggers the in vitro and in vivo release of potent antimicrobial agents. J Immunol. 2007;178(12):8036-45. doi:10.4049/jimmunol.178.12.8036.
198. Mancuso P, Standiford TJ, Marshall T, Peters-Golden M. 5-Lipoxygenase Reaction Products Modulate Alveolar Macrophage Phagocytosis of Klebsiella pneumoniae. Infect Immun. 1998;66(11).
199. Mancuso P, Nana-Sinkam P, Peters-Golden M. Leukotriene $B_4$ augments neutrophil phagocytosis of *Klebsiella pneumoniae*. Infect Immun. 2001;69(4):2011-6. doi:10.1128/IAI.69.4.2011-2016.2001.
200. Serezani CH, Aronoff DM, Jancar S, Mancuso P, Peters-Golden M. Leukotrienes enhance the bactericidal activity of alveolar macrophages against *Klebsiella pneumoniae* through the activation of NADPH oxidase. Blood. 2005;106(3):1067-75. doi:10.1182/blood-2004-08-3323.
201. Bailie MC, Standiford TJ, Laichalk LL, Coffey MJ, Strieter R, Peters-Golden M. leukotriene-Deficient Mice Manifest Enhanced lethality from KIebsieIIu Pneumonia in Association with Decreased Alveolar Macropha e Phagocytic and Bactericidal Activities. The Journal of Immunology. 1996;157.
202. Mancuso P, Lewis C, Serezani CH, Goel D, Peters-Golden M. Intrapulmonary administration of leukotriene $B_4$ enhances pulmonary host defense against pneumococcal pneumonia. Infect Immun. 2010;78(5):2264-71. doi:10.1128/IAI.01323-09.
203. Vincent WJB, Harvie EA, Sauer JD, Huttenlocher A. Neutrophil derived $LTB_4$ induces macrophage aggregation in response to encapsulated *Streptococcus iniae* infection. PLoS ONE. 2017;12(6):e0179574. doi:10.1371/journal.pone.0179574.
204. Tobin DM, Vary JC, Jr., Ray JP, Walsh GS, Dunstan SJ, Bang ND, et al. The lta4h locus modulates susceptibility to mycobacterial infection in zebrafish and humans. Cell. 2010;140(5):717-30. doi:10.1016/j.cell.2010.02.013.
205. Sorgi CA, Soares EM, Rosada RS, Bitencourt CS, Zoccal KF, Pereira PAT, et al. Eicosanoid pathway on host resistance and inflammation during *Mycobacterium tuberculosis* infection is comprised by $LTB_4$ reduction but not $PGE_2$ increment. Biochim Biophys Acta Mol Basis Dis. 2020;1866(3):165574. doi:10.1016/j.bbadis.2019.165574.
206. Brandt SL, Klopfenstein N, Wang S, Winfree S, McCarthy BP, Territo PR, et al. Macrophage-derived $LTB_4$ promotes abscess formation and clearance of *Staphylococcus aureus* skin infection in mice. PLoS Pathog. 2018;14(8):e1007244. doi:10.1371/journal.ppat.1007244.
207. Malaviya R, Abraham SN. Role of mast cell leukotrienes in neutrophil recruitment and bacterial clearance in infectious peritonitis. Journal of Leukocyte Biology. 2000;67.
208. Demitsu T, Katayama H, Saito-Taki T, Yaoita H, Nakano M. Phagocytosis and bactericidal action of mouse peritoneal macrophages treated with leukotriene B4. International Journal of Immunopharmacology. 1989;11(7):7.

209. Zhang Y, Olson RM, Brown CR. Macrophage $LTB_4$ drives efficient phagocytosis of *Borrelia burgdorferi* via BLT1 or BLT2. J Lipid Res. 2017;58(3):494-503. doi:10.1194/jlr.M068882.
210. Coffey MJ, Phare SM, Peters-Golden M. Role of leukotrienes in killing of *Mycobacterium bovis* by neutrophils. Prostaglandins Leukot Essent Fatty Acids. 2004;71(3):185-90. doi:10.1016/j.plefa.2004.03.012.
211. Soares EM, Mason KL, Rogers LM, Serezani CH, Faccioli LH, Aronoff DM. Leukotriene B4 enhances innate immune defense against the puerperal sepsis agent Streptococcus pyogenes. J Immunol. 2013;190(4):1614-22. doi:10.4049/jimmunol.1202932.
212. Goodarzi K, Goodarzi M, Tager AM, Luster AD, von Andrian UH. Leukotriene B4 and BLT1 control cytotoxic effector T cell recruitment to inflamed tissues. Nat Immunol. 2003;4(10):965-73. doi:10.1038/ni972.
213. Brandt SL, Serezani CH. Too much of a good thing: How modulating $LTB_4$ actions restore host defense in homeostasis or disease. Semin Immunol. 2017;33:37-43. doi:10.1016/j.smim.2017.08.006.
214. Rola-Pleszczynski M, Gagnon L, Chavaillaz PA. Immune Regulation by Leukotriene B4. Biology of Leukotrienes. 1988;524(1).
215. Liang M, Lv J, Jiang Z, He H, Chen C, Xiong Y, et al. Promotion of Myofibroblast Differentiation and Tissue Fibrosis by the Leukotriene B4 -Leukotriene B4 Receptor Axis in Systemic Sclerosis. Arthritis Rheumatol. 2020;72(6):1013-25. doi:10.1002/art.41192.
216. Xiong Y, Cui X, Li W, Lv J, Du L, Mi W, et al. BLT1 signaling in epithelial cells mediates allergic sensitization via promotion of IL-33 production. Allergy. 2019;74(3):495-506. doi:10.1111/all.13656.
217. Chaves MM, Sinflorio DA, Thorstenberg ML, Martins MDA, Moreira-Souza ACA, Rangel TP, et al. Non-canonical NLRP3 inflammasome activation and IL-1beta signaling are necessary to L. amazonensis control mediated by P2X7 receptor and leukotriene B4. PLoS Pathog. 2019;15(6):e1007887. doi:10.1371/journal.ppat.1007887.
218. Salina ACG, Brandt SL, Klopfenstein N, Blackman A, Bazzano JMR, Sa-Nunes A, et al. Leukotriene $B_4$ licenses inflammasome activation to enhance skin host defense. Proc Natl Acad Sci U S A. 2020;117(48):30619-27. doi:10.1073/pnas.2002732117.
219. Zoccal KF, Sorgi CA, Hori JI, Paula-Silva FW, Arantes EC, Serezani CH, et al. Opposing roles of $LTB_4$ and $PGE_2$ in regulating the inflammasome-dependent scorpion venom-induced mortality. Nat Commun. 2016;7:10760. doi:10.1038/ncomms10760.
220. von Moltke J, Trinidad NJ, Moayeri M, Kintzer AF, Wang SB, van Rooijen N, et al. Rapid induction of inflammatory lipid mediators by the inflammasome *in vivo*. Nature. 2012;490(7418):107-11. doi:10.1038/nature11351.
221. Song Z, Bhattacharya S, Clemens RA, Dinauer MC. Molecular regulation of neutrophil swarming in health and disease: Lessons from the phagocyte oxidase. iScience. 2023;26(10):108034. doi:10.1016/j.isci.2023.108034.
222. Brown L, Yipp BG. Neutrophil swarming: Is a good offense the best defense? iScience. 2023;26(9):107655. doi:10.1016/j.isci.2023.107655.
223. Irimia D. Neutrophil swarms are more than the accumulation of cells. Microbiol Insights. 2020;13:1178636120978272. doi:10.1177/1178636120978272.
224. Golenkina EA, Galkina SI, Pletjushkina O, Chernyak B, Gaponova TV, Romanova YM, et al. Gram-Negative Bacteria Salmonella typhimurium Boost Leukotriene Synthesis Induced by Chemoattractant fMLP to Stimulate Neutrophil Swarming. Front Pharmacol. 2021;12:814113. doi:10.3389/fphar.2021.814113.

225. Kienle K, Glaser KM, Eickhoff S, Mihlan M, Knopper K, Reategui E, et al. Neutrophils self-limit swarming to contain bacterial growth *in vivo*. Science. 2021;372(6548). doi:10.1126/science.abe7729.
226. Kienle K, Lammermann T. Neutrophil swarming: an essential process of the neutrophil tissue response. Immunol Rev. 2016;273(1):76-93. doi:10.1111/imr.12458.
227. Lammermann T, Afonso PV, Angermann BR, Wang JM, Kastenmuller W, Parent CA, et al. Neutrophil swarms require $LTB_4$ and integrins at sites of cell death *in vivo*. Nature. 2013;498(7454):371-5. doi:10.1038/nature12175.
228. Poplimont H, Georgantzoglou A, Boulch M, Walker HA, Coombs C, Papaleonidopoulou F, et al. Neutrophil swarming in damaged tissue is orchestrated by connexins and cooperative calcium alarm signals. Curr Biol. 2020;30(14):2761-76 e7. doi:10.1016/j.cub.2020.05.030.
229. Isles HM, Loynes CA, Alasmari S, Kon FC, Henry KM, Kadochnikova A, et al. Pioneer neutrophils release chromatin within in vivo swarms. Elife. 2021;10. doi:10.7554/eLife.68755.
230. Reategui E, Jalali F, Khankhel AH, Wong E, Cho H, Lee J, et al. Microscale arrays for the profiling of start and stop signals coordinating human-neutrophil swarming. Nat Biomed Eng. 2017;1. doi:10.1038/s41551-017-0094.
231. Frith J. The history of plague – Part 1. The three great pandemics. J Mil Vet Health. 2012;20(2):11-6. doi:11.2021-22485863/JMVH.
232. Bertherat E. Plague around the world, 2010–2015. World Health Organ. 2016;8(91):89-104.
233. Eisen RJ, Dennis DT, Gage KL. The role of early-phase transmission in the spread of *Yersinia pestis*. J Med Entomol. 2015;52(6):1183-92. doi:10.1093/jme/tjv128.
234. Coburn B, Sekirov I, Finlay BB. Type III secretion systems and disease. Clin Microbiol Rev. 2007;20(4):535-49. doi:10.1128/CMR.00013-07.
235. Straley SC, Skrzypek E, Plano GV, Bliska JB. Yops of *Yersinia* spp. pathogenic for humans. Infection and Immunity. 1993;61(8). doi:10.1128/iai.61.8.3105-3110.1993.
236. Bosio CF, Jarrett CO, Gardner D, Hinnebusch BJ. Kinetics of innate immune response to *Yersinia pestis* after intradermal infection in a mouse model. Infect Immun. 2012;80(11):4034-45. doi:10.1128/IAI.00606-12.
237. Banerjee SK, Crane SD, Pechous RD. A dual role for the plasminogen activator protease during the preinflammatory phase of primary pneumonic plague. J Infect Dis. 2020;222(3):407-16. doi:10.1093/infdis/jiaa094.
238. Demeure C, Dussurget O, Fiol GM, Le Guern AS, Savin C, Pizarro-Cerda J. *Yersinia pestis* and plague: an updated view on evolution, virulence determinants, immune subversion, vaccination and diagnostics. Microbes Infect. 2019;20(5):357-70. doi:10.1038/s41435-019-0065-0.
239. Marketon MM, DePaolo RW, DeBord KL, Jabri B, Schneewind O. Plague bacteria target immune cells during infection. Science. 2005;309(5741):1739-41. doi:10.1126/science.1114580.
240. Olson RM, Dhariwala MO, Mitchell WJ, Anderson DM. *Yersinia pestis* exploits early activation of MyD88 for growth in the lungs during pneumonic plague. Infection and Immunity. 2019;87(4). doi:10.1128/IAI.00757-18.
241. Afonso PV, Janka-Junttila M, Lee YJ, McCann CP, Oliver CM, Aamer KA, et al. $LTB_4$ is a signal-relay molecule during neutrophil chemotaxis. Dev Cell. 2012;22(5):1079-91. doi:10.1016/j.devcel.2012.02.003.

242. Peters-Golden M, Henderson WR. Leukotrienes. The New England Journal of Medicine. 2007;357(18). doi:10.1056/NEJMra071371.
243. Gaudreau R, Le Gouill C, Metaoui S, Lemire S, Stankovaa J, Rola-Pleszczynski M. Signalling through the leukotriene $B_4$ receptor involves both $a_i$ and $a_{16}$, but not $a_q$ or $a_{11}$ G-protein subunits. Biochem Journal. 1998;355(Pt. 1):15-8. doi:10.1042/bj3350015.
244. Powell WS, Rokach J. Biochemistry, biology and chemistry of the 5-lipoxygenase product 5-oxo-ETE. Prog Lipid Res. 2005;44(2-3):154-83. doi:10.1016/j.plipres.2005.04.002.
245. Radmark O, Samuelsson B. 5-Lipoxygenase: Mechanisms of regulation. J Lipid Res. 2009;50 Suppl(Suppl):S40-5. doi:10.1194/jlr.R800062-JLR200.
246. Scher JU, Pillinger MH. The anti-inflammatory effects of prostaglandins. J Investig Med. 2009;57(6). doi:10.231/JIM.0b013e31819aaa76.
247. Schmid T, Brune B. Prostanoids and resolution of inflammation - Beyond the lipid-mediator class switch. Front Immunol. 2021;12:714042. doi:10.3389/fimmu.2021.714042.
248. Yokomizo T, Izumi T, Chang K, Takuwa Y, Shimizu T. A G-protein-coupled receptor for leukotriene B4 that mediates chemotaxis. Nature. 1997;387(6633):620-4. doi:10.1038/42506.
249. Chaplin DD. Overview of the immune response. J Allergy Clin Immunol. 2010;125(2 Suppl 2):S3-23. doi:10.1016/j.jaci.2009.12.980.
250. Secatto A, Soares EM, Locachevic GA, Assis PA, Paula-Silva FW, Serezani CH, et al. The leukotriene $B_4$/$BLT_1$ axis is a key determinant in susceptibility and resistance to histoplasmosis. PLoS One. 2014;9(1):e85083. doi:10.1371/journal.pone.0085083.
251. Sun Y, Connor MG, Pennington JM, Lawrenz MB. Development of bioluminescent bioreporters for *in vitro* and *in vivo* tracking of *Yersinia pestis*. PLoS ONE. 2012;7(10):e47123. doi:10.1371/journal.pone.0047123.
252. Haribabu B, Verghese MW, Steeber DA, Sellars DD, Bock CB, Snyderman R. Targeted disruption of the leukotriene $B_4$ receptor in mice reveals its role in inflammation and platelet-activating factor–induced anaphylaxis. J Exp Med. 2000;192(3). doi:10.1084/jem.192.3.433.
253. Auerbuch V, Golenbock DT, Isberg RR. Innate immune recognition of *Yersinia pseudotuberculosis* type III secretion. PLoS Pathog. 2009;5(12):e1000686. doi:10.1371/journal.ppat.1000686.
254. Chung LK, Bliska JB. *Yersinia* versus host immunity: how a pathogen evades or triggers a protective response. Curr Opin Microbiol. 2016;29:56-62. doi:10.1016/j.mib.2015.11.001.
255. Davis AJ, Mecsas J. Mutations in the Yersinia pseudotuberculosis type III secretion system needle protein, YscF, that specifically abrogate effector translocation into host cells. J Bacteriol. 2007;189(1):83-97. doi:10.1128/JB.01396-06.
256. Kwuan L, Adams W, Auerbuch V. Impact of host membrane pore formation by the Yersinia pseudotuberculosis type III secretion system on the macrophage innate immune response. Infect Immun. 2013;81(3):905-14. doi:10.1128/IAI.01014-12.
257. Sorgi CA, Rose S, Court N, Carlos D, Paula-Silva FW, Assis PA, et al. GM-CSF priming drives bone marrow-derived macrophages to a pro-inflammatory pattern and downmodulates $PGE_2$ in response to TLR2 ligands. PLoS ONE. 2012;7(7):e40523. doi:10.1371/journal.pone.0040523.
258. Lacey DC, Achuthan A, Fleetwood AJ, Dinh H, Roiniotis J, Scholz GM, et al. Defining GM-CSF- and macrophage-CSF-dependent macrophage responses by *in vitro* models. J Immunol. 2012;188(11):5752-65. doi:10.4049/jimmunol.1103426.

259. Serezani CH, Divangahi M, Peters-Golden M. Leukotrienes in innate immunity: still underappreciated after all these years? J Immunol. 2023;210(3):221-7. doi:10.4049/jimmunol.2200599.
260. Subramanian BC, Moissoglu K, Parent CA. The $LTB_4$-BLT1 axis regulates the polarized trafficking of chemoattractant GPCRs during neutrophil chemotaxis. J Cell Sci. 2018;131(18). doi:10.1242/jcs.217422.
261. Kwak DW, Park D, Kim JH. Leukotriene $B_4$ receptors are necessary for the stimulation of NLRP3 inflammasome and IL-1beta synthesis in neutrophil-dominant asthmatic airway inflammation. Biomedicines. 2021;9(5). doi:10.3390/biomedicines9050535.
262. McDonald PP, McColl SR, Braquet P, Borgeat P. Autocrine enhancement of leukotriene synthesis by endogenous leukotriene $B_4$ and platelet-activating factor in human neutrophils. Br J Pharmacol. 1994;111(3). doi:10.1111/j.1476-5381.1994.tb14816.x.
263. Chou RC, Kim ND, Sadik CD, Seung E, Lan Y, Byrne MH, et al. Lipid-cytokine-chemokine cascade drives neutrophil recruitment in a murine model of inflammatory arthritis. Immunity. 2010;33(2):266-78. doi:10.1016/j.immuni.2010.07.018.
264. Oh C, Li L, Verma A, Reuven AD, Miao EA, Bliska JB, et al. Neutrophil inflammasomes sense the subcellular delivery route of translocated bacterial effectors and toxins. Cell Rep. 2022;41(8):111688. doi:10.1016/j.celrep.2022.111688.
265. Chen KW, Demarco B, Ramos S, Heilig R, Goris M, Grayczyk JP, et al. RIPK1 activates distinct gasdermins in macrophages and neutrophils upon pathogen blockade of innate immune signaling. Proc Natl Acad Sci U S A. 2021;118(28). doi:10.1073/pnas.2101189118.
266. Yokomizo T, Izumi T, Shimizu T. Leukotriene $B_4$: metabolism and signal transduction. Arch Biochem Biophys. 2001;385(2):231-41. doi:10.1006/abbi.2000.2168.
267. Eruslanov EB, Singhal S, Albelda SM. Mouse versus human neutrophils in cancer: a major knowledge gap. Trends Cancer. 2017;3(2):149-60. doi:10.1016/j.trecan.2016.12.006.
268. Mestas J, Hughes CC. Of mice and not men: differences between mouse and human immunology. J Immunol. 2004;172(5):2731-8. doi:10.4049/jimmunol.172.5.2731.
269. Shay T, Jojic V, Zuk O, Rothamel K, Puyraimond-Zemmour D, Feng T, et al. Conservation and divergence in the transcriptional programs of the human and mouse immune systems. Proc Natl Acad Sci U S A. 2013;110(8):2946-51. doi:10.1073/pnas.1222738110.
270. Zheng Y, Sefik E, Astle J, Karatepe K, Oz HH, Solis AG, et al. Human neutrophil development and functionality are enabled in a humanized mouse model. Proc Natl Acad Sci U S A. 2022;119(43):e2121077119. doi:10.1073/pnas.2121077119.
271. Zschaler J, Schlorke D, Arnhold J. Differences in innate immune response between man and mouse. Crit Rev Immunol. 2014. doi:10.1615/CritRevImmunol.2014011600.
272. Maddipati KR. Non-inflammatory physiology of "inflammatory" mediators - *unalamation*, a new paradigm. Front Immunol. 2020;11:580117. doi:10.3389/fimmu.2020.580117.
273. Murakami Y, Akahoshi T, Hayashi I, Endo H, Hashimoto A, Kono S, et al. Inhibition of monosodium urate monohydrate crystal-induced acute inflammation by retrovirally transfected prostaglandin D synthase. Arthritis Rheum. 2003;48(10):2931-41. doi:10.1002/art.11271.
274. Storer PD, Xu J, Chavis JA, Drew PD. Cyclopentenone prostaglandins $PGA_2$ and 15-deoxy-$D^{12,14}$ $PGJ_2$ suppress activation of murine microglia and astrocytes: implications for multiple sclerosis. J Neurosci Res. 2005;80(1):66-74. doi:10.1002/jnr.20413.
275. Loynes CA, Lee JA, Robertson AL, Steel MJ, Ellett F, Feng Y, et al. $PGE_2$ production at sites of tissue injury promotes an anti-inflammatory neutrophil phenotype and determines the outcome of inflammation resolution *in vivo*. Science Advances. 2018;4(9):eaar8320. doi:10.1126/sciadv.aar8320.

276. Serezani CH, Chung J, Ballinger MN, Moore BB, Aronoff DM, Peters-Golden M. Prostaglandin $E_2$ suppresses bacterial killing in alveolar macrophages by inhibiting NADPH oxidase. Am J Respir Cell Mol Biol. 2007;37(5):562-70. doi:10.1165/rcmb.2007-0153OC.
277. Aronoff DM, Canetti C, Serezani CH, Luo M, Peters-Golden M. Cutting edge: macrophage inhibition by cyclic AMP (cAMP): differential roles of protein kinase A and exchange protein directly activated by cAMP-1. J Immunol. 2005;174(2):595-9. doi:10.4049/jimmunol.174.2.595.
278. Lee SP, Serezani CH, Medeiros AI, Ballinger MN, Peters-Golden M. Crosstalk between prostaglandin $E_2$ and leukotriene $B_4$ regulates phagocytosis in alveolar macrophages via combinatorial effects on cyclic AMP. J Immunol. 2009;182(1):530-7. doi:10.4049/jimmunol.182.1.530.
279. Luo M, Jones SM, Phare SM, Coffey MJ, Peters-Golden M, Brock TG. Protein kinase A inhibits leukotriene synthesis by phosphorylation of 5-lipoxygenase on serine 523. J Biol Chem. 2004;279(40):41512-20. doi:10.1074/jbc.M312568200.
280. Price SL, Vadyvaloo V, DeMarco JK, Brady A, Gray PA, Kehl-Fie TE, et al. Yersiniabactin contributes to overcoming zinc restriction during *Yersinia pestis* infection of mammalian and insect hosts. Proc Natl Acad Sci U S A. 2021;118(44). doi:10.1073/pnas.2104073118.
281. Gong S, Bearden SW, Geoffroy VA, Fetherston JD, Perry RD. Characterization of the *Yersinia pestis* Yfu ABC inorganic iron transport system. Infect Immun. 2001;69(5):2829-37. doi:10.1128/IAI.67.5.2829-2837.2001.
282. Fodah RA, Scott JB, Tam HH, Yan P, Pfeffer TL, Bundschuh R, et al. Correlation of Klebsiella pneumoniae comparative genetic analyses with virulence profiles in a murine respiratory disease model. PLoS One. 2014;9(9):e107394. doi:10.1371/journal.pone.0107394.
283. Lane MC, Alteri CJ, Smith SN, Mobley HL. Expression of flagella is coincident with uropathogenic *Escherichia coli* ascension to the upper urinary tract. Proc Natl Acad Sci U S A. 2007;104(42):16669-74. doi:10.1073/pnas.0607898104.
284. Calderin EP, Zheng J-J, Boyd NL, McNally L, Audam TN, Lorkiewicz P, et al. Exercise-induced specialized proresolving mediators stimulate AMPK phosphorylation to promote mitochondrial respiration in macrophages. Molecular Metabolism. 2022;66:101637. doi:10.1016/j.molmet.2022.101637.
285. Maddipati KR, Zhou SL. Stability and analysis of eicosanoids and docosanoids in tissue culture media. Prostaglandins Other Lipid Mediat. 2011;94(1-2):59-72. doi:10.1016/j.prostaglandins.2011.01.003.
286. Maddipati KR, Romero R, Chaiworapongsa T, Chaemsaithong P, Zhou SL, Xu Z, et al. Lipidomic analysis of patients with microbial invasion of the amniotic cavity reveals up-regulation of leukotriene B4. FASEB J. 2016;30(10):3296-307. doi:10.1096/fj.201600583R.
287. Maddipati KR, Romero R, Chaiworapongsa T, Chaemsaithong P, Zhou SL, Xu Z, et al. Clinical chorioamnionitis at term: the amniotic fluid fatty acyl lipidome. J Lipid Res. 2016;57(10):1906-16. doi:10.1194/jlr.P069096.
288. Haslett C, Guthrie LA, Kopaniak MM, Johnston Jr. RB, Henson PM. Modulation of multiple neutrophil functions by preparative methods or trace concentrations of bacterial lipopolysaccharide. Am J Pathol. 1985;119.
289. Werz O, Gerstmeier J, Libreros S, De la Rosa X, Werner M, Norris PC, et al. Human macrophages differentially produce specific resolvin or leukotriene signals that depend on bacterial pathogenicity. Nat Commun. 2018;9(1):59. doi:10.1038/s41467-017-02538-5.

290. Li Q, Anderson CD, Egilmez NK. Inhaled IL-10 suppresses lung tumorigenesis via abrogation of inflammatory macrophage-Th17 cell axis. J Immunol. 2018;201(9):2842-50. doi:10.4049/jimmunol.1800141.
291. Bodduluri SR, Mathis S, Maturu P, Krishnan E, Satpathy SR, Chilton PM, et al. Mast cell-dependent CD8$^{+}$ T-cell recruitment mediates immune surveillance of intestinal tumors in Apc$^{Min/+}$ mice. Cancer Immunol Res. 2018;6(3):332-47. doi:10.1158/2326-6066.CIR-17-0424.
292. Schindelin J, Arganda-Carreras I, Frise E, Kaynig V, Longair M, Pietzsch T, et al. Fiji: an open-source platform for biological-image analysis. Nat Methods. 2012;9(7):676-82. doi:10.1038/nmeth.2019.
293. Jin J, Wahlang B, Thapa M, Head KZ, Hardesty JE, Srivastava S, et al. Proteomics and metabolic phenotyping define principal roles for the aryl hydrocarbon receptor in mouse liver. Acta Pharm Sin B. 2021;11(12):3806-19. doi:10.1016/j.apsb.2021.10.014.
294. Srivastava S, Merchant M, Rai A, Rai SN. Standardizing proteomics workflow for liquid chromatography-mass spectrometry: Technical and statistical considerations. J Proteomics Bioinform. 2019;12(3):48-55. doi:10.35248/0974-276x.19.12.496.
295. Srivastava S, Merchant M, McClain CJ, Rai A, Chaturvedi KK, Angadi UB, et al. Advanced multivariable statistical analysis interactive tool for handling missing data and confounding covariates for label-free LC-MS proteomics experiments. Curr Bioinform. 2023;18(2). doi:10.2174/1574893618666230223150253.
296. Haeggstrom JZ. Leukotriene biosynthetic enzymes as therapeutic targets. J Clin Invest. 2018;128(7):2680-90. doi:10.1172/JCI97945.
297. Brady A, Sheneman KR, Pulsifer AR, Price SL, Garrison TM, Maddipati KR, et al. Type 3 secretion system induced leukotriene B4 synthesis by leukocytes is actively inhibited by Yersinia pestis to evade early immune recognition. PLoS Pathog. 2024;20(1):e1011280. doi:10.1371/journal.ppat.1011280.
298. Zauberman A, Cohen S, Mamroud E, Flashner Y, Tidhar A, Ber R, et al. Interaction of Yersinia pestis with macrophages: limitations in YopJ-dependent apoptosis. Infect Immun. 2006;74(6):3239-50. doi:10.1128/IAI.00097-06.
299. Zhang G, Lu J, Zheng J, Mei S, Li H, Zhang X, et al. Spi1 regulates the microglial/macrophage inflammatory response via the PI3K/AKT/mTOR signaling pathway after intracerebral hemorrhage. Neural Regen Res. 2024;19(1):161-70. doi:10.4103/1673-5374.375343.
300. Krebs J, Agellon LB, Michalak M. Ca(2+) homeostasis and endoplasmic reticulum (ER) stress: An integrated view of calcium signaling. Biochem Biophys Res Commun. 2015;460(1):114-21. doi:10.1016/j.bbrc.2015.02.004.
301. Prakriya M, Lewis RS. Store-Operated Calcium Channels. Physiol Rev. 2015;95(4):1383-436. doi:10.1152/physrev.00020.2014.
302. Putney JW, Tomita T. Phospholipase C signaling and calcium influx. Adv Biol Regul. 2012;52(1):152-64. doi:10.1016/j.advenzreg.2011.09.005.
303. Bill CA, Vines CM. Phospholipase C. Adv Exp Med Biol. 2020;1131:215-42. doi:10.1007/978-3-030-12457-1_9.
304. Heemskerk JWM, Farndale RW, Sage SO. Effects of U73122 and U73343 on human platelet calcium signalling and protein tyrosine phosphorylation. Biochimica et Biophysica Acta. 1997;1355:81-8.
305. Hollywood MA, Sergeant GP, Thornbury KD, McHale NG. The PI-PLC inhibitor U-73122 is a potent inhibitor of the SERCA pump in smooth muscle. Br J Pharmacol. 2010;160(6):1293-4. doi:10.1111/j.1476-5381.2010.00795.x.

306. Macmillan D, McCarron JG. The phospholipase C inhibitor U-73122 inhibits Ca(2+) release from the intracellular sarcoplasmic reticulum Ca(2+) store by inhibiting Ca(2+) pumps in smooth muscle. Br J Pharmacol. 2010;160(6):1295-301. doi:10.1111/j.1476-5381.2010.00771.x.
307. Reed PW, Lardy HA. A23187: a divalent cation ionophore. J Biol Chem. 1972;247(21):6970-7.
308. Clemens RA, Lowell CA. Store-operated calcium signaling in neutrophils. J Leukoc Biol. 2015;98(4):497-502. doi:10.1189/jlb.2MR1114-573R.
309. Catacuzzeno L, Fioretti B, Franciolini F. Expression and Role of the Intermediate-Conductance Calcium-Activated Potassium Channel KCa3.1 in Glioblastoma. J Signal Transduct. 2012;2012:421564. doi:10.1155/2012/421564.
310. Staal RGW, Weinstein JR, Nattini M, Cajina M, Chandresana G, Moller T. Senicapoc: Repurposing a Drug to Target Microglia K(Ca)3.1 in Stroke. Neurochem Res. 2017;42(9):2639-45. doi:10.1007/s11064-017-2223-y.
311. Zhu YR, Jiang XX, Zhang DM. Critical regulation of atherosclerosis by the KCa3.1 channel and the retargeting of this therapeutic target in in-stent neoatherosclerosis. J Mol Med (Berl). 2019;97(9):1219-29. doi:10.1007/s00109-019-01814-9.
312. El Kebir D, Jozsef L, Khreiss T, Filep JG. Inhibition of K+ efflux prevents mitochondrial dysfunction, and suppresses caspase-3-, apoptosis-inducing factor-, and endonuclease G-mediated constitutive apoptosis in human neutrophils. Cell Signal. 2006;18(12):2302-13. doi:10.1016/j.cellsig.2006.05.013.
313. Munoz-Planillo R, Kuffa P, Martinez-Colon G, Smith BL, Rajendiran TM, Nunez G. K(+) efflux is the common trigger of NLRP3 inflammasome activation by bacterial toxins and particulate matter. Immunity. 2013;38(6):1142-53. doi:10.1016/j.immuni.2013.05.016.
314. Ruhl S, Broz P. Caspase-11 activates a canonical NLRP3 inflammasome by promoting K(+) efflux. Eur J Immunol. 2015;45(10):2927-36. doi:10.1002/eji.201545772.
315. Yaron JR, Gangaraju S, Rao MY, Kong X, Zhang L, Su F, et al. K(+) regulates Ca(2+) to drive inflammasome signaling: dynamic visualization of ion flux in live cells. Cell Death Dis. 2015;6(10):e1954. doi:10.1038/cddis.2015.277.
316. Roos J, DiGregorio PJ, Yeromin AV, Ohlsen K, Lioudyno M, Zhang S, et al. STIM1, an essential and conserved component of store-operated Ca2+ channel function. J Cell Biol. 2005;169(3):435-45. doi:10.1083/jcb.200502019.
317. You HJ, Woo CH, Choi E, Cho S, Yoo YH, Kim J. Roles of Rac and p38 kinase in the activation of cytosolic phospholipase $A_2$ in response to PMA. Biochemistry Journal. 2005;388:567-35.
318. Kramer RM, Roberts EF, Um SL, Borsch-Haubold AG, Watson SP, Fisher MH, et al. p38 Mitogen-activated Protein Kinase Phosphorylates Cytosolic Phospholipase A2 (cPLA2) in Thrombin-stimulated Platelets. The Journal of Biological Chemistry. 1996;271(44):27723-9.
319. Oliver Werz JK, Bengt Samuelsson, and Olof Rådmark. 5-Lipoxygenase is phosphorylated by p38 kinase-dependent MAPKAP kinases. PNAS. 2000;97(10):5261-6. doi:10.1073/pnas.050588997.
320. Rukoyatkina N, Mindukshev I, Walter U, Gambaryan S. Dual role of the p38 MAPK/cPLA2 pathway in the regulation of platelet apoptosis induced by ABT-737 and strong platelet agonists. Cell Death Dis. 2013;4(11):e931. doi:10.1038/cddis.2013.459.
321. Waterman WH, Molski TFP, Huang CK, Adams JL, Sha'afi RI. Tumour necrosis factor-α-induced phosphorylation and activation of cytosolic phospholipase A2 are abrogated by

an inhibitor of the p38 mitogen-activated protein kinase cascade in human neutrophils. Biochemistry Journal. 1996;319:17-20.

322. Ford-Hutchinson AW. Leukotriene B4 and neutrophil function: a review. Journal ofthe Royal Society of Medicine. 1981;74:831-3.

323. Baumann D, Drebant J, Hagele T, Burger L, Serger C, Lauenstein C, et al. p38 MAPK signaling in M1 macrophages results in selective elimination of M2 macrophages by MEK inhibition. J Immunother Cancer. 2021;9(7). doi:10.1136/jitc-2020-002319.

324. Chen W, Wang Y, Zhou Y, Xu Y, Bo X, Wu J. M1 Macrophages Increase Endothelial Permeability and Enhance p38 Phosphorylation via PPAR-gamma/CXCL13-CXCR5 in Sepsis. Int Arch Allergy Immunol. 2022;183(9):997-1006. doi:10.1159/000524272.

325. Traves PG, de Atauri P, Marin S, Pimentel-Santillana M, Rodriguez-Prados JC, Marin de Mas I, et al. Relevance of the MEK/ERK signaling pathway in the metabolism of activated macrophages: a metabolomic approach. J Immunol. 2012;188(3):1402-10. doi:10.4049/jimmunol.1101781.

326. Zhou Y, Takano T, Li X, Wang Y, Wang R, Zhu Z, et al. beta-elemene regulates M1-M2 macrophage balance through the ERK/JNK/P38 MAPK signaling pathway. Commun Biol. 2022;5(1):519. doi:10.1038/s42003-022-03369-x.

327. Waterman SR, Holden DW. Functions and effectors of the Salmonella pathogenicity island 2 type III secretion system. Cell Microbiol. 2003;5(8):501-11. doi:10.1046/j.1462-5822.2003.00294.x.

328. van der Velden AWM, Lindgren SW, Worley MJ, Heffron F. *Salmonella* pathogenicity island 1-independent induction of apoptosis in infected macrophages by *Salmonella enterica* Serotype Typhimurium. Infection and Immunity. 2000;68(10):5702-9. doi:10.1128/iai.68.10.5702-5709.2000.

329. Wang M, Qazi IH, Wang L, Zhou G, Han H. Salmonella Virulence and Immune Escape. Microorganisms. 2020;8(3). doi:10.3390/microorganisms8030407.

330. Marenne MN, Journet L, Mota LJ, Cornelis GR. Genetic analysis of the formation of the Ysc-Yop translocation pore in macrophages by Yersinia enterocolitica: role of LcrV, YscF and YopN. Microb Pathog. 2003;35(6):243-58. doi:10.1016/s0882-4010(03)00154-2.

331. Levillayer L, Cassonnet P, Declercq M, Santos MD, Lebreton L, Danezi K, et al. SKAP2 Modular Organization Differently Recognizes SRC Kinases Depending on Their Activation Status and Localization. Mol Cell Proteomics. 2023;22(1):100451. doi:10.1016/j.mcpro.2022.100451.

332. Malik HS, Bliska JB. The pyrin inflammasome and the *Yersinia* effector interaction. Immunol Rev. 2020;297(1):96-107. doi:10.1111/imr.12907.

333. Geddes K, Worley M, Niemann G, Heffron F. Identification of new secreted effectors in Salmonella enterica serovar Typhimurium. Infect Immun. 2005;73(10):6260-71. doi:10.1128/IAI.73.10.6260-6271.2005.

334. Pechous RD, Broberg CA, Stasulli NM, Miller VL, Goldman WE. In vivo transcriptional profiling of *Yersinia pestis* reveals a novel bacterial mediator of pulmonary inflammation. mBio. 2015;6(1):e02302-14. doi:10.1128/mBio.02302-14.

335. Glennon EK, Wei L, Roobsoong W, Primavera VI, Tongogara T, Yee CB, et al. Host kinase regulation of Plasmodium vivax dormant and replicating liver stages. bioRxiv. 2023. doi:10.1101/2023.11.13.566868.

336. Grabiec A, Meng G, Fichte S, Bessler W, Wagner H, Kirschning CJ. Human but not murine toll-like receptor 2 discriminates between tri-palmitoylated and tri-lauroylated peptides. J Biol Chem. 2004;279(46):48004-12. doi:10.1074/jbc.M405311200.

337. Hajjar AM, Ernst RK, Tsai JH, Wilson CB, Miller SI. Human Toll-like receptor 4 recognizes host-specific LPS modifications. Nat Immunol. 2002;3(4):354-9. doi:10.1038/ni777.
338. Renna SA, Michael JV, Kong X, Ma L, Ma P, Nieman MT, et al. Human and mouse PAR4 are functionally distinct receptors: Studies in novel humanized mice. J Thromb Haemost. 2022;20(5):1236-47. doi:10.1111/jth.15669.
339. Sah R, Reda A, Mehta R, Mohapatra RK, Dhama K. A situation analysis of the current plague outbreak in the Demographic Republic of Congo and counteracting strategies - Correspondence. Int J Surg. 2022;105:106885. doi:10.1016/j.ijsu.2022.106885.
340. Nguyen VK, Parra-Rojas C, Hernandez-Vargas EA. The 2017 plague outbreak in Madagascar: Data descriptions and epidemic modelling. Epidemics. 2018;25:20-5. doi:10.1016/j.epidem.2018.05.001.
341. Carlson CJ, Bevins SN, Schmid BV. Plague risk in the western United States over seven decades of environmental change. Global Change Biol. 2022;28(3):753-69. doi:10.1111/gcb.15966.
342. Benavides-Montaño JA, Vadyvaloo V. *Yersinia pestis* resists predation by *Acanthamoeba castellanii* and exhibits prolonged intracellular survival. Appl Environ Microbiol. 2017;83(13). doi:10.1128/AEM.00593-17.
343. Guidance on the inactivation or removal of select agents and toxins for future use. 2018. Available from: https://www.selectagents.gov/compliance/guidance/inactivation/docs/Inactivation_Guidance.pdf
344. Olsen SC, Boggiatto P, Vrentas C. Inactivation of virulent *Brucella* species in culture and animal samples. Appl Biosaf. 2017;22(4):145-51. doi:10.1177/1535676017734202.
345. Darnell ME, Subbarao K, Feinstone SM, Taylor DR. Inactivation of the coronavirus that induces severe acute respiratory syndrome, SARS-CoV. J Virol Methods. 2004;121(1):85-91. doi:10.1016/j.jviromet.2004.06.006.
346. McDonnell GaR, A. David. Antiseptics and disinfectants: activity, action, and resistance. Clin Microbiol Rev. 1999;12(1):147-79. doi:10.1128/cmr.12.1.147.
347. Heipieper HJ, Neumann G, Cornelissen S, Meinhardt F. Solvent-tolerant bacteria for biotransformations in two-phase fermentation systems. Appl Microbiol Biotechnol. 2007;74(5):961-73. doi:10.1007/s00253-006-0833-4.
348. Kabelitz N, Santos PM, Heipieper HJ. Effect of aliphatic alcohols on growth and degree of saturation of membrane lipids in *Acinetobacter calcoaceticus*. FEMS Microbiol Lett. 2003;220(2):223-7. doi:10.1016/s0378-1097(03)00103-4.
349. Weber FJ, de Bont JAM. Adaptation mechanisms of microorganisms to the toxic effects of organic solvents on membranes. Biochim Biophys Acta - Biomembranes. 1996;1286(3). doi:10.1016/S0304-4157(96)00010-X.
350. Calfee MW, Wendling M. Inactivation of vegetative bacterial threat agents on environmental surfaces. Sci Total Environ. 2013;443:387-96. doi:10.1016/j.scitotenv.2012.11.002.
351. Hilgren J, Swanson KMJ, Diez-Gonzalez F, Cords B. Inactivation of *Yersinia pseudotuberculosis,* as a Surrogate for *Yersinia pestis*, by Liquid Biocides in the Presence of Food Residue. J Food Prot. 2009;72(2):392-8. doi:10.4315/0362-028x-72.2.392.
352. Falaise C, Bouvattier C, Larigauderie G, Lafontaine V, Berchebru L, Marangon A, et al. Hydrogen Peroxide Vapor Decontamination of Hazard Group 3 Bacteria and Viruses in a Biosafety Level 3 Laboratory. Appl Biosaf. 2022;27(1):15-22. doi:10.1089/apb.2021.0022.
353. John J. Lowe SGG, Peter C. Iwen,Philip W. Smith &Angela L. Hewlett. Decontamination of a Hospital Room Using Gaseous Chlorine Dioxide: *Bacillus anthracis*, *Francisella tularensis*,

and *Yersinia pestis*. Journal of Occupational and Environmental Hygiene. 2013;10(10):533-9. doi:10.1080/15459624.2013.818241.

354. Pottage T, Lewis S, Lansley A, Fraser S, Hendon-Dunn C, Bacon J, et al. Hazard Group 3 agent decontamination using hydrogen peroxide vapour in a class III microbiological safety cabinet. J Appl Microbiol. 2020;128(1):116-23. doi:10.1111/jam.14461.

355. Rogers JV, Richter WR, Shaw MQ, Choi YW. Vapour-phase hydrogen peroxide inactivates *Yersinia pestis* dried on polymers, steel, and glass surfaces. Lett Appl Microbiol. 2008;47(4):279-85. doi:10.1111/j.1472-765x.2008.02421.x.

356. Shams AM, O'Connell H, Arduino MJ, Rose LJ. Chlorine dioxide inactivation of bacterial threat agents. Lett Appl Microbiol. 2011;53(2):225-30. doi:10.1111/j.1472-765X.2011.03095.x.

357. Paoli GC, Sommers CH, Scullen OJ, Wijey C. Inactivation of avirulent pgm(+) and Deltapgm Yersinia pestis by ultraviolet light (UV-C). Food Microbiol. 2014;44:168-72. doi:10.1016/j.fm.2014.06.002.

358. Sommers CH, Cooke PH. Inactivation of Avirulent *Yersinia pestis* in Butterfield's Phosphate Buffer and Frankfurters by UVC (254 nm) and Gamma Radiation. J Food Prot. 2009;72(4):755-9. doi:10.4315/0362-028x-72.4.755.

359. Sommers CH, Niemira BA. Inactivation of avirulent *Yersinia pestis* in beef bologna by gamma irradiation. J Food Prot. 2011;74(4):627-30. doi:10.4315/0362-028X.JFP-10-421.

360. Sommers CH, Sheen S. Inactivation of avirulent *Yersinia pestis* on food and food contact surfaces by ultraviolet light and freezing. Food Microbiol. 2015;50:1-4. doi:10.1016/j.fm.2015.02.008.

361. Wang C, Stanciu CE, Ehrhardt CJ, Yadavalli VK. Evaluation of whole cell fixation methods for the analysis of nanoscale surface features of Yersinia pestis KIM. J Microsc. 2016;263(3):260-7. doi:10.1111/jmi.12387.

362. Ye Z, Koutchma T, Parisi B, Larkin J, Forney LJ. Ultraviolet inactivation kinetics of Escherichia coli and Yersinia pseudotuberculosis in annular reactors. J Food Sci. 2007;72(5):E271-8. doi:10.1111/j.1750-3841.2007.00397.x.

363. Chua J, Bozue JA, Klimko CP, Shoe JL, Ruiz SI, Jensen CL, et al. Formaldehyde and glutaraldehyde inactivation of bacterial tier 1 select agents in tissues. Emerg Infect Dis. 2019;25(5):919-26. doi:10.3201/eid2505.180928.

364. Couderc C, Nappez C, Drancourt M. Comparing inactivation protocols of Yersinia organisms for identification with matrix-assisted laser desorption/ionization time-of-flight mass spectrometry. Rapid Commun Mass Spectrom. 2012;26(6):710-4. doi:10.1002/rcm.6152.

365. Lin A, Merkley ED, Clowers BH, Hutchison JR, Kreuzer HW. Effects of bacterial inactivation methods on downstream proteomic analysis. J Microbiol Methods. 2015;112:3-10. doi:10.1016/j.mimet.2015.01.015.

366. Torosian SD, Regan PM, Doran T, Taylor MA, Margolin A. A refrigeration temperature of 4 degrees C does not prevent static growth of Yersinia pestis in heart infusion broth. Can J Microbiol. 2009;55(9):1119-24. doi:10.1139/w09-060.

367. Cebrian G, Condon S, Manas P. Physiology of the inactivation of vegetative bacteria by thermal treatments: mode of action, influence of environmental factors and inactivation kinetics. Foods. 2017;6(12). doi:10.3390/foods6120107.

368. Laskowska E, Bohdanowicz J, Kuczynska-Wisnik D, Matuszewska E, Kedzierska S, Taylor A. Aggregation of heat-shock-denatured, endogenous proteins and distribution of the IbpA/B and Fda marker-proteins in *Escherichia coli* WT and *grpE*280 cells. Microbiology. 2004;150(Pt 1):247-59. doi:10.1099/mic.0.26470-0.

369. Mohácsi-Farkas C, Farkas J, Mészáros L, Reichart O, Andrássy É. Thermal denaturation of bacterial cells examined by differential scanning calorimetry. J Therm Anal Calorim. 1999;57(2):409-14. doi:10.1023/a:1010139204401.
370. Pollice AA, McCoy J, J. Philip , Shackney SE, Smith CA, Agarwal J, Burholt DR, et al. Sequential paraformaldehyde and methanol fixation for simultaneous flow cytometric analysis of DNA, cell surface proteins, and intracellular proteins. Cytometry. 1992;13(4). doi:10.1002/cyto.990130414.
371. Born F, Braun P, Scholz HC, Grass G. Specific detection of *Yersinia pestis* Based on receptor binding proteins of phages. Pathogens. 2020;9(8). doi:10.3390/pathogens9080611.
372. Foster B, Prussin C, Liu F, Whitmire JK, Whitton JL. Detection of intracellular cytokines by flow cytometry. Curr Protoc Immunol. 2007;Chapter 6(Chapter: Unit 624):Unit 6.24. doi:10.1002/0471142735.im0624s78.
373. Krutzik PO, Nolan GP. Intracellular phospho-protein staining techniques for flow cytometry: monitoring single cell signaling events. Cytometry Part A. 2003;55(2):61-70. doi:10.1002/cyto.a.10072.
374. Taddese R, Belzer C, Aalvink S, de Jonge MI, Nagtegaal ID, Dutilh BE, et al. Production of inactivated gram-positive and gram-negative species with preserved cellular morphology and integrity. J Microbiol Methods. 2021;184:106208. doi:10.1016/j.mimet.2021.106208.
375. Buesa RJ, Peshkov MV. How much formalin is enough to fix tissues? Ann Diagn Pathol. 2012;16(3):202-9. doi:10.1016/j.anndiagpath.2011.12.003.
376. Burnum-Johnson KE, Kyle JE, Eisfeld AJ, Casey CP, Stratton KG, Gonzalez JF, et al. MPLEx: a method for simultaneous pathogen inactivation and extraction of samples for multi-omics profiling. Analyst. 2017;142(3):442-8. doi:10.1039/c6an02486f.
377. Satomi Y, Hirayama M, Kobayashi H. One-step lipid extraction for plasma lipidomics analysis by liquid chromatography mass spectrometry. J Chromatogr B. 2017;1063:93-100. doi:10.1016/j.jchromb.2017.08.020.
378. Zhao Z, Xu Y. An extremely simple method for extraction of lysophospholipids and phospholipids from blood samples. J Lipid Res. 2010;51(3):652-9. doi:10.1194/jlr.D001503.
379. Patterson EI, Prince T, Anderson ER, Casas-Sanchez A, Smith SL, Cansado-Utrilla C, et al. Methods of inactivation of SARS-CoV-2 for downstream biological Assays. J Infect Dis. 2020;222(9):1462-7. doi:10.1093/infdis/jiaa507.
380. Metherel AH, Hogg RC, Buzikievich LM, Stark KD. Butylated hydroxytoluene can protect polyunsaturated fatty acids in dried blood spots from degradation for up to 8 weeks at room temperature. Lipids Health Dis. 2013;12(22). doi:10.1186/1476-511X-12-22.
381. Tranchida F, Shintu L, Rakotoniaina Z, Tchiakpe L, Deyris V, Hiol A, et al. Metabolomic and lipidomic analysis of serum samples following *Curcuma longa* extract supplementation in high-fructose and saturated fat fed rats. PLoS ONE. 2015;10(8):e0135948. doi:10.1371/journal.pone.0135948.
382. Center for Disease Control Select agents and toxins exclusions: excluded attenuated strains of HHS select agents. Atlanta, GA; 2023. Available from: https://www.selectagents.gov/sat/exclusions/hhs.htm#print [12/02/23].

# APPENDICES

Chapter 2 and Chapter 5 have both been previously published. Chapter 2 was published in PLoS pathogens, which applies the Creative Commons Attribution 4.0 International (CC BY) license, “allow(ing) free and unrestricted use” of published works. Chapter 5 was published in Applied Biosafety, which gives permission to publish under the exemption of dissertations.

**Eicosanoid synthesis pathways**

A

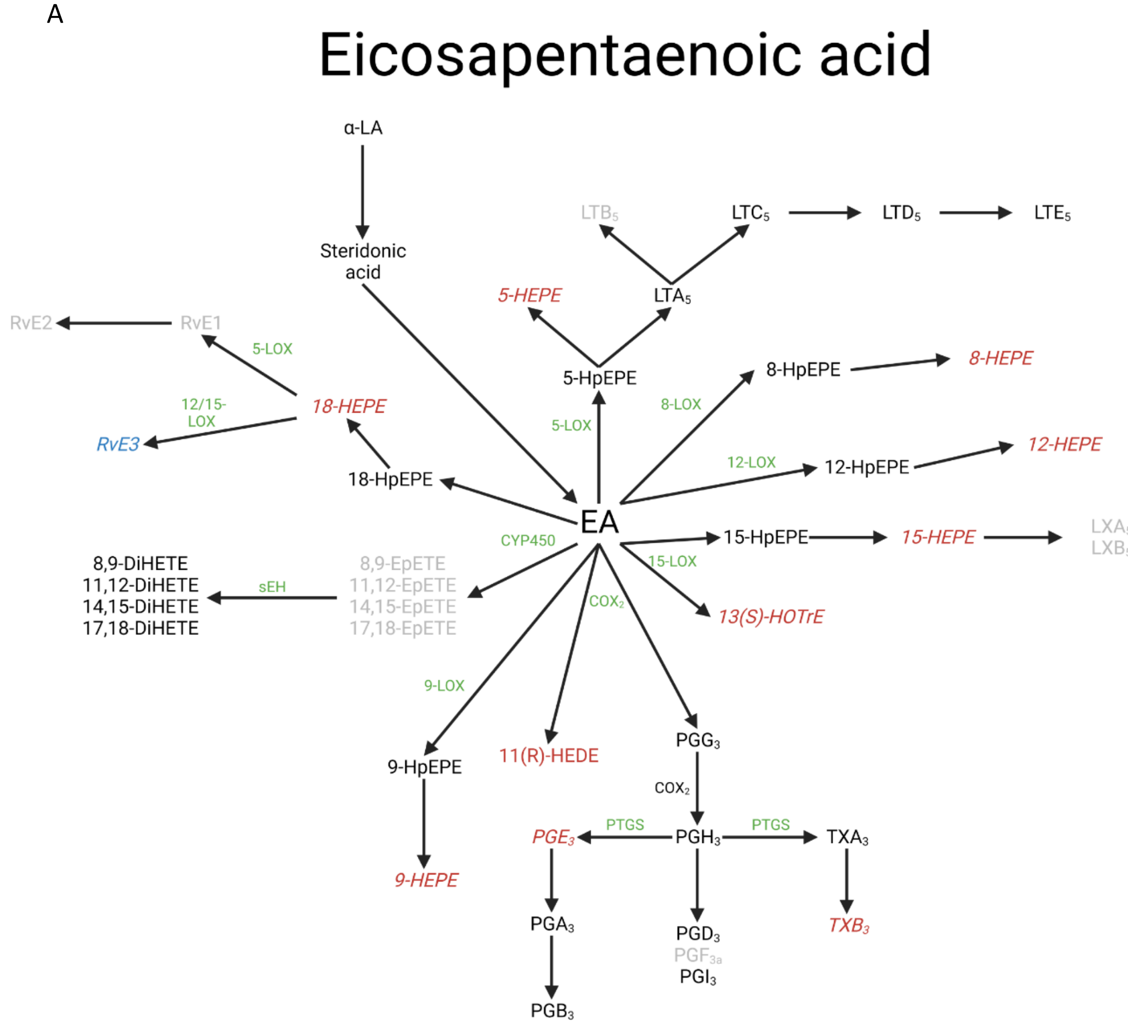

B

# Docosahexaenoic acid

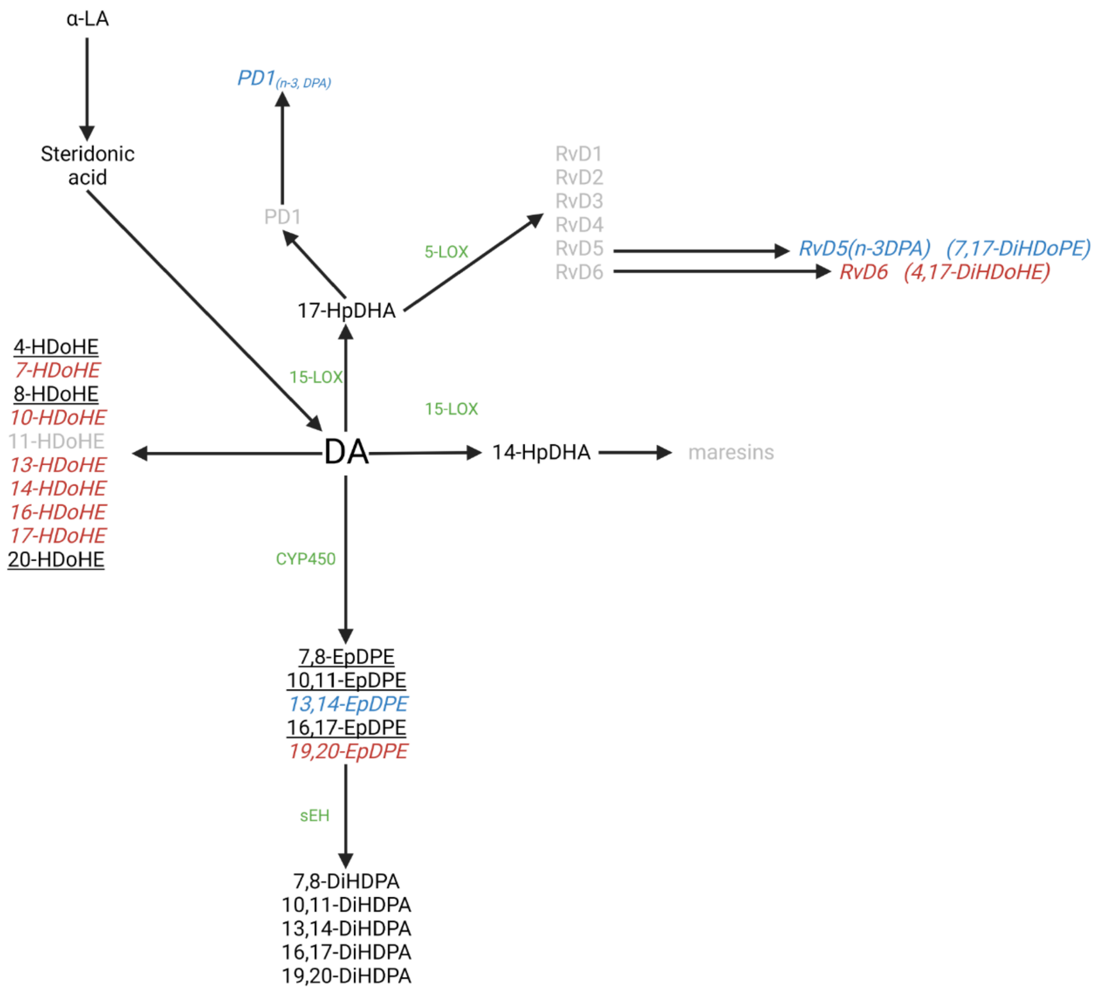

C

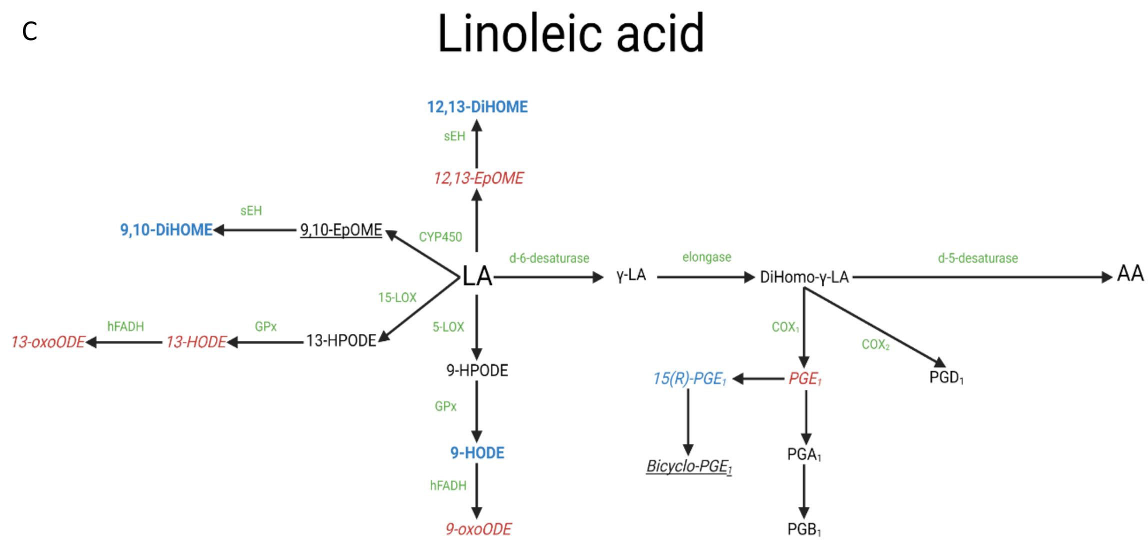
Linoleic acid
12,13-DiHOME
sEH
12,13-EpOME
sEH
9,10-DiHOME
9,10-EpOME
CYP450
LA
d-6-desaturase
γ-LA
elongase
DiHomo-γ-LA
d-5-desaturase
AA
15-LOX
5-LOX
hFADH
GPx
13-oxoODE
13-HODE
13-HPODE
9-HPODE
GPx
9-HODE
hFADH
9-oxoODE
COX1
COX2
15(R)-PGE1
PGE1
PGD1
PGA1
Bicyclo-PGE1
PGB1

D

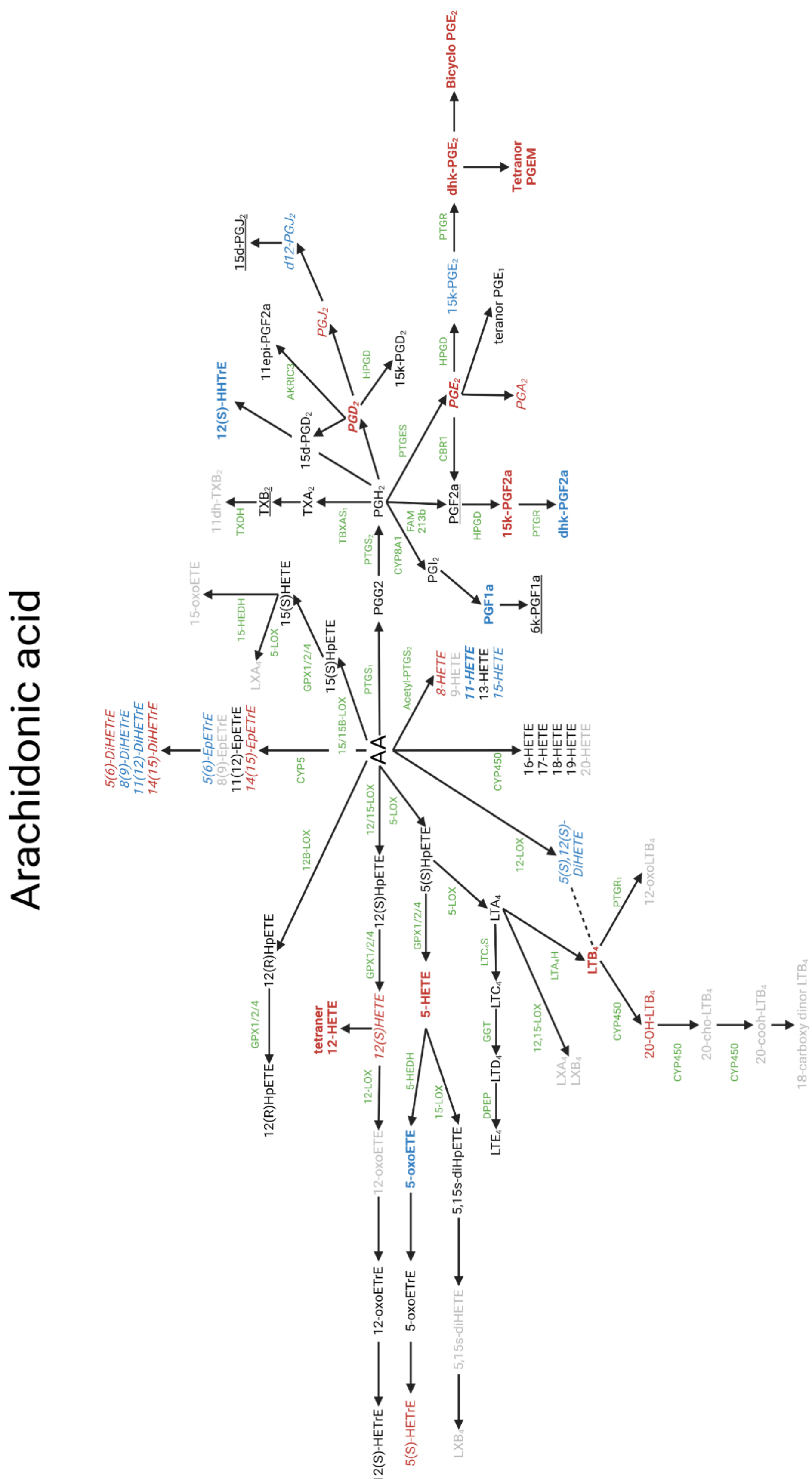

Arachidonic acid
AA
CYP5
5(6)-EpETrE
8(9)-EpETrE
11(12)-EpETrE
14(15)-EpETrE
5(6)-DiHETrE
8(9)-DiHETrE
11(12)-DiHETrE
14(15)-DiHETrE
15/15B-LOX
15(S)HpETE
GPX1/2/4
15(S)HETE
15-HEDH
15-oxoETE
5-LOX
LXA4
PTGS1
PGG2
PTGS2
PGH2
TBXAS1
TXA2
TXB2
TXDH
11dh-TXB2
15d-PGD2
12(S)-HHTrE
PGD2
AKRIC3
11epi-PGF2a
HPGD
15k-PGD2
PGJ2
d12-PGJ2
15d-PGJ2
PTGES
PGE2
CBR1
PGA2
teranor PGE1
HPGD
15k-PGE2
PTGR
dhk-PGE2
Bicyclo PGE2
Tetranor PGEM
FAM 213b
PGF2a
15k-PGF2a
dhk-PGF2a
CYP8A1
PGI2
PGF1a
6k-PGF1a
Acetyl-PTGS2
8-HETE
9-HETE
11-HETE
13-HETE
15-HETE
CYP450
16-HETE
17-HETE
18-HETE
19-HETE
20-HETE
12-LOX
5(S),12(S)-DiHETE
12B-LOX
12(R)HpETE
12(R)HpETE
12/15-LOX
12(S)HpETE
12(S)HETE
tetraner 12-HETE
12-oxoETE
12-oxoETrE
12(S)-HETrE
5(S)HpETE
5-HETE
5-HEDH
5-oxoETE
5-oxoETrE
5(S)-HETrE
15-LOX
5,15s-diHpETE
5,15s-diHETE
LXB4
LTA4
LTC4S
LTC4
GGT
LTD4
DPEP
LTE4
12,15-LOX
LXA4
LXB4
LTA4H
LTB4
PTGR1
12-oxoLTB4
20-OH-LTB4
20-cho-LTB4
20-cooh-LTB4
18-carboxy dinor LTB4

Synthesis pathways of eicosanoids

(A) Eicosapentaenoic acid, (B) docosahexaenoic acid, (C) linoleic acid, and (D) arachidonic acid pathways and the products measured in LC-MS. Black – Not screened; Red – significant increase compared to uninfected in at least one time point; Blue – significant decrease compared to uninfected in at least one time point; Grey – below the limit of detection; Green – enzyme responsible for lipid conversion (no enzyme indicates a non-enzymatic conversion via redox); Underlined – no change; Dotted line – epimers. Of the significant hits: Bold-pro-inflammatory; Italicized- anti-inflammatory/pro-resolving.

## *K. pneumoniae* lipidomic data

| | | UI | | | | | Kp | | | | |
|---|---|---|---|---|---|---|---|---|---|---|---|
| | | 48 hr | | | | | 6 hr | | | | |
| | Lipid | 1-A | 1-B | 1-C | 1-D | 1-E | 2-A | 2-B | 2-C | 2-D | 2-E |
| LA | 13,14dh-15k-PGE1 | 0.0182 | 0.0099 | 0.0176 | 0.0015 | 0.017 | 0.0015 | 0.0235 | 0.0015 | 0.0138 | 0.0201 |
| LA | **PGE1** | 0.1287 | 0.2363 | 0.1247 | 0.1645 | 0.1673 | 0.1855 | 0.1824 | 0.1336 | 0.1099 | 0.2118 |
| LA | 15(R)-PGE1 | 0.0959 | 0.1149 | 0.0778 | 0.0793 | 0.0015 | 0.0801 | 0.0015 | 0.0015 | 0.0015 | 0.0995 |
| LA | **15-keto PGE1** | 0.0015 | 0.0015 | 0.0015 | 0.0015 | 0.0015 | 0.0015 | 0.0132 | 0.0015 | 0.0052 | 0.0083 |
| LA | **Bicyclo PGE1** | 3.2853 | 5.6863 | 4.1312 | 3.156 | 4.1412 | 4.425 | 3.8544 | 3.6572 | 2.829 | 8.5985 |
| LA | 6kPGF1a | 3.6156 | 6.157 | 5.2604 | 5.9817 | 6.4715 | 4.9861 | 6.8791 | 4.9268 | 3.1575 | 3.7138 |
| LA | 6-keto PGE1 | 0.0015 | 0.0172 | 0.0149 | 0.0154 | 0.0136 | 0.0015 | 0.0154 | 0.0015 | 0.0106 | 0.0015 |
| AA | **PGE2** | 10.9409 | 12.1142 | 10.5898 | 10.3617 | 10.0851 | 11.3479 | 10.9362 | 8.663 | 7.983 | 11.9897 |
| AA | 15-keto PGE2 | 0.2065 | 0.4942 | 0.406 | 0.4265 | 0.3602 | 0.4194 | 0.5792 | 0.19 | 0.2313 | 0.5295 |
| AA | **13,14dh-15k-PGE2** | 0.4777 | 0.5916 | 0.5485 | 0.5033 | 0.411 | 0.5183 | 0.6096 | 0.3631 | 0.3668 | 0.6311 |
| AA | **Bicyclo PGE2** | 0.0401 | 0.0476 | 0.0262 | 0.0309 | 0.0386 | 0.0465 | 0.0292 | 0.01 | 0.0404 | 0.0445 |
| AA | **PGA2** | 0.354 | 0.3827 | 0.3073 | 0.2715 | 0.3636 | 0.3527 | 0.3616 | 0.228 | 0.3018 | 0.4269 |
| AA | tetranor PGEM | 0.0022 | 0.0015 | 0.0018 | 0.0015 | 0.0011 | 0.0024 | 0.004 | 0.0043 | 0.0024 | 0.002 |
| AA | PGD2 | 0.0015 | 0.0015 | 0.0015 | 0.0015 | 0.0015 | 0.0015 | 0.0015 | 0.0015 | 0.0015 | 0.0015 |
| AA | **PGJ2** | 0.1498 | 0.1779 | 0.1303 | 0.131 | 0.1644 | 0.1706 | 0.1773 | 0.1077 | 0.1512 | 0.1931 |
| AA | 15d-D12,14-PGJ2 | 0.0519 | 0.0727 | 0.0757 | 0.0773 | 0.0691 | 0.1028 | 0.0995 | 0.1094 | 0.0441 | 0.064 |
| AA | **13,14dh-15k-PGD2** | 1.696 | 1.5422 | 1.2874 | 1.2029 | 1.1678 | 1.1241 | 1.3755 | 1.3618 | 0.9286 | 1.2303 |
| AA | PGF1a | 0.036 | 0.0483 | 0.0286 | 0.017 | 0.0389 | 0.028 | 0.038 | 0.0199 | 0.038 | 0.0355 |
| AA | PGF2a | 1.3802 | 1.3584 | 1.2208 | 0.6895 | 1.2415 | 0.6102 | 1.368 | 0.5236 | 1.027 | 1.4609 |
| AA | **15-keto PGF2a** | 0.5871 | 0.6055 | 0.5364 | 0.5491 | 0.4648 | 0.5906 | 0.6056 | 0.4169 | 0.4099 | 0.6216 |
| AA | **13,14dh-15k-PGF2a** | 0.0547 | 0.0785 | 0.0912 | 0.0525 | 0.081 | 0.0967 | 0.0997 | 0.1235 | 0.0472 | 0.0789 |
| AA | **19(R)-OH PGF2a & 20-OH PGF2a** | 0.0015 | 0.0015 | 0.0015 | 0.0015 | 0.0015 | 0.0015 | 0.0015 | 0.0015 | 0.0015 | 0.0015 |
| AA | 8-isoPGF2a & 11bPGF2a | 0.0015 | 0.1033 | 0.0638 | 0.0015 | 0.097 | 0.1046 | 0.114 | 0.0896 | 0.0015 | 0.0015 |
| AA | TXB2 | 0.0015 | 3.6118 | 2.967 | 2.9934 | 2.9566 | 4.6639 | 3.9503 | 4.4347 | 2.2695 | 2.8638 |
| AA | **11dh-TXB2** | 0.0015 | 0.0015 | 0.0015 | 0.0015 | 0.0015 | 0.0015 | 0.0015 | 0.0015 | 0.0015 | 0.0075 |
| AA | **11dh-2,3-dinor TXB2** | 0.0108 | 0.0148 | 0.0071 | 0.02 | 0.008 | 0.0015 | 0.0373 | 0.0015 | 0.0078 | 0.0085 |
| AA | **LTB4** | 0.0283 | 0.0446 | 0.0495 | 0.0015 | 0.0388 | 0.3162 | 0.3433 | 0.1809 | 0.1025 | 0.0694 |
| AA | **20-hydroxy LTB4** | 0.0015 | 0.0015 | 0.0015 | 0.0015 | 0.0015 | 0.0015 | 0.0015 | 0.0015 | 0.0015 | 0.0015 |
| AA | 18-carboxy dinor LTB4 | 0.0015 | 0.0015 | 0.0015 | 0.0015 | 0.0015 | 0.0015 | 0.0015 | 0.0015 | 0.0015 | 0.0015 |
| AA | 5(S),12(S)-DiHETE | 0.12 | 0.2146 | 0.138 | 0.1362 | 0.1033 | 0.1301 | 0.3688 | 0.0918 | 0.1142 | 0.0554 |
| AA | **5(S),15(S)-DiHETE** | 0.0015 | 0.0015 | 0.0015 | 0.0015 | 0.0015 | 0.0015 | 0.0015 | 0.0015 | 0.0015 | 0.0015 |
| AA | **9-HODE** | 13.1826 | 17.9999 | 14.7776 | 15.0953 | 0.0015 | 26.2579 | 20.6841 | 26.3639 | 13.1375 | 0.0015 |
| AA | **13-HODE** | 102.5982 | 95.7632 | 76.3926 | 74.8717 | 73.3199 | 96.3259 | 96.1537 | 145.7021 | 69.3079 | 61.9694 |
| AA | **8(S)-HETrE** | 0.1078 | 0.1475 | 0.114 | 0.1546 | 0.1888 | 0.2069 | 0.2359 | 0.2226 | 0.1139 | 0.1598 |
| AA | **5(S)-HETrE** | 0.0015 | 0.0089 | 0.0072 | 0.0015 | 0.0178 | 0.0343 | 0.0296 | 0.0384 | 0.0129 | 0.0128 |
| AA | **5-HETE** | 1.1215 | 1.3183 | 1.0202 | 1.3526 | 1.6977 | 4.2268 | 4.0221 | 3.6432 | 1.7096 | 2.1517 |
| AA | **8-HETE** | 1.0683 | 0.7753 | 0.9253 | 1.0993 | 0.9928 | 1.1408 | 0.8703 | 1.1034 | 0.7182 | 0.9084 |
| AA | 9-HETE | 0.0015 | 0.0015 | 0.0015 | 0.0015 | 0.0015 | 0.0015 | 0.0015 | 0.0015 | 0.0015 | 0.0015 |
| AA | **11-HETE** | 79.7221 | 93.6908 | 66.3016 | 71.2922 | 70.8498 | 57.0665 | 68.2009 | 62.1644 | 58.665 | 78.6488 |
| AA | **12-HETE** | 72.5816 | 78.9431 | 61.3581 | 78.744 | 122.5452 | 104.5921 | 129.2191 | 73.9955 | 85.4262 | 88.7403 |
| AA | **15-HETE** | 20.13 | 23.4669 | 18.4581 | 17.9891 | 21.4737 | 21.1367 | 20.6926 | 19.6588 | 17.0474 | 20.7357 |
| AA | 20-HETE | 0.0015 | 0.7678 | 0.8797 | 0.7748 | 1.0269 | 0.9879 | 0.0015 | 0.0015 | 0.0015 | 1.1511 |
| AA | **tetranor 12-HETE** | 0.055 | 0.0659 | 0.0563 | 0.0908 | 0.0015 | 0.1754 | 0.122 | 0.3195 | 0.0992 | 0.1093 |
| AA | 12(S)-HHTrE | 25.4892 | 26.803 | 23.4114 | 17.5795 | 20.8156 | 24.5405 | 26.3298 | 22.1131 | 20.3876 | 19.8816 |
| AA | 9(10)-EpOME | 1.2526 | 0.9361 | 1.0894 | 0.778 | 1.2517 | 1.6848 | 1.1212 | 1.7062 | 1.0127 | 1.7666 |
| AA | **12(13)-EpOME** | 0.615 | 0.4682 | 0.4531 | 0.4299 | 0.5792 | 0.7871 | 0.6074 | 0.7019 | 0.5003 | 0.7908 |
| AA | **5(6)-EpETrE** | 0.1433 | 0.1314 | 0.1363 | 0.1291 | 0.1562 | 0.2169 | 0.106 | 0.1294 | 0.0671 | 0.117 |
| AA | 8(9)-EpETrE | 0.0015 | 0.0015 | 0.0395 | 0.0015 | 0.0015 | 0.0641 | 0.0284 | 0.0015 | 0.0015 | 0.0015 |
| AA | **11(12)-EpETrE** | 0.0782 | 0.0015 | 0.1706 | 0.1312 | 0.197 | 0.2687 | 0.0015 | 0.1267 | 0.0783 | 0.247 |
| AA | **14(15)-EpETrE** | 0.0015 | 0.0015 | 0.0015 | 0.0015 | 0.0015 | 0.0015 | 0.0015 | 0.0015 | 0.0015 | 0.1503 |
| AA | **9,10-DiHOME** | 2.301 | 1.1255 | 1.1798 | 1.2964 | 0.5984 | 1.1787 | 1.6376 | 1.6647 | 0.9409 | 0.381 |
| AA | **12,13-DiHOME** | 2.158 | 1.797 | 1.4632 | 1.5488 | 0.6811 | 2.0044 | 2.3045 | 2.0099 | 1.2584 | 0.4719 |
| AA | 5,6-DiHETrE | 0.0116 | 0.0015 | 0.0015 | 0.0144 | 0.0052 | 0.0015 | 0.0015 | 0.0143 | 0.0064 | 0.0015 |
| AA | **8,9-DiHETrE** | 0.0321 | 0.0314 | 0.0422 | 0.0336 | 0.0253 | 0.0516 | 0.0821 | 0.0364 | 0.0377 | 0.0207 |
| AA | **11,12-DiHETrE** | 0.3019 | 0.3424 | 0.2642 | 0.3698 | 0.1507 | 0.3583 | 0.6169 | 0.3908 | 0.2596 | 0.1508 |
| AA | 14,15-DiHETrE | 0.4157 | 0.5778 | 0.5527 | 0.4511 | 0.2352 | 0.594 | 0.8723 | 0.5552 | 0.4252 | 0.2602 |
| AA | 9-OxoODE | 4.1273 | 3.4742 | 3.2389 | 2.9265 | 3.3894 | 4.8823 | 3.3929 | 5.7275 | 3.1355 | 3.0685 |
| AA | **13-OxoODE** | 4.11 | 3.5354 | 3.4325 | 2.6608 | 4.4553 | 5.5084 | 6.3574 | 6.8265 | 3.3263 | 3.5223 |
| AA | 9-OxoOTrE | 0.0664 | 0.0015 | 0.0438 | 0.0509 | 0.0824 | 0.1042 | 0.0015 | 0.0731 | 0.0706 | 0.0447 |
| AA | 5-oxoETE | 0.0881 | 0.0988 | 0.1752 | 0.1365 | 0.2091 | 0.2665 | 0.2236 | 0.1629 | 0.1278 | 0.1496 |
| AA | 15-OxoETE | 0.0015 | 0.4128 | 0.5018 | 0.0015 | 0.4084 | 0.3731 | 0.0015 | 0.2829 | 0.2093 | 0.2143 |
| AA | 15-epi LXA4 | 0.0015 | 0.005 | 0.0015 | 0.0015 | 0.0025 | 0.0015 | 0.0015 | 0.0015 | 0.0015 | 0.0015 |
| EPA | **PGE3** | 0.0314 | 0.0405 | 0.0273 | 0.038 | 0.0373 | 0.0423 | 0.0428 | 0.0524 | 0.0252 | 0.0559 |
| EPA | **PGD3** | 0.0258 | 0.0956 | 0.1062 | 0.0015 | 0.082 | 0.0571 | 0.1036 | 0.0015 | 0.0015 | 0.1113 |
| EPA | **TXB3** | 0.0015 | 0.0015 | 0.0015 | 0.0015 | 0.0015 | 0.0219 | 0.0015 | 0.0305 | 0.0015 | 0.0098 |
| EPA | **5(S),15(S)-DiHEPE** | 0.0015 | 0.0954 | 0.0015 | 0.0015 | 0.035 | 0.0669 | 0.0015 | 0.0343 | 0.0015 | 0.0175 |
| EPA | 9(S)-HOTrE | 0.3026 | 0.1751 | 0.2697 | 0.2057 | 0.4403 | 0.2867 | 0.2504 | 0.4783 | 0.2829 | 0.1856 |
| EPA | **13(S)-HOTrE** | 1.8809 | 1.0374 | 1.2444 | 1.3337 | 1.1165 | 1.7941 | 1.8987 | 5.3499 | 1.8762 | 0.527 |
| EPA | **11(R)-HEDE** | 1.7474 | 1.6548 | 1.4651 | 1.4726 | 1.8574 | 1.6798 | 1.3978 | 1.9366 | 1.3672 | 1.9787 |
| EPA | 15(S)-HEDE | 0.1069 | 0.089 | 0.113 | 0.109 | 0.1254 | 0.1241 | 0.1103 | 0.23 | 0.1087 | 0.1255 |
| EPA | **5-HEPE** | 0.0015 | 0.0015 | 0.0015 | 0.0754 | 0.0854 | 0.0015 | 0.1787 | 0.2752 | 0.0556 | 0.1214 |
| EPA | **8-HEPE** | 0.0015 | 0.0015 | 0.0015 | 0.0015 | 0.0498 | 0.0015 | 0.0526 | 0.0015 | 0.0015 | 0.037 |
| EPA | **9-HEPE** | 0.1265 | 0.0015 | 0.1298 | 0.1464 | 0.2553 | 0.186 | 0.2995 | 0.2316 | 0.2103 | 0.1817 |
| EPA | **11-HEPE** | 0.3896 | 0.2435 | 0.3743 | 0.3234 | 0.3701 | 0.2714 | 0.24 | 0.4695 | 0.3658 | 0.4858 |
| EPA | **12-HEPE** | 2.9162 | 2.2473 | 2.4298 | 3.0685 | 6.7805 | 4.525 | 6.0519 | 6.4211 | 4.7991 | 5.4858 |
| EPA | **15(S)-HEPE** | 0.4564 | 0.0015 | 0.2618 | 0.2662 | 0.2317 | 0.2965 | 0.3645 | 0.8254 | 0.3593 | 0.2431 |
| EPA | **18-HEPE** | 0.0015 | 0.0015 | 0.0485 | 0.0015 | 0.0444 | 0.0015 | 0.0015 | 0.0724 | 0.0015 | 0.05 |
| EPA | 17(18)-EpETE | 0.0015 | 0.0015 | 0.0015 | 0.0052 | 0.0015 | 0.0015 | 0.0015 | 0.0134 | 0.0042 | 0.0015 |
| EPA | 5,6-DiHETE(EPA) | 0.0015 | 0.0015 | 0.0015 | 0.0151 | 0.0015 | 0.0015 | 0.0015 | 0.0015 | 0.0015 | 0.0015 |
| EPA | LXA5 | 0.0015 | 0.0047 | 0.0015 | 0.0015 | 0.0013 | 0.0015 | 0.0015 | 0.0015 | 0.003 | 0.0015 |
| EPA | **RvE3** | 0.6231 | 1.9823 | 1.2107 | 1.5691 | 0.3361 | 2.2328 | 2.1334 | 1.171 | 0.6929 | 0.4454 |
| DHA/EPA | 19,20-DiHDoPE | 0.1499 | 0.2146 | 0.1943 | 0.2219 | 0.083 | 0.269 | 0.4062 | 0.3043 | 0.1516 | 0.0854 |
| DHA | 4-HDoHE | 0.1009 | 0.1166 | 0.1178 | 0.1438 | 0.2012 | 0.2052 | 0.1402 | 0.2024 | 0.1475 | 0.197 |
| DHA | **7-HDoHE** | 0.0884 | 0.078 | 0.0788 | 0.1264 | 0.1118 | 0.3751 | 0.2634 | 0.5356 | 0.1232 | 0.1795 |
| DHA | 8-HDoHE | 0.0938 | 0.1141 | 0.1405 | 0.0758 | 0.1676 | 0.2302 | 0.1411 | 0.2917 | 0.1314 | 0.2029 |
| DHA | **10-HDoHE** | 0.1791 | 0.0015 | 0.2581 | 0.2886 | 0.3397 | 0.3303 | 0.3666 | 0.67 | 0.2583 | 0.3563 |
| DHA | 11-HDoHE | 0.0015 | 0.0015 | 0.4672 | 0.0015 | 0.0015 | 0.0015 | 0.6923 | 0.0015 | 0.0015 | 0.0015 |
| DHA | **13-HDoHE** | 1.1767 | 1.5264 | 1.2935 | 1.5491 | 1.4563 | 1.637 | 1.1393 | 2.386 | 1.2781 | 1.7422 |
| DHA | **14-HDoHE** | 4.085 | 3.8589 | 4.0309 | 5.0897 | 5.2854 | 6.8102 | 8.2815 | 10.3198 | 5.5975 | 3.949 |
| DHA | **16-HDoHE** | 0.4735 | 0.3834 | 0.4376 | 0.4385 | 0.5883 | 0.4609 | 0.3837 | 0.6644 | 0.3919 | 0.7497 |
| DHA | **17-HDoHE** | 0.3356 | 0.1855 | 0.1926 | 0.2292 | 0.2906 | 0.4894 | 0.3922 | 0.8726 | 0.5056 | 0.301 |
| DHA | 20-HDoHE | 0.4596 | 0.5278 | 0.4812 | 0.5438 | 0.5025 | 0.5803 | 0.6057 | 0.8026 | 0.4283 | 0.6752 |
| DHA | 7(8)-EpDPE | 0.0033 | 0.0054 | 0.0054 | 0.0074 | 0.0108 | 0.004 | 0.0066 | 0.0015 | 0.0039 | 0.0184 |
| DHA | 10(11)-EpDPE | 0.0326 | 0.0156 | 0.0317 | 0.0196 | 0.0443 | 0.0407 | 0.0166 | 0.0172 | 0.0187 | 0.0607 |
| DHA | 13(14)-EpDPE | 0.0112 | 0.0098 | 0.0015 | 0.0096 | 0.0132 | 0.0098 | 0.014 | 0.0015 | 0.0143 | 0.0193 |
| DHA | 16(17)-EpDPE | 0.0097 | 0.0126 | 0.0015 | 0.008 | 0.0183 | 0.0166 | 0.0119 | 0.0096 | 0.0097 | 0.0015 |
| DHA | **19(20)-EpDPE** | 0.0298 | 0.0203 | 0.0284 | 0.0189 | 0.0378 | 0.0374 | 0.0302 | 0.0404 | 0.0222 | 0.0577 |
| DHA | RvD1 & AT-RvD1 | 0.1682 | 0.0015 | 0.0015 | 0.0015 | 0.1145 | 0.4834 | 0.0015 | 0.0015 | 0.0015 | 0.0015 |
| DHA | RvD6 (4,17-DiHDoHE) | 0.0015 | 0.0015 | 0.0015 | 0.0015 | 0.0015 | 0.0015 | 0.0015 | 0.0015 | 0.0079 | 0.0015 |
| DHA | RvD5(n-3DPA) (7,17-DiHDoPE) | 0.0356 | 0.0633 | 0.0591 | 0.0926 | 0.0284 | 0.0543 | 0.0967 | 0.0534 | 0.0528 | 0.0201 |
| DHA | **PD1(n-3, DPA)** | 3.8907 | 11.0489 | 4.1335 | 6.3073 | 1.6294 | 8.0493 | 9.739 | 6.7326 | 3.2542 | 1.8407 |
| DHA | **10S,17S-DiHDoHE** | 0.0015 | 0.0015 | 0.0015 | 0.0015 | 0.0015 | 1.2959 | 0.5766 | 0.0015 | 0.0015 | 0.0015 |

| | |
|---|---|
| Green = | Statistical p-value found |
| Yellow = | LogFC was higher than control group |
| Blue = | LogFC was lower than control group |
| Red = | ≥3 values below the limit of detection |
| | |
| LA= | Linoleic acid |
| AA= | Arachidonic acid |
| EPA= | eicosapentaenoic acid |
| DHA= | docosahexaenoic acid |

| | | UI | | | | | Kp | | | | |
|---|---|---|---|---|---|---|---|---|---|---|---|
| | | 48 hr | | | | | 12 hr | | | | |
| | Lipid | 1-A | 1-B | 1-C | 1-D | 1-E | 4-A | 4-B | 4-C | 4-D | 4-E |
| LA | 13,14dh-15k-PGE1 | 0.0182 | 0.0099 | 0.0176 | 0.0015 | 0.017 | 0.0015 | 0.0287 | 0.0185 | 0.0295 | 0.0293 |
| LA | **PGE1** | 0.1287 | 0.2363 | 0.1247 | 0.1645 | 0.1673 | 0.2665 | 0.2516 | 0.2308 | 0.2825 | 0.2969 |
| LA | 15(R)-PGE1 | 0.0959 | 0.1149 | 0.0778 | 0.0793 | 0.0015 | 0.072 | 0.0015 | 0.0015 | 0.19 | 0.1562 |
| LA | **15-keto PGE1** | 0.0015 | 0.0015 | 0.0015 | 0.0015 | 0.0015 | 0.0015 | 0.0015 | 0.0071 | 0.0219 | 0.0145 |
| LA | **Bicyclo PGE1** | 3.2853 | 5.6863 | 4.1312 | 3.156 | 4.1412 | 2.1103 | 3.5703 | 2.7277 | 2.3301 | 2.4057 |
| LA | 6kPGF1a | 3.6156 | 6.157 | 5.2604 | 5.9817 | 6.4715 | 4.1311 | 0.0015 | 3.8716 | 14.9301 | 8.7684 |
| LA | 6-keto PGE1 | 0.0015 | 0.0172 | 0.0149 | 0.0154 | 0.0136 | 0.0097 | 0.017 | 0.0123 | 0.0015 | 0.0015 |
| AA | **PGE2** | 10.9409 | 12.1142 | 10.5898 | 10.3617 | 10.0851 | 10.9693 | 17.5176 | 11.9192 | 22.6208 | 17.6967 |
| AA | 15-keto PGE2 | 0.2065 | 0.4942 | 0.406 | 0.4265 | 0.3602 | 0.1933 | 0.7138 | 0.3211 | 1.0339 | 0.7219 |
| AA | **13,14dh-15k-PGE2** | 0.4777 | 0.5916 | 0.5485 | 0.5033 | 0.411 | 0.5118 | 1.1525 | 0.5435 | 1.3706 | 0.9934 |
| AA | **Bicyclo PGE2** | 0.0401 | 0.0476 | 0.0262 | 0.0309 | 0.0386 | 0.0307 | 0.0847 | 0.0551 | 0.1095 | 0.0708 |
| AA | **PGA2** | 0.354 | 0.3827 | 0.3073 | 0.2715 | 0.3636 | 0.4129 | 0.6629 | 0.4345 | 0.8895 | 0.76 |
| AA | tetranor PGEM | 0.0022 | 0.0015 | 0.0018 | 0.0015 | 0.0011 | 0.0016 | 0.0023 | 0.0015 | 0.0015 | 0.0019 |
| AA | PGD2 | 0.0015 | 0.0015 | 0.0015 | 0.0015 | 0.0015 | 0.0015 | 0.7555 | 0.0015 | 0.0015 | 0.0015 |
| AA | **PGJ2** | 0.1498 | 0.1779 | 0.1303 | 0.131 | 0.1644 | 0.1899 | 0.3452 | 0.2284 | 0.4485 | 0.3472 |
| AA | 15d-D12,14-PGJ2 | 0.0519 | 0.0727 | 0.0757 | 0.0773 | 0.0691 | 0.0701 | 0.0659 | 0.0571 | 0.0877 | 0.0786 |
| AA | **13,14dh-15k-PGD2** | 1.696 | 1.5422 | 1.2874 | 1.2029 | 1.1678 | 1.202 | 2.366 | 1.2442 | 2.56 | 2.4218 |
| AA | PGF1a | 0.036 | 0.0483 | 0.0286 | 0.017 | 0.0389 | 0.0312 | 0.0532 | 0.0447 | 0.0496 | 0.0522 |
| AA | PGF2a | 1.3802 | 1.3584 | 1.2208 | 0.6895 | 1.2415 | 0.9904 | 1.5466 | 1.2126 | 1.9472 | 1.9178 |
| AA | **15-keto PGF2a** | 0.5871 | 0.6055 | 0.5364 | 0.5491 | 0.4648 | 0.5395 | 1.0379 | 0.6056 | 1.2433 | 0.9292 |
| AA | **13,14dh-15k-PGF2a** | 0.0547 | 0.0785 | 0.0912 | 0.0525 | 0.081 | 0.0774 | 0.1036 | 0.0812 | 0.1133 | 0.0949 |
| AA | **19(R)-OH PGF2a & 20-OH PGF2a** | 0.0015 | 0.0015 | 0.0015 | 0.0015 | 0.0015 | 0.0015 | 0.0015 | 0.0015 | 0.0107 | 0.0015 |
| AA | 8-isoPGF2a & 11bPGF2a | 0.0015 | 0.1033 | 0.0638 | 0.0015 | 0.097 | 0.0015 | 0.1107 | 0.074 | 0.1597 | 0.0015 |
| AA | TXB2 | 0.0015 | 3.6118 | 2.967 | 2.9934 | 2.9566 | 3.2956 | 4.2458 | 4.0087 | 5.0769 | 4.5667 |
| AA | **11dh-TXB2** | 0.0015 | 0.0015 | 0.0015 | 0.0015 | 0.0015 | 0.0015 | 0.0064 | 0.0015 | 0.01 | 0.0161 |
| AA | **11dh-2,3-dinor TXB2** | 0.0108 | 0.0148 | 0.0071 | 0.02 | 0.008 | 0.0363 | 0.0201 | 0.0219 | 0.044 | 0.0245 |
| AA | **LTB4** | 0.0283 | 0.0446 | 0.0495 | 0.0015 | 0.0388 | 0.1945 | 0.1793 | 0.1184 | 0.21 | 0.1658 |
| AA | **20-hydroxy LTB4** | 0.0015 | 0.0015 | 0.0015 | 0.0015 | 0.0015 | 0.0015 | 0.0015 | 0.0015 | 0.0015 | 0.0015 |
| AA | 18-carboxy dinor LTB4 | 0.0015 | 0.0015 | 0.0015 | 0.0015 | 0.0015 | 0.0015 | 0.0015 | 0.0015 | 0.0015 | 0.0015 |
| AA | 5(S),12(S)-DiHETE | 0.12 | 0.2146 | 0.138 | 0.1362 | 0.1033 | 0.1098 | 0.0436 | 0.1611 | 0.2307 | 0.1567 |
| AA | **5(S),15(S)-DiHETE** | 0.0015 | 0.0015 | 0.0015 | 0.0015 | 0.0015 | 0.0015 | 0.0027 | 0.0015 | 0.0015 | 0.0015 |
| AA | **9-HODE** | 13.1826 | 17.9999 | 14.7776 | 15.0953 | 0.0015 | 15.3168 | 0.0015 | 0.0015 | 13.8187 | 11.2935 |
| AA | **13-HODE** | 102.5982 | 95.7632 | 76.3926 | 74.8717 | 73.3199 | 68.0189 | 69.4235 | 61.9668 | 76.3762 | 66.2997 |
| AA | **8(S)-HETrE** | 0.1078 | 0.1475 | 0.114 | 0.1546 | 0.1888 | 0.1291 | 0.1849 | 0.2808 | 0.3165 | 0.1862 |
| AA | **5(S)-HETrE** | 0.0015 | 0.0089 | 0.0072 | 0.0015 | 0.0178 | 0.0193 | 0.0315 | 0.0158 | 0.0308 | 0.0165 |
| AA | **5-HETE** | 1.1215 | 1.3183 | 1.0202 | 1.3526 | 1.6977 | 2.6646 | 4.6687 | 3.8812 | 5.8134 | 2.9401 |
| AA | **8-HETE** | 1.0683 | 0.7753 | 0.9253 | 1.0993 | 0.9928 | 0.556 | 0.8445 | 1.2941 | 1.1471 | 1.1679 |
| AA | 9-HETE | 0.0015 | 0.0015 | 0.0015 | 0.0015 | 0.0015 | 0.0015 | 0.0015 | 0.0015 | 0.0015 | 0.0015 |
| AA | **11-HETE** | 79.7221 | 93.6908 | 66.3016 | 71.2922 | 70.8498 | 61.2496 | 81.2088 | 76.568 | 98.1535 | 96.5233 |
| AA | **12-HETE** | 72.5816 | 78.9431 | 61.3581 | 78.744 | 122.5452 | 68.0563 | 87.5217 | 144.9424 | 140.511 | 122.8057 |
| AA | **15-HETE** | 20.13 | 23.4669 | 18.4581 | 17.9891 | 21.4737 | 17.3597 | 21.0824 | 20.3477 | 27.1312 | 27.7763 |
| AA | 20-HETE | 0.0015 | 0.7678 | 0.8797 | 0.7748 | 1.0269 | 0.0015 | 0.0015 | 0.9183 | 1.3782 | 0.0015 |
| AA | **tetranor 12-HETE** | 0.055 | 0.0659 | 0.0563 | 0.0908 | 0.0015 | 0.2228 | 0.221 | 0.0967 | 0.2157 | 0.0829 |
| AA | 12(S)-HHTrE | 25.4892 | 26.803 | 23.4114 | 17.5795 | 20.8156 | 14.5411 | 18.1839 | 21.4144 | 30.5334 | 28.2001 |
| AA | 9(10)-EpOME | 1.2526 | 0.9361 | 1.0894 | 0.778 | 1.2517 | 1.0766 | 1.301 | 1.4118 | 2.12 | 1.2676 |
| AA | **12(13)-EpOME** | 0.615 | 0.4682 | 0.4531 | 0.4299 | 0.5792 | 0.5639 | 0.5328 | 0.6206 | 0.8896 | 0.6134 |
| AA | **5(6)-EpETrE** | 0.1433 | 0.1314 | 0.1363 | 0.1291 | 0.1562 | 0.0786 | 0.1142 | 0.1083 | 0.1661 | 0.1103 |
| AA | 8(9)-EpETrE | 0.0015 | 0.0015 | 0.0395 | 0.0015 | 0.0015 | 0.0015 | 0.0015 | 0.0015 | 0.1026 | 0.0015 |
| AA | **11(12)-EpETrE** | 0.0782 | 0.0015 | 0.1706 | 0.1312 | 0.197 | 0.1169 | 0.2349 | 0.2141 | 0.318 | 0.2179 |
| AA | **14(15)-EpETrE** | 0.0015 | 0.0015 | 0.0015 | 0.0015 | 0.0015 | 0.0015 | 0.0015 | 0.1195 | 0.0015 | 0.0015 |
| AA | **9,10-DiHOME** | 2.301 | 1.1255 | 1.1798 | 1.2964 | 0.5984 | 1.0883 | 0.461 | 0.417 | 0.7774 | 0.4992 |
| AA | **12,13-DiHOME** | 2.158 | 1.797 | 1.4632 | 1.5488 | 0.6811 | 1.4089 | 0.6309 | 0.7442 | 1.2957 | 0.8028 |
| AA | 5,6-DiHETrE | 0.0116 | 0.0015 | 0.0015 | 0.0144 | 0.0052 | 0.0015 | 0.0015 | 0.0068 | 0.0139 | 0.0104 |
| AA | **8,9-DiHETrE** | 0.0321 | 0.0314 | 0.0422 | 0.0336 | 0.0253 | 0.0235 | 0.015 | 0.0204 | 0.0419 | 0.0355 |
| AA | **11,12-DiHETrE** | 0.3019 | 0.3424 | 0.2642 | 0.3698 | 0.1507 | 0.2672 | 0.1062 | 0.1702 | 0.3733 | 0.2814 |
| AA | 14,15-DiHETrE | 0.4157 | 0.5778 | 0.5527 | 0.4511 | 0.2352 | 0.3941 | 0.1874 | 0.1882 | 0.4699 | 0.4232 |
| AA | 9-OxoODE | 4.1273 | 3.4742 | 3.2389 | 2.9265 | 3.3894 | 2.3814 | 3.0936 | 2.6615 | 3.7399 | 2.7069 |
| AA | **13-OxoODE** | 4.11 | 3.5354 | 3.4325 | 2.6608 | 4.4553 | 6.1663 | 2.9167 | 3.0145 | 3.7234 | 3.6457 |
| AA | 9-OxoOTrE | 0.0664 | 0.0015 | 0.0438 | 0.0509 | 0.0824 | 0.0489 | 0.0433 | 0.0516 | 0.0447 | 0.048 |
| AA | 5-oxoETE | 0.0881 | 0.0988 | 0.1752 | 0.1365 | 0.2091 | 0.14 | 0.1915 | 0.241 | 0.2674 | 0.1688 |
| AA | 15-OxoETE | 0.0015 | 0.4128 | 0.5018 | 0.0015 | 0.4084 | 0.0015 | 0.0774 | 0.2319 | 0.0015 | 0.0015 |
| AA | 15-epi LXA4 | 0.0015 | 0.005 | 0.0015 | 0.0015 | 0.0025 | 0.0015 | 0.0015 | 0.0015 | 0.0015 | 0.0015 |
| EPA | **PGE3** | 0.0314 | 0.0405 | 0.0273 | 0.038 | 0.0373 | 0.0356 | 0.0826 | 0.0374 | 0.0658 | 0.0439 |
| EPA | **PGD3** | 0.0258 | 0.0956 | 0.1062 | 0.0015 | 0.082 | 0.0319 | 0.1294 | 0.0015 | 0.1883 | 0.1303 |
| EPA | **TXB3** | 0.0015 | 0.0015 | 0.0015 | 0.0015 | 0.0015 | 0.0015 | 0.0015 | 0.0015 | 0.0015 | 0.0015 |
| EPA | **5(S),15(S)-DiHEPE** | 0.0015 | 0.0954 | 0.0015 | 0.0015 | 0.035 | 0.0015 | 0.0015 | 0.0015 | 0.0015 | 0.0015 |
| EPA | 9(S)-HOTrE | 0.3026 | 0.1751 | 0.2697 | 0.2057 | 0.4403 | 0.1606 | 0.0015 | 0.2248 | 0.3837 | 0.2442 |
| EPA | **13(S)-HOTrE** | 1.8809 | 1.0374 | 1.2444 | 1.3337 | 1.1165 | 0.9869 | 0.9365 | 1.0588 | 1.2926 | 0.894 |
| EPA | **11(R)-HEDE** | 1.7474 | 1.6548 | 1.4651 | 1.4726 | 1.8574 | 1.2591 | 2.1551 | 1.5214 | 1.863 | 1.6931 |
| EPA | 15(S)-HEDE | 0.1069 | 0.089 | 0.113 | 0.109 | 0.1254 | 0.0697 | 0.1303 | 0.0957 | 0.1258 | 0.1104 |
| EPA | **5-HEPE** | 0.0015 | 0.0015 | 0.0015 | 0.0754 | 0.0854 | 0.0962 | 0.1483 | 0.1282 | 0.1449 | 0.1446 |
| EPA | **8-HEPE** | 0.0015 | 0.0015 | 0.0015 | 0.0015 | 0.0498 | 0.0015 | 0.0015 | 0.0382 | 0.0501 | 0.0015 |
| EPA | **9-HEPE** | 0.1265 | 0.0015 | 0.1298 | 0.1464 | 0.2553 | 0.0936 | 0.1533 | 0.3641 | 0.3373 | 0.1779 |
| EPA | **11-HEPE** | 0.3896 | 0.2435 | 0.3743 | 0.3234 | 0.3701 | 0.354 | 0.5124 | 0.2789 | 0.4969 | 0.3655 |
| EPA | **12-HEPE** | 2.9162 | 2.2473 | 2.4298 | 3.0685 | 6.7805 | 3.5338 | 4.676 | 8.0672 | 8.0281 | 5.0892 |
| EPA | **15(S)-HEPE** | 0.4564 | 0.0015 | 0.2618 | 0.2662 | 0.2317 | 0.1382 | 0.2028 | 0.1446 | 0.2117 | 0.1556 |
| EPA | **18-HEPE** | 0.0015 | 0.0015 | 0.0485 | 0.0015 | 0.0444 | 0.0544 | 0.0015 | 0.0015 | 0.0434 | 0.0463 |
| EPA | 17(18)-EpETE | 0.0015 | 0.0015 | 0.0015 | 0.0052 | 0.0015 | 0.0015 | 0.0015 | 0.0015 | 0.0015 | 0.006 |
| EPA | 5,6-DiHETE(EPA) | 0.0015 | 0.0015 | 0.0015 | 0.0151 | 0.0015 | 0.0015 | 0.0015 | 0.0015 | 0.0015 | 0.0015 |
| EPA | LXA5 | 0.0015 | 0.0047 | 0.0015 | 0.0015 | 0.0013 | 0.0015 | 0.0015 | 0.0015 | 0.0015 | 0.0027 |
| EPA | **RvE3** | 0.6231 | 1.9823 | 1.2107 | 1.5691 | 0.3361 | 1.1046 | 0.2445 | 0.4268 | 0.81 | 0.8672 |
| DHA/EPA | 19,20-DiHDoPE | 0.1499 | 0.2146 | 0.1943 | 0.2219 | 0.083 | 0.1863 | 0.0818 | 0.069 | 0.1518 | 0.1227 |
| DHA | 4-HDoHE | 0.1009 | 0.1166 | 0.1178 | 0.1438 | 0.2012 | 0.1343 | 0.2024 | 0.2018 | 0.1877 | 0.1829 |
| DHA | **7-HDoHE** | 0.0884 | 0.078 | 0.0788 | 0.1264 | 0.1118 | 0.1763 | 0.1985 | 0.1976 | 0.2516 | 0.1614 |
| DHA | 8-HDoHE | 0.0938 | 0.1141 | 0.1405 | 0.0758 | 0.1676 | 0.0635 | 0.1464 | 0.1902 | 0.1836 | 0.1496 |
| DHA | **10-HDoHE** | 0.1791 | 0.0015 | 0.2581 | 0.2886 | 0.3397 | 0.24 | 0.2705 | 0.235 | 0.2967 | 0.2805 |
| DHA | 11-HDoHE | 0.0015 | 0.0015 | 0.4672 | 0.0015 | 0.0015 | 0.3681 | 0.0015 | 0.0015 | 0.0015 | 0.0015 |
| DHA | **13-HDoHE** | 1.1767 | 1.5264 | 1.2935 | 1.5491 | 1.4563 | 1.3325 | 1.6993 | 1.1829 | 1.8955 | 1.5715 |
| DHA | **14-HDoHE** | 4.085 | 3.8589 | 4.0309 | 5.0897 | 5.2854 | 3.8008 | 4.1304 | 4.6884 | 5.3688 | 4.2584 |
| DHA | **16-HDoHE** | 0.4735 | 0.3834 | 0.4376 | 0.4385 | 0.5883 | 0.3769 | 0.5927 | 0.4047 | 0.5255 | 0.6289 |
| DHA | **17-HDoHE** | 0.3356 | 0.1855 | 0.1926 | 0.2292 | 0.2906 | 0.162 | 0.2912 | 0.2818 | 0.2851 | 0.2614 |
| DHA | 20-HDoHE | 0.4596 | 0.5278 | 0.4812 | 0.5438 | 0.5025 | 0.4708 | 0.5169 | 0.367 | 0.6146 | 0.5579 |
| DHA | 7(8)-EpDPE | 0.0033 | 0.0054 | 0.0054 | 0.0074 | 0.0108 | 0.0054 | 0.0158 | 0.0096 | 0.0132 | 0.0133 |
| DHA | 10(11)-EpDPE | 0.0326 | 0.0156 | 0.0317 | 0.0196 | 0.0443 | 0.0308 | 0.0623 | 0.0558 | 0.0703 | 0.047 |
| DHA | 13(14)-EpDPE | 0.0112 | 0.0098 | 0.0015 | 0.0096 | 0.0132 | 0.0079 | 0.0277 | 0.0155 | 0.0226 | 0.0239 |
| DHA | 16(17)-EpDPE | 0.0097 | 0.0126 | 0.0015 | 0.008 | 0.0183 | 0.0125 | 0.0153 | 0.0173 | 0.0271 | 0.0141 |
| DHA | **19(20)-EpDPE** | 0.0298 | 0.0203 | 0.0284 | 0.0189 | 0.0378 | 0.0185 | 0.0464 | 0.0409 | 0.049 | 0.0508 |
| DHA | RvD1 & AT-RvD1 | 0.1682 | 0.0015 | 0.0015 | 0.0015 | 0.1145 | 0.0015 | 0.0836 | 0.0816 | 0.0015 | 0.0015 |
| DHA | RvD6 (4,17-DiHDoHE) | 0.0015 | 0.0015 | 0.0015 | 0.0015 | 0.0015 | 0.0015 | 0.0015 | 0.0015 | 0.0015 | 0.0015 |
| DHA | RvD5(n-3DPA) (7,17-DiHDoPE) | 0.0356 | 0.0633 | 0.0591 | 0.0926 | 0.0284 | 0.0553 | 0.0121 | 0.0015 | 0.0275 | 0.0225 |
| DHA | **PD1(n-3, DPA)** | 3.8907 | 11.0489 | 4.1335 | 6.3073 | 1.6294 | 2.8265 | 0.8625 | 1.118 | 2.5176 | 2.2475 |
| DHA | **10S,17S-DiHDoHE** | 0.0015 | 0.0015 | 0.0015 | 0.0015 | 0.0015 | 0.0015 | 0.0015 | 0.0015 | 0.0015 | 0.0015 |

| | |
|---|---|
| Green = | Statistical p-value found |
| Yellow = | LogFC was higher than control group |
| Blue = | LogFC was lower than control group |
| Red = | ≥3 values below the limit of detection |
| | |
| LA= | Linoleic acid |
| AA= | Arachidonic acid |
| EPA= | eicosapentaenoic acid |
| DHA= | docosahexaenoic acid |

| | | UI | | | | | Kp | | | | |
|---|---|---|---|---|---|---|---|---|---|---|---|
| | | 48 hr | | | | | 24 hr | | | | |
| | Lipid | 1-A | 1-B | 1-C | 1-D | 1-E | 6-A | 6-B | 6-C | 6-D | 6-E |
| LA | 13,14dh-15k-PGE1 | 0.0182 | 0.0099 | 0.0176 | 0.0015 | 0.017 | 0.0235 | 0.0015 | 0.0122 | 0.021 | 0.0234 |
| LA | **PGE1** | 0.1287 | 0.2363 | 0.1247 | 0.1645 | 0.1673 | 0.3545 | 0.5591 | 0.4228 | 0.4129 | 0.5243 |
| LA | 15(R)-PGE1 | 0.0959 | 0.1149 | 0.0778 | 0.0793 | 0.0015 | 0.1262 | 0.2327 | 0.1722 | 0.167 | 0.1864 |
| LA | **15-keto PGE1** | 0.0015 | 0.0015 | 0.0015 | 0.0015 | 0.0015 | 0.0015 | 0.0079 | 0.0055 | 0.0015 | 0.0095 |
| LA | **Bicyclo PGE1** | 3.2853 | 5.6863 | 4.1312 | 3.156 | 4.1412 | 1.2875 | 1.4609 | 1.6754 | 1.4012 | 1.7342 |
| LA | 6kPGF1a | 3.6156 | 6.157 | 5.2604 | 5.9817 | 6.4715 | 8.9961 | 7.0321 | 8.4985 | 4.6059 | 0.0015 |
| LA | 6-keto PGE1 | 0.0015 | 0.0172 | 0.0149 | 0.0154 | 0.0136 | 0.021 | 0.0203 | 0.0015 | 0.0128 | 0.0015 |
| AA | **PGE2** | 10.9409 | 12.1142 | 10.5898 | 10.3617 | 10.0851 | 21.0323 | 29.4933 | 18.3468 | 18.9937 | 25.0177 |
| AA | 15-keto PGE2 | 0.2065 | 0.4942 | 0.406 | 0.4265 | 0.3602 | 0.5837 | 0.6664 | 0.394 | 0.3746 | 0.6662 |
| AA | **13,14dh-15k-PGE2** | 0.4777 | 0.5916 | 0.5485 | 0.5033 | 0.411 | 0.9089 | 1.2217 | 0.7811 | 0.7557 | 1.1309 |
| AA | **Bicyclo PGE2** | 0.0401 | 0.0476 | 0.0262 | 0.0309 | 0.0386 | 0.0987 | 0.1429 | 0.1069 | 0.1063 | 0.2043 |
| AA | **PGA2** | 0.354 | 0.3827 | 0.3073 | 0.2715 | 0.3636 | 0.8396 | 1.229 | 0.91 | 0.8424 | 1.4833 |
| AA | tetranor PGEM | 0.0022 | 0.0015 | 0.0018 | 0.0015 | 0.0011 | 0.0028 | 0.0029 | 0.0024 | 0.0022 | 0.0018 |
| AA | PGD2 | 0.0015 | 0.0015 | 0.0015 | 0.0015 | 0.0015 | 0.4458 | 0.0015 | 0.0015 | 0.0015 | 0.0015 |
| AA | **PGJ2** | 0.1498 | 0.1779 | 0.1303 | 0.131 | 0.1644 | 0.4298 | 0.6083 | 0.4065 | 0.4082 | 0.6872 |
| AA | 15d-D12,14-PGJ2 | 0.0519 | 0.0727 | 0.0757 | 0.0773 | 0.0691 | 0.0812 | 0.0876 | 0.0505 | 0.0513 | 0.0603 |
| AA | **13,14dh-15k-PGD2** | 1.696 | 1.5422 | 1.2874 | 1.2029 | 1.1678 | 2.755 | 3.8069 | 2.0748 | 1.9415 | 2.9571 |
| AA | PGF1a | 0.036 | 0.0483 | 0.0286 | 0.017 | 0.0389 | 0.0517 | 0.038 | 0.0543 | 0.0556 | 0.0777 |
| AA | PGF2a | 1.3802 | 1.3584 | 1.2208 | 0.6895 | 1.2415 | 1.5469 | 0.9796 | 1.5086 | 1.2796 | 1.747 |
| AA | **15-keto PGF2a** | 0.5871 | 0.6055 | 0.5364 | 0.5491 | 0.4648 | 1.0562 | 1.4321 | 1.0499 | 0.9774 | 1.3889 |
| AA | **13,14dh-15k-PGF2a** | 0.0547 | 0.0785 | 0.0912 | 0.0525 | 0.081 | 0.0232 | 0.0731 | 0.0015 | 0.0622 | 0.0404 |
| AA | **19(R)-OH PGF2a & 20-OH PGF2a** | 0.0015 | 0.0015 | 0.0015 | 0.0015 | 0.0015 | 0.0015 | 0.0127 | 0.0015 | 0.0015 | 0.0015 |
| AA | 8-isoPGF2a & 11bPGF2a | 0.0015 | 0.1033 | 0.0638 | 0.0015 | 0.097 | 0.0015 | 0.1447 | 0.0015 | 0.0883 | 0.1431 |
| AA | TXB2 | 0.0015 | 3.6118 | 2.967 | 2.9934 | 2.9566 | 0.0015 | 5.7561 | 3.6538 | 3.4136 | 4.3992 |
| AA | **11dh-TXB2** | 0.0015 | 0.0015 | 0.0015 | 0.0015 | 0.0015 | 0.0015 | 0.0073 | 0.0067 | 0.0015 | 0.0015 |
| AA | **11dh-2,3-dinor TXB2** | 0.0108 | 0.0148 | 0.0071 | 0.02 | 0.008 | 0.0474 | 0.1097 | 0.039 | 0.015 | 0.0782 |
| AA | **LTB4** | 0.0283 | 0.0446 | 0.0495 | 0.0015 | 0.0388 | 0.0821 | 0.0586 | 0.0504 | 0.0679 | 0.0804 |
| AA | **20-hydroxy LTB4** | 0.0015 | 0.0015 | 0.0015 | 0.0015 | 0.0015 | 0.0015 | 0.0015 | 0.0015 | 0.0015 | 0.0015 |
| AA | 18-carboxy dinor LTB4 | 0.0015 | 0.0015 | 0.0015 | 0.0015 | 0.0015 | 0.0166 | 0.0094 | 0.0015 | 0.0089 | 0.0015 |
| AA | 5(S),12(S)-DiHETE | 0.12 | 0.2146 | 0.138 | 0.1362 | 0.1033 | 0.1618 | 0.0768 | 0.1351 | 0.1353 | 0.1176 |
| AA | **5(S),15(S)-DiHETE** | 0.0015 | 0.0015 | 0.0015 | 0.0015 | 0.0015 | 0.0015 | 0.0104 | 0.0015 | 0.0015 | 0.0046 |
| AA | **9-HODE** | 13.1826 | 17.9999 | 14.7776 | 15.0953 | 0.0015 | 13.6497 | 0.0015 | 0.0015 | 0.0015 | 0.0015 |
| AA | **13-HODE** | 102.5982 | 95.7632 | 76.3926 | 74.8717 | 73.3199 | 120.0167 | 125.6052 | 134.5304 | 92.5377 | 135.0084 |
| AA | **8(S)-HETrE** | 0.1078 | 0.1475 | 0.114 | 0.1546 | 0.1888 | 0.2287 | 0.228 | 0.3314 | 0.2435 | 0.3803 |
| AA | **5(S)-HETrE** | 0.0015 | 0.0089 | 0.0072 | 0.0015 | 0.0178 | 0.0181 | 0.0364 | 0.024 | 0.0319 | 0.0295 |
| AA | **5-HETE** | 1.1215 | 1.3183 | 1.0202 | 1.3526 | 1.6977 | 3.9423 | 4.4906 | 4.1817 | 5.4693 | 7.1324 |
| AA | **8-HETE** | 1.0683 | 0.7753 | 0.9253 | 1.0993 | 0.9928 | 2.2569 | 1.5581 | 1.2963 | 1.2802 | 1.9151 |
| AA | 9-HETE | 0.0015 | 0.0015 | 0.0015 | 0.0015 | 0.0015 | 0.0015 | 0.0015 | 0.0015 | 0.0015 | 0.0015 |
| AA | **11-HETE** | 79.7221 | 93.6908 | 66.3016 | 71.2922 | 70.8498 | 126.1694 | 92.4727 | 92.3358 | 74.9885 | 113.8029 |
| AA | **12-HETE** | 72.5816 | 78.9431 | 61.3581 | 78.744 | 122.5452 | 132.7051 | 124.7226 | 157.3238 | 127.4447 | 178.9694 |
| AA | **15-HETE** | 20.13 | 23.4669 | 18.4581 | 17.9891 | 21.4737 | 37.4739 | 26.7927 | 26.5613 | 21.7353 | 30.9692 |
| AA | 20-HETE | 0.0015 | 0.7678 | 0.8797 | 0.7748 | 1.0269 | 0.9179 | 0.7526 | 0.0015 | 0.0015 | 0.9483 |
| AA | **tetranor 12-HETE** | 0.055 | 0.0659 | 0.0563 | 0.0908 | 0.0015 | 0.1805 | 0.0015 | 0.1288 | 0.1508 | 0.1587 |
| AA | 12(S)-HHTrE | 25.4892 | 26.803 | 23.4114 | 17.5795 | 20.8156 | 24.3759 | 25.0567 | 25.5405 | 15.0375 | 30.4354 |
| AA | 9(10)-EpOME | 1.2526 | 0.9361 | 1.0894 | 0.778 | 1.2517 | 1.1038 | 1.5313 | 1.7569 | 1.5358 | 1.6039 |
| AA | **12(13)-EpOME** | 0.615 | 0.4682 | 0.4531 | 0.4299 | 0.5792 | 0.5688 | 0.7158 | 0.8027 | 0.6577 | 0.7165 |
| AA | **5(6)-EpETrE** | 0.1433 | 0.1314 | 0.1363 | 0.1291 | 0.1562 | 0.0608 | 0.0484 | 0.0402 | 0.0377 | 0.0293 |
| AA | 8(9)-EpETrE | 0.0015 | 0.0015 | 0.0395 | 0.0015 | 0.0015 | 0.0015 | 0.0015 | 0.0015 | 0.0015 | 0.0015 |
| AA | **11(12)-EpETrE** | 0.0782 | 0.0015 | 0.1706 | 0.1312 | 0.197 | 0.0015 | 0.1298 | 0.188 | 0.1723 | 0.1835 |
| AA | **14(15)-EpETrE** | 0.0015 | 0.0015 | 0.0015 | 0.0015 | 0.0015 | 0.0015 | 0.0833 | 0.1694 | 0.1398 | 0.1105 |
| AA | **9,10-DiHOME** | 2.301 | 1.1255 | 1.1798 | 1.2964 | 0.5984 | 1.1734 | 0.6638 | 0.712 | 0.5042 | 0.5348 |
| AA | **12,13-DiHOME** | 2.158 | 1.797 | 1.4632 | 1.5488 | 0.6811 | 1.3585 | 0.6969 | 0.5859 | 0.6697 | 0.5614 |
| AA | 5,6-DiHETrE | 0.0116 | 0.0015 | 0.0015 | 0.0144 | 0.0052 | 0.011 | 0.0039 | 0.0018 | 0.0073 | 0.0052 |
| AA | **8,9-DiHETrE** | 0.0321 | 0.0314 | 0.0422 | 0.0336 | 0.0253 | 0.0308 | 0.0299 | 0.0293 | 0.0387 | 0.0201 |
| AA | **11,12-DiHETrE** | 0.3019 | 0.3424 | 0.2642 | 0.3698 | 0.1507 | 0.2747 | 0.2002 | 0.182 | 0.18 | 0.1636 |
| AA | 14,15-DiHETrE | 0.4157 | 0.5778 | 0.5527 | 0.4511 | 0.2352 | 0.4332 | 0.3084 | 0.2737 | 0.2658 | 0.2577 |
| AA | 9-OxoODE | 4.1273 | 3.4742 | 3.2389 | 2.9265 | 3.3894 | 3.8585 | 4.7184 | 4.4477 | 2.9599 | 5.7628 |
| AA | **13-OxoODE** | 4.11 | 3.5354 | 3.4325 | 2.6608 | 4.4553 | 4.2839 | 5.8375 | 4.7954 | 3.3265 | 6.6445 |
| AA | 9-OxoOTrE | 0.0664 | 0.0015 | 0.0438 | 0.0509 | 0.0824 | 0.0783 | 0.0366 | 0.0015 | 0.0499 | 0.0793 |
| AA | 5-oxoETE | 0.0881 | 0.0988 | 0.1752 | 0.1365 | 0.2091 | 0.2137 | 0.1506 | 0.1994 | 0.1398 | 0.3063 |
| AA | 15-OxoETE | 0.0015 | 0.4128 | 0.5018 | 0.0015 | 0.4084 | 1.5153 | 0.4963 | 1.1408 | 0.0015 | 0.2733 |
| AA | 15-epi LXA4 | 0.0015 | 0.005 | 0.0015 | 0.0015 | 0.0025 | 0.0015 | 0.0015 | 0.0024 | 0.0015 | 0.0023 |
| EPA | **PGE3** | 0.0314 | 0.0405 | 0.0273 | 0.038 | 0.0373 | 0.1096 | 0.2762 | 0.1282 | 0.1384 | 0.2288 |
| EPA | **PGD3** | 0.0258 | 0.0956 | 0.1062 | 0.0015 | 0.082 | 0.0778 | 0.0015 | 0.0015 | 0.0015 | 0.0015 |
| EPA | **TXB3** | 0.0015 | 0.0015 | 0.0015 | 0.0015 | 0.0015 | 0.0331 | 0.0624 | 0.034 | 0.0373 | 0.0518 |
| EPA | **5(S),15(S)-DiHEPE** | 0.0015 | 0.0954 | 0.0015 | 0.0015 | 0.035 | 0.1032 | 0.0191 | 0.0449 | 0.1062 | 0.0235 |
| EPA | 9(S)-HOTrE | 0.3026 | 0.1751 | 0.2697 | 0.2057 | 0.4403 | 0.4829 | 0.2858 | 0.4505 | 0.1939 | 0.3515 |
| EPA | **13(S)-HOTrE** | 1.8809 | 1.0374 | 1.2444 | 1.3337 | 1.1165 | 3.4966 | 3.2917 | 1.9539 | 1.3888 | 2.1463 |
| EPA | **11(R)-HEDE** | 1.7474 | 1.6548 | 1.4651 | 1.4726 | 1.8574 | 3.0414 | 2.8961 | 3.2521 | 2.3606 | 3.5495 |
| EPA | 15(S)-HEDE | 0.1069 | 0.089 | 0.113 | 0.109 | 0.1254 | 0.2633 | 0.2777 | 0.2192 | 0.1858 | 0.3164 |
| EPA | **5-HEPE** | 0.0015 | 0.0015 | 0.0015 | 0.0754 | 0.0854 | 0.2002 | 0.3644 | 0.2669 | 0.2905 | 0.4611 |
| EPA | **8-HEPE** | 0.0015 | 0.0015 | 0.0015 | 0.0015 | 0.0498 | 0.0671 | 0.0915 | 0.0901 | 0.0823 | 0.1141 |
| EPA | **9-HEPE** | 0.1265 | 0.0015 | 0.1298 | 0.1464 | 0.2553 | 0.4201 | 0.8631 | 0.8967 | 0.6717 | 0.8016 |
| EPA | **11-HEPE** | 0.3896 | 0.2435 | 0.3743 | 0.3234 | 0.3701 | 0.8822 | 1.6176 | 0.9801 | 0.9859 | 1.1276 |
| EPA | **12-HEPE** | 2.9162 | 2.2473 | 2.4298 | 3.0685 | 6.7805 | 8.6584 | 18.5483 | 20.2591 | 15.7728 | 20.6724 |
| EPA | **15(S)-HEPE** | 0.4564 | 0.0015 | 0.2618 | 0.2662 | 0.2317 | 0.7812 | 1.9213 | 0.8015 | 0.7832 | 0.8903 |
| EPA | **18-HEPE** | 0.0015 | 0.0015 | 0.0485 | 0.0015 | 0.0444 | 0.0015 | 0.0862 | 0.0674 | 0.0662 | 0.1041 |
| EPA | 17(18)-EpETE | 0.0015 | 0.0015 | 0.0015 | 0.0052 | 0.0015 | 0.0015 | 0.0114 | 0.0015 | 0.008 | 0.0015 |
| EPA | 5,6-DiHETE(EPA) | 0.0015 | 0.0015 | 0.0015 | 0.0151 | 0.0015 | 0.0015 | 0.0015 | 0.003 | 0.0015 | 0.0048 |
| EPA | LXA5 | 0.0015 | 0.0047 | 0.0015 | 0.0015 | 0.0013 | 0.0015 | 0.0015 | 0.0015 | 0.0015 | 0.0015 |
| EPA | **RvE3** | 0.6231 | 1.9823 | 1.2107 | 1.5691 | 0.3361 | 0.3879 | 0.3771 | 0.1237 | 0.2366 | 0.0986 |
| DHA/EPA | 19,20-DiHDoPE | 0.1499 | 0.2146 | 0.1943 | 0.2219 | 0.083 | 0.2496 | 0.2025 | 0.1648 | 0.1504 | 0.1502 |
| DHA | 4-HDoHE | 0.1009 | 0.1166 | 0.1178 | 0.1438 | 0.2012 | 0.2489 | 0.2233 | 0.251 | 0.2417 | 0.4164 |
| DHA | **7-HDoHE** | 0.0884 | 0.078 | 0.0788 | 0.1264 | 0.1118 | 0.2474 | 0.1915 | 0.2433 | 0.2526 | 0.2992 |
| DHA | 8-HDoHE | 0.0938 | 0.1141 | 0.1405 | 0.0758 | 0.1676 | 0.0015 | 0.1822 | 0.1646 | 0.1444 | 0.3035 |
| DHA | **10-HDoHE** | 0.1791 | 0.0015 | 0.2581 | 0.2886 | 0.3397 | 0.574 | 0.709 | 0.5384 | 0.5489 | 0.7907 |
| DHA | 11-HDoHE | 0.0015 | 0.0015 | 0.4672 | 0.0015 | 0.0015 | 0.0015 | 0.0015 | 0.0015 | 0.0015 | 0.0015 |
| DHA | **13-HDoHE** | 1.1767 | 1.5264 | 1.2935 | 1.5491 | 1.4563 | 3.8205 | 3.4087 | 3.0002 | 3.1154 | 3.8321 |
| DHA | **14-HDoHE** | 4.085 | 3.8589 | 4.0309 | 5.0897 | 5.2854 | 11.6945 | 14.7264 | 10.7255 | 11.8411 | 14.5475 |
| DHA | **16-HDoHE** | 0.4735 | 0.3834 | 0.4376 | 0.4385 | 0.5883 | 0.9489 | 0.9715 | 0.8518 | 0.7509 | 1.137 |
| DHA | **17-HDoHE** | 0.3356 | 0.1855 | 0.1926 | 0.2292 | 0.2906 | 1.9596 | 1.2792 | 1.0944 | 1.0675 | 1.5597 |
| DHA | 20-HDoHE | 0.4596 | 0.5278 | 0.4812 | 0.5438 | 0.5025 | 1.111 | 0.822 | 1.0167 | 0.7845 | 1.0497 |
| DHA | 7(8)-EpDPE | 0.0033 | 0.0054 | 0.0054 | 0.0074 | 0.0108 | 0.0084 | 0.0071 | 0.0107 | 0.0045 | 0.0099 |
| DHA | 10(11)-EpDPE | 0.0326 | 0.0156 | 0.0317 | 0.0196 | 0.0443 | 0.0338 | 0.0323 | 0.0341 | 0.0364 | 0.0531 |
| DHA | 13(14)-EpDPE | 0.0112 | 0.0098 | 0.0015 | 0.0096 | 0.0132 | 0.0015 | 0.0015 | 0.0177 | 0.0015 | 0.0292 |
| DHA | 16(17)-EpDPE | 0.0097 | 0.0126 | 0.0015 | 0.008 | 0.0183 | 0.0186 | 0.0118 | 0.0015 | 0.0112 | 0.0153 |
| DHA | **19(20)-EpDPE** | 0.0298 | 0.0203 | 0.0284 | 0.0189 | 0.0378 | 0.0615 | 0.0379 | 0.0575 | 0.0422 | 0.0496 |
| DHA | RvD1 & AT-RvD1 | 0.1682 | 0.0015 | 0.0015 | 0.0015 | 0.1145 | 0.2551 | 0.0015 | 0.0494 | 0.1134 | 0.0015 |
| DHA | RvD6 (4,17-DiHDoHE) | 0.0015 | 0.0015 | 0.0015 | 0.0015 | 0.0015 | 0.0015 | 0.0015 | 0.0015 | 0.0015 | 0.0015 |
| DHA | RvD5(n-3DPA) (7,17-DiHDoPE) | 0.0356 | 0.0633 | 0.0591 | 0.0926 | 0.0284 | 0.0402 | 0.0276 | 0.03 | 0.0339 | 0.0157 |
| DHA | **PD1(n-3, DPA)** | 3.8907 | 11.0489 | 4.1335 | 6.3073 | 1.6294 | 2.5796 | 0.8684 | 0.6302 | 1.1817 | 0.5771 |
| DHA | **10S,17S-DiHDoHE** | 0.0015 | 0.0015 | 0.0015 | 0.0015 | 0.0015 | 0.0015 | 0.0015 | 0.1477 | 0.0015 | 0.1996 |

| | |
|---|---|
| Green = | Statistical p-value found |
| Yellow = | LogFC was higher than control group |
| Blue = | LogFC was lower than control group |
| Red = | ≥3 values below the limit of detection |
| | |
| LA= | Linoleic acid |
| AA= | Arachidonic acid |
| EPA= | eicosapentaenoic acid |
| DHA= | docosahexaenoic acid |

| | | UI | | | | | Kp | | | | |
|---|---|---|---|---|---|---|---|---|---|---|---|
| | | 48 hr | | | | | 48 hr | | | | |
| | Lipid | 1-A | 1-B | 1-C | 1-D | 1-E | 9-A | 9-B | 9-C | 9-D | 9-E |
| LA | 13,14dh-15k-PGE1 | 0.0182 | 0.0099 | 0.0176 | 0.0015 | 0.017 | 0.0116 | 0.0219 | 0.0252 | 0.0157 | 0.0238 |
| LA | **PGE1** | 0.1287 | 0.2363 | 0.1247 | 0.1645 | 0.1673 | 0.6398 | 0.545 | 0.6947 | 1.0266 | 0.7337 |
| LA | 15(R)-PGE1 | 0.0959 | 0.1149 | 0.0778 | 0.0793 | 0.0015 | 0.2475 | 0.1962 | 0.2714 | 0.275 | 0.3028 |
| LA | **15-keto PGE1** | 0.0015 | 0.0015 | 0.0015 | 0.0015 | 0.0015 | 0.0062 | 0.0015 | 0.0015 | 0.0015 | 0.0015 |
| LA | **Bicyclo PGE1** | 3.2853 | 5.6863 | 4.1312 | 3.156 | 4.1412 | 0.8512 | 3.4445 | 2.6966 | 2.3555 | 1.9704 |
| LA | 6kPGF1a | 3.6156 | 6.157 | 5.2604 | 5.9817 | 6.4715 | 8.0596 | 11.4721 | 14.7188 | 5.9937 | 9.1885 |
| LA | 6-keto PGE1 | 0.0015 | 0.0172 | 0.0149 | 0.0154 | 0.0136 | 0.0053 | 0.0015 | 0.0015 | 0.0162 | 0.012 |
| AA | **PGE2** | 10.9409 | 12.1142 | 10.5898 | 10.3617 | 10.0851 | 26.2314 | 23.8297 | 40.0288 | 38.7041 | 37.648 |
| AA | 15-keto PGE2 | 0.2065 | 0.4942 | 0.406 | 0.4265 | 0.3602 | 0.3674 | 0.4806 | 0.5838 | 0.6016 | 0.5714 |
| AA | **13,14dh-15k-PGE2** | 0.4777 | 0.5916 | 0.5485 | 0.5033 | 0.411 | 1.2414 | 1.0058 | 1.6763 | 1.7746 | 1.8361 |
| AA | **Bicyclo PGE2** | 0.0401 | 0.0476 | 0.0262 | 0.0309 | 0.0386 | 0.2057 | 0.1628 | 0.2917 | 0.2639 | 0.3239 |
| AA | **PGA2** | 0.354 | 0.3827 | 0.3073 | 0.2715 | 0.3636 | 1.7932 | 1.4049 | 2.3353 | 2.2924 | 2.1026 |
| AA | tetranor PGEM | 0.0022 | 0.0015 | 0.0018 | 0.0015 | 0.0011 | 0.0017 | 0.0011 | 0.0032 | 0.0024 | 0.0042 |
| AA | PGD2 | 0.0015 | 0.0015 | 0.0015 | 0.0015 | 0.0015 | 0.0015 | 0.9875 | 0.0015 | 0.0015 | 0.0015 |
| AA | **PGJ2** | 0.1498 | 0.1779 | 0.1303 | 0.131 | 0.1644 | 0.9203 | 0.7029 | 1.0966 | 1.0912 | 1.0527 |
| AA | 15d-D12,14-PGJ2 | 0.0519 | 0.0727 | 0.0757 | 0.0773 | 0.0691 | 0.0615 | 0.0791 | 0.0715 | 0.0581 | 0.0711 |
| AA | **13,14dh-15k-PGD2** | 1.696 | 1.5422 | 1.2874 | 1.2029 | 1.1678 | 2.4702 | 2.656 | 3.6419 | 3.8531 | 3.8629 |
| AA | PGF1a | 0.036 | 0.0483 | 0.0286 | 0.017 | 0.0389 | 0.039 | 0.0692 | 0.0574 | 0.0521 | 0.0441 |
| AA | PGF2a | 1.3802 | 1.3584 | 1.2208 | 0.6895 | 1.2415 | 0.8598 | 1.4343 | 1.7901 | 1.3031 | 1.3332 |
| AA | **15-keto PGF2a** | 0.5871 | 0.6055 | 0.5364 | 0.5491 | 0.4648 | 1.6324 | 1.2417 | 2.048 | 2.26 | 2.0469 |
| AA | **13,14dh-15k-PGF2a** | 0.0547 | 0.0785 | 0.0912 | 0.0525 | 0.081 | 0.0342 | 0.0766 | 0.0675 | 0.0374 | 0.0516 |
| AA | **19(R)-OH PGF2a & 20-OH PGF2a** | 0.0015 | 0.0015 | 0.0015 | 0.0015 | 0.0015 | 0.0044 | 0.0063 | 0.012 | 0.0015 | 0.005 |
| AA | 8-isoPGF2a & 11bPGF2a | 0.0015 | 0.1033 | 0.0638 | 0.0015 | 0.097 | 0.096 | 0.1212 | 0.1301 | 0.0015 | 0.1043 |
| AA | TXB2 | 0.0015 | 3.6118 | 2.967 | 2.9934 | 2.9566 | 3.9883 | 4.061 | 4.7334 | 3.5814 | 0.0015 |
| AA | **11dh-TXB2** | 0.0015 | 0.0015 | 0.0015 | 0.0015 | 0.0015 | 0.0015 | 0.0015 | 0.0015 | 0.0053 | 0.0151 |
| AA | **11dh-2,3-dinor TXB2** | 0.0108 | 0.0148 | 0.0071 | 0.02 | 0.008 | 0.0062 | 0.0206 | 0.015 | 0.0246 | 0.017 |
| AA | **LTB4** | 0.0283 | 0.0446 | 0.0495 | 0.0015 | 0.0388 | 0.3237 | 0.1853 | 0.3483 | 0.6914 | 0.5464 |
| AA | **20-hydroxy LTB4** | 0.0015 | 0.0015 | 0.0015 | 0.0015 | 0.0015 | 0.0054 | 0.0038 | 0.0015 | 0.0046 | 0.0059 |
| AA | 18-carboxy dinor LTB4 | 0.0015 | 0.0015 | 0.0015 | 0.0015 | 0.0015 | 0.0022 | 0.0036 | 0.0015 | 0.0071 | 0.0053 |
| AA | 5(S),12(S)-DiHETE | 0.12 | 0.2146 | 0.138 | 0.1362 | 0.1033 | 0.0839 | 0.14 | 0.1066 | 0.0772 | 0.0513 |
| AA | **5(S),15(S)-DiHETE** | 0.0015 | 0.0015 | 0.0015 | 0.0015 | 0.0015 | 0.0041 | 0.0042 | 0.005 | 0.0117 | 0.0133 |
| AA | **9-HODE** | 13.1826 | 17.9999 | 14.7776 | 15.0953 | 0.0015 | 0.0015 | 0.0015 | 0.0015 | 0.0015 | 0.0015 |
| AA | **13-HODE** | 102.5982 | 95.7632 | 76.3926 | 74.8717 | 73.3199 | 113.6335 | 98.8232 | 197.9931 | 127.9384 | 164.1104 |
| AA | **8(S)-HETrE** | 0.1078 | 0.1475 | 0.114 | 0.1546 | 0.1888 | 0.3853 | 0.4082 | 0.2501 | 0.4208 | 0.4201 |
| AA | **5(S)-HETrE** | 0.0015 | 0.0089 | 0.0072 | 0.0015 | 0.0178 | 0.0702 | 0.0275 | 0.071 | 0.0568 | 0.0807 |
| AA | **5-HETE** | 1.1215 | 1.3183 | 1.0202 | 1.3526 | 1.6977 | 10.2491 | 5.2164 | 10.0207 | 16.4168 | 18.0179 |
| AA | **8-HETE** | 1.0683 | 0.7753 | 0.9253 | 1.0993 | 0.9928 | 1.6201 | 1.3031 | 1.5334 | 1.4248 | 1.7057 |
| AA | 9-HETE | 0.0015 | 0.0015 | 0.0015 | 0.0015 | 0.0015 | 0.0015 | 0.0015 | 0.0015 | 0.0015 | 0.0015 |
| AA | **11-HETE** | 79.7221 | 93.6908 | 66.3016 | 71.2922 | 70.8498 | 72.4572 | 88.8838 | 101.6297 | 109.9225 | 114.0362 |
| AA | **12-HETE** | 72.5816 | 78.9431 | 61.3581 | 78.744 | 122.5452 | 153.9741 | 203.6111 | 183.6814 | 162.7366 | 125.4316 |
| AA | **15-HETE** | 20.13 | 23.4669 | 18.4581 | 17.9891 | 21.4737 | 21.9837 | 21.4077 | 25.7038 | 30.6602 | 31.4807 |
| AA | 20-HETE | 0.0015 | 0.7678 | 0.8797 | 0.7748 | 1.0269 | 0.0015 | 0.0015 | 0.0015 | 0.9248 | 0.0015 |
| AA | **tetranor 12-HETE** | 0.055 | 0.0659 | 0.0563 | 0.0908 | 0.0015 | 0.188 | 0.1532 | 0.2263 | 0.1062 | 0.1469 |
| AA | 12(S)-HHTrE | 25.4892 | 26.803 | 23.4114 | 17.5795 | 20.8156 | 13.5153 | 17.0084 | 30.7323 | 15.5715 | 19.1766 |
| AA | 9(10)-EpOME | 1.2526 | 0.9361 | 1.0894 | 0.778 | 1.2517 | 1.4148 | 1.9546 | 2.2122 | 1.4135 | 2.0371 |
| AA | **12(13)-EpOME** | 0.615 | 0.4682 | 0.4531 | 0.4299 | 0.5792 | 0.8213 | 1.1278 | 1.3301 | 0.5401 | 0.8151 |
| AA | **5(6)-EpETrE** | 0.1433 | 0.1314 | 0.1363 | 0.1291 | 0.1562 | 0.0338 | 0.0454 | 0.0349 | 0.0251 | 0.0247 |
| AA | 8(9)-EpETrE | 0.0015 | 0.0015 | 0.0395 | 0.0015 | 0.0015 | 0.0237 | 0.0351 | 0.0207 | 0.0015 | 0.0015 |
| AA | **11(12)-EpETrE** | 0.0782 | 0.0015 | 0.1706 | 0.1312 | 0.197 | 0.1394 | 0.1647 | 0.1401 | 0.1681 | 0.1618 |
| AA | **14(15)-EpETrE** | 0.0015 | 0.0015 | 0.0015 | 0.0015 | 0.0015 | 0.0015 | 0.3199 | 0.2447 | 0.1205 | 0.0926 |
| AA | **9,10-DiHOME** | 2.301 | 1.1255 | 1.1798 | 1.2964 | 0.5984 | 0.5186 | 0.4567 | 0.6912 | 0.7113 | 0.9343 |
| AA | **12,13-DiHOME** | 2.158 | 1.797 | 1.4632 | 1.5488 | 0.6811 | 0.4799 | 0.5349 | 0.728 | 0.5992 | 0.7931 |
| AA | 5,6-DiHETrE | 0.0116 | 0.0015 | 0.0015 | 0.0144 | 0.0052 | 0.0051 | 0.0077 | 0.0015 | 0.0073 | 0.0048 |
| AA | **8,9-DiHETrE** | 0.0321 | 0.0314 | 0.0422 | 0.0336 | 0.0253 | 0.0154 | 0.0217 | 0.0278 | 0.017 | 0.0114 |
| AA | **11,12-DiHETrE** | 0.3019 | 0.3424 | 0.2642 | 0.3698 | 0.1507 | 0.1599 | 0.1916 | 0.1429 | 0.1483 | 0.129 |
| AA | 14,15-DiHETrE | 0.4157 | 0.5778 | 0.5527 | 0.4511 | 0.2352 | 0.3852 | 0.4358 | 0.2427 | 0.254 | 0.186 |
| AA | 9-OxoODE | 4.1273 | 3.4742 | 3.2389 | 2.9265 | 3.3894 | 3.3792 | 3.1769 | 6.175 | 2.8172 | 5.4344 |
| AA | **13-OxoODE** | 4.11 | 3.5354 | 3.4325 | 2.6608 | 4.4553 | 2.6447 | 3.3191 | 6.7989 | 3.2489 | 4.9008 |
| AA | 9-OxoOTrE | 0.0664 | 0.0015 | 0.0438 | 0.0509 | 0.0824 | 0.032 | 0.0556 | 0.0752 | 0.0015 | 0.0505 |
| AA | 5-oxoETE | 0.0881 | 0.0988 | 0.1752 | 0.1365 | 0.2091 | 0.2353 | 0.1685 | 0.2698 | 0.2329 | 0.414 |
| AA | 15-OxoETE | 0.0015 | 0.4128 | 0.5018 | 0.0015 | 0.4084 | 0.4264 | 0.5199 | 0.0015 | 0.5833 | 0.0015 |
| AA | 15-epi LXA4 | 0.0015 | 0.005 | 0.0015 | 0.0015 | 0.0025 | 0.0013 | 0.0018 | 0.0015 | 0.0059 | 0.0029 |
| EPA | **PGE3** | 0.0314 | 0.0405 | 0.0273 | 0.038 | 0.0373 | 0.3211 | 0.1986 | 0.4364 | 0.3497 | 0.404 |
| EPA | **PGD3** | 0.0258 | 0.0956 | 0.1062 | 0.0015 | 0.082 | 0.0481 | 0.0015 | 0.0015 | 0.0015 | 0.0015 |
| EPA | **TXB3** | 0.0015 | 0.0015 | 0.0015 | 0.0015 | 0.0015 | 0.0697 | 0.0392 | 0.0617 | 0.0368 | 0.0521 |
| EPA | **5(S),15(S)-DiHEPE** | 0.0015 | 0.0954 | 0.0015 | 0.0015 | 0.035 | 0.0446 | 0.022 | 0.0529 | 0.024 | 0.0333 |
| EPA | 9(S)-HOTrE | 0.3026 | 0.1751 | 0.2697 | 0.2057 | 0.4403 | 0.2565 | 0.4037 | 0.6746 | 0.2239 | 0.4423 |
| EPA | **13(S)-HOTrE** | 1.8809 | 1.0374 | 1.2444 | 1.3337 | 1.1165 | 2.0121 | 1.6627 | 3.8046 | 1.1907 | 2.7807 |
| EPA | **11(R)-HEDE** | 1.7474 | 1.6548 | 1.4651 | 1.4726 | 1.8574 | 4.3563 | 3.7785 | 4.112 | 4.0948 | 4.1918 |
| EPA | 15(S)-HEDE | 0.1069 | 0.089 | 0.113 | 0.109 | 0.1254 | 0.3204 | 0.2305 | 0.3614 | 0.267 | 0.2936 |
| EPA | **5-HEPE** | 0.0015 | 0.0015 | 0.0015 | 0.0754 | 0.0854 | 0.7294 | 0.3335 | 0.7371 | 0.9436 | 1.4106 |
| EPA | **8-HEPE** | 0.0015 | 0.0015 | 0.0015 | 0.0015 | 0.0498 | 0.0835 | 0.0814 | 0.1663 | 0.1145 | 0.1024 |
| EPA | **9-HEPE** | 0.1265 | 0.0015 | 0.1298 | 0.1464 | 0.2553 | 0.7379 | 0.8043 | 1.0064 | 0.6766 | 0.7718 |
| EPA | **11-HEPE** | 0.3896 | 0.2435 | 0.3743 | 0.3234 | 0.3701 | 0.861 | 0.8147 | 1.794 | 1.0791 | 1.3381 |
| EPA | **12-HEPE** | 2.9162 | 2.2473 | 2.4298 | 3.0685 | 6.7805 | 17.5191 | 18.0899 | 23.5702 | 16.9391 | 17.681 |
| EPA | **15(S)-HEPE** | 0.4564 | 0.0015 | 0.2618 | 0.2662 | 0.2317 | 1.0967 | 1.1842 | 1.8378 | 0.9596 | 1.2048 |
| EPA | **18-HEPE** | 0.0015 | 0.0015 | 0.0485 | 0.0015 | 0.0444 | 0.086 | 0.0775 | 0.0848 | 0.0905 | 0.0903 |
| EPA | 17(18)-EpETE | 0.0015 | 0.0015 | 0.0015 | 0.0052 | 0.0015 | 0.0015 | 0.0015 | 0.0015 | 0.0015 | 0.0015 |
| EPA | 5,6-DiHETE(EPA) | 0.0015 | 0.0015 | 0.0015 | 0.0151 | 0.0015 | 0.0056 | 0.0042 | 0.0015 | 0.0015 | 0.003 |
| EPA | LXA5 | 0.0015 | 0.0047 | 0.0015 | 0.0015 | 0.0013 | 0.0015 | 0.0015 | 0.0015 | 0.0015 | 0.0015 |
| EPA | **RvE3** | 0.6231 | 1.9823 | 1.2107 | 1.5691 | 0.3361 | 0.0647 | 0.0812 | 0.2271 | 0.2226 | 0.1406 |
| DHA/EPA | 19,20-DiHDoPE | 0.1499 | 0.2146 | 0.1943 | 0.2219 | 0.083 | 0.1626 | 0.1483 | 0.154 | 0.1308 | 0.1296 |
| DHA | 4-HDoHE | 0.1009 | 0.1166 | 0.1178 | 0.1438 | 0.2012 | 0.2649 | 0.2923 | 0.319 | 0.339 | 0.2832 |
| DHA | **7-HDoHE** | 0.0884 | 0.078 | 0.0788 | 0.1264 | 0.1118 | 0.6071 | 0.4596 | 0.3766 | 0.787 | 0.9896 |
| DHA | 8-HDoHE | 0.0938 | 0.1141 | 0.1405 | 0.0758 | 0.1676 | 0.2339 | 0.2211 | 0.217 | 0.2689 | 0.3361 |
| DHA | **10-HDoHE** | 0.1791 | 0.0015 | 0.2581 | 0.2886 | 0.3397 | 0.7828 | 0.7093 | 0.5334 | 0.6366 | 0.5689 |
| DHA | 11-HDoHE | 0.0015 | 0.0015 | 0.4672 | 0.0015 | 0.0015 | 0.0015 | 1.1825 | 0.0015 | 0.0015 | 0.0015 |
| DHA | **13-HDoHE** | 1.1767 | 1.5264 | 1.2935 | 1.5491 | 1.4563 | 3.5659 | 3.2772 | 3.0958 | 4.2139 | 3.9399 |
| DHA | **14-HDoHE** | 4.085 | 3.8589 | 4.0309 | 5.0897 | 5.2854 | 14.351 | 11.35 | 9.8781 | 11.7489 | 10.3192 |
| DHA | **16-HDoHE** | 0.4735 | 0.3834 | 0.4376 | 0.4385 | 0.5883 | 1.0177 | 0.8766 | 0.8746 | 1.0066 | 1.1109 |
| DHA | **17-HDoHE** | 0.3356 | 0.1855 | 0.1926 | 0.2292 | 0.2906 | 1.2626 | 0.7442 | 1.1758 | 1.1952 | 1.2199 |
| DHA | 20-HDoHE | 0.4596 | 0.5278 | 0.4812 | 0.5438 | 0.5025 | 0.9135 | 0.8585 | 0.9337 | 1.1688 | 1.0281 |
| DHA | 7(8)-EpDPE | 0.0033 | 0.0054 | 0.0054 | 0.0074 | 0.0108 | 0.0059 | 0.0066 | 0.0074 | 0.0042 | 0.0078 |
| DHA | 10(11)-EpDPE | 0.0326 | 0.0156 | 0.0317 | 0.0196 | 0.0443 | 0.024 | 0.0287 | 0.0323 | 0.056 | 0.0649 |
| DHA | 13(14)-EpDPE | 0.0112 | 0.0098 | 0.0015 | 0.0096 | 0.0132 | 0.0015 | 0.0015 | 0.0162 | 0.0193 | 0.0171 |
| DHA | 16(17)-EpDPE | 0.0097 | 0.0126 | 0.0015 | 0.008 | 0.0183 | 0.0101 | 0.0094 | 0.0015 | 0.0205 | 0.027 |
| DHA | **19(20)-EpDPE** | 0.0298 | 0.0203 | 0.0284 | 0.0189 | 0.0378 | 0.0486 | 0.0444 | 0.0438 | 0.0595 | 0.0764 |
| DHA | RvD1 & AT-RvD1 | 0.1682 | 0.0015 | 0.0015 | 0.0015 | 0.1145 | 0.0593 | 0.0015 | 0.122 | 0.0822 | 0.0015 |
| DHA | RvD6 (4,17-DiHDoHE) | 0.0015 | 0.0015 | 0.0015 | 0.0015 | 0.0015 | 0.0037 | 0.0064 | 0.0015 | 0.0015 | 0.0015 |
| DHA | RvD5(n-3DPA) (7,17-DiHDoPE) | 0.0356 | 0.0633 | 0.0591 | 0.0926 | 0.0284 | 0.0094 | 0.0171 | 0.0368 | 0.0222 | 0.022 |
| DHA | **PD1(n-3, DPA)** | 3.8907 | 11.0489 | 4.1335 | 6.3073 | 1.6294 | 0.1615 | 0.25 | 0.6527 | 0.7637 | 0.6181 |
| DHA | **10S,17S-DiHDoHE** | 0.0015 | 0.0015 | 0.0015 | 0.0015 | 0.0015 | 0.154 | 0.0957 | 0.3721 | 0.1938 | 0.1499 |

| | |
|---|---|
| Green = | Statistical p-value found |
| Yellow = | LogFC was higher than control group |
| Blue = | LogFC was lower than control group |
| Red = | ≥3 values below the limit of detection |
| | |
| LA= | Linoleic acid |
| AA= | Arachidonic acid |
| EPA= | eicosapentaenoic acid |
| DHA= | docosahexaenoic acid |

Changes in inflammatory lipids during first 48 h of pneumonic *K. pneumoniae*

C57BL/6J mice were infected with WT *K. pneumoniae* (Kp) at 10x the $LD_{50}$ and lungs were harvested at 6, 12, 24, and 48 h post-infection (n=5). Total lipids were isolated from homogenized lungs and lipids were quantified by LC-MS. Significant changes in lipid concentrations were observed in at least one time point for 59 lipids. Lipids that were below the limit of detection for all time points were excluded from statistical analysis. Green boxes = statistical p-value in at least one time point. Yellow boxes = LogFC was higher than control (UI). Blue boxes = LogFC was lower than control (UI). Red font = $\geq$ 3 values were below the limit of detection.

**Isolation of BMNs: Percoll vs positive selection**

As I was performing experiments, I noticed an increase in the basal (i.e. uninfected) levels of $LTB_4$ synthesis in my neutrophils. I suspected the purity of the neutrophil isolation may be the cause, so to determine this, I isolated neutrophils using my regular protocol of Percoll Plus density gradient or an Ultrapure Anti-Ly6G MacsBead positive selection kit and measured neutrophil purity by flow cytometry. I found that the Percoll isolated neutrophils were nearly 40% less pure than the positive selection kit (Fig 5-2, $p \leq 0.0001$). Additionally, the Percoll isolated neutrophils also exhibited a significantly higher level of $LTB_4$ synthesis when uninfected than the positive selection isolated neutrophils (Fig 5-2, $p \leq 0.01$). While this difference in synthesis was also observed in the *Y. pestis* infected neutrophils ($p \leq 0.01$), there was no significant difference in the *Y. pestis* T3E infected neutrophils (Fig 5-2). I later found the cause for the decrease in purity was due to an abnormal amount of band cells in the Percoll isolated samples (data not shown). It should be noted that the positive selection protocol called for pressure to be applied to the neutrophils to release them from the column, therefore, to confirm the neutrophils were not becoming distressed, I examined their morphology via cytospin. Neutrophils that were uninfected, infected with *Y. pestis* or *Y. pestis* T3E showed consitently healthy neutrophils (Fig 5-2). Additionally, the cytospins exhibited phagocytosis of the *Y. pestis* T3E, but not the *Y. pestis* strain (Fig 5-2B & C). Moving forward, I decided to solely isolate neutrophils using the Anti-Ly6G kit.

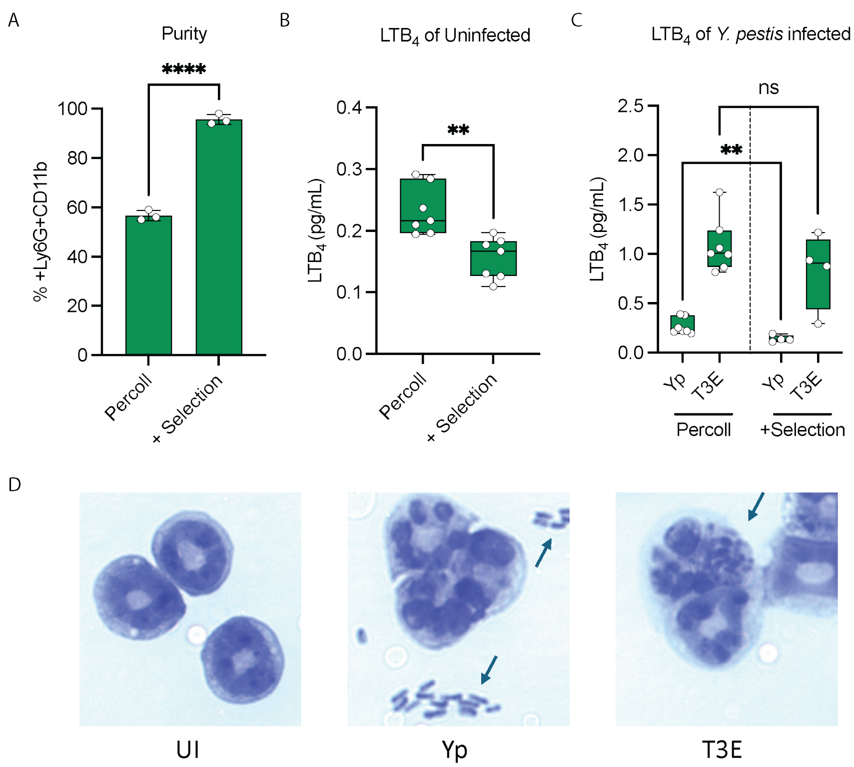


<u>BMN isolation with Anti-Ly6G +selection microbeads yields a higher purity more consistently than Percoll</u>

Neutrophils isolated from bone-marrow using a Percoll Plus density gradient (Percoll) (Cytiva, Cat. No. 17-5445-02) or an Anti-Ly-6G MicroBeads UltraPure (+selection) kit (Miltenyi Biotec, Cat. No. 130-120-337). (A) Neutrophil purity (+Ly6G+CD11b) measured by flow cytometry after isolation. (B) Basal $LTB_4$ levels measured from uninfected BMNs. (C) $LTB_4$ from BMNs infected with *Y. pestis* (Yp) or a *Y. pestis* T3E mutant (T3E) at an MOI of 20. (D) Cytospins showing the morphology of BMNs stained with H&E after Anti-Ly6G +selection isolation either uninfected or infected with *Y. pestis*, or *Y. pestis* T3E at an MOI of 20. (B-C) $LTB_4$ measured by ELISA after 1 h of incubation at 37°C. UI=uninfected. ns=not significant. (A-C) Each symbol represents an independent biological sample and the box plot or bar graph represents the median of the group ± the range or the mean ± the standard deviation, respectively. T-test with Welch's *post hoc* test. **=p≤0.01, ****=p≤0.0001.

CURRICULUM VITAE

Amanda Brady
University of Louisville School of Medicine
Clinical and Translational Research Building Rm 633
505 S. Hancock St., Louisville, KY 40202
Louisville, KY 40202
Phone: 720-296-7784
Email: a0rad06@louisville.edu

**EDUCATION**

2012-2017 B.S. in Biological Sciences, University of Northern Colorado, Greeley, CO

2018-2020 M.S. in Microbiology and Immunology, University of Louisville, Louisville, KY

2018-2024 Ph.D. in Microbiology and Immunology, University of Louisville, Louisville, KY

**RESEARCH EXPERIENCE**

2013-2017 Student Research Assistant, College of Education and Behavioral Science- University of Northern Colorado, Greeley, CO
Organized faculty and sensitive information and responsible for compiling research data for analysis.

2015-2018 Cytology Laboratory Aid, Summit Pathology, Loveland, CO
Processed cytology specimens for pathology analysis that were received from hospitals and clinics across the states of Colorado, Wyoming, and Nevada.

2015-2018 Primary Investigator, McNair Scholar Program, University of Northern Colorado, Greeley, CO
Mentor: Alan Price
Developed an independent project exploring the significance of mitochondrial DNA collected from human hair follicles and its use as trace evidence in forensic science applications.

2018-2024 Graduate Student Research Assistant, University of Louisville, Louisville, KY
Mentor: Matthew Lawrenz
Define the mechanisms in which *Yersinia pestis* targets the host to inhibit an appropriate immune response.

**TEACHING EXPERIENCE**

2020-2021 MBIO610: Research Methods in Microbiology and Immunology, Lecturer
Topic: Animal Models of Infection

2020 Louisville Science Pathways (LSP), Invited Lecturer
Topic: Using Confocal Microscopy in Research
LSP is a competitive high school summer research program designed to expose high school students to research and future career opportunities in the STEM fields.

2021,2022 Louisville Science Pathways (LSP), Research MentorMentored high school students during the 2021 and 2022 summer semesters. I developed projects for the students and assisted in their research and preparation of their scientific presentations at the end of their research internships.

**COMMUNITY OUTREACH, SERVICE, AND LEADERSHIP**

2018-2024 University of Louisville Microbiology and Immunology Student Organization (MISO)

Secretary (2019-2020); Administration representative (2021-2022)

MISO is a student run organization that supports expanding student-faculty relations within the Department of Microbiology and Immunology. In 2019 I served as the Secretary of MISO. As part of the MISO leadership team, I was directly involved in organizing student sponsored activities with the department, gathering and communicating suggestions from the students to improve the graduate program, and recruiting new students to the department.

2020-2024 Society for Advancement of Hispanics/Chicanos and Native Americans in Science (SACNAS) Student Chapter

President (2020-present)

SACNAS is a national organization that provides opportunities to aid Chicano/Hispanic and Native American students to obtain advanced degrees, careers, and equality in STEM fields. As president, I work towards keeping the UofL chapter active by planning monthly meetings, organizing events, and recruiting members.

2018-2024 Science Policy and Outreach Group (SPOG)

Outreach Coordinator (2020-2021)

SPOG is a graduate student organization at the University of Louisville Health Science Campus. The goal is to contribute to helping the community understand the importance of science. As Outreach Coordinator, I am responsible for initiating and executing events in which connections, mentoring, and communication can be performed between the science community and the greater community, focusing on younger pupils.

2020-2024 Institutional Biosafety committee (IBC) member

The IBC oversees all research performed at the University of Louisville and that research meets all the state and federal guidelines to ensure the research is completed in a safe manner. As the graduate student representative, I take part in monthly IBC meetings and contribute to the review of new IBC protocols.

2020-2021 Graduate Student Council Representative

The Graduate Student Council represents graduate students from all disciplines across the University of Louisville. As the representative from the Department of Microbiology and Immunology, I am responsible for conveying information between the Graduate Student Council and the students within the department and representing any M&I concerns to the council.

2020 Louisville Regional Science & Engineering Fair, Ambassador

Helped students develop their science fair presentations.

2021 Louisville Regional Science and Engineering Fair, Judge

Provided critical feedback on science fair projects.

2023-2024 Biomedical Integrative Opportunity for Mentored Experience Development Post-Baccalaureate Research Education Program (BIOMED-PREP), mentor

PREP is a NIH funded program aimed to increase diversity in the scientific workforce. As a mentor, I meet with PREP scholars on a monthly bases to provide guidance and support for the student as they navigate applying for graduate school.

**PROFESSIONAL MEMBERSHIPS**

| | |
|---|---|
| 2012-2017 | University of Northern Colorado Honors Interdisciplinary Program |
| 2016-2018 | American Academy of Forensic Science Affiliate |
| 2018-2024 | Presidential Diversity Fellow |
| 2020-2024 | Society for Leukocyte Biology |
| 2020-2024 | SACNAS |
| 2020-Current | American Society for Microbiology (ASM) |

**AWARDS AND HONORS**

| | |
|---|---|
| 2012, 2017 | First Generation Scholarship |
| 2012-2018 | Honors Interdisciplinary Program Scholarship |
| 2014-2017 | McNair Scholar |
| 2015 | University of Northern Colorado Research Competition Award (3rd Place Overall) |
| 2016 | McNair Scholars Travel Award |
| 2018-2020 | University of Louisville Presidential Diversity Fellowship |
| 2021-2023 | NIH Inflammation and Pathogenesis T32 Training Grant Fellow |
| 2022 | Graduate Student Council Travel Award |
| 2022 | Travel Award for the Mid-Atlantic Microbial Pathogenesis Meeting |
| 2022 | Carl Storm Underrepresented Minority Fellowship to attend the Microbial Toxins and Pathogenesis GRC |
| 2022 | Invited Oral Presentation - Microbial Toxins and Pathogenesis GRS |
| 2022 | NIH Abstract Award for the Midwest Microbial Pathogenesis Conference |
| 2022 | Travel Award to attend the SACNAS National Meeting |
| 2023 | Invited Oral Presentation – American Society for Microbiology Microbe Meeting |
| 2023 | American Society for Microbiology Future Leaders Mentoring Fellowship (FLMF) |
| 2023 | Graduate Student Council Travel Award |
| 2024 | John Richard Binford Memorial Award |
| 2024 | School of Medicine Student Diversity Award |
| 2024 | Graduate Dean's Citation award |

**PUBLICATIONS** (published as Amanda Landron prior to 2018)

1. **Landron, A.** and Price, A. (2019). "Trichology: A study of hair and its uses as trace evidence." Undergraduate Research Journal at the University of Northern Colorado 5(2): 41-46.

2. Price, S.L., Vadyvaloo, V., DeMarco, J.K., **Brady, A.**, Gray, P.A., Kehl-Fie, T.E., Garneau-Tsodikova, Sy., Perry, R.D., and Lawrenz, M.B. (2021). "Yersiniabactin Contributes to Overcoming Zinc Restriction during *Yersinia pestis* Infection of Mammalian and Insect Hosts." PNAS. 2021 Nov 2;118(44):e2104073118. doi: 10.1073/pnas.2104073118. PMID: 34716262

3. Price, S.L., Thibault, D., Garrison, T.M., **Brady, A.**, Guo, H., Kehl-Fie, T.E., Garneau-Tsodikova, S., Perry, R.D., van Opijnen, T., and Lawrenz, M.B. (2023). "Droplet Tn-Seq identifies the primary secretion mechanism for yersiniabactin in *Yersinia pestis*." EMBO Rep. 2023 Oct 9;24(10):e57369. doi: 10.15252/embr.202357369. Epub 2023 Jul 28. PMID: 37501563

4. Price, S.L., Oakes, R.S., Gonzalez, R.J., Edwards, C., **Brady, A.,** DeMarco, J.K., von Andrian, U.H., Jewell, C.M., and Lawrenz, M.B. (2023). "Microneedle array delivery of *Yersinia*

*pestis* recapitulates bubonic plague." iScience. 2023 Nov 30;27(1):108600. doi: 10.1016/j.isci.2023.108600. eCollection 2024 Jan 19. PMID: 38179062

5. **Brady, A.**, Sheneman, K.R., Pulsifer, A.B., Price, S.L., Garrison, T.M., Maddipati, K.R., Bodduluri, S.R., Pan, J., Boyd, N.L., Zheng, J., Rai, S.N., Hellmann, J., Haribabu, B., Uriarte, S.M., and Lawrenz, M.B. (2024). "Type 3 secretion system induced leukotriene B4 synthesis by leukocytes is actively inhibited by *Yersinia pestis* to evade early immune recognition". PLoS Pathog. 2024 Jan 25;20(1):e1011280. doi: 10.1371/journal.ppat.1011280. eCollection 2024 Jan. PMID: 38271464

6. **Brady, A.**, Tomaszewski, M., Garrison, T.M., and Lawrenz, M.B. (2024). "Approaches for the inactivation of *Yersinia pestis*." Applied Biosafety accepted for publication.

7. **Brady, A.**, Mora-Martinez, L., Hammond, B., Leus, P., Mecsas, J.C., Uriarte, S.M., and Lawrenz, M.B. (2024). "Signaling pathways required for $LTB_4$ synthesis in response to the bacterial type 3 secretion system differs between macrophages and neutrophils". In preparation.

8. **Brady, A.,** Hofstaedte, C., Smith, R., Sumner, K., Rasko, D., Ernst, R.K. and Lawrenz, M.B. (2024). "Evolution of lipid A in pathogenic *Yersinia* species". In preparation.

**ORAL PRESENTATIONS**

1. University of Louisville Microbiology and Immunology Departmental Seminar (2020). "Where has all the inflammation gone? Inhibition of $LTB_4$ synthesis by *Yersinia pestis."* **Brady, Amanda**, Pulsifer, Amanda R. and Lawrenz, Matthew B.

2. ASM KY-TN (2021). "*Yersinia pestis* inhibits host synthesis of Leukotriene B4, a potent mediator of inflammation"; **Amanda Brady**, Amanda R. Pulsifer, Sarah L. Price, Shesh N. Rai, Krishna Rao Maddipati, Haribabu Bodduluri, Silvia M. Uriarte and Matthew B. Lawrenz.

3. Center for Predictive Medicine Retreat (2022). "*Yersinia pestis* inhibits host synthesis of Leukotriene B4, a potent mediator of inflammation"; **Amanda Brady**, Amanda R. Pulsifer, Sarah L. Price, Shesh N. Rai, Krishna Rao Maddipati, Haribabu Bodduluri, Silvia M. Uriarte and Matthew B. Lawrenz.

4. University of Louisville Microbiology and Immunology Departmental Seminar (2022). "Yop effectors block $LTB_4$, which delays host inflammation*."* **Brady, Amanda.**, Pulsifer, Amanda R. and Lawrenz, Matthew B.

5. Inflammation and Pathogenesis T32 Colloquium (2022). "*Yersinia pestis* inhibits host synthesis of Leukotriene B4, a potent mediator of inflammation"; **Amanda Brady**, Amanda R. Pulsifer, Sarah L. Price, Shesh N. Rai, Krishna Rao Maddipati, Haribabu Bodduluri, Silvia M. Uriarte and Matthew B. Lawrenz.

6. GRS-Microbial Toxins and Pathogenicity (2022). "*Yersinia pestis* inhibits host synthesis of Leukotriene B4, a potent mediator of inflammation"; **Amanda Brady**, Amanda R. Pulsifer, Sarah L. Price, Shesh N. Rai, Krishna Rao Maddipati, Haribabu Bodduluri, Silvia M. Uriarte and Matthew B. Lawrenz.

7. University of Louisville Microbiology and Immunology Departmental Seminar (2023). "Yop effectors block $LTB_4$, which delays host inflammation*."* **Brady, Amanda.**, Pulsifer, Amanda R. and Lawrenz, Matthew B.

8. Inflammation and Pathogenesis T32 Colloquium (2023). “A mechanism of early immune evasion: Inhibition of $LTB_4$ synthesis by *Yersinia pestis*”; **Amanda Brady**, Amanda R. Pulsifer, Sarah L. Price, Shesh N. Rai, Krishna Rao Maddipati, Haribabu Bodduluri, Silvia M. Uriarte and Matthew B. Lawrenz.

9. ASM Microbe (2023). “The *Yersinia pestis* Type 3 secretion system triggers $LTB_4$ synthesis by leukocytes in an inflammasome-independent manner.” **Brady, Amanda**, Bodduluri, Haribabu, Uriarte, Silvia M., and Lawrenz, Matthew B.

10. Midwest Microbial Pathogenesis Conference (2023). “The *Yersinia pestis* Type 3 secretion system triggers $LTB_4$ synthesis by leukocytes in an inflammasome-independent manner”; **Amanda Brady**, Amanda R. Pulsifer, Sarah L. Price, Shesh N. Rai, Krishna Rao Maddipati, Haribabu Bodduluri, Silvia M. Uriarte and Matthew B. Lawrenz.

**POSTER PRESENTATIONS** (*presenter; published as Amanda Landron prior to 2018)

1. 23rd annual California McNair Scholars Symposium (2015). “Trichology: A Study of Hair and Its Uses as Trace Evidence”. ***Amanda Landron**

2. Research Day at the University of Northern Colorado (2016). “Trichology: A Study of Hair and Its Uses as Trace Evidence”. ***Amanda Landron**

3. American Academy of Forensic Science 68th Annual Scientific Meeting (2016). “Trichology: A Study of Hair and Its Uses as Trace Evidence”. *Amanda Landron

4. Research Day at the University of Northern Colorado (2017). “The Durability of Mitochondrial DNA in Hair Follicles”. ***Amanda Landron**

5. The American Academy of Forensic Science 70th Annual Scientific Meeting (2018). “The Durability of Mitochondrial DNA in Hair Follicles”. ***Amanda Brady**

6. University of Louisville Student Recruiting (2020). “Gain-of-function Approach Reveals Hidden Contributions of Yop Effectors During *Yersinia pestis* Infection of Human Neutrophils”; ***Amanda Brady**, Amanda R. Pulsifer, Aruna Vashishta, Sarah L. Price, Shane A. Reeves, Jennifer K. Wolfe, Samantha G. Palace, Jon D. Goguen, Sobha R. Bodduluri, Haribabu Bodduluri, Silvia M. Uriarte, and Matthew B. Lawrenz.

7. Midwest Microbial Pathogenesis Conference (2021). “*Yersinia pestis* inhibits host synthesis of Leukotriene B4, a potent mediator of inflammation”; ***Amanda Brady**, Amanda R. Pulsifer, Sarah L. Price, Krishna Rao Maddipati, Haribabu Bodduluri, Silvia M. Uriarte and Matthew B. Lawrenz.

8. Research Louisville (2021). “*Yersinia pestis* inhibits host synthesis of Leukotriene B4, a potent mediator of inflammation”; ***Amanda Brady**, Amanda R. Pulsifer, Sarah L. Price, Shesh N. Rai, Krishna Rao Maddipati, Haribabu Bodduluri, Silvia M. Uriarte and Matthew B. Lawrenz.

9. Mid-Atlantic Microbial Pathogenesis Meeting (2022). “*Yersinia pestis* inhibits host synthesis of Leukotriene B4, a potent mediator of inflammation”; **Amanda Brady**, Amanda R. Pulsifer, Sarah L. Price, Shesh N. Rai, Krishna Rao Maddipati, Haribabu Bodduluri, Silvia M. Uriarte and Matthew B. Lawrenz.

10. GRC-Microbial Toxins and Pathogenicity (2022). “*Yersinia pestis* inhibits host synthesis of Leukotriene B4, a potent mediator of inflammation”; **Amanda Brady**, Amanda R. Pulsifer,

Sarah L. Price, Shesh N. Rai, Krishna Rao Maddipati, Haribabu Bodduluri, Silvia M. Uriarte and Matthew B. Lawrenz.

11. Midwest Microbial Pathogenesis Conference (2022). "The *Yersinia pestis* Type 3 secretion system triggers LTB4 synthesis by leukocytes in an inflammasome-independent manner"; **Amanda Brady**, Amanda R. Pulsifer, Sarah L. Price, Shesh N. Rai, Krishna Rao Maddipati, Haribabu Bodduluri, Silvia M. Uriarte and Matthew B. Lawrenz.